

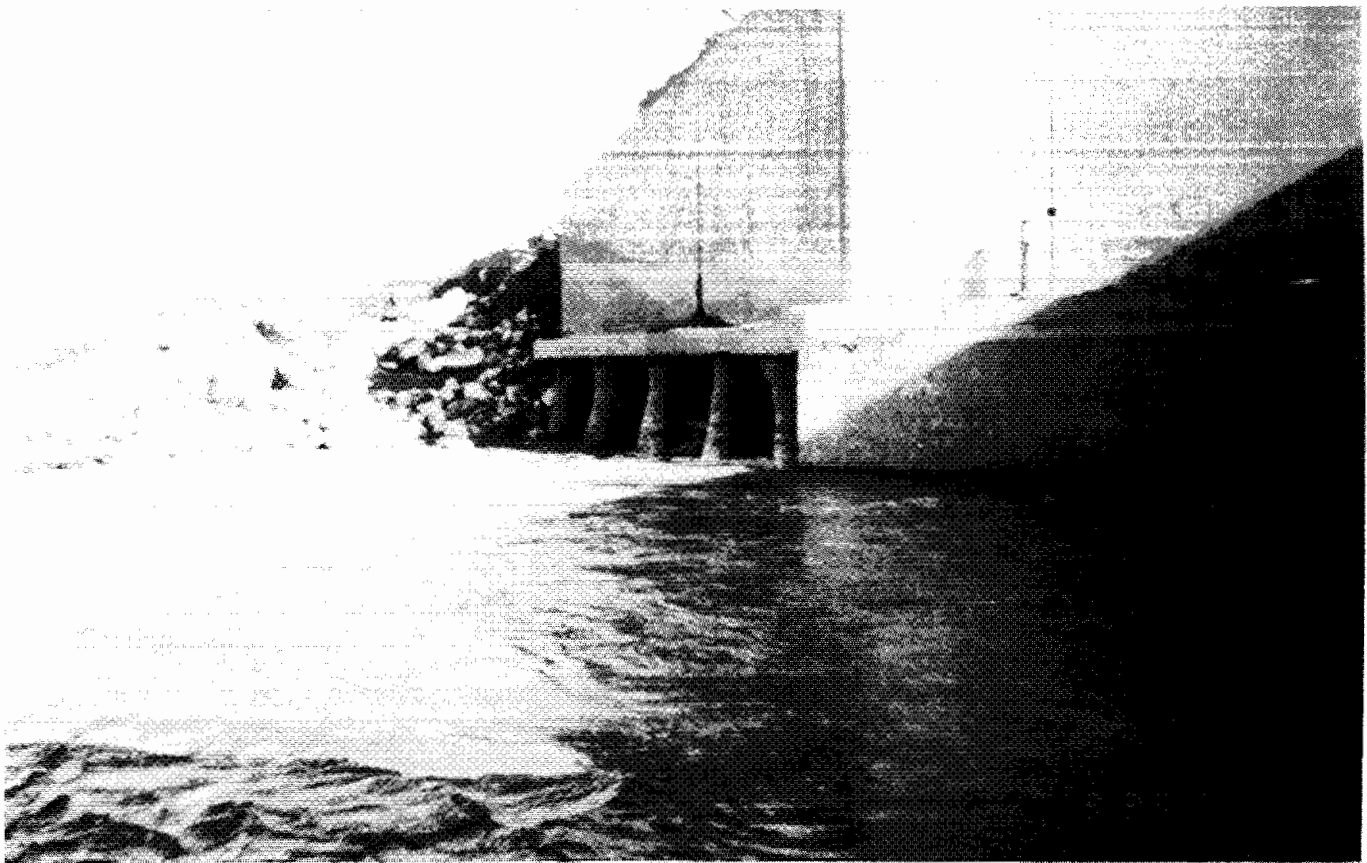
Channel Scour at Bridges in the United States



PB96-203195

Publication No. FHWA-RD-95-184

August 1996



U.S. Department of Transportation
Federal Highway Administration

Research and Development
Turner-Fairbank Highway Research Center
6300 Georgetown Pike
McLean, Virginia 22010-2296

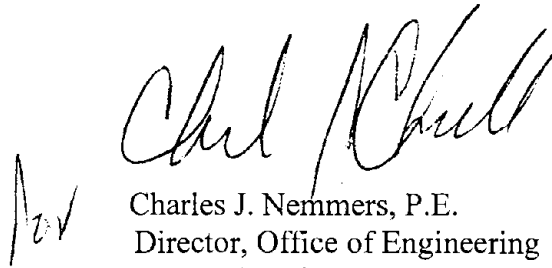
REPRODUCED BY:
U.S. Department of Commerce
National Technical Information Service
Springfield, Virginia 22161

NTIS

FOREWORD

This study documents more than 380 field measurements of local scour around bridge piers. The measurements were taken at 56 bridges in 14 States through cooperative agreements involving the U.S. Geological Survey, the Federal Highway Administration, and several State highway agencies.


This publication documents the methods used to measure and interpret the data and summarizes key information from the Bridge Scour Data Management System (BSDMS), which is a computer data base for mainframe and microcomputers that has the most comprehensive set of field measurements ever assembled on this topic.


Charles J. Nemmers, P.E.
Director, Office of Engineering
Research and Development

NOTICE

This document is disseminated under the sponsorship of the Department of Transportation in the interest of information exchange. The United States Government assumes no liability for its contents or use thereof. This report does not constitute a standard, specification, or regulation.

The United States Government does not endorse products or manufacturers. Trade and manufacturer's names appear in this report only because they are considered essential to the object of the document.

1. Report No. FHWA-RD-95-184	2. P896-203195 	3. Recipient's Catalog No.	
4. Title and Subtitle CHANNEL SCOUR AT BRIDGES IN THE UNITED STATES		5. Report Date August 1996	6. Performing Organization Code
7. Author(s) Mark N. Landers and David S. Mueller		8. Performing Organization Report No.	
9. Performing Organization Name and Address U.S. Geological Survey Water Resources Division 12201 Sunrise Valley Dr. Reston, VA 22092		10. Work Unit No. (TRAIS) 3D3C1-212	11. Contract or Grant No. DTFH61-87-Y-00123
12. Sponsoring Agency Name and Address Office of Engineering R&D Federal Highway Administration 6300 Georgetown Pike McLean, VA 22101-2296		13. Type of Report and Period Covered Final Report 1987 - 1994	14. Sponsoring Agency Code
15. Supplementary Notes Contracting Officer's Technical Representative (COTR): J. Sterling Jones, HNR-10 Final Document Preparation: David Pearson, Donna Pearson, GKY and Associates, Inc.			
16. Abstract Scour of the channel bed around bridge foundations is the leading cause of failure among more than 487,000 bridges over water in the United States. Field measurements of scour at bridges are needed to improve the understanding of scour processes and the ability to predict scour depths accurately. This report documents methods to measure and interpret bridge scour data, presents an extensive pier scour measurement data base, evaluates scour processes in an analysis of these data, and compares observed and predicted scour depths for several scour prediction equations. More than 380 measurements of local scour around bridge piers have been compiled from 56 bridges in 14 States in a cooperative investigation of the U.S. Geological Survey and the Federal Highway Administration. The data are stored in an interactive bridge scour data base management system developed in this study. Improved planning for scour measurements during floods and advances in scour measurement instrumentation and techniques have improved the quantity and quality of measured scour data. Consistent and representative methods are used to interpret scour measurement data that were compiled from several investigations. The relation of scour depth to several explanatory variables, including effective pier width, flow depth, flow intensity, and sediment parameters, is investigated. The data distributions of individual scour variables are typically right skewed. The effective pier width generally has the greatest influence on scour depth. Flow depth has a positive relation with scour depth over the range of measured data; but the influence of flow depth decreases with increasing scour. The positive relation of flow intensity to scour depth is apparent when bed-load transport is negligible, but appears insignificant for active bed-load transport conditions. The influence of sediment size and gradation on local scour depth is inconclusive on the basis of this analysis. Selected local scour prediction equations are evaluated and compared based on the field data. None of the selected equations accurately predict the depth of scour for all the measured conditions. Several equations did better than others when evaluated as design equations. The information in this report is provided to contribute to the improved design and evaluation of bridges, and to the safety of the traveling public.			
17. Key Words Bridge scour, field data, data base, hydraulics.		18. Distribution Statement No restrictions. This document is available to the public through the National Technical Information Service, Springfield, VA 22161.	
19. Security Classif. (of this report) Unclassified	20. Security Classif. (of this page) Unclassified	21. No. of Pages 140	22. Price

SI* (MODERN METRIC) CONVERSION FACTORS

APPROXIMATE CONVERSIONS TO SI UNITS

APPROXIMATE CONVERSIONS FROM SI UNITS

Symbol	When You Know	Multiply By	To Find	Symbol	Symbol	When You Know	Multiply By	To Find	Symbol
LENGTH					LENGTH				
in	inches	25.4	millimeters	mm	mm	millimeters	0.039	inches	in
ft	feet	0.305	meters	m	m	meters	3.28	feet	ft
yd	yards	0.914	meters	m	m	meters	1.09	yards	yd
mi	miles	1.61	kilometers	km	km	kilometers	0.621	miles	mi
AREA					AREA				
in ²	square inches	645.2	square millimeters	mm ²	mm ²	square millimeters	0.0016	square inches	in ²
ft ²	square feet	0.093	square meters	m ²	m ²	square meters	10.764	square feet	ft ²
yd ²	square yards	0.836	square meters	m ²	m ²	square meters	1.195	square yards	yd ²
ac	acres	0.405	hectares	ha	ha	hectares	2.47	acres	ac
mi ²	square miles	2.59	square kilometers	km ²	km ²	square kilometers	0.386	square miles	mi ²
VOLUME					VOLUME				
fl oz	fluid ounces	29.57	milliliters	mL	mL	milliliters	0.034	fluid ounces	fl oz
gal	gallons	3.785	liters	L	L	liters	0.264	gallons	gal
ft ³	cubic feet	0.028	cubic meters	m ³	m ³	cubic meters	35.71	cubic feet	ft ³
yd ³	cubic yards	0.765	cubic meters	m ³	m ³	cubic meters	1.307	cubic yards	yd ³
NOTE: Volumes greater than 1000 l shall be shown in m ³ .									
MASS					MASS				
oz	ounces	28.35	grams	g	g	grams	0.035	ounces	oz
lb	pounds	0.454	kilograms	kg	kg	kilograms	2.202	pounds	lb
T	short tons (2000 lb)	0.907	megagrams (or "metric ton")	Mg (or "t")	Mg (or "t")	megagrams (or "metric ton")	1.103	short tons (2000 lb)	T
TEMPERATURE (exact)					TEMPERATURE (exact)				
°F	Fahrenheit temperature	5(F-32)/9 or (F-32)/1.8	Celcius temperature	°C	°C	Celcius temperature	1.8C + 32	Fahrenheit temperature	°F
ILLUMINATION					ILLUMINATION				
fc	foot-candles	10.76	lux	lx	lx	lux	0.0929	foot-candles	fc
fl	foot-Lamberts	3.426	candela/m ²	cd/m ²	cd/m ²	candela/m ²	0.2919	foot-Lamberts	fl
FORCE and PRESSURE or STRESS					FORCE and PRESSURE or STRESS				
lbf	poundforce	4.45	newtons	N	N	newtons	0.225	poundforce	lbf
lbf/in ²	poundforce per square inch	6.89	kilopascals	kPa	kPa	kilopascals	0.145	poundforce per square inch	lbf/in ²

* SI is the symbol for the International System of Units. Appropriate rounding should be made to comply with Section 4 of ASTM E380.

TABLE OF CONTENTS

Section	Page
INTRODUCTION	1
CHANNEL SCOUR PROCESSES AT BRIDGES	5
<u>Long-Term Aggradation and Degradation</u>	5
<u>Contraction Scour and General Scour</u>	6
<u>Local Scour</u>	8
<u>Clear-Water and Live-Bed Scour</u>	11
PLANNING REGIONAL SCOUR MEASUREMENTS	15
<u>Reconnaissance and Site Selection</u>	15
<u>Measurement Preparation</u>	15
INSTRUMENTATION AND TECHNIQUES TO MEASURE SCOUR	19
<u>Streambed Elevation</u>	20
<u>Water Velocity</u>	23
<u>Bed Material</u>	25
<u>Sediment Transport</u>	27
<u>Instrument Deployment</u>	27
<u>Horizontal Position</u>	29
<u>Data Storage</u>	33
REFERENCE SURFACES FOR MEASURING SCOUR DEPTH	35
<u>Local Scour Reference Surfaces</u>	36
<u>Contraction Scour Reference Surfaces</u>	38
BRIDGE SCOUR DATA MANAGEMENT SYSTEM	41
<u>Characteristics and Capabilities</u>	41
<u>Structure and Elements of Data Set</u>	42
<u>Operation</u>	42
<u>Example Data Set</u>	43
SUMMARY OF SCOUR MEASUREMENTS AT BRIDGE PIERS	57
ANALYSIS OF LOCAL SCOUR PROCESSES AT BRIDGE PIERS	79
<u>Pier Width Effects</u>	80
<u>Pier Alignment Effects</u>	81
<u>Pier Nose Shape Effects</u>	82
<u>Flow Depth Effects</u>	83
<u>Flow Intensity Effects</u>	86
<u>Sediment Size Effects</u>	89
<u>Sediment Gradation Effects</u>	90
EVALUATION OF SELECTED PIER SCOUR EQUATIONS	95
<u>Description of Equations</u>	96
<u>AHMAD EQUATION</u>	96
<u>BLENCH-INGLIS EQUATIONS</u>	97

TABLE OF CONTENTS
(continued)

Section	Page
<i>SIMPLIFIED CHINESE EQUATIONS</i>	98
<i>CHITALE EQUATION</i>	100
<i>FROEHLICH EQUATIONS</i>	101
<i>HYDRAULIC ENGINEERING CIRCULAR 18 (HEC-18) EQUATION</i>	102
<i>INGLIS-POONA EQUATIONS</i>	103
<i>LARRAS EQUATION</i>	104
<i>LAURSEN EQUATION</i>	104
<i>SHEN EQUATIONS</i>	106
<u>Application of Equations to Measured Data</u>	107
<u>Comparison of Observed and Computed Scour</u>	108
SUMMARY AND CONCLUSIONS	117
REFERENCES	121

LIST OF FIGURES

No.		Page
1.	Percent total failures by failure mode [823 failures - Shirhole and Holt (1991)]	1
2.	Failure of pier 2 and span of I-90 crossing of Schoharie Creek, New York	3
3.	Locations of bridge scour data sites currently in the National Bridge Scour Data Management System	4
4.	Changes in channel geometry with flood discharge for Red River at U.S. Highway 71 near Index, Arkansas	7
5.	Scour and subsequent fill during flood passage, Colorado River at Lees Ferry, Arizona, water year 1956	8
6.	Bow wave and separation vortices at the nose of a pier	9
7.	Schematic representation of scour at a cylindrical pier	10
8.	Detailed measurement of local scour at the State Route 50/151 crossing of Mississippi River near Chester, Illinois	12
9.	Illustrative pier scour depth in a sand-bed stream as a function of time	13
10.	Clear-water contraction scour in a vegetated overbank area	13
11.	Columbus-type weight with fathometer transducer suspended by hydrologic equipment crane	21
12.	Example of side echoes from bridge pier	22
13.	Effect of transducer cone angle on the acoustic footprint of an echo sounder	23
14.	Approach velocity measurement locations for local pier scour	24
15.	Fathometer mounted on a two-wheel handcart with two-wheel base and boom, sounding weight, and transducer	28
16.	Design of knee-board for deploying a transducer to measure channel bathymetry near a bridge	29
17.	Knee-board deployed downstream from the bridge deck	30
18.	Range-azimuth positioning systems	32
19.	Reference surface for local scour	37

LIST OF FIGURES
(continued)

No.	Page
20.	Reference surface for local scour at pier 13 of the Interstate 95 crossing of South Altamaha River, near Brunswick, Georgia 37
21.	Example of a data set output from the Bridge Scour Data Management System 44
22.	Characteristics of: (A) drainage area, (B) log-transformed drainage area, (C) channel slope, and (D) log-transformed channel slope for scour measurement sites in data base 68
23.	Characteristics of: (A) pier nose shape, (B) pier type, and (C) foundation type for scour measurements 69
24.	Characteristics of: (A) pier width, (B) log-transformed pier width, (C) pier length, and (D) pier skew to flow for scour measurements 71
25.	Characteristics of: (A) flow velocity, (B) square-root transformed velocity, (C) flow depth, and (D) square-root transformed flow depth for scour measurements 72
26.	Characteristics of: (A) D_{50} grain size, (B) log-transformed D_{50} grain size, (C) D_{84} grain size, and (D) log-transformed D_{84} grain size 73
27.	Characteristics of: (A) untransformed and (B) log-transformed geometric standard deviation (σ_g) of the bed material for scour measurements 74
28.	Classification of bed material cohesion for scour measurements 74
29.	Distribution and characteristics of scour depth measured under clear-water and live-bed conditions 75
30.	Characteristics of measured scour depth (y_s) for: (A) standard and (B) log-transformed units, and (C) estimated error of scour measurements 76
31.	Characteristics of top width of measured local scour holes in: (A) standard and (B) log-transformed units 77
32.	Characteristics of side slope of measured local scour holes in: (A) untransformed and (B) log-transformed units 78
33.	Illustrations of dynamic influence of variables on scour depth or volume 79
34.	Relation of effect of pier width (b_c) and scour depth (y_{sp}) 81
35.	Relation of effective pier width to dimensionless scour depth for piers skewed to the flow 82

LIST OF FIGURES
(continued)

No.	Page
36. Distribution of scour depth data according to pier shape	82
37. Relation of ratio of flow depth to effective pier width to: (A) scour depth normalized for pier width, and (B) scour depth normalized for pier width and flow intensity	84
38. Characteristics of: (A) untransformed and (B) log-transformed scour depth to effective pier width ratio, and (C) untransformed and (D) log-transformed flow depth to effective pier width ratio	85
39. Relation of ratio of flow depth to effective pier width to: (A) scour depth normalized for pier width, and (B) scour depth normalized for pier width and flow intensity	86
40. Relation of normalized maximum scour depth to flow intensity (v_o/v_c)	87
41. Relation of flow intensity variable v_o/v_c to normalized scour depth	87
42. Relation of flow intensity variable $[v_o-(v_{c(DB4)}-v_c)]/v_c$ and normalized scour depth	88
43. Relation of Froude number to normalized scour depth	89
44. Relation of dimensionless sediment size variable to normalized scour depth	90
45. Relation of the geometric standard deviation of the bed material (σ_g) to normalized scour depth (y_{sp}/b_c) for clear-water scour measurements ^g compared with relation in Raudkivi and Ettema (1977)	92
46. Relation of geometric standard deviation of the bed material (σ_g) to normalized scour depth (y_{sp}/b_c) for live-bed scour measurements ^g compared with relation in Raudkivi and Ettema (1977)	93
47. Relation of sediment factor to normalized scour depth	93
48. Effect of angle of attack	105
49. Box plot of residuals for all data	109
50. Box plot of ratio of computed to observed scour for all data	110

LIST OF FIGURES
(continued)

No.		Page
51.	Comparison of computed and observed scour for: (A) Froehlich, (B) Froehlich Design, (C) HEC-18, and (D) Simplified Chinese equations with live-bed and clear-water scour identified	112
52.	Comparison of computed and observed scour for: (A) Shen, (B) Blench-Inglis I, (C) Larras, and (D) Inglis-Poona II equations with live-bed and clear-water scour identified	113
53.	Comparison of computed and observed scour for: (A) Froehlich, (B) Froehlich Design, (C) HEC-18, and (D) Simplified Chinese equations with skew of pier to flow categorized	114
54.	Comparison of computed and observed scour for: (A) Shen, (B) Blench-Inglis I, (C) Larras, and (D) Inglis-Poona II equations with skew of pier to flow categorized ..	115

LIST OF TABLES

No.		Page
1.	Checklist for scour measurement site selection	16
2.	Measured local scour on Sacramento River using several reference surfaces	36
3.	Organization of Bridge Scour Data Management System	42
4.	Summary of data collection sites	54
5.	Summary of local scour measurements at bridge piers	58
6.	Characteristics of principal variables of local scour at bridge piers	67
7.	Pier shape coefficients	105

SYMBOLS

- b — Width of bridge pier.
- b_e — Width of bridge pier projected normal to approach flow.
- c — Exponent related to bed load such that if $V_o \leq V_c$, $c=1$ and if $V_o > V_c$, $c < 1$.
- D_g — Grain size of bed material.
- D_m — Mean grain size of bed material.
- D_{16} — Grain size for which 16 percent of bed material is finer.
- D_{50} — Median grain size of bed material.
- D_{50a} — Median grain size of armor layer.
- D_{84} — Grain size for which 84 percent of bed material is finer.
- D_{90} — Grain size for which 90 percent of bed material is finer.
- F_o — Froude number of flow just upstream from pier or abutment.
- F_p — Pier Froude number, defined as $\frac{V_o}{\sqrt{gb}}$.
- f_b — Bed factor.
- g — Acceleration of gravity.
- K — Coefficient that is a function of boundary geometry, abutment shape, width of piers, shape of piers, and angle of approach flow.
- K_s — Coefficient for pier shape.
- K_{S1} — Coefficient for shape of pier nose.
- K_{S2} — Coefficient for shape of pier nose.
- K_1 — Coefficient for shape of pier nose.
- K_2 — Coefficient for pier shape and flow alignment.
- K_3 — Coefficient based on bed conditions.
- $K_{\alpha L}$ — Coefficient based on angle of approach flow referenced to bridge pier.
- K_{ξ} — Coefficient for pier shape and flow alignment.
- L — Length of bridge pier.
- q — Discharge per unit width just upstream from pier.
- Q — Discharge.
- R_p — Pier Reynolds number, defined as $\frac{V_o b}{\nu}$.

- S — Dimensionless slope of energy grade line near bridge.
 u_* — Shear velocity, defined as $\sqrt{gy_u S}$.
 V — Average velocity of channel cross section.
 V_o — Velocity of approach flow just upstream from bridge pier or abutment.
 V_c — Critical (incipient-motion) velocity for a given sediment size.
 $V_{c(D_{84})}$ — Critical (incipient-motion) velocity for D_{84} sediment size.
 V_c' — Approach velocity at which scour at pier is initiated.
 y — Average depth of channel cross section.
 y_o — Depth of flow just upstream from bridge pier or abutment, excluding local scour.
 y_p — Depth of flow at bridge pier, including local pier scour.
 y_r — Regime depth of flow, defined as $\left(\frac{q^2}{f_b}\right)^{1/3}$.
 y_{sp} — Depth of local pier scour below ambient bed.
 ν — Kinematic viscosity of water.
 α — Angle of approach flow referenced to bridge pier, in degrees.
 ϕ — Coefficient for shape of the pier nose.
 ρ — Density of water.
 ρ_s — Density of sediment particles.
 σ_g — Geometric standard deviation of bed material.

Page Intentionally Left Blank

INTRODUCTION

Rivers have played a major role in transportation history by supporting travel along and hindering travel across their winding courses. In the past, crossing an unknown stream required a traveler to assess the risk of the ford or bridge and the importance of the journey. Addressing the problem of public transportation across rivers produced some of the earliest and best examples of civil engineering and continues to fuel progress in engineering and earth science. Advances in transportation engineering have generally relieved the public from any thought of risk assessment when crossing rivers on today's highways. However, the accuracy of channel scour estimates for bridge foundation design remains uncertain in many cases because of inadequate knowledge about the complex dynamics of river channels during rare flood events.

River channels scour and aggrade due to complex interrelated natural processes. Bridge crossings frequently disrupt and intensify the natural river processes by constricting the flow area of the stream at flood stage, by constricting the portion of the channel from which sediment is supplied, and by disturbing the flow with local obstructions (i.e., piers) that locally constrict and redirect the flow. Estimates of the potential scour at bridge sites are essential for both the design of new bridges and for the evaluation of existing bridges to provide safe reliable public transportation corridors.

There are more than 580,000 bridges in the United States and about 84 percent of these are over waterways. The U.S. Federal Highway Administration (1988) states:

“Most waterways can be expected to experience scour over a bridge's service life (which is now approaching 100 years). The added cost of making a bridge less vulnerable is small when compared to the total cost of a failure which can easily be two or three times the original cost of the bridge itself.”

Channel scour around bridge foundations is the leading cause of bridge failure, exceeding all other causes combined. In a survey of 823 bridge failures since 1950, Shirhole and Holt (1991) found that 60 percent were associated with hydraulics (figure 1), which includes channel bed scour around bridge foundations and channel instability. Murillo (1987) also reported that channel scour in the vicinity of bridge piers and foundations resulted in more bridge failures than all other causes in recent history. The predominance of the hydraulics failure mode clearly indicates the need for improved scour analysis and prediction techniques.

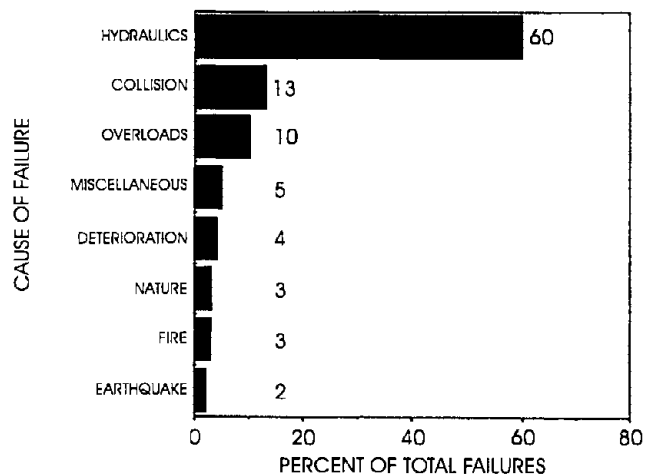


Figure 1. Percent total failures by failure mode [823 failures - Shirhole and Holt (1991)].

The need for improved scour design techniques has long been recognized and scour processes have been extensively researched by many investigators. Numerous equations have been developed to predict contraction scour and local scour at bridges (Shen et al., 1969; Laursen, 1960; Melville and Sutherland, 1988; Richardson et al., 1993; Froehlich, 1988). Most of these equations are based on laboratory investigations. Scour predictions based on the many available equations produce a wide range of scour depths for the same set of conditions, probably due to the typically limited and somewhat unique conditions associated with each investigation. Scour predictions also differ from many scour measurements at bridge sites, probably due to the range of deterministic scour variables in the field that are difficult to reproduce or measure in the laboratory, and due to dynamic dissimilarity between field conditions and laboratory investigations. The recommendation of many scour investigations has been to measure scour data at bridges during floods to improve the understanding of scour processes and the bridge scour prediction methods.

A considerable amount of historic scour data exists in the files of hydrologic data collection agencies such as the U.S. Geological Survey (USGS). Field measurements of local scour have been compiled by Froehlich (1988), Zhuravljov (1978), and others. These historical data sets contain valuable information, but most do not contain information on all of the major factors known to affect scour. Thus, there is a continuing need for measurements of bridge scour and its deterministic factors over the broad range of conditions encountered in the field.

Field measurements of bridge scour remain limited because of the past infrequency of focused scour measurement investigations and because of the difficulty of measuring bridge scour during floods. However, awareness of the problem of bridge scour has escalated in the last decade as a result of several catastrophic, scour-related bridge failures. There are more bridge scour measurement investigations currently underway than all those previously conducted in the United States. The most severe bridge failure of the 1980's was the catastrophic collapse of the I-90 crossing of Schoharie Creek near Amsterdam, New York, on April 5, 1987. Two spans of the bridge fell about 24 m (80 ft) into the flooding stream after pier 3, which partially supported the spans, was undermined by local scour and collapsed. Four passenger cars and a tractor-trailer plunged into the creek and 10 persons were killed. Ninety minutes after the first collapse, pier 2 and a third span collapsed (figure 2). The principal proponent of research into bridge scour processes has been the U.S. Federal Highway Administration (FHWA). The FHWA (1988) stated,

“The FHWA recognizes the subject of scour at bridges as a long-range high-priority national problem area for research and recommends that appropriate studies be carried out to improve the state-of-practice of designing new bridges and inspecting existing bridges for scour.”

Cooperative investigations to collect bridge scour data during floods have been initiated between the USGS and many State departments of transportation, including Alabama, Arkansas, California, Colorado, Delaware, Indiana, Kansas, Maryland, Mississippi, Missouri, Montana, New York, North Dakota, Ohio, South Dakota, and Virginia.



Figure 2. Failure of pier 2 and span of I-90 crossing of Schoharie Creek, New York.

This report documents the results of the National Scour Study, initiated in 1987 as a cooperative investigation of the FHWA and the USGS, Office of Surface Water. The purpose of this investigation is to collect measurements of bridge scour, to provide quality assurance and technical support to other investigations of scour processes, and to provide a national bridge scour data repository. These objectives address limited- and detailed-scope measurements of contraction scour in the bridge opening and local scour at bridge piers and abutments. However, only local pier scour data were successfully collected in this investigation and are presented in the scope of this report. Contraction scour and local scour at abutments have proven very difficult to measure and, when measured, to interpret conclusively. Experience has shown that investigations must be specifically designed to collect these types of scour data, which are particularly needed by bridge designers. The more than 380 local scour measurements presented in this study/investigation were collected at 56 bridge sites in Alaska, Arkansas, Colorado, Delaware, Georgia, Illinois, Indiana, Louisiana, Maryland, Mississippi, Montana, New York, Ohio, and Virginia (figure 3). Additional data have been collected in some of these and other States and will be included in the national data base as they are analyzed and reviewed. These data represent the results of studies funded by many State highway agencies and the creative, professional efforts of many hydrologists to develop programs, chase floods, and measure scour to provide bridge designers with information to reduce the risk to the public from bridge scour.

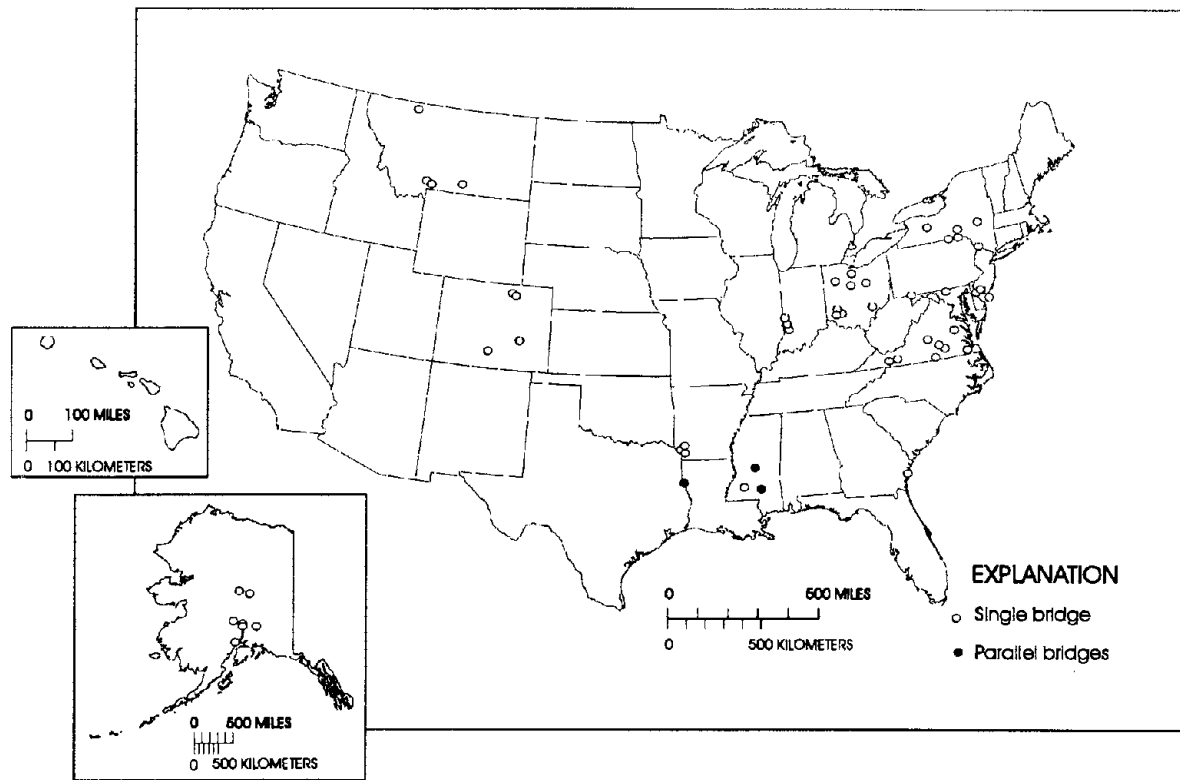


Figure 3. Locations of bridge scour data sites currently in the National Bridge Scour Data Management System.

This report is the principal product of the National Scour Study. Following the introduction is a review of scour processes, then a discussion of the methods employed in this investigation, including planning, field instrumentation and techniques, and interpreting scour reference surfaces from channel geometry data. A Bridge Scour Data Management System (BSDMS) was developed as a repository for the national scour data base (Landers et al., 1994). Its characteristics and function are described in the main body of the report, and a user's manual for the BSDMS is being published separately. The principal variables from the scour measurements in the national data base are tabulated and their data characteristics are summarized. Scour processes at bridge piers are evaluated in the relations of scour depth and several deterministic variables. Observed local scour depths are compared with predicted values for several published equations, and the equations are evaluated based on their residuals.

CHANNEL SCOUR PROCESSES AT BRIDGES

Flow velocity and shear stress typically increase when a flood passes through a river reach, so that the stream has an increased capacity to erode and transport sediment from the channel boundaries. As a result, there is a tendency for channels to scour during flood flows. If bed material is being transported to a scoured reach from upstream, there is typically some filling of the scoured areas as the flood recedes and shear stresses and velocities decrease. "Channel scour" and "fill" are terms that describe erosion and deposition occurring over individual flood events and perhaps seasons, while the terms "aggradation" and "degradation" apply to persistent mean changes over periods of time measured in years (Leopold et al., 1964). Bridge scour applies to short- and long-term channel processes that may undermine and threaten the stability of bridge foundations during the life of the structure. The total scour at a bridge is a function of hydrologic and hydraulic parameters, bridge characteristics, and bed material characteristics.

The magnitude of total scour is defined as the vertical distance between the scoured channel geometry and a reference datum that represents the channel geometry for a baseline condition, i.e., for current or historic conditions in the absence of the bridge structure. The total scour has three components that are usually additive in effect. These are long-term aggradation and degradation, contraction and general scour, and local scour. In addition to vertical scour, lateral erosion and migration of stream boundaries may erode roadway approaches, particularly at bridge abutments. These components of bridge scour are described and discussed in *Highways in the River Environment* (Richardson et al., 1990), *HEC-18: Evaluating Scour at Bridges* (Hydraulic Engineering Circular 18, Richardson et al., 1993), and in other publications. Therefore, the discussion here will be brief, with a particular emphasis on general scour, which has been used with different meanings in the past.

Predictions of total scour require evaluation of each individual component of scour based on deterministic parameters. Analysis of observed scour data also requires that measured total scour be broken into its individual components. Analyses of scour processes are limited when the contribution of the components of total scour cannot be isolated. The key to evaluating the individual components of observed total scour is to determine appropriate reference surfaces for each scour component (Landers and Mueller, 1993). Methods to determine appropriate reference surfaces are described in a later section of this report. The terms "scour depth" and "depth of scour" both refer to the eroded depth below a channel bed reference surface, while the term "scoured depth" refers to depth of water at a scoured location (Klingeman, 1973; Neill, 1968).

Long-Term Aggradation and Degradation

The landscape presented to us by the earth, including its rivers, is often perceived as one of the most unchanging aspects of our experience. River boundaries are, in fact, dynamic; although major changes are typically defined in historical, if not geologic, timeframes. Long-term aggradation and degradation at bridges should be evaluated in the timeframe of the design life of the structure; 50 or 100 yr is often used. Long-term changes in riverbed elevations occur due to natural and man-made changes that affect the stream energy and sediment load. Factors

that affect stream energy include channelization, changes in the downstream hydraulic control, cutoffs of meander loops (natural or man-made), regulation or diversion of stream flow, changes in basin rainfall-runoff characteristics, and climate changes. Factors that affect the sediment load of a river reach include changes in stream energy, gravel mining from the stream bed, dams and reservoirs, changes in basin land use, and catastrophic floods. Methods to evaluate long-term stability of streams are described in Richardson et al. (1990), and Lagasse et al. (1991). These methods require investigation of the drainage basin or an extended stream reach, as compared with methods for other scour components that require investigation only of the reach affected by the bridge. Methods to determine reference surfaces for and to quantify local and contraction scour from measured scour data are designed to exclude the component of long-term degradation and aggradation.

Contraction Scour and General Scour

Contraction scour is caused by a contraction of the channel flow area that increases the scouring and sediment transport capacity of the flow in the contracted channel reach. The flow contraction can be formed by a naturally occurring, relatively narrow channel and flood plain reach; and such reaches are often selected for bridge locations because of reduced costs associated with shorter bridge spans. Contraction scour is more often associated with flow contraction by roadway embankments and guide banks. Contraction scour can be intensified where the flow area is decreased by accumulations of debris or ice, or by the cumulative effect of piers. Contraction scour is also caused by the effect of redirecting flow from vegetated overbank areas, where sediment-supply and bed-load transport are negligible, to the main channel at the bridge crossing. The concentration of this "sediment-hungry" water can increase scour in the bridge opening, particularly at the abutments or guide banks where the water re-enters the main channel.

Flow area contractions cause increased average velocities and bed shear stress so that more bed material can be scoured and transported out of the contracted reach than is transported into it. As scour progresses, the flow area increases so that (by continuity) the velocity and shear stress decrease until there is equilibrium between the bed material transported into and out of the contracted reach. This is an idealized description of the process because discharge and bed material transport are typically unsteady and true equilibrium conditions are rarely achieved in nature. Unlike long-term aggradation and degradation, contraction scour approaches a limit for steady-state flood conditions if bed-load transport is active, and may be refilled during the flood recession.

Some confusion may exist among engineers and scientists regarding the terms "general scour" and "contraction scour." Both terms describe short-term processes that cause scour over the general channel cross section. The term "general scour" is used in *Highways in the River Environment* (Richardson et al., 1990) to inclusively describe contraction scour and other short-term (flood event-associated, seasonal, and annual) scour processes caused by variable backwater conditions and variable bed material load. In *HEC-18: Evaluating Scour at Bridges* (Hydraulic Engineering Circular 18, Richardson et al., 1993), the term "contraction scour" is used to inclusively describe these short-term processes, and the term "general scour" is not used. In

Guide to Bridge Hydraulics (Neill, 1973), the term “general scour” refers to contraction scour as defined above, and the term “natural scour” refers to other short-term scour processes that cause scour across a channel opening.

In the previous paragraphs of this report, contraction scour is defined consistent with Richardson et al. (1990), and *HEC-18: Evaluating Scour at Bridges* (Richardson et al., 1993). In this report, general scour is defined as scour due to short-term processes caused by variable backwater conditions and variable bed material transport. General scour tends to be distributed across a bridge opening (though usually not uniformly) rather than localized. Contraction and general scour are defined independently so that their distinct deterministic processes may be isolated and analyzed independently. Contraction and general scour cannot be distinguished in most field measurements made using limited-detail methods. Figure 4 shows the total scour for a 100-yr recurrence interval flood at the U.S. Highway 71 crossing of Red River near Index, Arkansas. The maximum total scour is about 4.9 m (16 ft). Concurrent channel geometry was not measured outside of the contracted reach, so the contraction scour cannot be distinguished from the general scour.

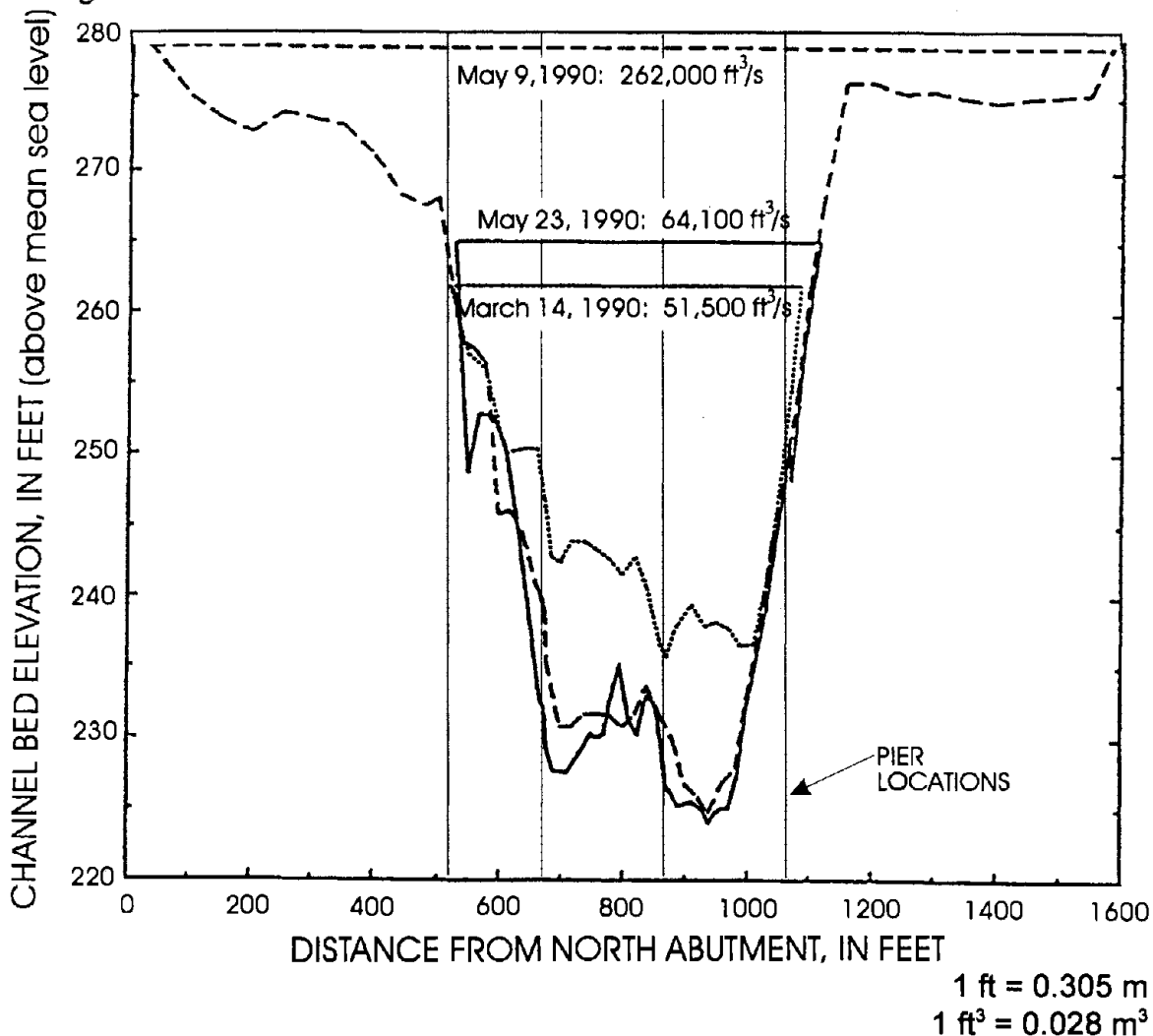


Figure 4. Changes in channel geometry with flood discharge for Red River at U.S. Highway 71 near Arkansas.

General scour can be very significant, particularly on streams in semiarid climates and on ephemeral streams where sediment transport is more intermittent over time and more concentrated during flood events. Figure 5 (from Leopold et al., 1964) illustrates general scour and fill of about 2.7 m (9 ft) over one flood season at Colorado River at Lees Ferry, Arizona.

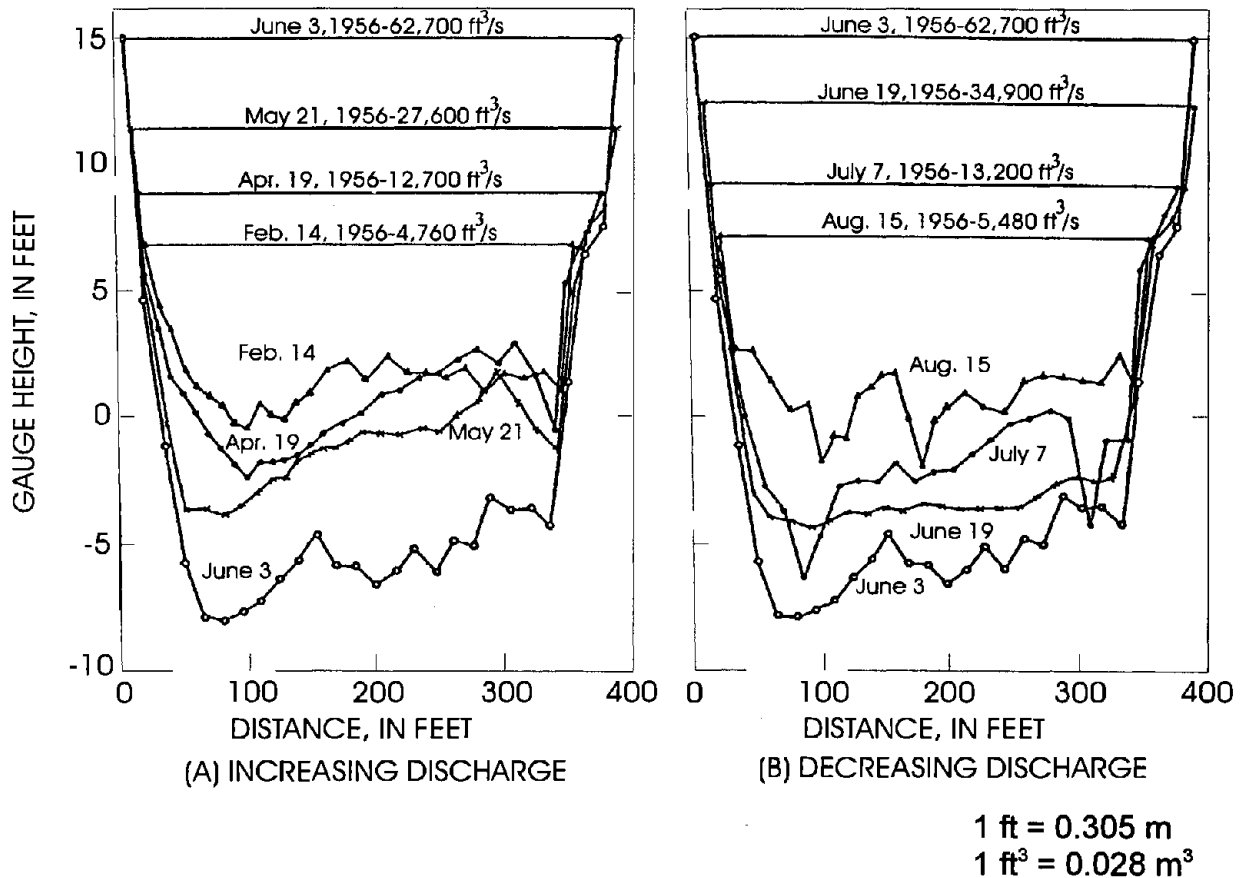


Figure 5. Scour and subsequent fill during flood passage, Colorado River at Lees Ferry, Arizona, water year 1956.

Local Scour

Local scour of the channel bed occurs where flow obstructions cause acceleration and the formation of vortices around the base of the obstruction, which locally increase the erosive capacity of the flow. Local scour typically occurs around bridge piers, abutments, spurs, and embankments. The depth of local scour is the difference between the scoured bed level with, and the unscoured bed level without, the flow obstruction for a given flow condition. The maximum local scour from a measurement is the quantity usually reported, unless otherwise noted.

At the upstream face of a flow obstruction such as a bridge pier, a pressure field develops and causes vortices and accelerations in the magnitude and direction of the flow. For example, a horizontally oriented, reverse rolling vortex or bow wave, may be observed rising above the surrounding water surface at the head of a flow obstruction (figure 6). A similar vortex (known as the horseshoe vortex) is formed at the base of the pier and is an effective mechanism for eroding and transporting bed material away from the base of the pier (figure 7). Investigators also report the formation of a groove in the bed, at the location where the vertical velocity along the face of the pier intersects the channel bed (Raudkivi, 1986; Melville, 1984). A local scour hole develops as the bed material transport away from the local area exceeds the transport into the area. As the volume of the scour hole increases, the strength of the vortices and boundary shear stress are reduced. Scouring ceases when sediment transport out of the scour hole does not exceed the sediment transport into the scour hole or when there is no transport out of the hole.



Figure 6. Bow wave and separation vortices at the nose of a pier.

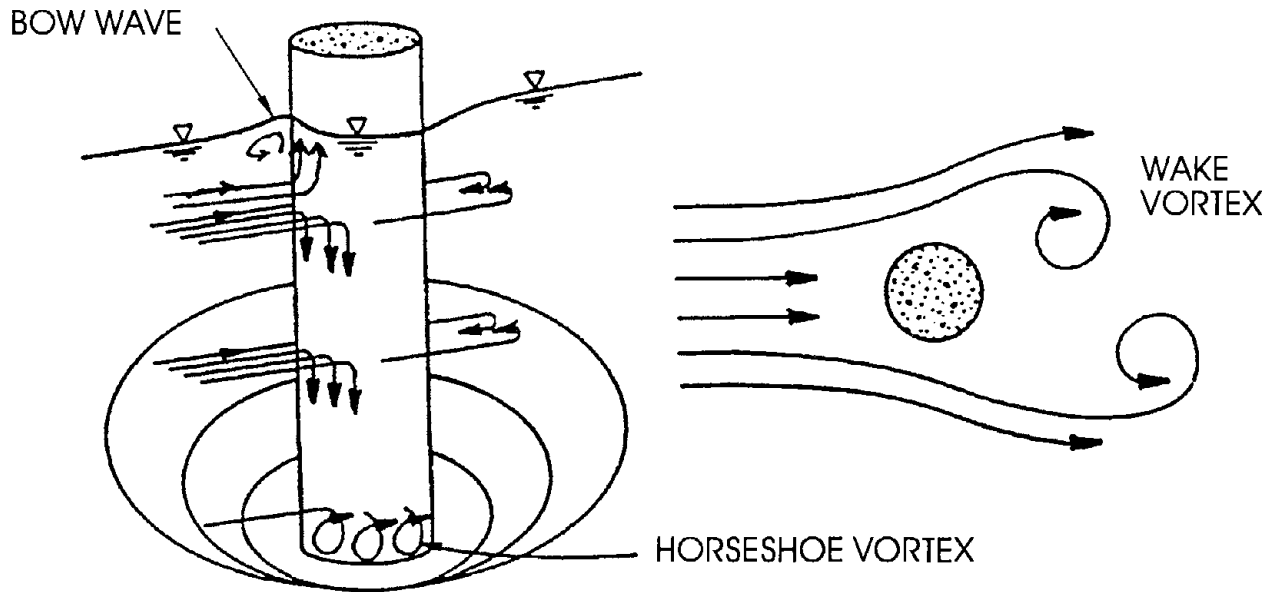


Figure 7. Schematic representation of scour at a cylindrical pier.

Figure 8 shows detailed local scour hole measurements made at the State Route 50/151 crossing of the Mississippi River near Chester, Illinois, for three dates during the 1993 Midwest flood. The three measurements are vertically offset in this illustration so that changes in the shape of the scour hole can be observed. For the perspective shown in figure 8, the flow is from the lower right to the upper left. The measurement of August 3 was made near the flood peak and has a maximum local scour of 7.1 m (23.3 ft), pier width of 4.0 m (13 ft), and depth and velocity of 22.5 m (73.9 ft) and 2.4 m/s (8.0 ft/s). The maximum local scour on August 12 and September 13 is 6.2 and 6.5 m (20.4 and 21.4 ft), respectively; however, the volume of the local scour hole for the three measurements does not change beyond the limits of measurement accuracy.

Vertical vortices typically form immediately downstream from local flow obstructions, and are known as wake vortices (figure 7). The wake vortex may extend the local scour effects for some distance downstream from the pier in fine-grained materials; however, more typically, a deposition zone may be observed just downstream from the pier.

Factors that affect local scour at piers and abutments include: (1) pier width; (2) projected length of the abutment into the flow; (3) length of the pier (if the pier is skewed to the approach flow); (4) depth of flow approaching the scour hole; (5) velocity of the approach flow; (6) bed material size, gradation, and cohesion; (7) alignment of the obstruction to the flow; (8) the shape of the pier nose or abutment edge; (9) channel bed configuration (dunes, plane bed, etc.); and (10) ice and debris effects.

Clear-Water and Live-Bed Scour

Contraction and local scour processes can occur under clear-water or live-bed conditions. Clear-water conditions occur when transport of bed material into the channel section at the bridge crossing is negligible. Live-bed conditions occur when transport of bed material into the channel section at the bridge crossing is not negligible. It is important to identify the condition under which the scour is occurring, because both the rate at which scour develops over time and the relation between scour depth and approach flow velocity depend on whether clear-water or live-bed conditions predominate (Shen et al., 1969). Figure 9 illustrates that live-bed scour develops rapidly and then fluctuates over time (due to the passage of dunes) around an equilibrium scour depth. In steady-state laboratory tests, clear-water scour develops more slowly and has a maximum scour depth about 10 percent greater than the equilibrium scour depth for live-bed scour (Richardson et al., 1993; Raudkivi and Ettema, 1983).

Examples of clear-water scour situations include coarse bed material streams, armored stream beds, vegetated channels and overbank areas where the cover is penetrated only in the scoured area, and flat gradient streams during low flow. Figure 10 shows clear-water contraction scour at a bridge in a vegetated overbank area.

Equilibrium scour depth (or volume) for live-bed scour in fine-grained materials is reached quickly when hydraulic and sediment transport conditions are steady state. The typically unsteady rate of bed material transport into a scoured region is highly significant for live-bed scour. This study has observed, even for sand-size materials, the progression from clear-water scour conditions to live-bed conditions and back to clear-water scour conditions over a single flow event. Multiple flood events may be required before maximum clear-water scour depth is reached for a specific flow condition; in some armored cobble or cohesive bed streams, this may require decades.

Surficial bed material movement usually does not begin suddenly at a critical or incipient condition. However, the transition from negligible (clear-water) to significant (live-bed) bed material transport conditions will be centered over some critical shear stress condition. Shields' diagram is often used to estimate the critical shear stress at which bed particles just begin to move. Neill (1968) presented an equation based on Shields' diagram to compute the critical, channel mean velocity for the incipient motion of large particles, on which viscous boundary forces are not significant. On Shields' diagram, the dimensionless shear stress for this fully turbulent condition is constant at 0.060 at grain Reynolds numbers greater than about 600. Neill and others have noted that marginal transport of bed load occurs at much lower dimensionless shear stress values. Andrews and Smith (1992) observed that bed-load transport of individual particles by rolling (rather than saltating) occurs over a range of dimensionless shear stress between 0.020 and 0.060, and they state that gravel transport is not significant in this range. Neill (1968) suggests that his equation may be applicable for dimensionless shear stress values greater than 0.03.

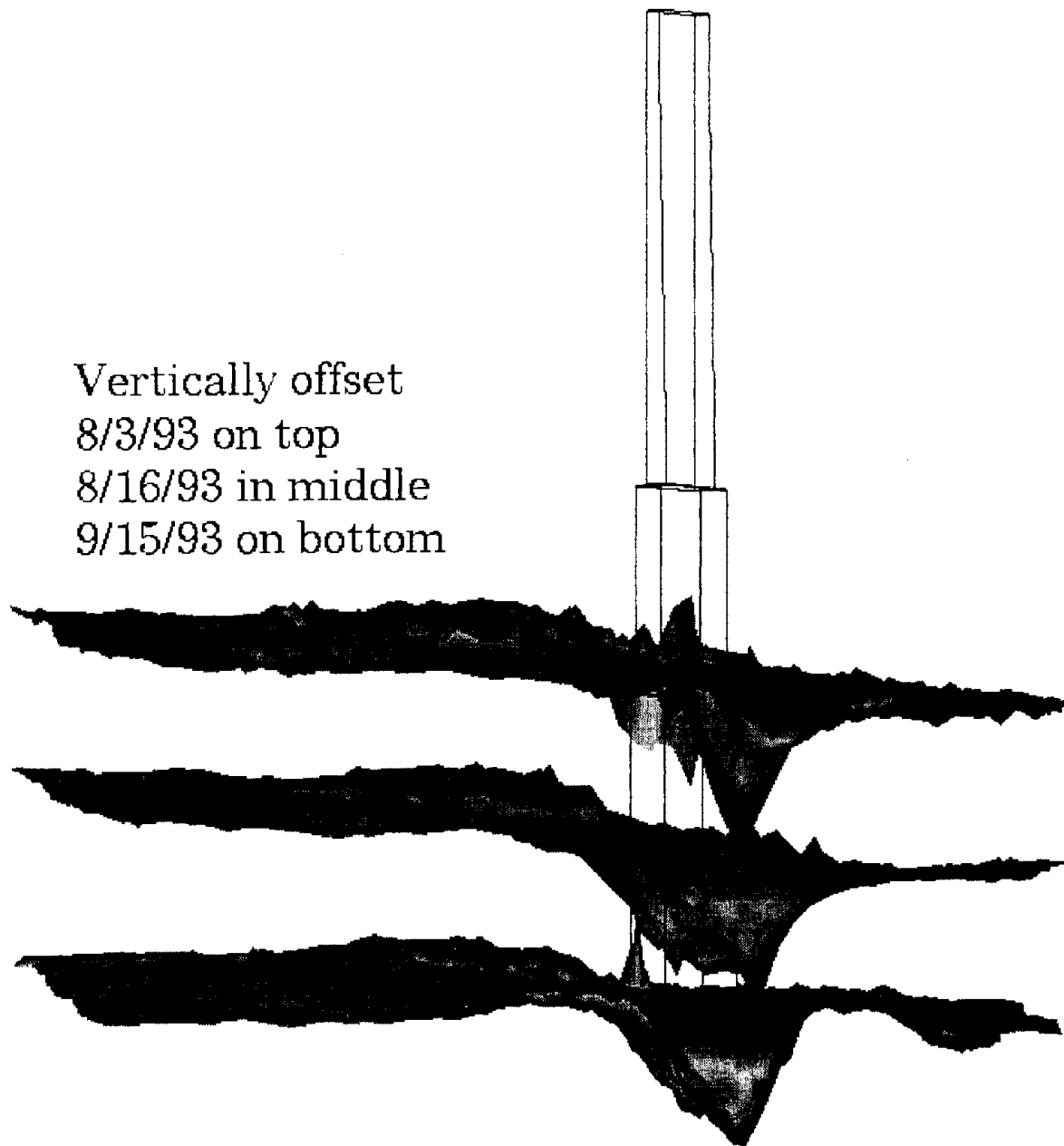


Figure 8. Detailed measurement of local scour at the State Route 50/151 crossing of Mississippi River near Chester, Illinois.

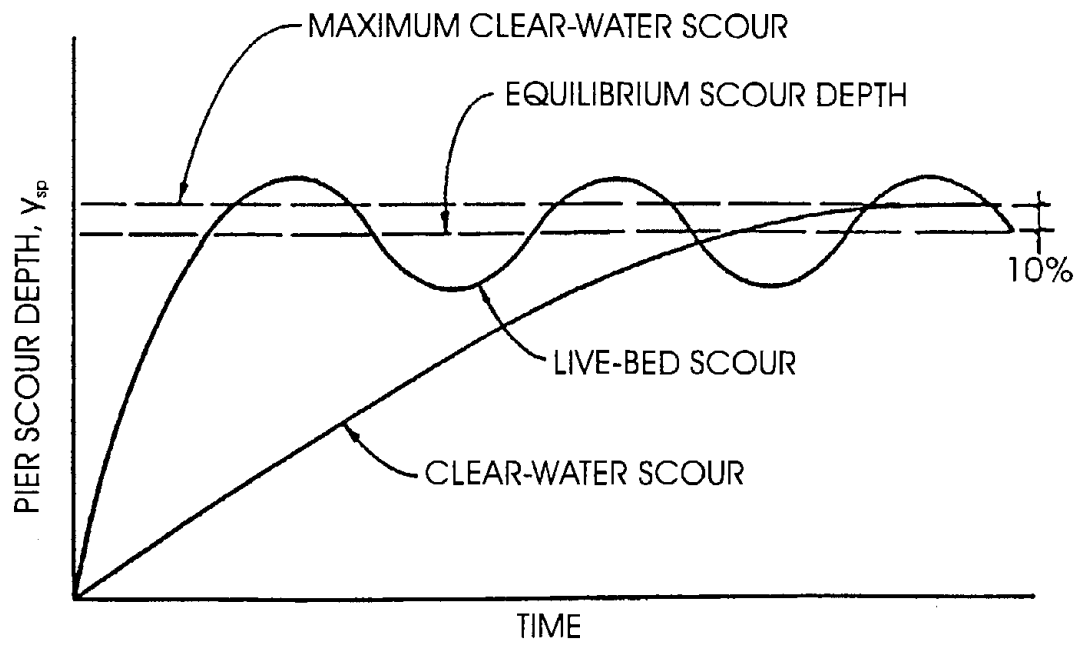


Figure 9. Illustrative pier scour depth in a sand-bed stream as a function of time (not to scale).

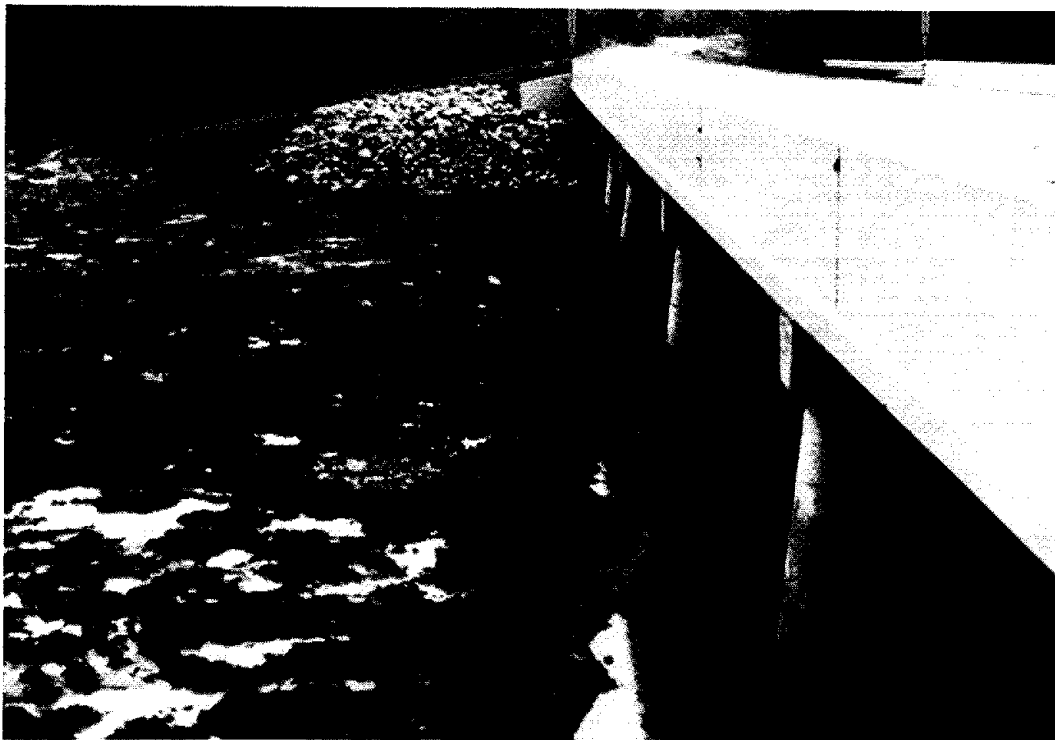


Figure 10. Clear-water contraction scour in a vegetated overbank area.

For the flow conditions at which scour measurements were made for this investigation, the equation is probably a reasonable indicator of bed-load transport condition. Neill's (1968) equation for the critical velocity of incipient motion is:

$$V_c = 1.41[(S_s - 1)g D_g]^{1/2} \left(\frac{y}{D_g} \right)^{1/6} \quad (1)$$

where V_c is the critical velocity for incipient motion of the bed material;
 S_s is the specific gravity of bed material;
 y is the depth of flow;
 D_g is the grain size of bed material; and
 g is the acceleration of gravity.

This equation can be derived assuming the ratio of the critical velocity to shear velocity is given by:

$$\frac{V_c}{u_*} = 6.45 \left(\frac{y}{D_{50}} \right)^{1/6} \quad (2)$$

where u_* is the shear velocity.

In *HEC-18: Evaluating Scour at Bridges* (Richardson et al., 1993), Neill's equation is slightly modified and presented as:

$$V_c = 1.58[(S_s - 1)g D_{50}]^{1/2} \left(\frac{y}{D_{50}} \right)^{1/6} \quad (3)$$

where V_c is the critical velocity for incipient motion of the median (D_{50}) grain size of bed material; and
 D_{50} is the median grain size of bed material.

The sediment transport condition was usually assessed by field personnel during scour measurement in this investigation. Where a field determination was not made, equation 3 was used to determine whether the measured scour occurred in clear-water or live-bed conditions.

Knowledge of these scour processes at bridges was used in designing several aspects of the approach for this investigation; including planning scour measurements, and selecting appropriate instrumentation and data collection methods.

PLANNING REGIONAL SCOUR MEASUREMENTS

Successful regional scour measurement investigations require planning to select scour measurement sites; acquire measurement instrumentation; train personnel; and coordinate with local, State, and Federal agencies. Preparation of a scour measurement plan requires site reconnaissance, site selection, and site establishment. The goal of this plan is to maximize the potential to measure scour data sets that are regionally representative and that cover a broad range of conditions for each of the measured parameters. The scour measurement plan should include more sites than must be measured to meet the project objectives, because factors required for successful measurements will only occur at some of the sites. Note that valuable measurements can also be obtained at sites that have not been reconnoitered or established; however, it is very useful to have advanced knowledge of bridge and hydraulic conditions.

Reconnaissance and Site Selection

Previous records of channel geometry and scour problems at bridges should be reviewed to identify potential scour measurement sites. These records are found in files of local, State, and Federal agencies. Valuable channel geometry and channel stability information may be found in discharge measurement notes and reports of sediment transport studies. Information on potential scour problems at bridges may be obtained from the bridge owner in records of bridge plans, geotechnical data, bridge inspections, hydraulic analyses, and periodic maintenance. These records are reviewed to select a set of sites where field reconnaissance will be made. Experience has shown field reconnaissance to be valuable because some important site information is usually not available in site files. Site selection criteria evaluated in the office and field reconnaissance are listed in table 1. Sites that meet all of these criteria are very rare. Site selections are based not on all of the criteria being met, but on the basis of maximizing the opportunity to measure useful and transferable data. Site selection within a region should also maximize the distribution of scour-related parameters, including geographic distribution, bridge foundation type and size, stream hydraulics, bed material characteristics, and watershed features.

Measurement Preparation

Scour measurements during floods are more likely to be obtained if preparations are made at selected sites and if there is a scour measurement plan that includes flood monitoring and personnel training. The information gathered in the reconnaissance should be summarized and extended. The scour measurement plan should include a listing of flood stages above which scour measurements will be attempted and a procedure to monitor sites for measurable events. Road access and boat access during flood events should be evaluated and described. Flood conditions may be monitored using local weather reports, data from stream gauges with telemetry, and local observers. Equipment and personnel should be ready to make flood scour measurements at any time. Site preparations typically include surveying or sounding channel geometry at the bridge entrance and exit and at approach and tailwater sections. Bed material samples will be required if a scour measurement is made at a site. If bed material characteristics are assumed to be temporally constant, bed material measurements may be postponed until after

Table 1. Checklist for scour measurement site selection.

Site Selection Criteria	
	The site must be accessible during floods.
	Bridge-related channel scour should occur during annual (or more frequent) floods; less frequently for armored streams.
	Flood duration should be long enough for field crews to receive notification from flood monitoring, and to travel to the site to obtain a measurement during a flood event.
	The bridge must be wide enough to provide safe workspace for a two-person crew and measuring equipment.
	The location of the bridge piers relative to the edge of the bridge deck must permit measurement of local scour hole geometry.
	The bridge should provide significant contraction of high flows (for contraction scour studies).
	Bridge and pier geometries should be simple and typical, except where complex geometries are being specifically investigated.
	Piers should be aligned to the flood flows.
	Sites with scour countermeasures, such as riprap, are not desirable.
	The quantity of woody debris at the site should be minimal; sites with a history of collecting debris are not desirable (unless the study specifically targets this type of measurement).
	Boat access during floods is desirable at larger stream sites and is essential for detailed measurement sites.
	Truss bridges are undesirable for limited-detail measurements made from the bridge deck.
	Sites with soil profile data from streambed borings are desirable.
	The channel should be relatively uniform through the study reach to avoid dynamic channel conditions unrelated to the bridge structure.

a scour measurement is obtained. This is cost-effective because scour measurements may not be made at all sites on the scour measurement plan. If temporally constant bed material size and distribution cannot be assumed, then bed material samples are needed before and after each scour measurement.

Training of scour measurement personnel is required to familiarize them with the scour measurement plan, instruments, and methods. Instrumentation and methods training may be

done on a suitable stream during normal flow conditions. A great commitment by project personnel and managers to carry out the scour measurement plan is essential to the success of this approach. The success or failure of the scour process studies depends as much upon this commitment of personnel as upon the quality of the instrumentation and techniques required to make scour measurements.

Page Intentionally Left Blank

INSTRUMENTATION AND TECHNIQUES TO MEASURE SCOUR

Recent advances in instrumentation to measure bridge scour are a major reason for the increased success in obtaining these data sets over the last few years. New instrumentation and methods for bridge scour measurement have improved the quantity and quality of data being collected, particularly when the measurement scope is detailed. The instrumentation and techniques appropriate to a scour measurement are determined by the scope or detail required in the measured data set. Bridge scour data sets can be categorized into one of three classes according to the detail of the measurement objectives: inspection measurements, limited-detail measurements, and detailed measurements. Inspection measurements are made for the purpose of determining bridge safety during either a routine inspection or during flood conditions. Inspection measurements require only a few soundings around the bridge foundations. Limited-detail measurements are made for the purposes of documenting the maximum observed scour, evaluating published scour equations, and exploring relations between scour and explanatory variables. Detailed data are collected primarily for the purpose of developing a better understanding of the processes causing scour and can be used to evaluate and develop improved predictive models of these processes.

Data requirements of limited-detail and detailed data sets are different; although the types of data are the same. Unless otherwise noted, the data should be measured during the flood for the conditions causing, or concurrent with, the measured scour. A limited-detail data set should contain the following data:

- water discharge;
- water-surface elevation at the bridge;
- cross-section data along the upstream and downstream sides of the bridge;
- cross sections approximately one bridge width upstream and downstream of the bridge (it is desirable to measure this during the flood, but low-water approach and exit sections are usually acceptable);
- approach flow velocity for each pier location;
- bed material samples (it is desirable to collect these during the flood, but low-water samples are usually acceptable);
- visual analysis and notes on debris accumulations, surface velocity directions, channel and overbank roughness, vegetation cover, and whether bed-load transport is occurring;
- photographs of the channel and bridge for both flood and low-flow conditions;
- water temperature;
- bridge and pier geometry measured in the field or from bridge plans; and
- soil-boring logs for the bridge crossing (from geotechnical analyses).

A detailed data set should contain the following data:

- water discharge hydrograph;
- water-surface elevation hydrograph;

- water-surface slope at one or more times during the flood;
- detailed channel geometry data at and near the bridge during the rising limb, peak, and recession of the flood;
- channel geometry data from upstream of to downstream of the hydraulic influence of the bridge during the rising limb, peak, and recession of the flood;
- approach flow velocities over the study reach, with additional measurements near bridge piers, collected during the rising limb, peak, and recession of the flood;
- bed material samples collected one or more times (if possible) during the flood (pre- and post-flood samples are also desirable);
- suspended-load and bed-load measurements (if possible) collected during the rising limb, peak, and recession of the flood;
- visual analysis and notes on the surface velocity direction, channel and overbank roughness, and vegetation cover;
- approximate measurements of the extent and composition of debris present;
- photographs of channel and bridge for both flood and low-flow conditions;
- water temperature;
- bridge and pier geometry measured in the field or from bridge plans; and
- soil-boring logs for the bridge crossing (from geotechnical analyses).

A portable scour data collection system has four components: (1) instruments to measure stream flow and channel geometry data, (2) instruments to deploy equipment in the water, (3) an instrument to measure the horizontal position of the data collected, and (4) a data storage device. The spatial extent and resolution for a detailed data set are much greater than for a limited-detail data set. Consequently, the instrumentation and techniques required to collect detailed data sets are more extensive and complex than those required to collect limited-data sets.

Instrumentation and techniques are discussed for the channel geometry, water velocity, bed material, sediment transport, instrument deployment, and horizontal position components of a bridge scour measurement. These instruments and techniques were used extensively by the USGS to collect the bridge scour data presented in this report.

Streambed Elevation

Channel geometry is the most fundamental part of a bridge scour data set and requires concurrent measurements of streambed elevation and horizontal position. The elevation of the streambed is determined by measuring the distance from a known datum to the streambed. The most common devices for measuring the streambed elevation during floods are a sounding weight and an echo sounder.

Most of the USGS bridge scour studies initially used a Columbus-type lead sounding weight (figure 11) to measure the elevation of the cross section along the upstream and downstream edges of a bridge. For scour data collection, a 45- to 136-kg (100- to 300-lb) weight is often required, depending on the depth and velocity of the flow. Lead sounding weights are widely used with hydrologic equipment cranes and current meters for standard discharge measurements in the USGS, thus requiring little acquisition and training. Sounding weights can

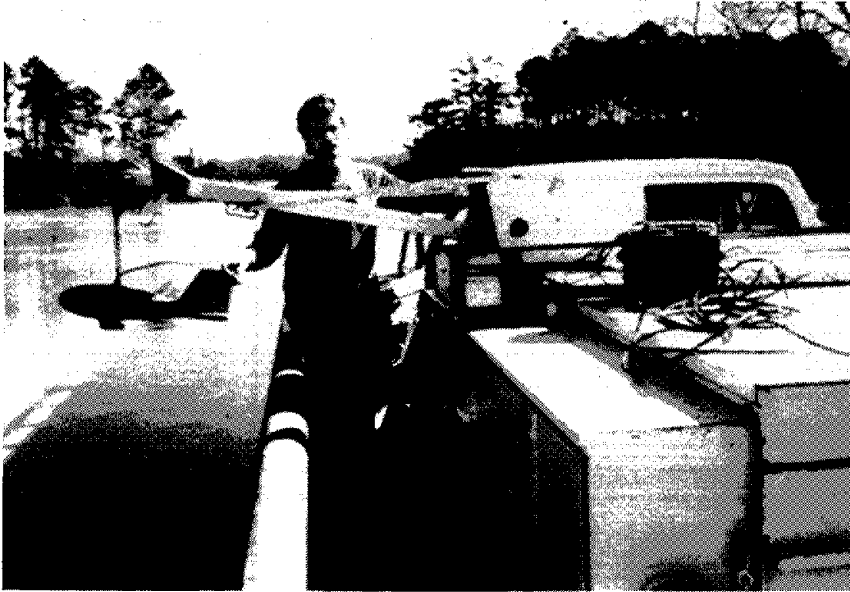


Figure 11. Columbus-type weight with fathometer transducer suspended by hydrologic equipment crane.

be used to collect data where extreme turbulence and air entrainment prevent the use of echo sounders. For example, the May 1990 flooding on the Red River at I-30 resulted in flow through a relief opening where USGS personnel measured velocity at 4.5 m/s (14.8 ft/s). Attempts to use an echo sounder failed due to excessive turbulence and entrained air. The 2.4- to 2.7-m (8- to 9-ft) depth was sounded by allowing a 90.7-kg (200-lb) weight to free fall to the bottom before being pulled downstream.

However, in more typical conditions, the sounding weight method has several limitations. The weight may be swept downstream on its descent to the bottom in deep channels with high velocities. Vertical angle corrections may be applied in this case, but the streambed elevation at the location of the weight may be significantly different from the streambed elevation directly below the point of suspension where the measurement is desired. In deep streams with velocities greater than 3 m/s (10 ft/s), it may not be possible to sound the depth with a weight at all. Debris near the bottom, especially around piers, can snag suspension lines and cause loss of the sounding weight, breakage of the suspension cable, and a safety hazard to the field crew (Trent and Landers, 1991). This method is also slower than using an echo sounder because the weight must be lowered through the water column at each sounding. Complete documentation of smaller channel geometry features such as scour holes is difficult because soundings are only made at discrete points.

Echo sounders measure the distance from a transducer to the streambed by emitting an acoustic pulse and measuring the time required for the pulse to reflect off the streambed and return to the transducer. The streambed elevation is usually determined by subtracting the depth below the transducer and the transducer draft from the water-surface elevation. Echo sounders can be grouped into three general classes: non-recording, analog recording, and digital recording. Non-recording echo sounders simply display a graph or numeric value of the depth measured and are not typically used for collecting limited-detail or detailed data. Recording echo sounders provide a continuous record of the cross section, thus eliminating any gaps in the data, except where obstructions prohibit an instrument from being lowered into the water. Analog echo sounders can record depths on a paper chart. Digital recording echo sounders process the signal and provide a single digital value through a computer port. Many recording echo sounders provide paper chart recording and digital output. The paper chart is used to verify the digital data because occasional echoes off of the side or base of the pier can be strong enough to cause the

signal processor to digitize an incorrect depth (figure 12). Analog recording echo sounders are often used to collect limited-detail channel geometry data. The detail and spatial coverage of detailed data requires the use of a digital recording echo sounder.

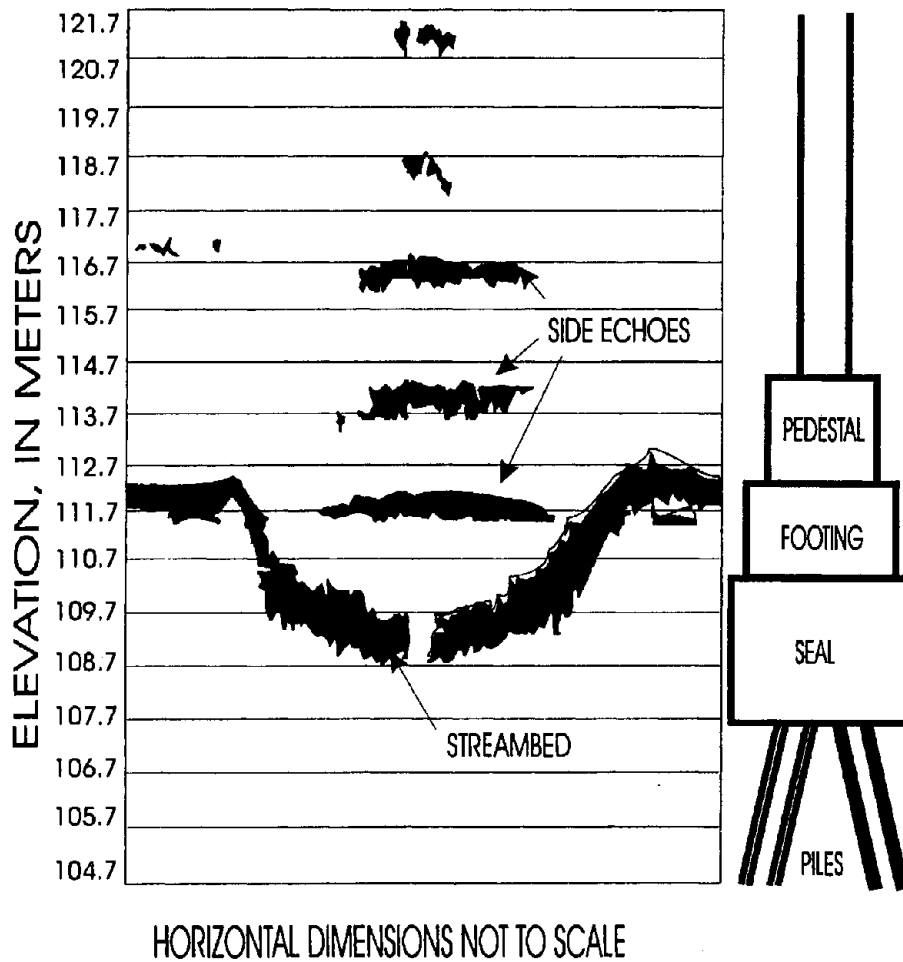


Figure 12. Example of side echoes from bridge pier.

The accuracy of an elevation measurement made with an echo sounder is dependent on the stability of the distance between the datum and the transducer, the angular stability of the platform deploying the transducer, and the accuracy of the echo sounder. Uncompensated vertical displacement of the transducer, such as by wave action, changes the distance between the transducer and the datum, thus causing errors in the measured streambed elevation.

Uncompensated angular displacement of the transducer will cause it to measure a distance to the streambed that is not vertical, resulting in an inaccurate streambed elevation. The accuracy of the echo sounder is significantly affected by the cone angle of the transducer and the scheme used to digitize the data. A wide cone angle results in a large acoustic footprint and less accurate measurements of steep channel bottom slopes (figure 13).

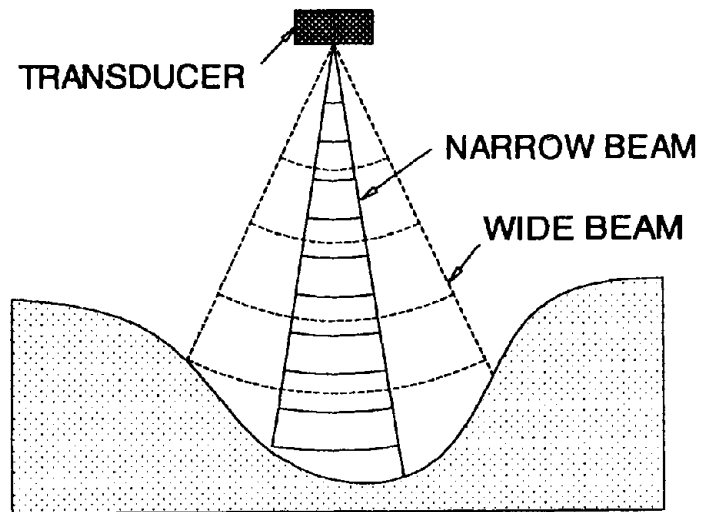


Figure 13. Effect of transducer cone angle on the acoustic footprint of an echo sounder.

Transducers with cone angles between 3 and 8 degrees are typically used for limited-detail and detailed data collection. Digital recording echo sounders typically employ one of two methods to digitize the analog signal. The most common method is threshold detection, which measures the distance based on the time from acoustic release until the reflected signal exceeds a predetermined acoustic energy threshold. Peak value detection analyzes the entire reflected pulse and computes the distance associated with the peak energy of the return signal. The peak detection method is less sensitive to acoustic reflectors in the water column (sediment, fish, debris, etc.) and tends to measure the approximate center of the acoustic footprint rather than the edge of the footprint, effectively reducing the acoustic footprint. With proper deployment, an accuracy of 0.06 to 0.3 m (0.2 to 1 ft) can be obtained under most conditions with either type of recording echo sounder; however, less satisfactory results were obtained in shallow [1.8 to 2.4 m (6 to 8 ft)], swift [1.8 to 4.6 m/s (6 to 15 ft/s)] water (G.K. Butch, USGS, written communication, 1992). Streambed elevations are combined with concurrent measurements of horizontal position to obtain channel geometry.

Water Velocity

Water velocity is an important bridge scour parameter that is used to quantify the available scouring energy of the stream flow. Use of traditional stream gauging techniques is adequate for limited-detail measurements of water velocity. Traditional methods are marginally acceptable for collecting velocity profiles for detailed data sets. The development of new technology now allows three-dimensional water velocity profiles to be collected and is the preferred method of data collection for detailed data sets.

Measurement of a vertically averaged water velocity is accomplished using standard discharge measurement methods as described in Rantz et al. (1982, pp. 79-183). The vertically averaged velocity is taken from the average of velocity measurements at 0.2 and 0.8 times the depth, referenced to the water surface. Where measurements at 0.2 and 0.8 times the depth cannot be made or when the stage is changing rapidly, an acceptable estimate of the vertically averaged velocity may be measured at 0.6 times the depth, referenced to the water surface. In

situations that do not permit the deployment of a current meter into the water, the vertically averaged velocity may be estimated as 0.85 to 0.86 times the surface velocity. A standard discharge measurement is part of a limited-detail data set and usually contains between 25 and 30 vertically averaged velocities.

Velocity measurements must be taken in the proper locations to estimate the approach velocity for local scour at piers. Ideally, the velocity just upstream of the pier and outside the zone of accelerated flow should be measured (location A in figure 14A). However, a velocity meter often cannot be suspended at this location from the bridge deck. If the flow is aligned with the pier, the approach velocity can be approximated by averaging measurements made on each side of the pier, outside of the zones of accelerated flow (locations B and C in figure 14A). If the flow is skewed to the alignment of the pier, the velocity measured on the back side of the pier may be low and nonrepresentative of the approach velocity (location C in figure 14B). In this situation, the person making the measurement must decide which measured velocity best represents the approach velocity. Water velocity measurements made with a horizontal or vertical axis meter contain only velocity magnitude. The horizontal direction of the velocity is typically estimated from the direction of the surface currents. The inclusion of a flux gate compass in the weight deployed with the meters would allow the horizontal direction of the velocity to be measured.

Detailed data sets would ideally include detailed velocity profiles. Multiple measurements at different depths are required to obtain a vertical velocity profile using standard current meters. The recently developed Broadband Acoustic Doppler Current Profiler (BB-ADCP) measures detailed three-dimensional velocity profiles from a moving boat.

The BB-ADCP measures velocity magnitude and direction using the Doppler shift associated with the reflection of acoustic waves off moving objects. The BB-ADCP has four transducers offset by 90 degrees in the horizontal plane. The instrument sends an encoded pair of acoustic pulses through the water column and records the acoustic signals reflected from particulate matter in the water column. The reflected signal is then discretized by time difference into individual segments representing specific depth cells within the water column. Further

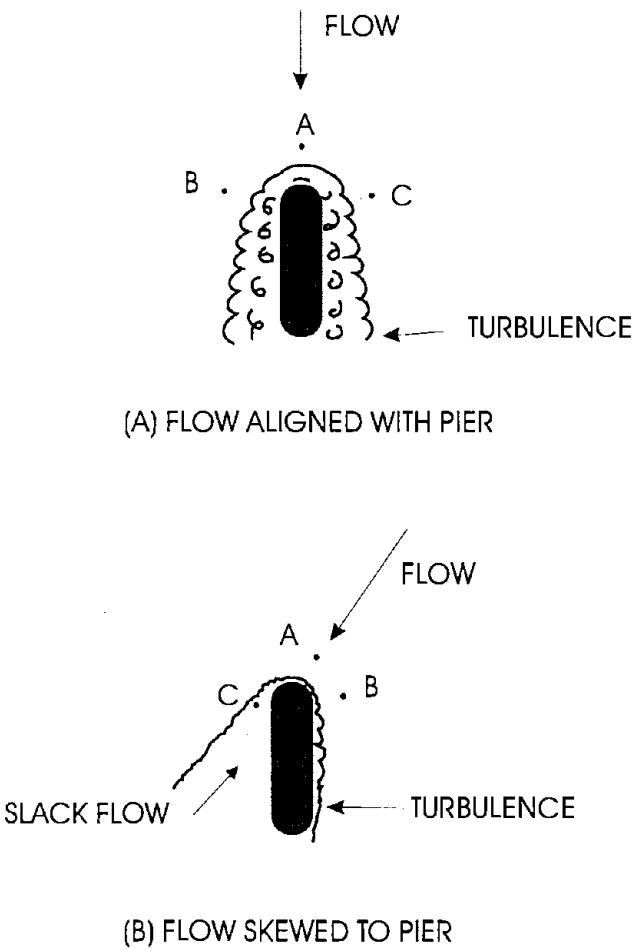


Figure 14. Approach velocity measurement locations for local pier scour.

acoustic signal analysis provides the velocity of the acoustic reflectors along each of the beams for each depth cell. The geometric arrangement of the four transducers allows the horizontal and vertical components of the velocity to be resolved for each depth cell, producing a current profile for the water column. Only three beams are needed to resolve the three-dimensional velocity; the fourth beam provides a quality check of the measurement (RD Instruments, 1993). When deploying the BB-ADCP from a moving boat, the measured water velocity (relative to the instrument on the boat) must be corrected for the speed and direction of the boat. Under most conditions, the BB-ADCP does this by tracking the streambed speed and direction relative to the instrument. If the bed material has not become mobilized at the streambed, the velocity of the boat can be measured accurately based on this principle. However, if the stream is actively transporting bed material along the streambed, this technique may not adequately measure the speed and direction of the boat. During the 1993 flood on the Mississippi River, a 1200-kHz instrument failed to provide adequate bottom tracking under conditions of water depths greater than 18 m (60 ft), high suspended sediment load, and bed load characterized by 1.8-m (6-ft) dunes. A 300-kHz instrument was able to penetrate the mobile bed layer and provide adequate bottom tracking and water velocity profiles.

The BB-ADCP allows very detailed velocity data to be collected in the approach and exit sections and in the vicinity of the bridge. However, extreme care must be taken when using the BB-ADCP to collect velocity information in the vortices at the bridge piers. The BB-ADCP assumes the water velocity is uniform along a horizontal plane passing through the four beams. The size of the vortices are often smaller than the area bounded by the four beams, so that flow measured by one beam may not be uniform with flow measured by the other beams. Although the BB-ADCP can measure three-dimensional velocity profiles under most conditions, it may not accurately measure the velocity profile in the vortices around bridge piers.

Bed Material

Bed material characteristics are important determinants of streambed erodibility and bed material transport conditions. Both limited-detail and detailed data sets must contain an analysis of bed material samples. Bed material samples collected during the conditions causing the scour are preferable; but this is often impractical. If bed material samples are collected at another time, the temporal variation of bed material size and distribution should be evaluated. Techniques for bed material sampling in sand-bed streams are described in Edwards and Glysson (1988), and Ashmore et al. (1988). Techniques for bed material sampling in coarse gravel, cobble, and boulder bed streams are described in Yuzyk (1986) and International Organization for Standardization (1992). These references should be consulted to select a suitable method and sampler, which will depend on the bed material size, cohesion, and armoring, and on the flow depth and velocity. The objective for any of the collection techniques is to ensure that a representative sample is collected. The BMH-53 or BMH-80 handsamplers may be used to collect the samples in sand-bed streams that can be waded. A BM-54 may be used to collect

samples in sand-bed streams that are too deep to be waded. Additional weight may be added to the BM-54 for sampling in high velocities; however, there may be flood conditions in which bed material samples cannot be collected. Procedures are not well defined for sampling cohesive bed materials; but a BMH-53 may be used on streams that can be waded. A clamshell, drag sampler, or other sampler described in Yuzyk (1986) may be used to collect samples from streams with bed material that is coarser than can be sampled with the BM-54; however, these samplers may allow fine-grained materials to wash out of the sample. The type of sampler used should always be noted with the bed material data.

The sampling location should be selected so that the samples are representative of the bed material controlling the sediment transport processes in the study reach. In sand channels with uniform bed material characteristics, this is not difficult; but in coarse bed streams with riffles and pools, bed material characteristics vary significantly and a representative sample is much more difficult to obtain. Bed material in a scour hole is often coarser than and atypical of the bed material controlling the sediment transport processes of the stream. Thus, samples collected directly from the scour hole should be avoided for determining representative bed material characteristics for the channel reach. A representative sample collected by deploying samplers from the bridge should be a composite of samples collected between the piers, but not in scour holes that may be present at the piers. Samples collected from scour holes may provide valuable information on the natural armoring that can occur there.

On coarse, armored bed material streams, an armor-layered sample should be taken along a transection using a grid-sampling technique (International Organization for Standardization, 1992). A subsurface bulk sample should also be obtained after removal of the armor layer at a location near the grid transection. According to Yuzyk (1986) and the International Organization for Standardization (1992), a representative sample for these types of streambeds may be collected at the upstream end of a major bar or at the head of a riffle. Detailed data sets may provide a description of the spatial distribution of fine and coarse sediments by collecting numerous sediment samples with the location of each sample identified.

Research on the erodibility of cohesive bed materials have used the following parameters to describe the erodibility of cohesive material: shear strength (Sundborg, 1956), plasticity index (Smerdon and Beasley, 1961), saturated unconfined compressive strength (Flaxman, 1963), and vane shear strength (Abdel-Rahmann, 1964). However:

“It is clear from this work that the properties of the sediment that determine its resistance to erosion are not completely defined. Shear strength and plasticity index, and perhaps clay content, have an important bearing on the phenomenon, but they apparently do not describe it completely.” (Vanoni, 1975, p. 114)

Therefore, there is not a recommended procedure or universally accepted parameters that can be used to characterize the erodibility of cohesive sediments.

Sediment Transport

Bed material load is an important parameter for the analysis of scour processes to quantify the amount of material transported into the scour area from upstream. The total load or sediment transported by the stream can be subdivided by mode of transport (suspended load and bed load), by origin (wash load and bed material load), or by method of measurement (measured load and unmeasured load). Measurements of bed material load, or bed load, are difficult to obtain and are often of very limited accuracy. An alternative to direct measurement is to derive the bed material load based on the measured suspended sediment load and the sediment grain size distribution. Techniques and samplers for the measurement of bed load are described by Edwards and Glysson (1988). Techniques for computing sediment transport are described by Porterfield (1972).

Instrument Deployment

Instrument deployment systems requirements depend on the spatial extent of the channel reach to be measured and the detail required for the measurement. Deploying instruments from the bridge deck is adequate for typical limited-detail measurements for which the spatial coverage of the data set is between the upstream and downstream sides of the bridge. Detailed data sets require measurements over the reach from upstream to downstream of the hydraulic influence of the bridge. This coverage usually requires instruments to be deployed from boats.

Limited-detail deployment systems include manual and electric-powered hydrologic equipment cranes mounted on a truck or a four-wheel base, and hand-held systems. The truck-mounted cranes are typically easier to use and are required for weights in excess of about 68 kg (150 lb). The electric-powered crane mounted on a truck or a four-wheel base has been the most common system used by the USGS. A typical truck-mounted hydrologic equipment crane being used to deploy an echo sounder on a Columbus-type weight is shown in figure 11. A two-wheel base and boom configured for a limited-detail scour measurement is shown in figure 15. These systems can be used to deploy lead weights for direct soundings, echo sounders, velocity meters, or sediment samples. To measure the geometry of a cross section by sounding with a Columbus weight, the horizontal position, depths, and the water-surface elevation are recorded along the upstream and downstream sides of the bridge. To measure limited-detail channel geometry with an echo sounder, a transducer is mounted on the bottom of the weight (figure 15) and lowered into the water so that the transducer is submerged about 0.6 m (2 ft). The echo sounder is slowly moved across the bridge and the chart is annotated for the stationing, location of the piers, and other important features. The depth of the transducer below the water surface must be checked often to provide an accurate record of the streambed elevation. Where the piers are inset from the edge of the bridge, the sounding weight may be lowered further to increase the drag and allow the flow of water to carry the sounding weight closer to the pier (Trent and Landers, 1991).

Floats have been used to maneuver the transducer beneath the bridge and along the sides of the piers. Various types of floats have been tried, including a spherical warning marker for electric power lines, rubber balls, a raft made from polyvinyl carbonate (PVC) pipe, and water skis. Spherical floats did not work well due to substantial drag on the sphere when partly submerged and the resulting instability that caused the transducer to be raised and tilted out of the vertical position. A raft

made of PVC pipe worked reasonably well (G.H. Carlson, USGS, written communication, 1991). Both the Texas and Arkansas DOT's had success using a water ski to deploy a transducer. The primary problems associated with the water skis are air entrainment and instability during high flows (Garland Land, Arkansas DOT, oral communication, 1992).

A recreational "knee-board" (similar to a small surfboard) worked well to deploy an echo sounder transducer for inspection and limited-detail data collection during the 1993 flood in the Midwest (figure 16). The design of the knee-board resulted in only a small amount of drag and allowed the system to be deployed by hand without the use of manual or electric-operated booms and reels (figure 17). The board was stable except under the most turbulent conditions and easily deployed the transducer along the edges of the bridge and along the sides of the piers underneath the bridge. Air entrainment was only a problem in very turbulent water. The size and weight of the system make it much more portable and easy to use than sounding weight deployment systems.

The collection of detailed-data sets requires the use of a boat. Experience using manned boats for bridge scour data collection on the Red River in 1990 and on the Mississippi River in 1993 revealed many important considerations for collecting data from a manned boat during floods. Flood conditions and clearance underneath the bridge must be adequate for the safety of the crew. These criteria severely limit data collection on small rivers where clearance under bridges is often small during floods. Reliability, handling, and adequate launch facilities are also important for the use of a manned boat during floods. During extreme conditions, boat ramps are flooded and velocities can be high near the shore. Flooded local streets with sufficient slope or

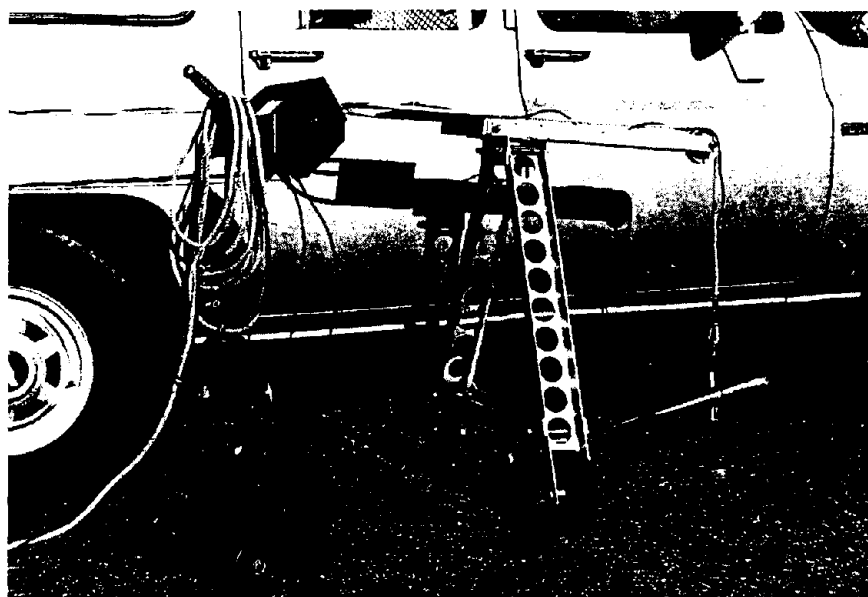


Figure 15. Fathometer mounted on a two-wheel handcart with two-wheel base and boom, sounding weight, and transducer.

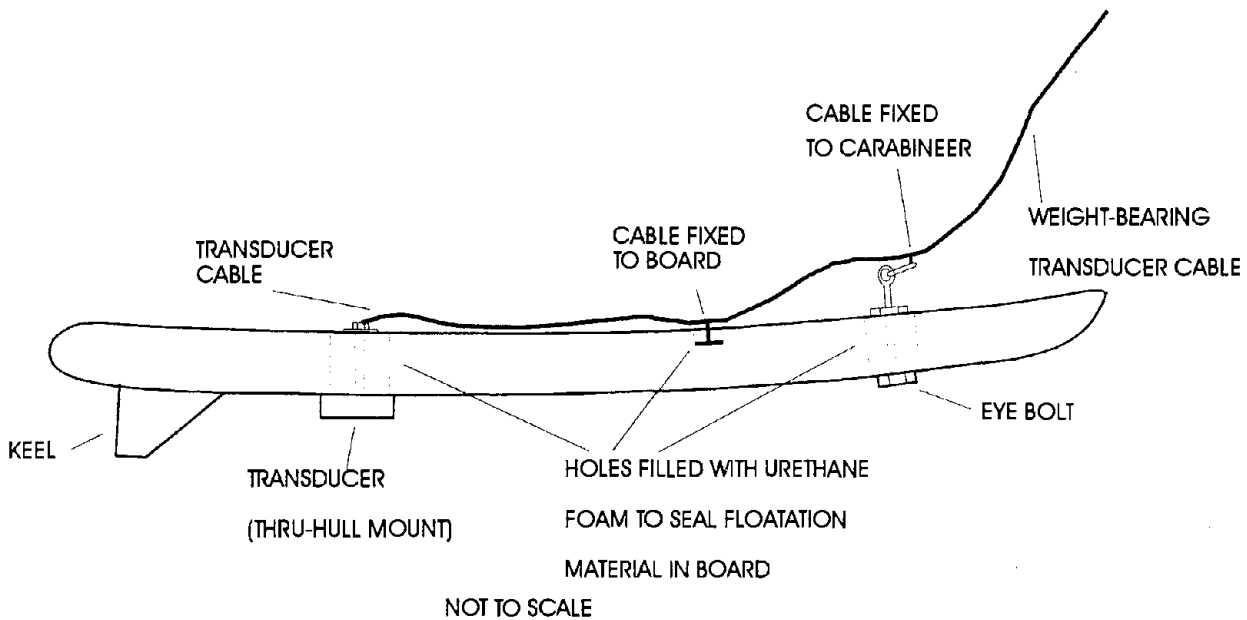


Figure 16. Design of knee-board for deploying a transducer to measure channel bathymetry near a bridge.

the river side of levees are often the only options for deploying a survey vessel. Local citizens and government agencies can usually help locate adequate launching facilities. Excellent vessel reliability and handling characteristics and a skilled pilot are required for safety and to maneuver the vessel around the bridge piers (Mueller and Landers, 1994).

A remote-controlled boat is currently under development to deploy instruments to collect bathymetric and three-dimensional velocity data. The remote-controlled boat will reduce the bridge clearance requirements, eliminate personnel safety hazards associated with a manned boat, and launch much more easily. Skinner (1985) reviewed remote-control platforms, but was unable to find a recommendable system. However, recreational remote-control boat technology has advanced rapidly and is readily adaptable for scientific applications. Key design criteria are viability, stability, and operability in a flood environment (Landers et al., 1993). It is anticipated that the remote-controlled boat measurement system will significantly enhance the collection of detailed scour data.

Horizontal Position

Bridge scour data sets require horizontal position measurements concurrent with streambed-elevation and velocity measurements. A horizontal positioning system consists of the instrumentation and techniques used to measure the position at which data are collected. The instrumentation and techniques used are dependent on the accuracy required and whether the data are collected only at the bridge or in the reaches upstream and downstream of the bridge.



Figure 17. Knee-board deployed downstream from the bridge deck.

The distance across the stream is usually measured from stationing marked on the bridge or from a measuring tape or tag line stretched along the bridge handrail for limited-detail measurements at the upstream and downstream edges of the bridge. Marked stationing is easiest to use during scour measurements. The transverse stationing should be repeatable during subsequent measurements. Stations on the left edge, centerline, and right edge of piers must also be recorded. When trying to collect data directly below the edge of the bridge, the echo sounder transducer or sounding weight may be pulled downstream by the flow and the measured location may be downstream of the planned location. The distance upstream or downstream from the edge of the bridge should be visually estimated and recorded.

Detailed measurements of channel bathymetry and velocities from a moving boat require real-time measurement and recording of horizontal positions. In general, horizontal positions are measured using range-range instruments, range-azimuth instruments, or a Global Positioning System (GPS). Hydrographic surveyors have used positioning systems for many years, but the accuracy attainable by most of the systems is less stringent than that required for the purpose of analyzing and modeling river processes. Technology related to horizontal position determination has improved dramatically in recent years. Previous technology could not typically provide real-time position measurements with an accuracy of less than 1 m and often required time-consuming pre-surveying of setup locations. Current technology can provide better than 1-m accuracy with no pre-surveying requirements and fast setup time.

Range-range systems use the measured distance from the survey vessel to three or more transponders to triangulate the vessel position in real time. The systems measure the average time it takes for a known frequency signal to travel between the transmitters and the receiver, and solve for the survey vessel position. Microwave-based systems are typical, but radio wave, laser, and underwater-acoustic systems are also available. Typical accuracy for these systems is 1 to 3 m. The setup time required to locate transponders at pre-surveyed positions and the weight of range-range systems are significantly greater than for range-azimuth and GPS systems.

Range-azimuth tracking systems are similar to total stations used for land surveying (figure 18). The width of the distance-measuring laser beam is enlarged from that of the standard survey beam so that it can obtain a reading even when the laser is not centered on the target reflector. For some systems, this beam is 4 mrad for the vertical by 7 mrad for the horizontal, so that at a 1000-m range, the beam would reflect from the target within an area of 4 m by 7 m. If the instrument is not centered on the target, the horizontal and vertical angles will not be correct and some error (up to 3.5 m for the example) will result. These systems usually have a powerful, yet eye-safe laser capable of reflecting from objects up to 300 m away and from prisms up to 10,000 m away. They have the capability to update readings every 0.5 s, to filter out spurious readings, and to automatically resume tracking after the target is lost for a period of time. Some systems have accuracies of less than 0.1 m; however, in practice, it is very difficult to keep the instrument centered on a moving target. During data collection on the Mississippi River, an accuracy of approximately 0.7 m was achieved with a range-azimuth system tracking a prism mounted on the moving survey vessel.



Figure 18. Range-azimuth positioning systems.

The power of the laser allows setup points to be referenced to the bridge quickly and often without the need of a prism. Setups can often be referenced to the centerlines of several piers by pointing the instrument at the centerline of each pier and reflecting the laser directly off the concrete pier. This provides fast setups so that more time may be spent collecting data rather than setting up instruments and surveying control points.

The Global Positioning System (GPS) is a \$10 billion satellite positioning and navigation network developed by the U.S. Department of Defense. GPS is providing accurate navigation and position fixing for a broad range of applications. Development of GPS began in 1973 and the system became fully operational in 1993 with 21 satellites and 3 operational spare satellites. The accuracy and applicability of GPS in hydrographic surveying during floods had been difficult to assess because of its rapid development. According to manufacturers and literature, differential GPS (DGPS) in kinematic mode can provide centimeter accuracy. The principal disadvantage of GPS for this application is that four or more satellites must be kept locked in view during the entire survey. This is an unrealistic constraint when operating very close to and under bridges during scour measurement.

Real-time kinematic DGPS was used for horizontal positioning during scour measurement on the Mississippi River in 1993. DGPS allowed rapid collection of velocity and bathymetric data in the approach and exit reaches of the river. Because DGPS requires no setups (if a base station is already established) on shore and no personnel to track the boat, data were collected rapidly and over a much longer reach of river than would have been feasible with the range-azimuth tracking system. However, data collection near trees and bridges was hampered by loss of adequate satellite coverage. The optimum positioning system for collecting detailed data may be a combination of DGPS and range-azimuth tracking systems. DGPS provides accurate positions in areas where adequate satellite coverage can be maintained. The range-azimuth system provides accurate positions under the bridge, around the piers, and on small streams where DGPS may not be usable due to lack of satellite visibility.

Data Storage

Efficient and reliable data storage is a key component to any data collection system. Limited-detail data are typically recorded in field notebooks and written directly on the echo sounder chart when an analog recording echo sounder is used. Bridge scour data are often collected during wet and less than ideal conditions; therefore, waterproof notebooks and/or pens are highly recommended to prevent loss of any data. A field computer could be used to record limited-detail data, but it may not be the most efficient method and it has not been used extensively to date. However, a computer is required for the large amounts of digital data that must be collected and stored in a detailed data set. A rugged field computer with at least two serial data ports is required to collect streambed elevation or velocity data and horizontal position data simultaneously. In addition to the digital data collected by the field computer, a field notebook is used to describe the various data collection activities, to record water-surface elevations, to record reference point survey notes, and for sketches of the study reach.

Page Intentionally Left Blank

REFERENCE SURFACES FOR MEASURING SCOUR DEPTH

Scour cannot be measured directly; it must be determined by interpretation of channel geometry data. The magnitude of scour for a scour data set is the vertical distance between the measured channel geometry and a surface, line, or point that represents the reference channel geometry for the baseline condition, i.e., for conditions in the absence of the bridge structure. The term "reference surface" is used here even when the three-dimensional surface is represented by a line or a point. This reference surface has also been referred to as "reference datum" in the literature.

Several methods have been used to establish reference surfaces from which bridge scour depths are measured using channel geometry data. Reference surfaces in previous bridge scour investigations have been based on mean bed elevation, concurrent ambient bed elevation, water-surface elevation, and maximum observed bed elevation. Different methods of defining reference surfaces can result in measured scour depths that vary by as much as 100 percent for a given data set. Published discussions of articles by Laursen (1962) and Neill (1965) were confused because some contributors referenced scour depth to a water-surface datum, while the original articles referenced scour depth to a channel-bed reference datum. Neill (1965) addresses this issue in response to discussions of his 1965 paper and suggests that the term "scoured depth" be used to refer to the flow depth over a scoured area. The terms "scour depth" and "depth of scour" refer to the depth of the scoured channel bed below a channel reference surface representing an unscoured condition.

Methods to determine reference surfaces were evaluated in this study to ensure the correct and consistent interpretation of bridge scour data collected in this and other ongoing studies (Landers and Mueller, 1993). Reference surfaces should be selected so that the local, contraction, general, and long-term process components of total scour may be quantified separately. The reference surface for each component of scour will be unique; however, the technique for determining each reference surface requires consideration of the overall scour process at the bridge. This discussion covers techniques for establishing reference surfaces from which local and contraction scour are measured using channel geometry data at bridges. Potential problems in applying these methods to field data are also discussed.

Reference surfaces for computed (not measured) scour depths to predict minimum channel elevations for bridge foundation design are not addressed in detail in this report. Klingeman (1973) recommends:

"The designer should carefully assess the permanence of channel alignment and bed configuration when selecting the reference streambed elevation from which to determine the scour depth and lowest scour elevation. In alluvial rivers, it is recommended that the lowest undisturbed streambed elevation at or near the bridge crossing (other than a local scour hole) be used as a reference level in setting scour elevations of principal piers in or near the main channel. This recognizes that the main part of the channel may shift within the banks over the

years and provides a conservative estimate of design scour to allow for such a possibility.”

Local Scour Reference Surfaces

Local scour processes were discussed in a previous section of this report. Local scour typically occurs around bridge piers, abutments, spurs, and embankments. *The depth of local scour is the difference between the bed level with and without the flow obstruction present for a given flow condition.* The maximum local scour from a measurement is the quantity usually reported, unless otherwise noted. Scour measurement data have often been obtained from models in laboratory flumes where bed elevations outside of the scour hole usually do not change significantly during an experiment. The reference surface is typically taken as the average of several points measured in the unscoured region around the obstruction after equilibrium bed conditions are established and after the model run is completed. This ambient or mean equilibrium (in the case of dunes) bed level has been used as the reference surface in most flume studies of local scour (Shen et al., 1969; Melville, 1984; Santoro, 1991; Posey, 1974; Tison, 1961; Chiew and Melville, 1987; and others). Other reference surfaces used in flume studies include the initial condition bed level and the water surface. Field measurements of local scour have generally used concurrent ambient bed level as a reference (Neill, 1965; Harrington and McLean, 1984; Norman, 1975; Chang, 1980). However, in field data studies by Inglis (1949), the water surface was used as the reference surface, and Jarrett and Boyle (1986) use the highest observed bed elevation at the point where local scour is being measured. Results from a comparison by Blodgett (1989) of reference surfaces for a scour measurement on Sacramento River are shown in table 2.

Table 2. Measured local scour on Sacramento River using several reference surfaces (Blodgett, 1989).

Method	Description of Reference Surface	Local Scour	
		(m)	(ft)
1	Concurrent ambient bed level	1.3	4.3
2	Concurrent thalweg at upstream side of bridge	0.9	3.0
3	Projected upstream to downstream thalweg profile	1.4	4.5
4	Projected upstream to downstream mean bed elevation	2.5	8.3
5	Highest bed elevation observed at same pier	0.5	1.7

Local scour measurements using reference surfaces other than concurrent ambient bed level may include amounts of contraction, general, or long-term scour, which would reduce the analytical value of these data. Such total scour measurements cannot be effectively analyzed in relation to separate local, contraction, and sediment supply deterministic processes. Therefore, concurrent ambient bed level is the preferred reference surface for measurement of local scour depth from scoured channel geometry.

The concept and description of this preferred surface are simple. However, a representative, concurrent ambient bed level is not always apparent, given the range of channel geometry conditions and data limitations. Two examples are presented to illustrate the method for different scoured channel geometry measurements. Figure 19 shows data from a model of pressure flow for a rectangular pier in a sand bed from a flume with a sediment box, thus clear-water conditions (J.S. Jones, personal communication, 1993). The reference surface is taken as the concurrent ambient bed level, illustrated by the heavy line.

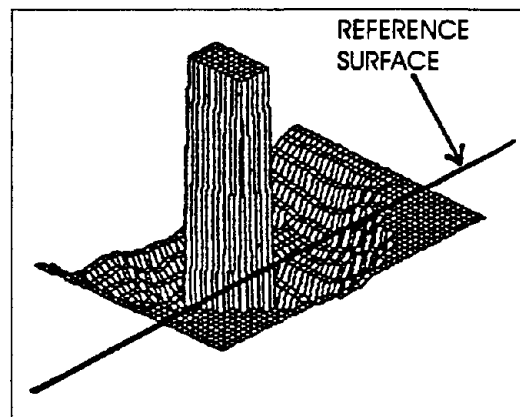
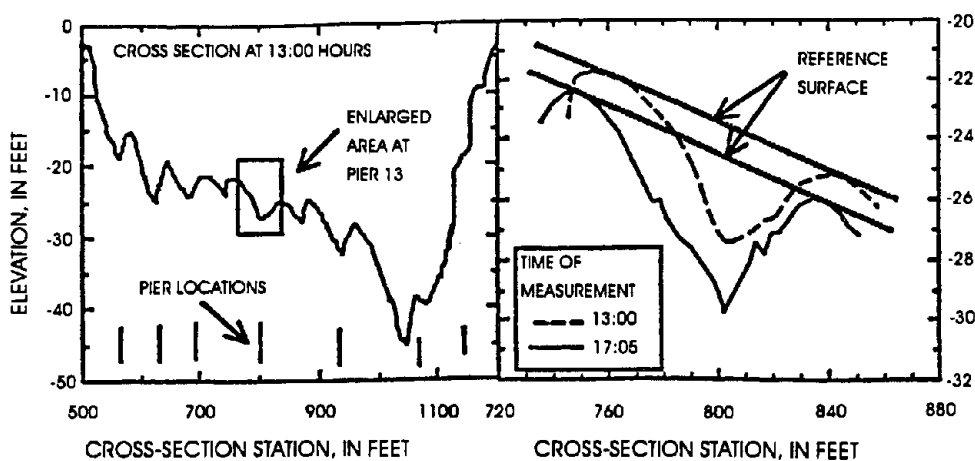


Figure 19. Reference surface for local scour.

Figure 20 shows data from a scour measurement on South Altamaha River at southbound Interstate Highway 95, near Brunswick, Georgia. The reference surface is represented by the sloping line, and the maximum vertical distance between this line and the locally scoured bed is the measured scour. Establishment of local scour reference surfaces can be difficult and require much judgment for some complex cross-sectional geometries, such as where the thalweg coincides with the local scour hole. Additional factors that must be evaluated in measuring local scour include remnant scour holes, debris, scour countermeasures, time-rate of scour, and dune-bed forms. It is often difficult to determine a representative and repeatable reference surface for local scour; however, the surface is even more difficult for the case of contraction scour.



1 ft = 0.305 m

Figure 20. Reference surface for local scour at pier 13 of the Interstate 95 crossing of South Altamaha River, near Brunswick, Georgia.

Contraction Scour Reference Surfaces

Contraction scour is caused by a decrease in the channel flow area due to natural or man-made contractions such as highway embankments. The depth of contraction scour is the difference between bed levels with and without the contraction in place for a particular flow. Contraction scour depth is usually defined as the difference between the average bed elevations of contracted and uncontracted sections. Blodgett (1989) reported one of the few field investigations in which contraction scour was quantified separately from general scour or long-term degradation. Blodgett's contraction scour reference surface was represented by a straight line (or flat surface) projected over the contracted section, connecting a thalweg profile running upstream and downstream from the hydraulic influence of the bridge. The thalweg profile was measured during moderate flow conditions. The contraction scour was reported as the difference between this reference surface and the thalweg (minimum elevation) of the contracted section. Blodgett stated that using the thalweg to measure contraction scour represented a worst-case condition. However, contraction scour may affect the entire contracted section. A thalweg-based reference surface would not be consistent with existing contraction scour equations that are based on average changes in the contracted section. The equations do not have the ability to compute the distribution of contraction scour; thus, the location and magnitude of maximum contraction scour cannot be predicted. A two-dimensional sediment transport model could predict the spatial distribution of contraction scour.

Neill (1965) measured combined contraction and/or general scour at two sites on the Beaver River for a June 1962 flood by comparing scoured channel geometry measured before, during, and after the flood. At the La Corey bridge site, the post-flood channel geometry was practically coincident with the pre-flood channel geometry, indicating that the scour observed during the flood did not include any long-term aggradation or degradation. This measurement can be classified as bridge contraction scour given the assumption that the scour was occurring only at, and due to, the bridge contraction during the flood. At the Beaver Crossing bridge, post-flood longitudinal profiles running 244 m (800 ft) upstream and downstream from the bridge indicated that the measured scour was not occurring in the approach and exit sections and was associated only with contraction of flow by the embankments.

The reference surface should characterize the mean bed elevation of an uncontracted section at the location of the contraction scour measurement. *The reference surface can be established by passing a line through the average elevation of uncontracted sections, located upstream and downstream from the contracted section.* Ideally, the contracted and uncontracted sections would be measured concurrently. The effects of local scour should be removed by excluding locally scoured areas when determining the average contracted bed elevation. Cross sections that have some sub-areas with live-bed and others with clear-water bed-load transport conditions require separate analysis of those sub-areas. The reference surface and the contraction-scoured bed elevation would be the average elevation of the portion of the uncontracted and contracted sections, respectively, where the specific bed-load transport is occurring.

There are several potential problems with this ideal reference surface for live-bed conditions:

- (1) Because of irregular cross-section geometry, it is often difficult to identify the bottom width over which active bed-load transport is occurring.
- (2) Upstream and downstream cross sections may be in natural contractions or expansions, due to channel bends or other factors, so that they do not represent an uncontracted condition at the bridge.
- (3) Large dune-bed forms can produce misleading results when dune crests or troughs predominate in one of the measured sections.
- (4) Slow, downstream migration of large sand and gravel bars can make a measurement nonrepresentative of equilibrium conditions.
- (5) Measured contraction scour may not represent equilibrium scour if the scour develops over many years due to the infrequency of channel-formative flows and the resistance of the bed to scour.
- (6) Most flood-flow scour measurements are made only from the bridge deck along the upstream and downstream sides of the bridge because boats are usually unavailable to obtain concurrent uncontracted channel geometry.

Pre- and/or post-flood measurements of uncontracted sections are often used to establish a contraction scour reference surface. These are usually obtained upstream and downstream from the hydraulic influence of the bridge contraction. This reference surface may be useful, even for live-bed contraction scour measurements, if there are sufficient data to support the assumption of stable approach and exit sections. The stability of the uncontracted sections and the accuracy of the measurement should be assessed by comparing pre- and post-flood measurements through the study reach.

Clear-water contraction scour occurs when sediment transported into the scour hole is insignificant, so that the geometry of the uncontracted section will remain the same after the flood has passed. Post-flood surveys can be used to measure clear-water contraction scour because there is no infilling, although real-time flood measurements of hydraulic characteristics are still desirable. Post-flood surveys should extend downstream beyond the influence of deposited scour-hole material.

Page Intentionally Left Blank

BRIDGE SCOUR DATA MANAGEMENT SYSTEM

A portable and interactive computer data base management system is needed to support data preparation, compilation, and analysis, and to serve as a repository for bridge scour measurement data. The Bridge Scour Data Management System (BSDMS) was developed in this investigation to support these needs. This user-friendly software requires no training and has online documentation of its operation and data management, editing, computation, and output characteristics. The BSDMS supports bridge scour data set preparation by providing a complete, formatted list and description of the data elements that should be included. The list of relevant data for a bridge scour measurement data set is extensive and a checklist is needed to evaluate the completeness of a given data set. The BSDMS prompts users for more than 200 data set attributes and interactively provides descriptions of those attributes so that the data sets are defined using consistent methods of interpretation. The BSDMS is a national repository for scour data sets from historic records and ongoing studies, and additional records are being added as they become available. As a compilation of all available bridge scour field measurements, the BSDMS will facilitate both regional scour analyses and investigation of specific scour processes. Consistent and high quality assurance standards are essential to the value of the BSDMS. The basic quality assurance criteria are that a data set includes all of the essential information needed to evaluate scour processes at a site and that the data were measured directly or indirectly using sound and consistent methods. The BSDMS will be enhanced and probably superseded at some point in the future; however, more important than the characteristics and operation of BSDMS software is its function as a long-term repository of scour data for existing and future bridge scour measurement data.

Characteristics and Capabilities

The basic functions of the BSDMS are data storage and retrieval. The principal features are portability and ease of use. The program enables users to interactively store, retrieve, select, update, and display bridge scour and associated data. User interaction features full-screen menus and form fill-ins, including prompts, help information, and default values. The program is written in Fortran 77 and is portable to microcomputers, engineering workstations, and mainframes. The data are stored in an unformatted, direct-access file with internal pointer systems for rapid access to the data and for efficient management of disk space. Data management functions enable a user to add, delete, or modify data sets. Searches can be conducted to select data sets that meet user-specified criteria of data element values or value ranges. Data sets in the data base that satisfy search criteria are added to a working buffer for further processing. Graphic capabilities include plotting the locations of selected sites on an outline map of the United States, and hydrographs and cross sections. Information from all or selected data sets can be output to files that can be read by separate programs for statistical analysis, mapping, or other purposes.

A computational option computes predicted scour depths for published equations so that observed and predicted values may be compared at selected sites. A limited number of equations are included for estimation of local pier scour, local abutment scour, and contraction scour. The

equations should only be applied to streams characteristic of the conditions for which the equations were developed, and some sites may not be represented by any of the equations.

Structure and Elements of Data Set

The structure of a data set in the BSDMS is shown in table 3. Approximately 200 attributes may be used to describe scour in a data set for a given bridge site. All of the data for a bridge site are stored in a single data set. Each data set has four categories: site data; scour measurement data; flood event data; and channel geometry data. Channel geometry data include coordinate reference information, channel cross sections, and time of measurement data. Each site data set may include several sets of channel geometry data for several flood events. Several sets of scour measurement data may be stored for each flood event. The BSDMS is designed to store the essential information from a detailed scour measurement; however, most data sets are more limited and do not contain all of the information that can be stored.

Table 3. Organization of Bridge Scour Data Management System.

Site Data	Scour Measurement Data	Flood Even Data	Channel Geometry Data
Location	Pier Scour	Peak Stage	Reference Points
Site Description	Abutment Scour	Peak Discharge	Channel Geometry
Elevation Control	Contraction Scour	Hydrographs	
Stream Attributes	General Scour	Debris Attributes	
Bridge Attributes			
Abutment Attributes			
Pier Attributes			

Operation

The operation of the BSDMS is described in the *BSDMS User's Manual* (Landers et al., in press). Interactive features of the BSDMS include option menus, data entry forms, processing instructions, and help information (Kittle et al., 1990). The BSDMS screen has at least two windows and a command line. These two windows are the data window and the instruction window. The data window is where most user interaction takes place through option menus and user-prompting data entry forms. The data window also displays explanatory program messages on tasks being performed. The instruction window displays information on the appropriate user response to interact with the program at any point. Error messages related to invalid responses are also displayed in the instruction window. A third window, the assistance window, can be displayed or hidden. The assistance window displays help information or valid ranges for data attributes that are highlighted in the data window, or the identification of the data set being used.

Help information includes the definition and default values for the selected data attribute. Command line options control movement through the program and the display of the assistance window.

Example Data Set

An example of a National Scour Study data set output from the BSDMS is shown in figure 21. This data set is for Pearl River at westbound (upstream) U.S. Highway 98, near Columbia, Mississippi. The format shown in figure 21 is the standard BSDMS output. Definitions of each attribute of the data set are provided in the interactive BSDMS help utility. U.S. Highway 98 crosses Pearl River on two, parallel bridges, and each bridge is a unique site data set in the BSDMS. This example data set indicates the detail of the information that can be stored in the BSDMS. The absence of abutment, contraction, and general scour data is, unfortunately, typical of the data sets in the National Scour Study Data Base. Every scour measurement in the data base includes the channel geometry data from which it was measured. These (lengthy) data are not included in the output shown in figure 21.

Much of the information contained in the data sets of the National Scour Study Data Base are attendant to the key variables that quantitatively describe bridge scour processes. However, this attendant information is essential to an informed analysis and interpretation of those key data. The most important quantitative variables for each scour measurement are summarized in table 4 and are described in the following section.

Bridge Scour Data Management System
Data Set Output
Units are feet, feet per second, and degrees

LOCATION SITE DATA

Site Description > Pearl River at westbound U.S. 98 nr Columbia, MS
County > Marion
State > MS

Latitude (ddmmss) > 311414
Longitude (dddmmss) > 895054
Station ID (integer) > 2489000
Route Number > 98
Service Level > 1
Route Class > 2
Route Direction > 4
Mile Point > 118.5

Site description:

This is a 785-ft-long bridge crossing the Pearl River about 1.5 miles southwest of Columbia at river mile 137.8. This entry is for the westbound lanes, which are upstream from the eastbound lanes. The bridge has three 4-ft-diameter pier bents (Nos. 4-6) within the low-water channel supporting the main span over the channel and five interior double-18 x 18-in-pile bents (Nos. 2-3 & 7-9) supporting the approach spans on the flood plain. The bridge is in a 680-ft-long vertical curve with 4.0% approach grades. A 150-ft-long spur dike is located at the right (west) abutment. The left (east) bank is covered with riprap through the bridge. The spill-through abutments are paved under the bridge but are not paved on the upstream slope.

The upstream left (east) bank has experienced lateral erosion in recent years. The bridge crossing is in a channel reach in a transition between a 125-degree bend about 1,600 ft upstream and a 145-degree bend about 1,200 ft downstream of the bridge. In an effort to control the bank erosion on the left bank, five flow deflectors were constructed in 1985-86 along the left bank from the bridge to about 1500 ft upstream.

Scour data were collected during high and low flows using a fathometer. The flow velocities approaching the bridge piers were determined from velocity soundings during discharge measurements at the upstream side of the bridge.

On October 4-9, 1991, bed samples were collected from the main channel at selected intervals along three channel cross sections. Individual samples with similar characteristics were combined for gradation analyses. The following is a brief description of the bed samples collected:

Figure 21. Example of a data set output from the Bridge Scour Data Management System.

Cross section No.	Distance upstream (ft)	Sample No.	Comments
1	100	1	Represents right part of channel beginning near station 8180.
1	100	2	Represents left part of channel ending near station 8180.
2	1,100	3	Within main flow of low-water channel, from tip of 4th jetty upstream to about 100 ft right.
2	1,100	4	Right part of channel, 175 ft from tip of 4th jetty to RWE.
2	1,100	5	Near upstream end of 4th jetty.
3	2,000	6	At upstream end of sand/gravel bar, all samples here combined.

No bed samples were obtained at the piers due to debris, etc. Based on rod probings at the piers, the material at the base of the piers is thought to be mostly gravel with some sand and debris. Also, soil borings by the MDOT indicate gravel is present. Therefore, bed sample no. 6 is thought to be most representative for the bed material at the base of pier nos. 4-6.

The International Standard ISO 9195, "Liquid flow measurement in open channels—Sampling and analysis of gravel-bed material," prepared by Technical Committee ISO/TC 113 suggests sampling at the upstream end of gravel bars. The coarse material is associated with the channel-forming processes and sediment transport. Therefore, sample no. 6 was selected as the most representative.

ELEVATION SITE DATA
Datum type > MSL
Conversion to MSL (ft) > (none)

Description of reference points and bench marks:
Wire-weight gauge attached to the upstream side of the upstream bridge. Check-bar reading at 61.00 ft (Elev. 176.81 ft (NGVD)).
Centerline elevation of downstream bridge at the left (east) abutment (Elev. 155.46 ft).
BM-6—Chiseled square on downstream streamward corner of bridge seat of left (east) abutment (Elev. 151.47 ft).

STREAM SITE DATA
Drainage area (sq mi) > 5720.0
Slope in vicinity (ft/ft) > 0.000189
Flow impact > LEFT
Channel evolution > UNKNOWN
Observed armoring > UNKNOWN
Debris frequency > OCCASIONAL
Debris effect > LOCAL
Stream size > WIDE
Flow habit > UNKNOWN
Bed material > GRAVEL
Valley/Other setting > MODERATE
Flood plain > WIDE
Natural levees > LITTLE
Apparent incision > NONE
Channel boundaries > ALLUVIAL
Tree cover on banks > MEDIUM
Degree of sinuosity > MEANDERING
Degree of braiding > NONE
Degree of anabranching > NONE
Development of bars > NARROW
Variability of width > RANDOM

Figure 21. Example of a data set output from the Bridge Scour Data Management System (continued).

Values for Manning's "n":

	Left Overbank	Main Channel	Right Overbank
High	0.20	0.033	0.20
Typical	0.18	0.03	0.18
Low	0.16	0.028	0.16

Bed Material Characteristics (Di in mm)

Sample No.	Date		Type	Specific							
	Yr	Mo		Dy	Sampler	D95	D84	D50	D16	Grav.	Shape
1	1991	10	4	BMH-60	5.8	0.36	0.25	0.16	2.65	(none)	NONCOH
2	1991	10	4	BMH-60	0.28	0.19	0.14	0.092	2.65	(none)	NONCOH
3	1991	10	4	BMH-60	17.3	10.4	2.1	0.35	2.65	(none)	NONCOH
4	1991	10	4	BMH-60	15.0	10.0	2.0	0.33	2.65	(none)	NONCOH
5	1991	10	9	BMH-60	0.86	0.5	0.32	0.13	2.65	(none)	MILD
6	1991	10	9	SHOVEL	20.0	15.0	6.9	0.39	2.65	(none)	NONCOH

BRIDGE SITE DATA

Structure Number > 118.5A

Length (ft) > 785.0

Width (ft) > 32

Lower low chord elev. (ft) > 159.8

Upper low chord elev. (ft) > 167.4

Overtopping elevation (ft) > (none)

Skew to flow (deg) > 0.0

Guide banks > ELLIPTICAL

Plans on file? YES

Parallel bridges? YES

Continuous Abutments > NO

Distance/center lines (ft) > 75.0

Distance/pier faces (ft) > 51.0

Upstream/Downstream? > UP

Number of spans > 9

Vertical bridge config > 3

Average daily traffic > 5295

Year built > 1970

Waterway classification > 1

Description for this bridge:

ABUTMENT SITE DATA

Left Abutment: Highway Station > 7688.0

Right Abutment: Highway Station > 8471.0

Left abutment skew to flow (deg) > 0

Right abutment skew to flow (deg) > 0

Figure 21. Example of a data set output from the Bridge Scour Data Management System (continued).

Abutment/Contracted opening type > III
 Abutment slope (ft/ft) > 2.0
 Embankment slope (ft/ft) > 3.0
 Left abutment length (ft) > (none)
 Right abutment length (ft) > (none)
 Embankment skew to flow (deg) > 0.0

Wingwalls? > NO
 Wingwall angle > 0.0

Distance from Left abutment to channel bank (ft) > 170.0
 Distance from Right abutment to channel bank (ft) > 95.0

PIER SITE DATA

<For Pile Bent Piers>

Pier ID	Bridge Station (ft)	Highway Alignment (deg)	Pier Station (ft)	Pier Type	Number of Piles	Pile Spacing (ft)
6	7980.0	0.0	7980.0	GROUP	2	17.0
5	8110.0	0.0	8110.0	GROUP	2	17.0
4	8240.0	0.0	8240.0	GROUP	2	17.0

Pier Width (ft)	Pier Shape	Pier Shape Factor	Pier Length (ft)	Pier Protection
4.0	CYLINDER	(none)	21.0	NONE
4.0	CYLINDER	(none)	21.0	NONE
4.0	CYLINDER	(none)	21.0	NONE

Pier Foundation	<-----Foot or Pile Cap-----> <---Elevations---> <---(ft)--->		Width (ft)	Shape	Pile Tip Elevation (ft)
	Top	Bottom			
PILES	122.1	118.1	11.2	SQUARE	82.0
PILES	122.3	118.3	11.2	SQUARE	81.0
PILES	122.1	118.1	11.2	SQUARE	79.0

Pier description for pier ID 6:

Pier consists of two 4-ft-diameter concrete columns spaced 17.0 ft apart. Each column is on an 11.2-ft-wide, 8.5-ft-long, 4.0-ft-deep concrete footing supported by 12 18x18-in concrete piles. There are four piles at the upstream side of the footing, four in the middle, and four at the downstream side.

Figure 21. Example of a data set output from the Bridge Scour Data Management System (continued).

Pier coordinates for pier ID 6:

-5.6	118.1
-5.6	122.1
-2.0	122.1
-2.0	162.4
-2.0	166.9
2.0	166.9
2.0	162.4
-2.0	162.4
2.0	162.4
2.0	122.1
5.6	122.1
5.6	118.1
-5.6	118.1

Pier description for pier ID 5:

Pier consists of two 4-ft-diameter concrete columns spaced 17.0 ft apart. Each column is on an 11.2-ft-wide, 8.5-ft-long, 4.0-ft-deep concrete footing supported by 12 18x18-in concrete piles. There are four piles at the upstream side of the footing, four in the middle, and four at the downstream side.

Pier coordinates for pier ID 5:

-5.6	118.3
-5.6	122.3
-2.0	122.3
-2.0	163.6
-2.0	168.1
2.0	168.1
2.0	163.6
-2.0	163.6
2.0	163.6
2.0	122.3
5.6	122.3
5.6	118.3
-5.6	118.3

Pier description for pier ID 4:

Pier consists of two 4-ft-diameter concrete columns spaced 17.0 ft apart. Each column is on an 11.2-ft-wide, 8.5-ft-long, 4.0-ft-deep concrete footing supported by 12 18x18-in concrete piles. There are four piles at the upstream side of the footing, four in the middle, and four at the downstream side.

Figure 21. Example of a data set output from the Bridge Scour Data Management System (continued).

Pier coordinates for pier ID 4:

```

-5.6    118.1
-5.6    122.1
-2.0    122.1
-2.0    160.4
-2.0    164.9
 2.0    164.9
 2.0    160.4
-2.0    160.4
 2.0    160.4
 2.0    122.1
 5.6    122.1
 5.6    118.1
-5.6    118.1
    
```

CONTACT/PUBLICATION REFERENCE DATA

Contact reference for this site:

U.S. Geological Survey, WRD, MS District
 100 W. Capitol Street, Suite 710
 Jackson, MS 39269
 (601) 965-4600

Publication reference for this site:

Turnipseed, D.P., and Smith, J.A., 1992, "Monitoring lateral movement of channel banks on the Pearl River in Mississippi," *Mississippi Water Resources Conference Proceedings*, 1992, pp.101-108.

PIER SCOUR DATA

For pier ID 6:

<--Date of Measurement--> Upstream/Downstream
 Year Mon Day Hr Min (0=UNKNOWN, 1=UP, 2=DOWN)

```

1990 1 27 14 55 1
1990 1 30 15 0 2
1990 2 5 17 35 2
1991 5 10 10 45 1
    
```

<-Scour Depth->		<-Scour Hole->		<-Approach Flow->		Effective Skew to	
Value	Accuracy	Side Slope	Top Width	Velocity	Depth	Pier Width	Flood Flow
(ft)	(ft)	(ft/ft)	(ft)	(ft/s)	(ft)	(ft)	(deg)
4.9	0.5	3.4	46.0	5.55	30.1	5.5	16.0
6.5	0.5	4.1	62.0	6.94	27.7	5.5	14.0
6.6	0.5	2.1	30.0	4.24	25.1	5.8	18.0
9.9	0.5	2.1	49.0	7.17	27.3	5.4	14.0

Figure 21. Example of a data set output from the Bridge Scour Data Management System (continued).

Sediment Transpt	Bed Material	Sand Bed Form	<--Dune Scour-->		<Bed Mat Size>		Debris Effects
			Trough (ft)	Crest (ft)	D50 (mm)	Sigma	
LIVE	NON-COH	UNKNOWN	(none)	(none)	6.9	6.2	INSIGNIF
LIVE	NON-COH	UNKNOWN	(none)	(none)	6.9	6.2	UNKNOWN
LIVE	NON-COH	UNKNOWN	(none)	(none)	6.9	6.2	UNKNOWN
LIVE	NON-COH	UNKNOWN	(none)	(none)	6.9	6.2	UNKNOWN

Comments for pier scour measurement on 1/27/90 14:55:
Reference bed is at elev. 110.3 ft.
Minimum bed elev. at pier is at upstream side at 105.4 ft.
Scour-hole depth = 110.3 - 105.4 = 4.9 ft. Effective pier width is a
depth-weighted average of the column, footing, and piling widths.

Comments for pier scour measurement on 1/30/90 15:00:
Reference bed is at elev. 111.4 ft.
Minimum bed elev. at pier is at downstream side at 104.9 ft.
Scour-hole depth = 111.4 - 104.9 = 6.5 ft. Effective pier width is a
depth-weighted average of the column, footing, and piling widths.

Comments for pier scour measurement on 2/5/90 17:35:
Reference bed is at elev. 109.6 ft at downstream side.
Minimum bed elev. at pier is at downstream side at 103.0 ft.
Scour-hole depth = 109.6 - 103.0 = 6.6 ft, at upstream side, 109.3 - 105.6 = 3.7 ft.
Eff. pier width is a depth-weighted ave. of the column, footing, and piling widths.

Comments for pier scour measurement on 5/10/91 10:45:
Reference bed is at elev. 113.1 ft.
Minimum bed elev. at pier is at upstream side at 103.2 ft.
Scour-hole depth = 113.1 - 103.2 = 9.9 ft. Effective pier width is a
depth-weighted average of the column, footing, and piling widths.

For pier ID 5:

<--Date of Measurement-->						Upstream/Downstream
Year	Mon	Day	Hr	Min		(0=UNKNOWN, 1=UP, 2=DOWN)
1990	1	27	12	30	1	
1990	1	30	15	0	1	
1990	2	5	17	35	1	
1991	5	10	10	45	2	

Figure 21. Example of a data set output from the Bridge Scour Data Management System (continued).

<-Scour Depth->		<-Scour Hole->				Effective Skew to	
Value	Accuracy	Side Slope	Top Width	<-Approach Flow->		Pier	Flood
(ft)	(ft)	(ft/ft)	(ft)	Velocity	Depth	Width	Flow
				(ft/s)	(ft)	(ft)	(deg)
7.5	0.5	4.8	82.0	7.69	28.4	5.5	22.0
3.3	0.5	3.3	44.0	5.69	28.6	6.4	8.0
2.0	0.5	5.2	38.0	4.34	25.7	5.8	16.0
4.5	0.5	2.8	36.0	6.64	28.9	5.5	11.0

Sedimnt	Bed	Sand	<-Dune Scour-->		<Bed Mat Size>		Debris
Transpt	Material	Bed Form	Trough	Crest	D50	Sigma	Effects
			(ft)	(ft)	(mm)		
LIVE	NON-COH	UNKNOWN	(none)	(none)	6.9	6.2	UNKNOWN
LIVE	NON-COH	UNKNOWN	(none)	(none)	6.9	6.2	UNKNOWN
LIVE	NON-COH	UNKNOWN	(none)	(none)	6.9	6.2	UNKNOWN
LIVE	NON-COH	UNKNOWN	(none)	(none)	6.9	6.2	UNKNOWN

Comments for pier scour measurement on 1/27/90 12:30:
Reference bed is at elev. 112.0 ft.
Minimum bed elev. at pier is upstream side at 104.5 ft.
Scour-hole depth = 112.0 - 104.5 = 7.5 ft. Effective pier width is a depth-weighted average of the column, footing, and piling widths.

Comments for pier scour measurement on 1/30/90 15:00:
Reference bed is at elev. 110.5 ft.
Minimum bed elev. at pier is at upstream side of pier at 107.2 ft.
Scour-hole depth = 110.5 - 107.2 = 3.3 ft. Effective pier width is a depth-weighted average of the column, footing, and piling widths.

Comments for pier scour measurement on 2/5/90 17:35:
Reference bed is at elev. 109.0 ft.
Minimum bed at pier is at upstream side at 107.0 ft.
Scour-hole depth = 109.0 - 107.0 = 2.0 ft. Effective pier width is a depth-weighted average of the column, footing, and piling widths.

Comments for pier scour measurement on 5/10/91 10:45:
Reference bed is at elev. 111.5 ft.
Minimum bed elev. at pier is at downstream side at 107.0 ft.
Scour-hole depth = 111.5 - 107.0 = 4.5 ft, at upstream side, 112.0 - 107.9 = 4.1 ft.
Eff. pier width is a depth-weighted ave. of the column, footing, and piling widths.

For pier ID 4:

<-Date of Measurement-->					Upstream/Downstream
Year	Mon	Day	Hr	Min	(0=UNKNOWN, 1=UP, 2=DOWN)
1990	1	27	14	55	1
1990	1	30	15	0	1
1991	5	10	10	45	1

Figure 21. Example of a data set output from the Bridge Scour Data Management System (continued).

<-Scour Depth->		<-Scour Hole->		<-Approach Flow->		Effective Skew to	
Value	Accuracy	Side Slope	Top Width	Velocity	Depth	Pier Width	Flood Flow
(ft)	(ft)	(ft/ft)	(ft)	(ft/s)	(ft)	(ft)	(deg)
1.9	0.5	7.2	34.0	5.33	26.9	5.4	8.0
3.2	0.5	4.5	41.0	4.64	25.0	5.5	8.0
1.4	0.5	4.4	13.0	5.14	29.1	5.5	11.0

Sedimnt	Bed	Sand	<--Dune Scour-->		<Bed Mat Size>		Debris
Transpt	Material	Bed Form	Trough	Crest	D50	Sigma	Effects
			(ft)	(ft)	(mm)		
LIVE	NON-COH	UNKNOWN	(none)	(none)	6.9	6.2	UNKNOWN
LIVE	NON-COH	UNKNOWN	(none)	(none)	6.9	6.2	UNKNOWN
LIVE	NON-COH	UNKNOWN	(none)	(none)	6.9	6.2	UNKNOWN

Comments for pier scour measurement on 1/27/90 14:55:
Reference bed is at elev. 113.5 ft. Scour-hole side slope is rough due to close proximity of bank. Minimum bed elev. at pier is at upstream side at 111.6 ft.
Scour-hole depth = 113.5 - 111.6 = 1.9 ft. Effective pier width is a depth-weighted average of the column, footing, and piling widths.

Comments for pier scour measurement on 1/30/90 15:00:
Reference bed is at elev. 114.1 ft.
Minimum bed at upstream side is at 110.9 ft. At downstream side, bed is at 110.4 ft.
Scour-hole depth = 114.1 - 110.9 = 3.2 ft. Effective pier width is a depth-weighted average of the column, footing, and piling widths.

Comments for pier scour measurement on 5/10/91 10:45:
Reference bed is at elev. 111.3 ft.
Minimum bed elev. at pier is at upstream side at 109.9 ft.
Scour-hole depth = 111.3 - 109.9 = 1.4 ft. Effective pier width is a depth-weighted average of the column, footing, and piling widths.

ABUTMENT SCOUR DATA

No scour measurements for the LEFT Abutment.

No scour measurements for the RIGHT Abutment.

CONTRACTION SCOUR DATA

No contraction scour measurements for this site.

GENERAL SCOUR DATA

No general scour measurements for this site.

Figure 21. Example of a data set output from the Bridge Scour Data Management System (continued).

STAGE AND DISCHARGE DATA

<-----Peak Discharge----->						<-----Peak Stage----->					Water	Return		
Year	Mo	Dy	Hr	Min	Flow	Accuracy	Year	Mo	Dy	Hr	Mi	Stage	Temp.	Period
(cfs)						(ft)					(deg C)	(years)		
1991	5	10	13	20	71700.0	5.0	1991	5	10	13	20	140.37	(none)	25.0
1990	1	27	13	35	73000.0	5.0	1990	1	27	13	35	140.38	(none)	25.0
none	0	0	0	0	(none)	(none)	1990	1	30	0	0	139.09	(none)	(none)
none	0	0	0	0	(none)	(none)	1990	2	5	0	0	134.73	(none)	(none)
none	0	0	0	0	(none)	(none)	1990	2	14	0	0	134.09	(none)	(none)
none	0	0	0	0	(none)	(none)	1990	3	28	0	0	123.43	(none)	(none)

HYDROGRAPH FLOOD DATA

No HYDROGRAPH FLOOD data exists for this site.

DEBRIS FLOOD DATA

No DEBRIS FLOOD data exists for this site.

CHANNEL GEOMETRY DESCRIPTION

Description of the channel geometry:

Figure 21. Example of a data set output from the Bridge Scour Data Management System (continued).

Table 4. Summary of data collection sites.

Site number	Site name	Drainage area (mi ²)	Channel slope (ft/ft)
1	Susitna River near Sunshine, AK	11,500	0.0004
2	Knik River at Old Glenn Highway near Palmer, AK	1,200	0.00069
3	Knik River near Eklutna, AK	--	0.001
4	Tazlina River at Richardson Hwy near Glennallen, AK	2,670	0.0021
5	Tanana River at Richardson Hwy at Big Delta, AK	13,500	0.0006
6	Tanana River at Nenana, AK	25,600	0.00015
7	Snow River at Seward Highway near Seward, AK	150	--
8	Red River at U.S. 71 at Index, AR	48,030	--
9	Red River at I-30 near Fulton, AR	52,336	--
10	Red River at U.S. 82 at Garland, AR	52,675	--
11	South Platte River at S.R. 37 near Kersey, CO	9,598	0.00093
12	South Platte River at C.R. 87 near Masters, CO	12,120	0.00132
13	Arkansas River at C.R. 613 near Nepesta, CO	--	0.0005
14	Rio Grande River at U.S. 285 near Monte Vista, CO	1,590	0.00075
15	Leipsic River at S.R. 9 at Leipsic, DE	--	--
16	Assawoman Bay at S.R. 54 near Fenwick Island, DE	--	--
17	South Altamaha River at I-95 near Brunswick, GA	14,000	--
18	Eel River at S.R. 59 near Clay City, IN	880	0.00035
19	Wabash River at S.R. 163 at Clinton, IN	11,720	0.00014
20	White River at S.R. 157 at Worthington, IN	4,392	0.0002
21	Red River at S.R. 3032 near Shreveport, LA, EB	60,700	0.0001
22	Red River at S.R. 3032 near Shreveport, LA, WB	60,700	0.0001
23	Youghiogheny River at S.R. 42 at Friendsville, MD	295	0.005
24	Big Pipe Creek at S.R. 194 at Bruceville, MD	102	0.00157
25	Choptank River at S.R. 287 near Goldsboro, MD	--	--
26	Pearl River at westbound S.R. 25 at Jackson, MS	3,130	0.00019
27	Pearl River at eastbound S.R. 25 at Jackson, MS	3,130	0.00019
28	Homochitto River at U.S. 84 at Eddiceton, MS	181	0.000928
29	Pearl River at eastbound U.S. 98 near Columbia, MS	5,720	0.000189
30	Pearl River at westbound U.S. 98 near Columbia, MS	5,720	0.000189

Table 4. Summary of data collection sites (continued).

Site number	Site name	Drainage area (mi ²)	Channel slope (ft/ft)
31	Clarks Fork Yellowstone River near Bridger, MT	1,809	0.007
32	Gallatin River at U.S. 191 near Gallatin Gateway, MT	825	0.0063
33	Yellowstone River at U.S. 89 near Emigrant, MT	2,844	0.0022
34	Badger Creek at U.S. 89 near Browning, MT	239	0.0039
35	Otselic River at S.R. 23 at Cincinnatus, NY	153	0.0004
36	Chemung River at S.R. 427 at Chemung, NY	2,506	0.00075
37	Schoharie Creek at S.R. 30 at Middleburg, NY	534	0.002
38	Susquehanna River at C.R. 314 at Conklin, NY	2,232	0.00057
39	Genesee River at Bailey Road at Portageville, NY	984	0.0009
40	Delaware River at Route 6 at Port Jervis, NY	3,070	0.00114
41	Great Miami River at S.R. 128 at Hamilton, OH	3,630	0.00049
42	Hocking River at S.R. 278 at Nelsonville, OH	576	0.00038
43	Honey Creek at S.R. 67 at Melmore, OH	149	0.0014
44	Little Miami River at S.R. 350 at Fort Ancient, OH	675	0.00084
45	Ottawa River at Township Road 122 at Lima, OH	130	0.00144
46	Scioto River at S.R. 4 near Prospect, OH	528	0.00008
47	Todd Fork at S.R. 22 at Morrow, OH	262	0.00179
48	Killbuck Creek at C.R. 621 at Killbuck, OH	462	0.00023
49	Pamunkey River at S.R. 614 near Hanover, VA	1,081	0.00012
50	Nottoway River at S.R. 653 near Sebrell, VA	1,421	0.00016
51	Bush River at U.S. 460 near Rice, VA	64	0.0011
52	Dan River at U.S. 501 at South Boston, VA	2,730	0.00025
53	Tye River at S.R. 56 near Lovingston, VA	93	0.0029
54	Little Nottoway River at S.R. 603 near Blackstone, VA	--	0.002
55	Reed Creek at S.R. 649 near Wytheville, VA	--	0.0001
56	North Fork Holston River near North Holston, VA	--	0.001

[I, Interstate; S.R., State Route; C.R., County Road; EB, eastbound; WB, westbound;
1 mi² = 2.59 km²; 1 ft = 0.305 m]

Page Intentionally Left Blank

SUMMARY OF SCOUR MEASUREMENTS AT BRIDGE PIERS

The scour measurement data summarized here were collected to provide an improved understanding of scour processes that contributes to better scour prediction and bridge design. A summary and characterization of the individual scour variables are an initial but important step toward understanding scour processes. Analytical procedures (and results) typically assume the data possess certain characteristics regarding their distribution, symmetry, linearity of relation to other variables, etc. Those characteristics are discussed in this section for the principal scour variables. The key variables from 384 measurements of local scour at bridge piers are presented in tables 4 and 5, and are characterized in table 6 and in the following discussion and associated figures.

The data distribution, range, median, mode, and spread of each quantitative scour measurement variable are illustrated in a paired histogram and box plot. Selected statistical properties of the variables are also listed in table 6. Each box plot and histogram pair has the same horizontal scale. The box plot illustrates the median of the data (vertical line inside the box); the 25th and 75th percentiles of the data (left and right ends of the box); the ratio of the 25th and 75th percentiles or quartile skew (relative size of box sections); and the range of the data, including unusual values (whiskers and outlier points; figure 22C). The box plot whiskers are drawn to any points within the range of 1.5 times the box length (interquartile range). The asterisks represent outlier values and the circles represent extreme outliers to the data set.

The distributions of most of the quantitative variables are right (positive) skewed, as is typical for water resources data. The data were transformed, where appropriate, to make their distribution more symmetrical and their relations more linear. Note that nothing is lost in the transformation process, as one unit of measurement is not, in itself, more valid than another. The sample correlation coefficient measures the strength of only the linear relation between two variables. The sample mean is a measure of the center of the data only for symmetrical distributions. The relation between two variables, such as pier scour depth and velocity, can be defined more effectively if the variables can be transformed to be represented by a similar distribution that is linear and symmetrical. Transformations that approximate the bivariate normal distribution are particularly desirable for analysis, because it is symmetrical and has constant variance in both tails. The curve for a normal distribution with the sample variable's mean and standard deviation is shown on the histograms for several of the transformed variables.

Table 5. Summary of local scour measurements at bridge piers.

Mea- sure- ment num- ber	Site num- ber	State	Date M/D/Y	Time	Pier ID	UP/DN	Bed- load trans- port	Bed mat- erial cohe- sion	Debris	Pier shape	Pier type	Founda- tion type	Mea- sure- ment num- ber	Pier length (ft)	Pier skew (deg)	Pier width (ft)	Flow velo- city (ft/s)	Flow depth (ft)	D ₅₀ (mm)	D ₈₄ (mm)	σ	Scour		Side slope (ft)	Top width (ft)
																						depth (ft)	Error (ft/ft)		
1	1	AK	7/2/71	0000	1	1	Clear	Non-coh	Insig	Sharp	Single	Piles	1	20.0	0.0	5.0	6.5	19.0	70.0	90.0	1.3	2.5	0.5	--	--
2	1	AK	8/11/71	0000	1	1	Clear	Non-coh	Insig	Sharp	Single	Piles	2	20.0	0.0	5.0	10.0	17.5	70.0	90.0	1.3	2.0	0.5	--	--
3	1	AK	7/2/71	0000	2	1	Clear	Non-coh	Insig	Sharp	Single	Piles	3	20.0	0.0	5.0	8.5	13.5	70.0	90.0	1.3	2.5	0.5	--	--
4	1	AK	8/11/71	0000	2	0	Clear	Non-coh	Insig	Sharp	Single	Piles	4	20.0	0.0	5.0	9.5	21.5	70.0	90.0	1.3	2.0	1.0	--	--
5	1	AK	7/2/71	0000	3	1	Clear	Non-coh	Insig	Sharp	Single	Piles	5	20.0	0.0	5.0	7.0	11.0	70.0	90.0	1.3	2.0	0.5	--	--
6	1	AK	8/11/71	0000	3	0	Clear	Non-coh	Insig	Sharp	Single	Piles	6	20.0	0.0	5.0	11.5	17.0	70.0	90.0	1.3	2.0	1.0	--	--
7	1	AK	7/2/71	0000	4	2	Clear	Non-coh	Subst	Sharp	Single	Piles	7	20.0	0.0	5.0	5.0	13.5	70.0	90.0	1.3	5.0	0.5	--	--
8	1	AK	8/11/71	0000	4	2	Clear	Non-coh	Subst	Sharp	Single	Piles	8	20.0	0.0	5.0	9.5	17.5	70.0	90.0	1.3	5.0	1.0	--	--
9	2	AK	7/11/65	1530	5	1	Live	Non-coh	Unkn	Sharp	Single	Poured	9	29.0	0.0	6.0	12.0	18.0	5.0	25.0	9.0	3.5	0.5	--	--
10	3	AK	6/24/66	0000	1	1	Live	Non-coh	Unkn	Round	Single	Piles	10	36.9	0.0	5.0	5.0	7.0	1.8	13.0	7.2	2.0	0.5	--	--
11	3	AK	6/28/66	0000	1	1	Live	Non-coh	Unkn	Round	Single	Piles	11	36.9	0.0	5.0	3.1	3.0	1.8	13.0	7.2	1.5	0.5	--	--
12	3	AK	6/24/66	0000	2	1	Live	Non-coh	Unkn	Round	Single	Piles	12	36.9	0.0	5.0	5.1	6.5	1.8	13.0	7.2	2.0	0.5	--	--
13	3	AK	6/28/66	0000	2	1	Live	Non-coh	Unkn	Round	Single	Piles	13	36.9	0.0	5.0	3.2	3.0	1.8	13.0	7.2	2.0	0.5	--	--
14	3	AK	6/17/66	0000	3	1	Live	Non-coh	Unkn	Round	Single	Piles	14	36.9	0.0	5.0	1.6	4.0	0.58	7.0	12.1	1.0	0.5	--	--
15	3	AK	6/24/66	0000	3	1	Live	Non-coh	Unkn	Round	Single	Piles	15	36.9	0.0	5.0	5.2	10.0	1.8	13.0	7.2	3.0	0.5	--	--
16	3	AK	6/28/66	0000	3	1	Live	Non-coh	Unkn	Round	Single	Piles	16	36.9	0.0	5.0	3.6	6.0	1.8	13.0	7.2	1.5	0.5	--	--
17	3	AK	6/17/66	0000	4	1	Live	Non-coh	Unkn	Round	Single	Piles	17	36.9	0.0	5.0	2.5	5.0	0.58	7.0	12.1	1.0	0.5	--	--
18	3	AK	6/24/66	0000	4	1	Live	Non-coh	Unkn	Round	Single	Piles	18	36.9	0.0	5.0	6.5	10.5	1.8	13.0	7.2	4.0	0.5	--	--
19	3	AK	6/28/66	0000	4	1	Live	Non-coh	Unkn	Round	Single	Piles	19	36.9	0.0	5.0	3.8	8.0	1.8	13.0	7.2	2.0	0.5	--	--
20	3	AK	6/17/66	0000	5	1	Live	Non-coh	Unkn	Round	Single	Piles	20	36.9	0.0	5.0	2.9	4.0	0.58	7.0	12.1	1.0	0.5	--	--
21	3	AK	6/24/66	0000	5	1	Live	Non-coh	Unkn	Round	Single	Piles	21	36.9	0.0	5.0	5.9	10.0	1.8	13.0	7.2	4.5	0.5	--	--
22	3	AK	6/28/66	0000	5	1	Live	Non-coh	Unkn	Round	Single	Piles	22	36.9	0.0	5.0	3.7	7.5	1.8	13.0	7.2	2.5	0.5	--	--
23	3	AK	6/17/66	0000	6	1	Live	Non-coh	Unkn	Round	Single	Piles	23	36.9	0.0	5.0	0.9	1.5	0.58	7.0	12.1	2.5	0.5	--	--
24	3	AK	6/24/66	0000	6	1	Live	Non-coh	Unkn	Round	Single	Piles	24	36.9	0.0	5.0	6.8	8.5	1.8	13.0	7.2	3.5	0.5	--	--
25	3	AK	6/28/66	0000	6	1	Live	Non-coh	Unkn	Round	Single	Piles	25	36.9	0.0	5.0	3.7	5.0	1.8	13.0	7.2	1.5	0.5	--	--
26	3	AK	6/17/66	0000	7	1	Live	Non-coh	Unkn	Round	Single	Piles	26	36.9	0.0	5.0	0.5	2.0	0.58	7.0	12.1	4.0	0.5	--	--
27	3	AK	6/24/66	0000	7	1	Live	Non-coh	Unkn	Round	Single	Piles	27	36.9	0.0	5.0	6.0	10.0	1.8	13.0	7.2	6.0	0.5	--	--
28	3	AK	6/28/66	0000	7	1	Live	Non-coh	Unkn	Round	Single	Piles	28	36.9	0.0	5.0	3.2	6.5	1.8	13.0	7.2	2.5	0.5	--	--
29	4	AK	9/2/71	0000	1	1	Live	Non-coh	Insig	Round	Group	Piles	29	--	0.0	15.0	9.5	12.0	90.0	130.0	1.44	5.0	0.5	--	--
30	4	AK	9/4/71	0000	1	1	Live	Non-coh	Insig	Round	Group	Piles	30	--	0.0	15.0	11.5	15.0	90.0	130.0	1.44	5.5	0.5	--	--
31	5	AK	7/16/71	0000	1	1	Live	Non-coh	Moder	Round	Single	Piles	31	31.0	37.0	5.0	7.1	12.0	14.0	58.0	4.14	6.0	0.5	--	--
32	5	AK	7/16/71	0000	2	2	Live	Non-coh	Moder	Round	Single	Poured	32	31.0	37.0	5.0	7.3	12.0	14.0	58.0	4.14	7.0	0.5	--	--
33	5	AK	7/16/71	0000	3	3	Live	Non-coh	Moder	Round	Single	Poured	33	31.0	37.0	5.0	6.8	15.0	14.0	58.0	4.14	6.0	0.5	--	--
34	5	AK	7/16/71	0000	4	4	Live	Non-coh	Moder	Round	Single	Poured	34	44.4	37.0	5.0	5.7	14.0	14.0	58.0	4.14	8.0	0.5	--	--
35	6	AK	8/17/67	0000	1	2	Live	Non-coh	Moder	Sharp	Group	Piles	35	48.0	0.0	10.0	8.5	22.0	15.0	21.0	1.4	6.0	0.5	--	--
36	7	AK	9/23/70	0000	5	5	Live	Non-coh	Insig	Round	Single	Unkn	36	--	0.0	3.2	5.3	5.0	7.6	23.0	3.0	2.5	0.5	--	--
37	8	AR	5/9/90	1500	8	2	Live	Unkn	Unkn	Round	Group	Piles	37	31.0	11.0	7.0	8.7	40.4	0.119	--	--	7.6	0.5	8.6	179.0
38	8	AR	5/9/90	1500	9	2	Live	Unkn	Unkn	Round	Group	Piles	38	31.0	8.0	7.0	12.8	42.8	0.119	--	--	11.2	0.5	9.5	170.0
39	9	AR	5/12/90	1400	4	1	Live	Unkn	Unkn	Sharp	Unkn	Unkn	39	--	0.0	7.0	9.5	35.3	0.18	--	--	14.6	0.5	3.4	220.0
40	9	AR	5/12/90	1400	5	1	Live	Unkn	Unkn	Sharp	Unkn	Unkn	40	--	0.0	6.5	2.4	26.7	0.18	--	--	8.7	0.5	11.4	140.0
41	10	AR	5/14/90	1400	7	2	Live	Unkn	Unkn	Round	Group	Piles	41	35.8	0.0	9.8	6.2	38.5	0.32	--	--	14.4	0.5	7.4	195.0
42	10	AR	5/14/90	1400	8	2	Live	Unkn	Unkn	Round	Group	Piles	42	35.8	14.0	9.8	7.7	44.2	0.32	--	--	5.9	0.5	11.5	105.0
43	10	AR	5/14/90	1400	10	2	Live	Unkn	Unkn	Round	Group	Piles	43	35.8	0.0	9.8	4.8	29.9	0.32	--	--	10.7	0.5	6.4	87.0

Table 5. Summary of local scour measurements at bridge piers (continued).

Mea- sure- ment num- ber	Site		Date			Pier		Bed- load trans- port	Bed mat- erial cohe- sion	Debris	Pier shape	Pier type	Foun- dation type	Mea- sure- ment num- ber	Pier length (ft)	Pier skew (deg)	Pier width (ft)	Flow					Side slope (ft)	Top width (ft)	
	num- ber	State	M/D/Y	Time	ID	UP/DN	Mea- sure- ment num- ber											velocity (ft/s)	Flow depth (ft)	D ₅₀ (mm)	D ₈₄ (mm)	σ			Scour depth (ft)
44	11	CO	5/21/84	1000	3	1	Live	Non-coh	Unkn	Sharp	Single	Piles	44	23.25	20.0	1.75	4.6	6.0	1.1	5.12	3.45	1.1	0.5	20.0	29.0
45	11	CO	5/21/84	1300	3	2	Live	Non-coh	Unkn	Sharp	Single	Piles	45	23.25	20.0	1.75	4.6	6.0	1.1	5.12	3.45	2.2	0.5	9.9	38.0
46	11	CO	5/21/84	1000	4	1	Live	Non-coh	Unkn	Sharp	Single	Piles	46	23.25	20.0	1.75	5.8	5.1	1.1	5.12	3.45	1.0	0.5	22.0	28.0
47	11	CO	5/21/84	1300	4	2	Live	Non-coh	Unkn	Sharp	Single	Piles	47	23.25	20.0	1.75	5.8	5.1	1.1	5.12	3.45	2.6	0.5	7.2	32.0
48	11	CO	6/26/84	1400	4	1	Live	Non-coh	Unkn	Sharp	Single	Piles	48	23.25	43.0	1.75	3.2	4.6	1.1	5.12	3.45	1.5	0.5	7.5	21.0
49	11	CO	6/26/84	1600	4	2	Live	Non-coh	Unkn	Sharp	Single	Piles	49	23.25	43.0	1.75	3.2	4.6	1.1	5.12	3.45	2.2	0.5	9.3	41.0
50	11	CO	5/21/84	1300	5	2	Live	Non-coh	Unkn	Sharp	Single	Piles	50	23.25	20.0	1.75	4.6	4.3	1.1	5.12	3.45	3.0	0.5	6.7	40.0
51	11	CO	6/26/84	1600	5	2	Live	Non-coh	Unkn	Sharp	Single	Piles	51	23.25	43.0	1.75	3.4	3.3	1.1	5.12	3.45	1.6	0.5	8.0	26.0
52	12	CO	5/18/84	1100	1	1	Live	Non-coh	Unkn	Square	Single	Piles	52	24.0	26.0	0.95	2.6	3.3	0.94	3.51	2.98	2.0	0.5	10.5	44.0
53	12	CO	5/18/84	1330	1	2	Live	Non-coh	Unkn	Square	Single	Piles	53	24.0	26.0	0.95	2.6	3.3	0.94	3.51	2.98	1.9	0.5	5.9	18.0
54	12	CO	6/25/84	1400	1	1	Live	Non-coh	Unkn	Square	Single	Piles	54	24.0	15.0	0.95	2.3	1.9	0.94	3.51	2.98	0.7	0.5	10.7	17.0
55	12	CO	6/25/85	1630	1	2	Live	Non-coh	Unkn	Square	Single	Piles	55	24.0	15.0	0.95	2.3	1.9	0.94	3.51	2.98	1.4	0.5	6.2	17.0
56	12	CO	5/18/84	1100	2	1	Live	Non-coh	Subst	Square	Single	Piles	56	24.0	26.0	0.95	3.5	3.3	0.94	3.51	2.98	0.5	0.5	5.1	16.0
57	12	CO	5/18/84	1330	2	2	Live	Non-coh	Subst	Square	Single	Piles	57	24.0	26.0	0.95	3.5	3.3	0.94	3.51	2.98	1.5	0.5	5.7	15.0
58	12	CO	5/18/84	1100	3	1	Live	Non-coh	Unkn	Square	Single	Piles	58	24.0	14.0	0.95	3.8	3.3	0.94	3.51	2.98	1.0	0.5	15.2	24.0
59	12	CO	5/18/84	1330	3	2	Live	Non-coh	Unkn	Square	Single	Piles	59	24.0	14.0	0.95	3.8	3.3	0.94	3.51	2.98	1.1	0.5	9.0	16.0
60	12	CO	6/25/84	1400	3	1	Live	Non-coh	Unkn	Square	Single	Piles	60	24.0	20.0	0.95	2.7	1.1	0.94	3.51	2.98	1.0	0.5	11.5	23.0
61	12	CO	6/25/84	1630	3	2	Live*	Non-coh	Unkn	Square	Single	Piles	61	24.0	20.0	0.95	2.7	1.1	0.94	3.51	2.98	0.0	0.5	--	--
62	12	CO	5/18/84	1100	4	1	Live	Non-coh	Subst	Square	Single	Piles	62	24.0	23.0	0.95	3.9	4.3	0.94	3.51	2.98	0.6	0.5	5.5	10.0
63	12	CO	5/18/84	1330	4	2	Live	Non-coh	Subst	Square	Single	Piles	63	24.0	23.0	0.95	3.9	4.3	0.94	3.51	2.98	1.1	0.5	51.0	25.0
64	12	CO	6/25/84	1400	4	1	Live	Non-coh	Unkn	Square	Single	Piles	64	24.0	16.0	0.95	3.3	1.1	0.94	3.51	2.98	1.2	0.5	7.5	22.0
65	12	CO	6/25/84	1630	4	2	Live	Non-coh	Unkn	Square	Single	Piles	65	24.0	16.0	0.95	3.3	1.1	0.94	3.51	2.98	0.8	0.5	9.9	15.0
66	12	CO	5/18/84	1100	5	1	Live	Non-coh	Unkn	Square	Single	Piles	66	24.0	16.0	0.95	4.1	6.1	0.94	3.51	2.98	2.1	0.5	4.9	18.0
67	12	CO	5/18/84	1330	5	2	Live	Non-coh	Unkn	Square	Single	Piles	67	24.0	16.0	0.95	4.1	6.1	0.94	3.51	2.98	1.6	0.5	14.4	18.0
68	12	CO	6/25/84	1400	5	1	Live	Non-coh	Unkn	Square	Single	Piles	68	24.0	11.0	0.95	3.7	1.4	0.94	3.51	2.98	1.8	0.5	2.5	9.0
69	12	CO	6/25/84	1630	5	2	Live	Non-coh	Unkn	Square	Single	Piles	69	24.0	11.0	0.95	3.7	1.4	0.94	3.51	2.98	1.3	0.5	5.5	16.0
70	12	CO	5/18/84	1100	6	1	Live	Non-coh	Unkn	Square	Single	Piles	70	24.0	16.0	0.95	3.9	8.7	0.94	3.51	2.98	2.4	0.5	5.8	30.0
71	12	CO	5/18/84	1330	6	2	Live	Non-coh	Unkn	Square	Single	Piles	71	24.0	16.0	0.95	3.9	8.7	0.94	3.51	2.98	2.5	0.5	7.4	37.0
72	12	CO	6/25/84	1400	6	1	Live	Non-coh	Unkn	Square	Single	Piles	72	24.0	8.0	0.95	3.6	1.7	0.94	3.51	2.98	1.7	0.5	5.1	16.0
73	12	CO	6/25/84	1630	6	2	Live	Non-coh	Unkn	Square	Single	Piles	73	24.0	8.0	0.95	3.6	1.7	0.94	3.51	2.98	1.3	0.5	6.9	15.0
74	12	CO	5/18/84	1100	7	1	Live	Non-coh	Subst	Square	Single	Piles	74	24.0	14.0	0.95	5.2	9.2	0.94	3.51	2.98	1.3	0.5	2.6	8.0
75	12	CO	5/18/84	1330	7	2	Live	Non-coh	Subst	Square	Single	Piles	75	24.0	14.0	0.95	5.2	9.2	0.94	3.51	2.98	1.3	0.5	8.1	17.0
76	12	CO	6/25/84	1400	7	1	Live	Non-coh	Unkn	Square	Single	Piles	76	24.0	13.0	0.95	3.7	2.2	0.94	3.51	2.98	1.7	0.5	5.2	14.0
77	12	CO	6/25/84	1630	7	2	Live	Non-coh	Unkn	Square	Single	Piles	77	24.0	13.0	0.95	3.7	2.2	0.94	3.51	2.98	1.2	0.5	6.2	17.0
78	12	CO	5/18/84	1100	8	1	Live	Non-coh	Subst	Square	Single	Piles	78	24.0	11.0	0.95	4.3	9.4	0.94	3.51	2.98	0.7	0.5	3.3	10.0
79	12	CO	5/18/84	1330	8	2	Live	Non-coh	Subst	Square	Single	Piles	79	24.0	11.0	0.95	4.3	9.4	0.94	3.51	2.98	2.0	0.5	7.5	23.0
80	13	CO	5/23/84	0900	1	1	Live	Non-coh	Unkn	Round	Single	Unkn	80	21.0	12.0	4.0	3.3	6.9	1.19	5.15	3.61	2.1	0.5	3.9	15.0
81	13	CO	5/23/84	1030	1	2	Live	Non-coh	Unkn	Round	Single	Unkn	81	21.0	12.0	4.0	3.3	6.9	1.19	5.15	3.61	1.4	0.5	5.2	12.0
82	13	CO	6/5/84	1400	1	1	Live	Non-coh	Unkn	Round	Single	Unkn	82	21.0	0.0	4.0	5.4	7.5	1.19	5.15	3.61	4.3	1.0	3.7	32.0
83	13	CO	6/5/84	1500	1	2	Live	Non-coh	Unkn	Round	Single	Unkn	83	21.0	0.0	4.0	5.4	7.5	1.19	5.15	3.61	1.5	0.5	5.7	15.0
84	13	CO	5/23/84	0900	3	1	Live	Non-coh	Unkn	Round	Single	Unkn	84	21.0	0.0	4.0	2.2	2.1	1.19	5.15	3.61	1.0	0.5	5.4	15.0
85	13	CO	5/23/84	1030	3	2	Live	Non-coh	Unkn	Round	Single	Unkn	85	21.0	0.0	4.0	2.2	2.1	1.19	5.15	3.61	1.0	0.5	3.2	6.0
86	13	CO	6/5/84	1400	3	1	Live	Non-coh	Unkn	Round	Single	Unkn	86	21.0	0.0	4.0	3.3	3.4	1.19	5.15	3.61	1.0	0.5	5.7	26.0
87	13	CO	6/5/84	1500	3	2	Live	Non-coh	Unkn	Round	Single	Unkn	87	21.0	0.0	4.0	3.3	3.4	1.19	5.15	3.61	1.1	0.5	7.4	15.0

Table 5. Summary of local scour measurements at bridge piers (continued).

Mea- sure- ment num- ber	Site num- ber	Date M/D/Y	Time	Pier		Bed- load trans- port	Bed mat- erial cohe- sion	Debris	Pier shape	Pier type	Foun- dation type	Mea- sure- ment num- ber	Pier length (ft)	Pier skew (deg)	Pier width (ft)	Flow velo- city (ft/s)	Flow depth (ft)	D_{50} (mm)	D_{84} (mm)	σ	Scour		Side slope (ft)	Top width (ft)	
				ID	UP/DN																depth (ft)	Error (ft/ft)			
88	14	CO	5/22/84	1200	1	1	Live	Non-coh	Unkn	Sharp	Single	Piles	88	90.0	26.0	3.0	5.4	4.0	29.8	68.9	3.03	1.7	0.5	9.5	27.0
89	14	CO	5/22/84	1400	1	2	Live	Non-coh	Unkn	Sharp	Single	Piles	89	90.0	26.0	3.0	5.4	4.0	29.8	68.9	3.03	1.5	0.5	9.8	23.0
90	15	DE	11/28/88	1600	C2	1	Clear*	Unkn	Unkn	Square	Group	Piles	90	27.0	0.0	1.25	1.82	15.4	0.4	1.4	5.05	0.5	1.0	20.0	20.0
91	15	DE	11/15/90	1330	C2	1	Live*	Unkn	Unkn	Square	Group	Piles	91	27.0	0.0	1.25	2.22	17.3	0.4	1.4	5.05	0.8	1.0	6.0	10.0
92	15	DE	12/2/90	1300	C2	1	Clear*	Unkn	Unkn	Square	Group	Piles	92	27.0	0.0	1.25	1.33	15.7	0.4	1.4	5.05	1.0	1.0	7.5	15.0
93	15	DE	12/2/90	1400	C2	1	Live*	Unkn	Unkn	Square	Group	Piles	93	27.0	0.0	1.25	2.18	13.9	0.4	1.4	5.05	0.8	1.0	8.0	13.0
94	15	DE	12/4/90	1500	C2	1	Clear*	Unkn	Unkn	Square	Group	Piles	94	27.0	0.0	1.25	1.42	15.5	0.4	1.4	5.05	1.0	1.0	7.5	15.0
95	15	DE	10/7/91	1300	C2	1	Clear*	Unkn	Unkn	Square	Group	Piles	95	27.0	0.0	1.25	1.6	15.2	0.4	1.4	5.05	0.5	1.0	20.0	20.0
96	15	DE	6/10/92	0930	C2	1	Clear*	Unkn	Unkn	Square	Group	Piles	96	27.0	0.0	1.25	1.65	15.0	0.4	1.4	5.05	0.6	1.0	16.0	52.0
97	15	DE	6/10/92	1030	C2	1	Clear*	Unkn	Unkn	Square	Group	Piles	97	27.0	0.0	1.25	1.62	13.9	0.4	1.4	5.05	0.7	1.0	10.0	14.0
98	15	DE	6/10/92	1130	C2	1	Clear*	Unkn	Unkn	Square	Group	Piles	98	27.0	0.0	1.25	1.52	12.3	0.4	1.4	5.05	0.5	1.0	10.0	10.0
99	15	DE	11/15/90	1330	C3	1	Clear*	Unkn	Unkn	Square	Group	Piles	99	27.0	0.0	1.25	1.74	13.2	0.4	1.4	5.05	0.3	1.0	8.5	5.0
100	15	DE	6/10/92	1030	C3	1	Clear*	Unkn	Unkn	Square	Group	Piles	100	27.0	0.0	1.25	1.72	16.2	0.4	1.4	5.05	0.9	1.0	6.0	11.0
101	16	DE	9/24/91	1400	C	1	Clear*	Unkn	Unkn	Cylind	Group	Piles	101	43.0	0.0	2.5	0.88	10.4	0.18	0.37	2.03	2.4	1.0	7.0	33.0
102	16	DE	6/8/92	0900	C	1	Clear*	Unkn	Unkn	Cylind	Group	Piles	102	43.0	0.0	2.5	1.08	10.1	0.18	0.37	2.03	1.7	1.0	6.5	22.0
103	16	DE	6/8/92	1030	C	1	Clear*	Unkn	Unkn	Cylind	Group	Piles	103	43.0	0.0	2.5	0.84	10.2	0.18	0.37	2.03	1.1	1.0	7.5	17.0
104	16	DE	9/24/91	1400	E	1	Clear*	Unkn	Unkn	Cylind	Group	Piles	104	43.0	0.0	2.5	1.13	26.2	0.18	0.37	2.03	5.2	1.0	4.0	44.0
105	16	DE	6/8/92	0900	E	1	Clear*	Unkn	Unkn	Cylind	Group	Piles	105	43.0	0.0	2.5	1.55	25.5	0.18	0.37	2.03	4.5	1.0	4.5	41.0
106	16	DE	6/8/92	1030	E	1	Clear*	Unkn	Unkn	Cylind	Group	Piles	106	43.0	0.0	2.5	1.58	25.5	0.18	0.37	2.03	4.5	1.0	5.5	50.0
107	16	DE	9/24/91	1400	F	1	Clear*	Unkn	Unkn	Cylind	Group	Piles	107	43.0	0.0	2.5	1.42	23.4	0.18	0.37	2.03	1.5	1.0	9.0	27.0
108	16	DE	6/8/92	0900	F	1	Live*	Unkn	Unkn	Cylind	Group	Piles	108	43.0	0.0	2.5	1.67	25.0	0.18	0.37	2.03	4.0	1.0	5.0	39.0
109	16	DE	6/8/92	1030	F	1	Clear*	Unkn	Unkn	Cylind	Group	Piles	109	43.0	0.0	2.5	1.62	24.8	0.18	0.37	2.03	4.0	1.0	4.5	35.0
110	16	DE	9/24/91	1400	G	1	Clear*	Unkn	Unkn	Cylind	Group	Piles	110	43.0	0.0	2.5	0.92	12.6	0.18	0.37	2.03	1.4	1.0	2.0	3.0
111	16	DE	6/8/92	1030	G	1	Clear*	Unkn	Unkn	Cylind	Group	Piles	111	43.0	0.0	2.5	1.04	12.2	0.18	0.37	2.03	0.5	1.0	7.0	3.5
112	16	DE	6/8/92	0900	H	1	Clear*	Unkn	Unkn	Cylind	Group	Piles	112	43.0	0.0	2.5	0.8	4.9	0.18	0.37	2.03	1.5	1.0	7.5	23.0
113	16	DE	6/8/92	1030	H	1	Clear*	Unkn	Unkn	Cylind	Group	Piles	113	43.0	0.0	2.5	0.6	4.8	0.18	0.37	2.03	1.5	1.0	7.0	21.0
114	16	DE	6/8/92	0900	I	1	Clear*	Unkn	Unkn	Cylind	Group	Piles	114	43.0	0.0	2.5	0.72	1.0	0.18	0.37	2.03	0.7	1.0	15.0	20.0
115	17	GA	2/12/90	1445	11	1	Live	Non-coh	Insig	Square	Group	Piles	115	32.5	0.0	4.0	1.9	18.7	1.0	2.45	2.1	7.0	0.25	3.8	62.0
116	17	GA	2/12/90	1705	11	1	Live	Non-coh	Insig	Square	Group	Piles	116	32.5	0.0	4.0	1.7	18.1	1.0	2.45	2.1	6.6	0.25	3.4	58.0
117	17	GA	2/12/90	1300	12	1	Live	Non-coh	Insig	Square	Group	Piles	117	35.5	0.0	4.0	1.8	23.2	1.0	2.45	2.1	4.0	0.25	6.7	65.0
118	17	GA	2/12/90	1445	12	1	Live	Non-coh	Insig	Square	Group	Piles	118	35.5	0.0	4.0	2.3	20.9	1.0	2.45	2.1	4.7	0.25	5.0	73.0
119	17	GA	2/12/90	1705	12	1	Live	Non-coh	Insig	Square	Group	Piles	119	35.5	0.0	4.0	2.3	20.2	1.0	2.45	2.1	5.5	0.25	4.5	68.0
120	17	GA	2/12/90	1300	13	1	Live	Non-coh	Insig	Square	Group	Piles	120	35.5	0.0	6.0	1.7	26.4	1.0	2.45	2.1	3.9	0.25	6.2	87.0
121	17	GA	2/12/90	1445	13	1	Live	Non-coh	Insig	Square	Group	Piles	121	35.5	0.0	6.0	2.15	24.8	1.0	2.45	2.1	4.8	0.25	5.8	78.0
122	17	GA	2/12/90	1705	13	1	Live	Non-coh	Insig	Square	Group	Piles	122	35.5	0.0	6.0	2.23	23.1	1.0	2.45	2.1	5.2	0.25	5.2	83.0
123	18	IN	11/13/92	1230	1	2	Live	Non-coh	Unkn	Round	Single	Poured	123	33.5	0.0	3.0	1.01	16.8	0.5	2.25	3.0	1.4	0.5	3.6	9.6
124	18	IN	11/13/92	1030	2	1	Live	Non-coh	Unkn	Round	Single	Poured	124	33.5	0.0	3.0	2.5	19.5	0.5	2.25	3.0	3.4	0.5	5.4	34.0
125	19	IN	1/3/91	1100	8	1	Live	Non-coh	Unkn	Round	Single	Poured	125	34.5	5.0	3.0	5.2	30.9	0.34	0.46	1.38	2.3	0.5	15.7	24.5
126	19	IN	1/3/91	1145	8	2	Live	Non-coh	Unkn	Round	Single	Poured	126	34.5	5.0	3.0	5.2	30.9	0.3	0.46	1.38	1.5	0.5	7.0	22.0
127	20	IN	1/3/91	1230	2	1	Live	Non-coh	Unkn	Round	Single	Poured	127	47.5	5.0	3.0	3.6	11.3	0.9	4.2	4.2	1.2	0.5	9.5	24.0
128	20	IN	1/4/91	1200	2	1	Live	Non-coh	Unkn	Round	Single	Poured	128	47.5	5.0	3.0	3.3	10.4	0.9	4.2	4.2	1.3	0.5	6.7	14.0
129	20	IN	1/4/91	1300	2	2	Live	Non-coh	Unkn	Round	Single	Poured	129	47.5	5.0	3.0	3.3	10.4	0.9	4.2	4.2	0.8	0.5	11.4	19.0
130	20	IN	1/3/91	1230	3	1	Live	Non-coh	Unkn	Round	Single	Poured	130	43.0	0.0	3.0	4.2	16.7	0.9	4.2	4.2	2.2	0.5	6.7	56.0
131	20	IN	1/3/91	1230	4	1	Live	Non-coh	Unkn	Round	Single	Poured	131	42.0	10.0	2.0	5.4	21.5	0.9	4.2	4.2	3.5	0.5	5.7	91.0

Table 5. Summary of local scour measurements at bridge piers (continued).

Measurement number	Site number	State	Date M/D/Y	Time	Pier		Bed-load transport	Bed-material cohesion	Debris	Pier shape	Pier type	Foundation type	Measurement number	Pier length (ft)	Pier skew (deg)	Pier width (ft)	Flow velocity (ft/s)	Flow depth (ft)	D ₅₀ (mm)	D ₈₄ (mm)	σ	Scour depth (ft)	Error (ft/ft)	Side slope (ft)	Top width (ft)
					ID	UP/DN																			
132	20	IN	1/4/91	1200	4	1	Live	Non-coh	Unkn	Round	Single	Poured	132	42.0	10.0	2.0	6.1	20.2	0.9	4.2	4.2	4.1	0.5	5.7	78.0
133	21	LA	5/19/90	1420	4	1	Live	Non-coh	Insig	Sharp	Single	Piles	133	54.0	0.0	14.0	8.4	38.0	0.3	0.4	1.4	12.2	2.0	3.0	172.0
134	21	LA	5/19/90	1530	4	2	Live	Non-coh	Insig	Sharp	Single	Piles	134	54.0	0.0	14.0	8.4	40.2	0.3	0.4	1.4	3.0	1.0	9.0	121.0
135	21	LA	5/22/90	1335	4	1	Live	Non-coh	Insig	Sharp	Single	Piles	135	54.0	0.0	14.0	6.9	30.9	0.3	0.4	1.4	11.4	1.0	4.5	119.0
136	21	LA	5/22/90	1445	4	2	Live	Non-coh	Insig	Sharp	Single	Piles	136	54.0	0.0	14.0	6.9	30.8	0.3	0.4	1.4	3.7	1.0	9.7	95.0
137	21	LA	5/19/90	1420	5	1	Live	Non-coh	Insig	Sharp	Single	Piles	137	54.0	0.0	14.0	10.4	39.2	0.3	0.4	1.4	22.9	2.0	4.7	279.0
138	21	LA	5/19/90	1530	5	2	Live	Non-coh	Insig	Sharp	Single	Piles	138	54.0	0.0	14.0	10.4	41.4	0.3	0.4	1.4	17.0	2.0	5.9	221.0
139	21	LA	5/22/90	1335	5	1	Live	Non-coh	Insig	Sharp	Single	Piles	139	54.0	0.0	14.0	9.5	32.1	0.3	0.4	1.4	25.1	1.0	4.2	281.0
140	21	LA	5/22/90	1445	5	2	Live	Non-coh	Insig	Sharp	Single	Piles	140	54.0	0.0	14.0	9.5	32.1	0.3	0.4	1.4	18.5	1.0	5.9	264.0
141	22	LA	5/17/90	1330	4	1	Live	Non-coh	Insig	Round	Single	Poured	141	40.0	0.0	14.0	8.2	38.3	0.3	0.4	1.4	14.4	1.0	4.0	133.0
142	22	LA	5/17/90	1510	4	2	Live	Non-coh	Insig	Round	Single	Poured	142	40.0	0.0	14.0	8.2	38.5	0.3	0.4	1.4	12.9	2.0	6.6	181.0
143	22	LA	5/19/90	1025	4	1	Live	Non-coh	Insig	Round	Single	Poured	143	40.0	0.0	14.0	8.4	35.5	0.3	0.4	1.4	10.8	2.0	6.6	136.0
144	22	LA	5/19/90	1255	4	2	Live	Non-coh	Insig	Round	Single	Poured	144	40.0	0.0	14.0	8.4	37.0	0.3	0.4	1.4	6.8	1.0	11.0	173.0
145	22	LA	5/22/90	1030	4	1	Live	Non-coh	Insig	Round	Single	Poured	145	40.0	0.0	14.0	6.9	30.6	0.3	0.4	1.4	12.6	1.0	6.0	117.0
146	22	LA	5/22/90	0855	4	2	Live	Non-coh	Insig	Round	Single	Poured	146	40.0	0.0	14.0	6.9	30.4	0.3	0.4	1.4	13.7	1.0	4.9	138.0
147	22	LA	5/17/90	1510	5	2	Live	Non-coh	Insig	Round	Single	Poured	147	40.0	0.0	14.0	9.8	38.5	0.3	0.4	1.4	15.6	2.0	3.3	234.0
148	22	LA	5/17/90	1330	5	1	Live	Non-coh	Insig	Round	Single	Poured	148	40.0	0.0	14.0	9.8	39.5	0.3	0.4	1.4	14.9	1.0	3.3	125.0
149	22	LA	5/19/90	1025	5	1	Live	Non-coh	Insig	Round	Single	Poured	149	40.0	0.0	14.0	10.4	36.7	0.3	0.4	1.4	18.1	1.0	4.0	218.0
150	22	LA	5/19/90	1255	5	2	Live	Non-coh	Insig	Round	Single	Poured	150	40.0	0.0	14.0	10.4	38.3	0.3	0.4	1.4	16.9	1.0	6.7	235.0
151	22	LA	5/22/90	1030	5	1	Live	Non-coh	Insig	Round	Single	Poured	151	40.0	0.0	14.0	9.5	31.8	0.3	0.4	1.4	12.3	1.0	5.0	163.0
152	22	LA	5/22/90	0855	5	2	Live	Non-coh	Insig	Round	Single	Poured	152	40.0	0.0	14.0	9.5	31.6	0.3	0.4	1.4	18.5	2.0	5.9	210.0
153	23	MD	7/13/90	1300	Left	1	Clear*	Unkn	Unkn	Sharp	Single	Poured	153	41.7	0.0	5.0	7.66	7.9	108.0	233.0	1.8	1.1	1.0	15.0	25.0
154	23	MD	4/1/93	0930	Left	1	Clear*	Unkn	Unkn	Sharp	Single	Poured	154	41.7	0.0	5.0	6.85	6.8	108.0	233.0	1.8	1.4	1.0	13.0	35.0
155	23	MD	7/13/90	1300	Rt	1	Clear*	Unkn	Unkn	Sharp	Single	Poured	155	41.7	0.0	5.0	8.62	9.9	108.0	233.0	1.8	2.7	1.0	9.5	52.0
156	23	MD	4/1/93	0930	Rt	1	Clear*	Unkn	Unkn	Sharp	Single	Poured	156	41.7	0.0	5.0	6.2	8.0	108.0	233.0	1.8	1.7	1.0	16.0	55.0
157	24	MD	6/23/72	1730	1	1	Clear*	Unkn	Unkn	Round	Single	Poured	157	32.0	0.0	4.0	2.64	11.6	22.0	76.0	2.4	1.2	1.0	6.0	15.0
158	24	MD	9/25/75	1900	1	1	Clear*	Unkn	Unkn	Round	Single	Poured	158	32.0	0.0	4.0	4.28	10.2	22.0	76.0	2.4	1.4	1.0	8.5	24.0
159	24	MD	6/23/72	1730	2	1	Clear*	Unkn	Unkn	Round	Single	Poured	159	32.0	0.0	4.0	3.72	8.0	22.0	76.0	2.4	2.4	1.0	10.0	50.0
160	24	MD	9/25/75	1900	2	1	Clear*	Unkn	Unkn	Round	Single	Poured	160	32.0	0.0	4.0	5.2	8.0	22.0	76.0	2.4	1.8	1.0	3.5	12.0
161	24	MD	5/29/90	2030	2	1	Clear*	Unkn	Unkn	Round	Single	Poured	161	32.0	0.0	4.0	3.32	6.3	22.0	76.0	2.4	1.0	1.0	6.0	12.0
162	24	MD	10/23/90	1530	2	1	Clear*	Unkn	Unkn	Round	Single	Poured	162	32.0	0.0	4.0	5.39	6.6	22.0	76.0	2.4	1.2	1.0	4.0	10.0
163	24	MD	10/23/90	2000	2	1	Clear*	Unkn	Unkn	Round	Single	Poured	163	32.0	0.0	4.0	5.26	10.1	22.0	76.0	2.4	1.7	1.0	4.5	16.0
164	25	MD	2/23/89	1100	Left	1	Live*	Non-coh	Unkn	Unkn	Single	Unkn	164	35.0	0.0	4.0	2.18	6.2	0.38	0.94	2.29	4.0	1.0	6.0	50.0
165	25	MD	3/25/89	1400	Left	1	Live*	Non-coh	Unkn	Unkn	Single	Unkn	165	35.0	0.0	4.0	2.53	10.1	0.38	0.94	2.29	5.4	1.0	6.5	72.0
166	25	MD	7/28/91	1030	Left	1	Live*	Non-coh	Unkn	Unkn	Single	Unkn	166	35.0	0.0	4.0	2.52	7.3	0.38	0.94	2.29	4.3	1.0	3.5	55.0
167	25	MD	3/25/89	1400	Cntr	1	Clear*	Unkn	Unkn	Unkn	Single	Unkn	167	35.0	0.0	4.0	1.36	7.1	0.38	0.94	2.29	2.4	1.0	5.0	25.0
168	25	MD	7/28/91	1030	Cntr	1	Clear*	Unkn	Unkn	Unkn	Single	Unkn	168	35.0	0.0	4.0	0.71	4.9	0.38	0.94	2.29	2.0	1.0	7.0	27.0
169	25	MD	2/23/89	1100	Rt	1	Clear*	Unkn	Unkn	Unkn	Single	Unkn	169	35.0	0.0	4.0	0.9	3.7	0.38	0.94	2.29	1.6	1.0	18.0	58.0
170	25	MD	2/23/89	1400	Rt	1	Live*	Unkn	Unkn	Unkn	Single	Unkn	170	35.0	0.0	4.0	1.89	7.0	0.38	0.94	2.29	2.3	1.0	13.0	60.0
171	25	MD	7/28/91	1030	Rt	1	Clear*	Unkn	Unkn	Unkn	Single	Unkn	171	35.0	0.0	4.0	1.04	4.8	0.38	0.94	2.29	2.2	1.0	11.0	48.0
172	26	MS	2/25/91	1430	12L	1	Clear	Cohesive	Insig	Square	Group	Piles	172	26.3	28.0	1.33	2.52	9.6	--	--	--	2.0	0.5	1.6	16.0
173	26	MS	5/1/91	1000	12L	2	Clear	Cohesive	Insig	Square	Group	Piles	173	26.3	23.0	1.33	2.78	16.7	--	--	--	2.5	0.5	2.5	18.0
174	26	MS	2/25/91	1430	14L	1	Clear	Cohesive	Insig	Square	Group	Piles	174	26.3	18.0	1.33	3.14	24.1	--	--	--	0.0	0.5	--	--
175	26	MS	5/1/91	1000	14L	1	Clear	Cohesive	Insig	Square	Group	Piles	175	26.3	16.0	1.33	4.16	21.0	--	--	--	0.0	0.5	--	--

Table 5. Summary of local scour measurements at bridge piers (continued).

Mea- sure- ment num- ber	Site num- ber	State	Date M/D/Y	Time	Pier ID	UP/DN	Bed- load trans- port	Bed mat- erial cohe- sion	Debris	Pier shape	Pier type	Foun- dation type	Mea- sure- ment num- ber	Pier length (ft)	Pier skew (deg)	Pier width (ft)	Flow velo- city (ft/s)	Flow depth (ft)	D ₅₀ (mm)	D ₈₄ (mm)	σ	Scour depth (ft)	Error (ft/ft)	Side slope (ft)	Top width (ft)
176	26	MS	2/25/91	1430	15L	1	Live	Non-coh	Insig	Square	Group	Piles	176	26.3	16.0	1.33	3.78	29.2	0.54	1.2	1.8	1.3	0.5	2.7	20.0
177	26	MS	5/1/91	1000	15L	2	Live	Non-coh	Insig	Square	Group	Piles	177	26.3	14.0	1.33	4.39	29.0	0.54	1.2	1.8	3.0	0.5	5.8	40.0
178	26	MS	2/25/91	1430	16L	1	Live	Non-coh	Insig	Square	Group	Piles	178	26.3	16.0	2.66	3.96	29.0	0.54	1.2	1.8	1.4	0.5	4.6	23.0
179	26	MS	5/1/91	1000	16L	1	Live	Non-coh	Mod	Square	Group	Piles	179	26.3	8.0	2.66	4.68	26.9	0.54	1.2	1.8	1.4	0.5	--	24.0
180	26	MS	1/31/90	1500	17L	1	Live	Non-coh	Insig	Cylind	Group	Poured	180	20.5	11.0	5.8	2.84	17.5	0.39	0.9	1.9	2.0	0.5	4.7	25.0
181	26	MS	2/25/91	1430	17L	1	Live	Non-coh	Insig	Cylind	Group	Poured	181	20.5	16.0	5.4	3.37	22.0	0.39	0.9	1.9	3.6	0.5	3.8	41.0
182	26	MS	5/1/91	1000	17L	1	Live	Non-coh	Insig	Cylind	Group	Poured	182	20.5	11.0	4.7	3.47	21.4	0.39	0.9	1.9	4.1	0.5	3.9	41.0
183	26	MS	1/31/90	1500	18L	1	Live	Non-coh	Mod	Cylind	Group	Poured	183	20.5	11.0	5.8	1.3	17.4	0.39	0.9	1.9	1.6	0.5	2.4	19.0
184	26	MS	2/25/91	1430	18L	1	Live	Non-coh	Mod	Cylind	Group	Poured	184	20.5	16.0	5.3	1.91	21.1	0.39	0.9	1.9	2.0	0.5	3.9	21.0
185	26	MS	5/1/91	1000	18L	2	Live	Non-coh	Insig	Cylind	Group	Poured	185	20.5	14.0	4.9	2.21	22.3	0.39	0.9	1.9	2.6	0.5	2.0	18.0
186	27	MS	5/1/91	1120	15R	1	Live	Non-coh	Insig	Square	Group	Piles	186	26.3	16.0	1.33	5.1	30.6	0.54	1.2	1.8	1.4	0.5	5.9	20.0
187	27	MS	2/25/91	1520	16R	1	Live	Non-coh	Insig	Square	Group	Piles	187	26.3	16.0	2.67	3.9	27.5	0.54	1.2	1.8	2.9	0.5	2.8	19.0
188	27	MS	5/1/91	1120	16R	2	Live	Non-coh	Insig	Square	Group	Piles	188	26.3	11.0	2.67	4.7	26.6	0.54	1.2	1.8	2.1	0.5	3.9	26.0
189	27	MS	2/25/91	1520	17R	1	Live	Non-coh	Insig	Cylind	Group	Poured	189	20.5	16.0	5.5	2.8	23.3	0.39	0.9	1.9	1.6	0.5	6.4	27.0
190	27	MS	5/1/91	1120	17R	1	Live	Non-coh	Insig	Cylind	Group	Poured	190	20.5	8.0	4.8	3.2	21.7	0.39	0.9	1.9	3.9	0.5	2.2	28.0
191	27	MS	2/25/91	1520	18R	1	Live	Non-coh	Insig	Cylind	Group	Poured	191	20.5	20.0	5.1	2.4	20.2	0.39	0.9	1.9	5.7	0.5	2.3	31.0
192	27	MS	5/1/91	1120	18R	1	Live	Non-coh	Insig	Cylind	Group	Poured	192	20.5	14.0	5.1	2.0	23.0	0.39	0.9	1.9	3.7	0.5	3.2	26.0
193	28	MS	1/25/90	0900	3	1	Live	Non-coh	Insig	Cylind	Single	Poured	193	8.0	0.0	8.0	6.2	10.0	7.51	23.2	6.9	4.1	1.0	--	--
194	28	MS	8/27/92	1010	3	2	Live	Non-coh	Subst	Cylind	Single	Poured	194	8.0	0.0	8.0	6.24	8.5	7.51	23.2	6.9	3.2	1.0	8.0	50.0
195	28	MS	12/21/72	0600	4	1	Live	Non-coh	Unkn	Cylind	Single	Poured	195	8.0	0.0	8.0	7.0	12.9	7.51	23.2	6.9	2.9	0.5	--	--
196	28	MS	4/25/73	0530	4	1	Live	Non-coh	Unkn	Cylind	Single	Poured	196	8.0	0.0	8.0	6.1	8.7	7.51	23.2	6.9	2.9	0.5	--	--
197	28	MS	1/25/90	0900	4	1	Live	Non-coh	Insig	Cylind	Single	Poured	197	8.0	0.0	8.0	6.94	9.5	7.51	23.2	6.9	3.9	1.0	--	--
198	28	MS	8/27/92	1110	4	1	Live	Non-coh	Insig	Cylind	Single	Poured	198	8.0	0.0	8.0	7.4	8.7	7.51	23.2	6.9	6.4	1.0	--	--
199	28	MS	1/25/90	0900	5	1	Live	Non-coh	Insig	Cylind	Single	Poured	199	8.0	0.0	8.0	5.74	10.0	7.51	23.2	6.9	4.7	1.0	--	--
200	28	MS	8/27/92	1055	5	1	Live	Non-coh	Insig	Cylind	Single	Poured	200	8.0	0.0	8.0	6.55	10.2	7.51	23.2	6.9	4.5	1.0	--	--
201	29	MS	1/30/90	1415	4	2	Live	Non-coh	Insig	Square	Single	Poured	201	26.8	14.0	5.4	7.0	22.3	6.9	15.0	6.2	4.8	0.5	3.1	35.0
202	29	MS	5/10/91	1445	4	1	Live	Non-coh	Insig	Square	Single	Poured	202	26.8	8.0	5.4	7.0	24.6	6.9	15.0	6.2	2.3	0.5	3.3	21.0
203	29	MS	1/30/90	1415	5	1	Live	Non-coh	Insig	Square	Single	Poured	203	26.8	8.0	6.1	6.5	28.1	6.9	15.0	6.2	5.3	0.5	2.8	35.0
204	29	MS	5/10/91	1445	5	2	Live	Non-coh	Insig	Square	Single	Poured	204	26.8	11.0	6.0	6.4	28.9	6.9	15.0	6.2	3.9	0.5	4.4	47.0
205	29	MS	1/30/90	1415	6	1	Live	Non-coh	Insig	Square	Single	Poured	205	26.5	0.0	5.5	3.5	26.4	6.9	15.0	6.2	5.7	1.0	2.6	37.0
206	29	MS	5/10/91	1445	6	2	Live	Non-coh	Insig	Square	Single	Poured	206	26.5	11.0	5.7	5.1	30.1	6.9	15.0	6.2	7.4	1.0	3.0	61.0
207	29	MS	1/30/90	1415	7	1	Live	Non-coh	Insig	Square	Group	Poured	207	23.0	0.0	3.9	1.9	23.0	6.9	15.0	6.2	4.1	0.5	3.8	27.0
208	29	MS	5/10/91	1445	7	2	Live	Non-coh	Insig	Square	Group	Poured	208	23.0	0.0	4.1	2.9	28.9	6.9	15.0	6.2	2.5	1.0	3.0	35.0
209	30	MS	1/27/90	1455	6	1	Live	Non-coh	Insig	Cylind	Group	Piles	209	21.0	16.0	5.5	5.55	30.1	6.9	15.0	6.2	4.9	0.5	3.4	46.0
210	30	MS	1/30/90	1500	6	2	Live	Non-coh	Unkn	Cylind	Group	Piles	210	21.0	14.0	5.5	6.94	27.7	6.9	15.0	6.2	6.5	0.5	4.1	62.0
211	30	MS	2/5/90	1735	6	2	Live	Non-coh	Unkn	Cylind	Group	Piles	211	21.0	18.0	5.8	4.24	25.1	6.9	15.0	6.2	6.6	0.5	2.1	30.0
212	30	MS	5/10/91	1045	6	1	Live	Non-coh	Unkn	Cylind	Group	Piles	212	21.0	14.0	5.4	7.17	27.3	6.9	15.0	6.2	9.9	0.5	2.1	49.0
213	30	MS	1/27/90	1230	5	1	Live	Non-coh	Unkn	Cylind	Group	Piles	213	21.0	22.0	5.5	7.69	28.4	6.9	15.0	6.2	7.5	0.5	4.8	82.0
214	30	MS	1/30/90	1500	5	1	Live	Non-coh	Unkn	Cylind	Group	Piles	214	21.0	8.0	6.4	5.69	28.6	6.9	15.0	6.2	3.3	0.5	3.3	44.0
215	30	MS	2/5/90	1735	5	1	Live	Non-coh	Unkn	Cylind	Group	Piles	215	21.0	16.0	5.8	4.34	25.7	6.9	15.0	6.2	2.0	0.5	5.2	38.0
216	30	MS	5/10/91	1045	5	2	Live	Non-coh	Unkn	Cylind	Group	Piles	216	21.0	11.0	5.5	6.64	28.9	6.9	15.0	6.2	4.5	0.5	2.8	36.0
217	30	MS	1/27/90	1455	4	1	Live	Non-coh	Unkn	Cylind	Group	Piles	217	21.0	8.0	5.4	5.33	26.9	6.9	15.0	6.2	1.9	0.5	7.2	34.0
218	30	MS	1/30/90	1500	4	1	Live	Non-coh	Unkn	Cylind	Group	Piles	218	21.0	8.0	5.5	4.64	25.0	6.9	15.0	6.2	3.2	0.5	4.5	41.0
219	30	MS	5/10/91	1045	4	1	Live	Non-coh	Unkn	Cylind	Group	Piles	219	21.0	11.0	5.5	5.14	29.1	6.9	15.0	6.2	1.4	0.5	4.4	13.0

Table 5. Summary of local scour measurements at bridge piers (continued).

Measurement number	Site number	State	Date M/D/Y	Time	Pier ID	UP/DN	Bed-load transport	Bed material cohesion	Debris	Pier shape	Pier type	Foundation type	Measurement number	Pier length (ft)	Pier skew (deg)	Pier width (ft)	Flow velocity (ft/s)	Flow depth (ft)	D ₅₀ (mm)	D ₈₄ (mm)	σ	Scour depth (ft)	Error (ft/ft)	Side slope (ft)	Top width (ft)
220	31	MT	6/6/91	1115	P1	1	Clear	Non-coh	Insig	Sharp	Single	Poured	220	50.0	5.0	4.3	8.35	8.6	39.0	90.0	2.3	3.7	0.3	7.0	54.0
221	31	MT	6/10/91	1230	P1	1	Clear	Non-coh	Insig	Sharp	Single	Poured	221	50.0	5.0	4.3	7.04	6.4	39.0	90.0	2.3	2.7	0.3	12.4	47.0
222	31	MT	6/13/91	1230	P1	1	Clear	Non-coh	Insig	Sharp	Single	Poured	222	50.0	5.0	4.3	6.98	7.5	39.0	90.0	2.3	2.7	0.3	7.6	45.0
223	31	MT	6/18/91	1245	P1	1	Clear	Non-coh	Insig	Sharp	Single	Poured	223	50.0	5.0	4.3	5.0	4.6	39.0	90.0	2.3	3.2	0.3	9.8	45.0
224	31	MT	6/6/91	1115	P2	1	Clear	Non-coh	Insig	Sharp	Single	Poured	224	50.0	5.0	4.3	6.53	7.1	39.0	90.0	2.3	2.6	0.3	6.4	45.0
225	31	MT	6/10/91	1230	P2	1	Clear	Non-coh	Insig	Sharp	Single	Poured	225	50.0	5.0	4.3	6.01	5.6	39.0	90.0	2.3	3.0	0.3	6.7	45.0
226	31	MT	6/13/91	1230	P2	1	Clear	Non-coh	Insig	Sharp	Single	Poured	226	50.0	5.0	4.3	6.98	6.3	39.0	90.0	2.3	2.8	0.3	8.7	45.0
227	31	MT	6/18/91	1245	P2	1	Clear	Non-coh	Insig	Sharp	Single	Poured	227	50.0	5.0	4.3	3.63	4.1	39.0	90.0	2.3	3.0	0.3	7.0	45.0
228	32	MT	6/6/91	1335	P1	1	Clear	Non-coh	Insig	Sharp	Single	Poured	228	39.3	3.0	3.4	8.4	4.8	95.0	230.0	2.5	0.8	0.3	6.5	15.0
229	32	MT	6/18/92	1445	P1	1	Clear	Non-coh	Insig	Sharp	Single	Poured	229	39.3	3.0	3.4	5.1	3.3	95.0	230.0	2.5	1.2	0.3	12.1	19.0
230	32	MT	6/23/93	0000	P1	1	Clear	Non-coh	Insig	Sharp	Single	Poured	230	39.3	3.0	3.4	6.2	3.4	95.0	230.0	2.5	1.9	0.3	8.3	23.0
231	32	MT	6/6/91	1335	P2	1	Clear	Non-coh	Insig	Sharp	Single	Poured	231	39.5	3.0	3.4	10.6	5.5	95.0	230.0	2.5	5.5	0.5	4.1	44.0
232	32	MT	6/18/92	1445	P2	1	Clear	Non-coh	Insig	Sharp	Single	Poured	232	39.5	3.0	3.4	7.0	3.7	95.0	230.0	2.5	4.6	0.5	5.3	44.0
233	32	MT	6/23/93	0000	P2	1	Clear	Non-coh	Insig	Sharp	Single	Poured	233	39.5	3.0	3.4	7.0	3.8	95.0	230.0	2.5	4.5	0.5	5.7	48.0
234	33	MT	5/21/93	1610	P1	1	Clear	Non-coh	Unkn	Sharp	Single	Poured	234	34.0	0.0	3.1	8.0	8.7	73.0	150.0	2.3	2.5	0.5	6.8	34.0
235	33	MT	5/27/93	1000	P1	1	Clear	Non-coh	Unkn	Sharp	Single	Poured	235	34.0	0.0	3.1	8.2	8.3	73.0	150.0	2.3	2.3	0.5	9.8	46.0
236	33	MT	6/30/93	1030	P1	1	Clear	Non-coh	Unkn	Sharp	Single	Poured	236	34.0	0.0	3.1	4.9	6.6	73.0	150.0	2.3	1.9	0.5	4.8	18.0
237	33	MT	5/21/93	1610	P2	1	Clear	Non-coh	Unkn	Sharp	Single	Poured	237	34.0	0.0	3.2	7.6	8.2	73.0	150.0	2.3	1.6	0.3	15.3	49.0
238	33	MT	5/27/93	1000	P2	1	Clear	Non-coh	Unkn	Sharp	Single	Poured	238	34.0	0.0	3.1	8.0	7.8	73.0	150.0	2.3	1.8	0.3	11.1	41.0
239	33	MT	6/30/93	1030	P2	1	Clear	Non-coh	Unkn	Sharp	Single	Poured	239	34.0	0.0	3.2	4.8	6.2	73.0	150.0	2.3	1.1	0.3	7.7	18.0
240	33	MT	5/21/93	1610	P3	1	Clear	Non-coh	Unkn	Sharp	Single	Poured	240	34.0	0.0	3.1	3.3	7.4	73.0	150.0	2.3	0.3	0.3	2.5	6.0
241	33	MT	5/27/93	1000	P3	1	Clear	Non-coh	Unkn	Sharp	Single	Poured	241	34.0	0.0	3.1	3.6	6.8	73.0	150.0	2.3	0.4	0.3	2.5	6.0
242	33	MT	6/30/93	1030	P3	1	Clear	Non-coh	Unkn	Sharp	Single	Poured	242	34.0	0.0	3.1	3.5	6.0	73.0	150.0	2.3	0.4	0.3	2.5	11.0
243	34	MT	5/21/91	1530	P1	1	Live	Non-coh	Mod	Sharp	Single	Poured	243	36.0	0.0	3.4	5.4	1.7	8.0	30.0	9.3	1.2	0.5	10.0	24.0
244	34	MT	6/4/91	1240	P1	1	Live	Non-coh	Mod	Sharp	Single	Poured	244	36.0	0.0	3.4	4.4	1.5	8.0	30.0	9.3	1.7	0.5	4.7	16.0
245	34	MT	6/21/91	1450	P1	1	Live	Non-coh	Mod	Sharp	Single	Poured	245	36.0	0.0	3.4	4.2	1.3	8.0	30.0	9.3	1.5	0.5	10.7	32.0
246	34	MT	5/21/91	1530	P3	1	Live	Non-coh	Mod	Sharp	Single	Poured	246	36.0	0.0	3.4	5.4	1.3	8.0	30.0	9.3	3.2	0.3	7.0	45.0
247	34	MT	6/4/91	1240	P3	1	Live	Non-coh	Mod	Sharp	Single	Poured	247	36.0	0.0	3.4	4.7	1.0	8.0	30.0	9.3	3.4	0.3	6.6	45.0
248	34	MT	6/21/91	1450	P3	1	Live	Non-coh	Mod	Sharp	Single	Poured	248	36.0	0.0	3.4	5.4	1.5	8.0	30.0	9.3	3.5	0.3	6.4	45.0
249	34	MT	5/21/91	1530	P4	1	Live	Non-coh	Mod	Sharp	Single	Poured	249	36.0	0.0	3.4	4.1	0.9	8.0	30.0	9.3	1.6	0.3	8.8	14.0
250	34	MT	6/4/91	1240	P4	1	Live	Non-coh	Mod	Sharp	Single	Poured	250	36.0	0.0	3.4	2.5	0.4	8.0	30.0	9.3	1.0	0.3	4.1	12.0
251	34	MT	6/21/91	1450	P4	1	Live	Non-coh	Mod	Sharp	Single	Poured	251	36.0	0.0	3.4	2.1	0.5	8.0	30.0	9.3	1.2	0.3	5.2	15.0
252	35	NY	10/24/90	0000	1	1	Clear	Non-coh	Insig	Round	Single	Piles	252	40.0	30.0	3.0	6.8	10.3	32.0	55.0	1.75	5.2	0.2	6.6	52.0
253	36	NY	10/23/70	0000	6	1	Clear*	Non-coh	Unkn	Round	Single	Piles	253	48.0	0.0	5.0	1.6	5.7	27.0	58.0	2.3	0.0	0.5	--	--
254	36	NY	6/24/72	0000	6	1	Live*	Non-coh	Unkn	Round	Single	Piles	254	48.0	0.0	5.0	8.7	19.0	27.0	58.0	2.3	2.0	0.5	11.4	112.0
255	36	NY	9/28/75	0000	6	1	Clear*	Non-coh	Unkn	Round	Single	Piles	255	48.0	0.0	5.0	7.4	12.4	27.0	58.0	2.3	0.9	0.5	16.6	30.0
256	36	NY	3/25/80	0000	6	1	Clear	Non-coh	Unkn	Round	Single	Piles	256	48.0	0.0	5.0	5.4	8.5	27.0	58.0	2.3	0.0	0.5	--	--
257	36	NY	10/23/70	0000	5	1	Clear*	Non-coh	Unkn	Round	Single	Piles	257	48.0	0.0	5.0	2.5	6.7	27.0	58.0	2.3	0.0	0.5	--	--
258	36	NY	6/24/72	0000	5	1	Live*	Non-coh	Unkn	Round	Single	Piles	258	48.0	0.0	5.0	10.5	26.5	27.0	58.0	2.3	3.9	0.5	7.8	60.0
259	36	NY	9/28/75	0000	5	1	Live*	Non-coh	Unkn	Round	Single	Piles	259	48.0	0.0	5.0	8.9	17.8	27.0	58.0	2.3	1.9	0.5	20.5	86.0
260	36	NY	3/25/80	0000	5	1	Clear	Non-coh	Unkn	Round	Single	Piles	260	48.0	0.0	5.0	6.5	11.8	27.0	58.0	2.3	0.0	0.5	--	--
261	36	NY	10/23/70	0000	4	1	Clear*	Non-coh	Unkn	Round	Single	Piles	261	48.0	0.0	5.0	3.3	7.8	27.0	58.0	2.3	0.0	0.5	--	--
262	36	NY	6/24/72	0000	4	1	Live*	Non-coh	Unkn	Round	Single	Piles	262	48.0	0.0	5.0	11.2	31.9	27.0	58.0	2.3	4.3	1.0	10.5	95.0
263	36	NY	9/28/75	0000	4	1	Live*	Non-coh	Unkn	Round	Single	Piles	263	48.0	0.0	5.0	9.5	18.7	27.0	58.0	2.3	1.9	0.5	17.0	85.0

Table 5. Summary of local scour measurements at bridge piers (continued).

Measure- ment num- ber	Site num- ber	State	Date M/D/Y	Time	Pier ID	UP/DN	Bed	Bed- load trans- port	Bed mat- erial cohe- sion	Debris	Pier shape	Pier type	Foun- dation type	Mea- sure- ment num- ber	Pier length (ft)	Pier skew (deg)	Pier width (ft)	Flow velo- city (ft/s)	Flow depth (ft)	D ₅₀ (mm)	D ₈₄ (mm)	σ	Scour depth (ft)	Error (ft/ft)	Side slope (ft)	Top width (ft)
							Clear																			
264	36	NY	3/25/80	0000	4	1	Clear	Non-coh	Unkn	Round	Single	Piles	264	48.0	0.0	5.0	7.0	12.3	27.0	58.0	2.3	0.0	0.5	--	--	
265	36	NY	10/23/70	0000	3	1	Clear*	Non-coh	Unkn	Round	Single	Piles	265	48.0	0.0	5.0	5.0	11.2	27.0	58.0	2.3	0.0	0.5	--	--	
266	36	NY	6/24/72	0000	3	1	Live*	Non-coh	Unkn	Round	Single	Piles	266	48.0	0.0	5.0	12.3	31.4	27.0	58.0	2.3	3.9	0.5	7.6	61.0	
267	36	NY	9/28/75	0000	3	1	Live*	Non-coh	Unkn	Round	Single	Piles	267	48.0	0.0	5.0	10.4	19.0	27.0	58.0	2.3	2.3	0.5	14.0	70.0	
268	36	NY	3/25/80	0000	3	1	Clear	Non-coh	Unkn	Round	Single	Piles	268	48.0	0.0	5.0	7.6	12.6	27.0	58.0	2.3	3.3	0.5	--	--	
269	36	NY	10/23/70	0000	2	1	Clear*	Non-coh	Unkn	Round	Single	Piles	269	48.0	0.0	5.0	6.0	12.0	27.0	58.0	2.3	0.9	0.5	31.2	75.0	
270	36	NY	6/24/72	0000	2	1	Live*	Non-coh	Unkn	Round	Single	Piles	270	48.0	0.0	5.0	12.9	31.1	27.0	58.0	2.3	4.1	0.5	12.9	109.0	
271	36	NY	3/25/80	0000	2	1	Clear	Non-coh	Unkn	Round	Single	Piles	271	48.0	0.0	5.0	8.0	16.2	27.0	58.0	2.3	3.0	0.5	7.3	79.0	
272	36	NY	10/23/70	0000	1	1	Clear*	Non-coh	Unkn	Round	Single	Piles	272	48.0	0.0	5.0	6.5	12.5	27.0	58.0	2.3	1.7	0.5	9.5	38.0	
273	36	NY	6/24/72	0000	1	1	Live*	Non-coh	Unkn	Round	Single	Piles	273	48.0	0.0	5.0	13.4	27.3	27.0	58.0	2.3	5.1	0.5	7.9	64.0	
274	37	NY	11/17/89	0000	2	1	Clear	Non-coh	Insig	Round	Single	Piles	274	43.0	0.0	5.5	11.0	16.7	33.0	60.0	2.0	3.5	0.2	6.6	41.0	
275	37	NY	11/17/89	0000	1	1	Clear	Non-coh	Insig	Round	Single	Piles	275	43.0	0.0	5.5	12.0	17.9	33.0	60.0	2.0	1.9	0.2	10.9	37.0	
276	38	NY	8/27/91	0000	2	1	Clear	Non-coh	Unkn	Round	Single	Piles	276	40.0	0.0	5.0	8.3	18.1	28.0	53.0	1.9	1.1	0.2	--	--	
277	38	NY	8/27/91	0000	3	1	Clear	Non-coh	Unkn	Round	Single	Piles	277	40.0	0.0	5.0	9.0	18.3	28.0	53.0	1.9	0.9	0.2	--	--	
278	38	NY	8/27/91	0000	4	1	Clear	Non-coh	Mod	Round	Single	Piles	278	40.0	0.0	5.0	7.3	16.8	28.0	53.0	1.9	3.2	0.2	--	--	
279	39	NY	10/21/88	0000	3	1	Clear	Non-coh	Unkn	Sharp	Single	Poured	279	22.0	0.0	6.0	9.5	21.0	27.0	42.0	1.5	3.2	0.5	--	--	
280	40	NY	9/16/92	0000	1	1	Clear	Non-coh	Unkn	Round	Single	Piles	280	58.0	0.0	10.0	14.7	25.1	45.0	103.0	2.7	3.1	0.5	5.4	25.0	
281	41	OH	5/16/90	1000	2	1	Live*	Non-coh	Insig	Round	Single	Piles	281	81.8	0.0	3.5	4.5	12.7	1.82	5.0	2.6	1.6	0.25	15.5	50.0	
282	41	OH	5/16/90	1000	3	1	Live*	Unkn	Insig	Round	Single	Piles	282	81.8	0.0	3.5	4.5	13.4	0.78	1.6	3.4	1.0	0.25	5.7	11.0	
283	42	OH	12/31/90	1300	1	1	Live*	Non-coh	Insig	Round	Single	Piles	283	30.0	22.0	2.5	5.0	17.5	2.85	4.7	2.3	2.5	0.25	4.9	17.0	
284	42	OH	12/31/90	1300	2	1	Live*	Non-coh	Insig	Round	Single	Piles	284	30.0	16.0	2.5	2.2	13.9	0.17	0.25	2.8	1.1	0.25	3.1	7.0	
285	43	OH	2/2/90	1530	2	1	Clear*	Non-coh	Insig	Round	Single	Poured	285	35.6	0.0	3.2	3.9	6.4	18.0	34.0	1.9	1.8	0.25	3.3	20.0	
286	44	OH	5/16/90	1430	1	1	Clear*	Non-coh	Insig	Round	Single	Piles	286	24.3	0.0	2.5	4.6	8.4	10.2	37.0	8.1	0.6	0.25	4.9	5.7	
287	44	OH	12/19/90	1010	1	1	Clear*	Non-coh	Insig	Round	Single	Piles	287	24.3	0.0	2.5	4.8	7.6	10.2	37.0	8.1	2.7	1.0	9.9	30.0	
288	44	OH	12/19/90	1010	2	1	Clear*	Non-coh	Insig	Round	Single	Piles	288	24.3	0.0	2.5	3.7	5.6	60.0	71.0	2.4	0.7	0.25	7.0	5.2	
289	45	OH	8/22/90	1040	1	1	Clear*	Non-coh	Unkn	Round	Single	Poured	289	37.3	0.0	2.5	2.5	5.4	4.0	26.0	5.7	2.5	0.25	4.4	20.0	
290	45	OH	12/30/90	1430	1	1	Live*	Non-coh	Unkn	Round	Single	Poured	290	37.3	0.0	2.5	4.2	10.4	4.0	26.0	5.7	2.2	0.5	7.8	35.0	
291	45	OH	8/22/90	1040	2	1	Clear*	Non-coh	Insig	Round	Single	Poured	291	37.3	0.0	2.5	0.8	4.9	0.245	5.0	8.0	0.5	0.25	2.1	4.0	
292	45	OH	12/30/90	1430	2	1	Live*	Non-coh	Insig	Round	Single	Poured	292	37.3	0.0	2.5	2.2	10.2	0.245	5.0	8.0	0.5	0.25	6.1	11.0	
293	46	OH	5/14/90	1605	1	1	Clear*	Cohesive	Mod	Sharp	Single	Piles	293	33.4	8.0	3.75	1.2	6.0	0.165	0.36	3.5	0.7	0.25	6.9	10.0	
294	46	OH	5/18/90	1050	1	1	--	Cohesive	Insig	Sharp	Single	Piles	294	33.4	8.0	3.75	1.6	8.3	0.165	0.36	3.5	0.4	0.25	10.2	7.0	
295	46	OH	12/31/90	1155	1	1	--	Cohesive	Insig	Sharp	Single	Piles	295	33.4	8.0	3.75	2.5	13.9	0.165	0.36	3.5	0.5	0.25	4.8	9.0	
296	47	OH	5/16/90	1145	1	1	Live*	Non-coh	Insig	Round	Single	Piles	296	39.0	0.0	3.7	5.2	5.1	5.0	16.0	4.9	1.3	0.25	5.9	20.0	
297	47	OH	5/17/90	0905	1	1	Live*	Non-coh	Insig	Round	Single	Piles	297	39.0	0.0	3.7	7.0	9.4	5.0	16.0	4.9	2.4	0.25	9.2	40.0	
298	47	OH	12/18/90	1430	1	1	Live*	Non-coh	Insig	Round	Single	Piles	298	39.0	0.0	3.7	5.9	10.1	5.0	16.0	4.9	1.6	0.25	6.0	23.0	
299	47	OH	5/16/90	1145	2	1	Clear*	Non-coh	Insig	Round	Single	Piles	299	39.0	0.0	4.3	5.5	6.7	17.0	29.0	2.5	2.4	0.25	8.9	45.0	
300	47	OH	5/17/90	0905	2	1	Live*	Non-coh	Insig	Round	Single	Piles	300	39.0	0.0	4.4	7.0	10.5	17.0	29.0	2.5	3.0	0.25	6.2	40.0	
301	47	OH	12/18/90	1430	2	1	Clear*	Non-coh	Insig	Round	Single	Piles	301	39.0	0.0	4.5	6.5	11.1	17.0	29.0	2.5	3.2	0.25	6.7	40.0	
302	48	OH	5/17/90	1215	1	1	--	Cohesive	Insig	Round	Single	Piles	302	31.5	0.0	2.5	2.4	7.3	0.185	0.54	2.6	1.3	0.25	5.6	14.0	
303	48	OH	7/23/90	1305	1	1	--	Cohesive	Insig	Round	Single	Piles	303	31.5	0.0	2.5	3.0	9.1	0.185	0.54	2.6	1.4	0.25	3.6	19.0	
304	49	VA	5/31/90	1330	Left	1	Clear*	Unkn	Unkn	Round	Single	Piles	304	35.0	0.0	3.0	1.73	21.2	0.7	1.6	2.24	3.2	1.0	3.5	23.0	
305	49	VA	1/12/93	1030	Left	1	Clear*	Unkn	Unkn	Round	Single	Piles	305	35.0	0.0	3.0	1.01	16.4	0.7	1.6	2.24	3.0	1.0	4.0	24.0	
306	49	VA	12/13/92	1130	Left	1	Clear*	Unkn	Unkn	Round	Single	Piles	306	35.0	0.0	3.0	1.21	16.5	0.7	1.6	2.24	1.6	1.0	10.0	34.0	
307	49	VA	12/14/92	1000	Left	1	Clear*	Unkn	Unkn	Round	Single	Piles	307	35.0	0.0	3.0	1.3	17.5	0.7	1.6	2.24	3.0	1.0	5.5	33.0	

Table 5. Summary of local scour measurements at bridge piers (continued).

Measurement number	Site number	State	Date M/D/Y	Time	Pier ID	UP/DN	Bed- load trans- port	Bed mat- erial cohe- sion	Debris	Pier shape	Pier type	Foun- dation type	Mea- sure- ment num- ber	Pier length (ft)	Pier skew (deg)	Pier width (ft)	Flow velo- city (ft/s)	Flow depth (ft)	D ₅₀ (mm)	D ₈₄ (mm)	Scour depth (ft)	Error (ft/ft)	Side slope (ft)	Top width (ft)	
																									Clear*
308	49	VA	12/15/92	1100	Left	1	Clear*	Unkn	Unkn	Round	Single	Piles	308	35.0	0.0	3.0	1.02	16.9	0.7	1.6	2.24	2.0	1.0	6.0	23.0
309	49	VA	1/11/93	1200	Left	1	Clear*	Unkn	Unkn	Round	Single	Piles	309	35.0	0.0	3.0	0.95	15.6	0.7	1.6	2.24	1.8	1.0	6.0	22.0
310	49	VA	4/12/93	1200	Left	1	Clear*	Unkn	Unkn	Round	Single	Piles	310	35.0	0.0	3.0	1.56	18.1	0.7	1.6	2.24	1.6	1.0	6.0	19.0
311	49	VA	4/13/93	0930	Left	1	Clear*	Unkn	Unkn	Round	Single	Piles	311	35.0	0.0	3.0	1.35	18.4	0.7	1.6	2.24	2.0	1.0	7.5	30.0
312	49	VA	4/19/93	1000	Left	1	Clear*	Unkn	Unkn	Round	Single	Piles	312	35.0	0.0	3.0	1.7	18.9	0.7	1.6	2.24	2.3	1.0	6.0	28.0
313	49	VA	5/31/90	1330	Cntr	1	Live*	Unkn	Unkn	Round	Single	Piles	313	35.0	0.0	3.0	4.56	28.7	0.7	1.6	2.24	5.0	1.0	7.5	75.0
314	49	VA	1/14/91	1200	Cntr	1	Live*	Unkn	Unkn	Round	Single	Piles	314	35.0	0.0	3.0	3.16	24.0	0.7	1.6	2.24	2.5	1.0	7.0	35.0
315	49	VA	12/13/92	1130	Cntr	1	Live*	Unkn	Unkn	Round	Single	Piles	315	35.0	0.0	3.0	3.18	16.2	0.7	1.6	2.24	4.5	1.0	4.0	34.0
316	49	VA	12/14/92	1000	Cntr	1	Live*	Unkn	Unkn	Round	Single	Piles	316	35.0	0.0	3.0	3.31	22.8	0.7	1.6	2.24	3.5	1.0	3.5	24.0
317	49	VA	12/15/92	1100	Cntr	1	Live*	Unkn	Unkn	Round	Single	Piles	317	35.0	0.0	3.0	3.01	22.0	0.7	1.6	2.24	4.5	1.0	4.0	35.0
318	49	VA	1/11/93	1200	Cntr	1	Live*	Unkn	Unkn	Round	Single	Piles	318	35.0	0.0	3.0	2.84	21.3	0.7	1.6	2.24	5.1	1.0	3.5	37.0
319	49	VA	1/12/93	1030	Cntr	1	Live*	Unkn	Unkn	Round	Single	Piles	319	35.0	0.0	3.0	3.08	21.7	0.7	1.6	2.24	4.2	1.0	3.0	25.0
320	49	VA	4/12/93	1200	Cntr	1	Live*	Unkn	Unkn	Round	Single	Piles	320	35.0	0.0	3.0	3.34	24.6	0.7	1.6	2.24	4.0	1.0	4.0	30.0
321	49	VA	4/13/93	0930	Cntr	1	Live*	Unkn	Unkn	Round	Single	Piles	321	35.0	0.0	3.0	3.22	24.4	0.7	1.6	2.24	3.5	1.0	3.5	23.0
322	49	VA	4/19/93	1000	Cntr	1	Live*	Unkn	Unkn	Round	Single	Piles	322	35.0	0.0	3.0	3.26	24.8	0.7	1.6	2.24	3.6	1.0	3.5	25.0
323	49	VA	5/31/90	1330	Rt	1	Clear*	Unkn	Unkn	Round	Single	Piles	323	35.0	0.0	3.0	1.87	26.3	0.7	1.6	2.24	3.0	1.0	3.5	20.0
324	49	VA	12/13/92	1130	Rt	1	Clear*	Unkn	Unkn	Round	Single	Piles	324	35.0	0.0	3.0	1.25	19.5	0.7	1.6	2.24	1.5	1.0	10.0	30.0
325	49	VA	12/14/92	1000	Rt	1	Clear*	Unkn	Unkn	Round	Single	Piles	325	35.0	0.0	3.0	1.2	20.0	0.7	1.6	2.24	2.0	1.0	7.0	27.0
326	49	VA	12/15/92	1100	Rt	1	Clear*	Unkn	Unkn	Round	Single	Piles	326	35.0	0.0	3.0	0.82	18.8	0.7	1.6	2.24	1.2	1.0	8.5	20.0
327	49	VA	1/11/93	1200	Rt	1	Clear*	Unkn	Unkn	Round	Single	Piles	327	35.0	0.0	3.0	1.07	18.5	0.7	1.6	2.24	1.5	1.0	2.0	6.0
328	49	VA	1/12/93	1030	Rt	1	Clear*	Unkn	Unkn	Round	Single	Piles	328	35.0	0.0	3.0	0.95	19.3	0.7	1.6	2.24	1.3	1.0	2.5	6.0
329	49	VA	4/12/93	1200	Rt	1	Clear*	Unkn	Unkn	Round	Single	Piles	329	35.0	0.0	3.0	1.16	20.8	0.7	1.6	2.24	1.5	1.0	2.5	7.0
330	49	VA	4/13/93	0930	Rt	1	Clear*	Unkn	Unkn	Round	Single	Piles	330	35.0	0.0	3.0	1.08	21.0	0.7	1.6	2.24	1.5	1.0	3.5	10.0
331	49	VA	4/19/93	1000	Rt	1	Clear*	Unkn	Unkn	Round	Single	Piles	331	35.0	0.0	3.0	1.08	23.4	0.7	1.6	2.24	3.0	1.0	1.5	9.0
332	50	VA	1/16/91	1030	Left	1	Live*	Unkn	Unkn	Round	Single	Piles	332	32.0	0.0	2.9	2.8	14.0	0.74	2.0	2.4	0.9	1.0	30.0	55.0
333	50	VA	1/18/91	1030	Left	1	Live*	Unkn	Unkn	Round	Single	Piles	333	32.0	0.0	2.9	2.56	14.4	0.74	2.0	2.4	0.8	1.0	25.0	40.0
334	50	VA	4/4/91	1430	Left	1	Live*	Unkn	Unkn	Round	Single	Piles	334	32.0	0.0	2.9	3.03	14.8	0.74	2.0	2.4	0.9	1.0	25.0	46.0
335	50	VA	4/5/91	1200	Left	1	Live*	Unkn	Unkn	Round	Single	Piles	335	32.0	0.0	2.9	2.81	14.0	0.74	2.0	2.4	1.1	1.0	15.0	33.0
336	50	VA	3/12/92	1130	Left	1	Live*	Unkn	Unkn	Round	Single	Piles	336	32.0	0.0	2.9	2.82	14.4	0.74	2.0	2.4	1.6	1.0	14.0	46.0
337	50	VA	3/11/93	0930	Left	1	Live*	Unkn	Unkn	Round	Single	Piles	337	32.0	0.0	2.9	3.32	15.2	0.74	2.0	2.4	1.4	1.0	16.0	60.0
338	50	VA	3/17/93	0930	Left	1	Live*	Unkn	Unkn	Round	Single	Piles	338	32.0	0.0	2.9	3.14	14.3	0.74	2.0	2.4	1.4	1.0	20.0	56.0
339	50	VA	3/18/93	1200	Left	1	Live*	Unkn	Unkn	Round	Single	Piles	339	32.0	0.0	2.9	3.35	15.2	0.74	2.0	2.4	1.8	1.0	10.0	34.0
340	50	VA	3/19/93	1100	Left	1	Live*	Unkn	Unkn	Round	Single	Piles	340	32.0	0.0	2.9	3.13	15.2	0.74	2.0	2.4	1.5	1.0	7.5	23.0
341	50	VA	4/1/93	1000	Left	1	Live*	Unkn	Unkn	Round	Single	Piles	341	32.0	0.0	2.9	3.24	15.4	0.74	2.0	2.4	1.3	1.0	9.0	24.0
342	50	VA	1/16/91	1030	Cntr	1	Live*	Unkn	Unkn	Round	Single	Piles	342	32.0	0.0	2.9	2.97	15.5	0.74	2.0	2.4	1.1	1.0	22.0	50.0
343	50	VA	1/18/91	1030	Cntr	1	Live*	Unkn	Unkn	Round	Single	Piles	343	32.0	0.0	2.9	2.62	16.0	0.74	2.0	2.4	1.5	1.0	14.0	44.0
344	50	VA	4/4/91	1430	Cntr	1	Live*	Unkn	Unkn	Round	Single	Piles	344	32.0	0.0	2.9	3.26	16.5	0.74	2.0	2.4	1.2	1.0	19.0	46.0
345	50	VA	4/5/91	1200	Cntr	1	Live*	Unkn	Unkn	Round	Single	Piles	345	32.0	0.0	2.9	3.42	15.7	0.74	2.0	2.4	1.2	1.0	22.0	54.0
346	50	VA	3/12/92	1130	Cntr	1	Live*	Unkn	Unkn	Round	Single	Piles	346	32.0	0.0	2.9	3.03	14.7	0.74	2.0	2.4	1.2	1.0	19.0	44.0
347	50	VA	3/11/93	0930	Cntr	1	Live*	Unkn	Unkn	Round	Single	Piles	347	32.0	0.0	2.9	3.69	16.5	0.74	2.0	2.4	1.3	1.0	23.0	60.0
348	50	VA	3/17/93	0930	Cntr	1	Live*	Unkn	Unkn	Round	Single	Piles	348	32.0	0.0	2.9	3.28	16.7	0.74	2.0	2.4	1.8	1.0	17.0	62.0
349	50	VA	3/18/93	1200	Cntr	1	Live*	Unkn	Unkn	Round	Single	Piles	349	32.0	0.0	2.9	3.66	15.9	0.74	2.0	2.4	2.0	1.0	15.0	62.0
350	50	VA	3/19/93	1100	Cntr	1	Live*	Unkn	Unkn	Round	Single	Piles	350	32.0	0.0	2.9	3.45	16.9	0.74	2.0	2.4	2.0	1.0	19.0	75.0
351	50	VA	4/1/93	1000	Cntr	1	Live*	Unkn	Unkn	Round	Single	Piles	351	32.0	0.0	2.9	3.56	15.4	0.74	2.0	2.4	2.0	1.0	17.0	70.0

Table 5. Summary of local scour measurements at bridge piers (continued).

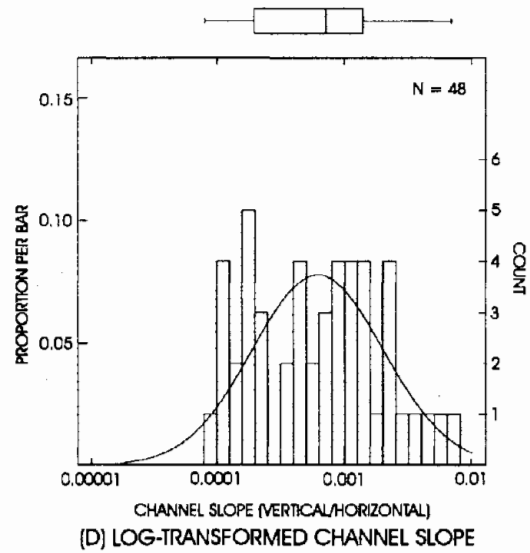
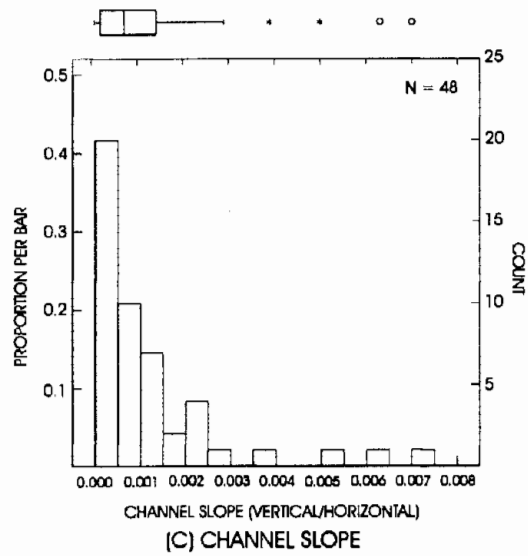
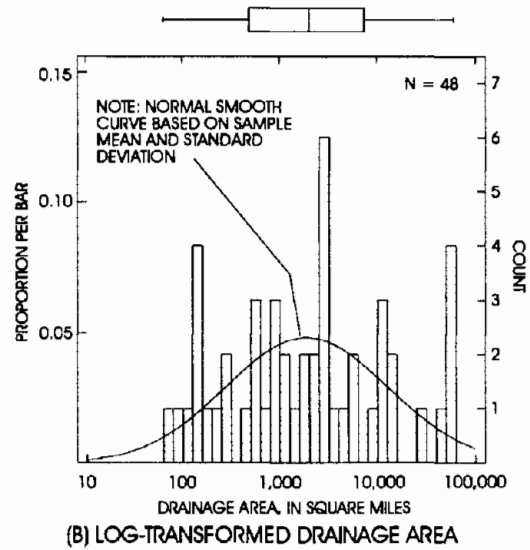
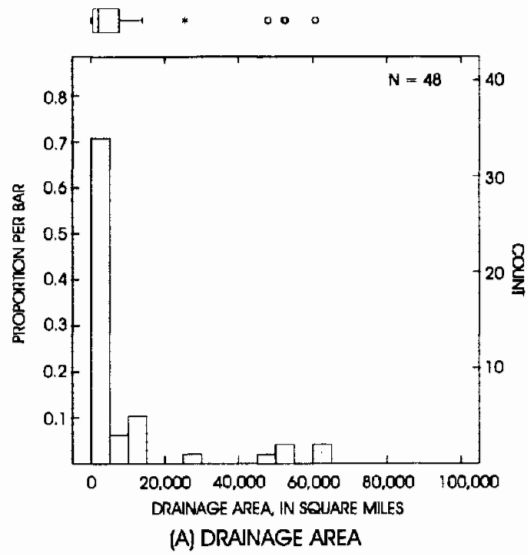
Mea- sure- ment num- ber	Site num- ber	State	Date M/D/Y	Time	Pier ID	UP/DN	Bed- load trans- port	Bed mat- erial cohe- sion	Debris	Pier shape	Pier type	Foun- dation type	Mea- sure- ment num- ber	Pier length (ft)	Pier skew (deg)	Pier width (ft)	Flow velo- city (ft/s)	Flow depth (ft)	D ₅₀ (mm)	D ₈₄ (mm)	σ	Scour depth (ft)	Error (ft/ft)	Side slope (ft)	Top width (ft)
352	51	VA	5/29/90	1200	2	1	Clear*	Unkn	Unkn	Round	Single	Piles	352	43.0	0.0	2.5	2.1	8.9	0.92	4.8	4.1	2.5	1.0	3.5	17.0
353	52	VA	10/24/90	1100	1	1	Live*	Non-coh	Unkn	Round	Single	Piles	353	83.0	0.0	3.2	5.24	20.5	0.28	0.46	1.8	3.5	1.0	8.5	60.0
354	52	VA	10/25/90	1100	1	1	Live*	Non-coh	Unkn	Round	Single	Piles	354	83.0	0.0	3.2	6.16	26.0	0.28	0.46	1.8	4.0	1.0	5.0	40.0
355	52	VA	4/22/92	1200	1	1	Live*	Non-coh	Unkn	Round	Single	Piles	355	83.0	0.0	3.2	4.32	19.1	0.28	0.46	1.8	2.7	1.0	4.5	23.0
356	52	VA	10/25/90	1100	2	1	Live*	Non-coh	Unkn	Round	Single	Piles	356	83.0	0.0	3.2	7.11	30.5	0.28	0.46	1.8	3.5	1.0	9.0	62.0
357	52	VA	4/22/92	1200	2	1	Live*	Non-coh	Unkn	Round	Single	Piles	357	83.0	0.0	3.2	5.46	27.5	0.28	0.46	1.8	5.0	1.0	3.5	36.0
358	53	VA	5/3/89	1200	2	1	Clear*	Non-coh	Unkn	Round	Single	Poured	358	41.0	0.0	2.0	1.84	1.5	72.0	170.0	2.3	0.8	1.0	5.5	9.0
359	53	VA	5/7/89	0900	2	1	Live*	Non-coh	Unkn	Round	Single	Poured	359	41.0	0.0	2.0	5.1	2.2	72.0	170.0	2.3	0.6	1.0	5.0	6.0
360	53	VA	4/22/92	1100	2	1	Live*	Non-coh	Unkn	Round	Single	Poured	360	41.0	0.0	2.0	5.22	5.5	72.0	170.0	2.3	1.6	1.0	6.0	19.0
361	53	VA	5/3/89	1200	3	1	Live*	Non-coh	Unkn	Round	Single	Poured	361	41.0	0.0	2.0	4.05	4.0	72.0	170.0	2.3	1.0	1.0	9.5	17.0
362	53	VA	5/7/89	0900	3	1	Live*	Non-coh	Unkn	Round	Single	Poured	362	41.0	0.0	2.0	5.31	5.0	72.0	170.0	2.3	1.2	1.0	9.5	20.0
363	53	VA	4/22/92	1100	3	1	Live*	Non-coh	Unkn	Round	Single	Poured	363	41.0	0.0	2.0	8.5	8.6	72.0	170.0	2.3	2.5	1.0	5.0	26.0
364	54	VA	5/2/89	1300	1	1	Live*	Unkn	Unkn	Round	Single	Piles	364	28.0	0.0	2.25	2.15	5.6	0.69	1.3	1.9	1.3	1.0	7.0	18.0
365	54	VA	8/24/90	1030	1	1	Live*	Unkn	Unkn	Round	Single	Piles	365	28.0	0.0	2.25	2.25	5.9	0.69	1.3	1.9	1.2	1.0	4.0	9.0
366	54	VA	8/24/90	1430	1	1	Live*	Unkn	Unkn	Round	Single	Piles	366	28.0	0.0	2.25	2.1	5.1	0.69	1.3	1.9	0.7	1.0	6.5	9.0
367	54	VA	3/29/91	1230	1	1	Clear*	Unkn	Unkn	Round	Single	Piles	367	28.0	0.0	2.25	1.26	2.9	0.69	1.3	1.9	1.3	1.0	3.5	9.0
368	54	VA	3/29/91	1530	1	1	Clear*	Unkn	Unkn	Round	Single	Piles	368	28.0	0.0	2.25	1.7	4.6	0.69	1.3	1.9	1.4	1.0	3.0	9.0
369	54	VA	3/29/91	1730	1	1	Clear*	Unkn	Unkn	Round	Single	Piles	369	28.0	0.0	2.25	1.72	5.3	0.69	1.3	1.9	1.2	1.0	4.0	10.0
370	54	VA	5/2/89	1300	2	1	Clear*	Unkn	Unkn	Round	Single	Piles	370	28.0	0.0	2.25	0.62	3.2	0.69	1.3	1.9	1.8	1.0	5.5	9.0
371	54	VA	8/24/90	1030	2	1	Clear*	Unkn	Unkn	Round	Single	Piles	371	28.0	0.0	2.25	1.06	2.9	0.69	1.3	1.9	2.4	1.0	1.5	10.0
372	54	VA	5/2/89	1300	3	1	Clear*	Unkn	Unkn	Round	Single	Piles	372	28.0	0.0	2.25	0.79	2.9	0.69	1.3	1.9	1.6	1.0	7.0	22.0
373	54	VA	8/24/90	1030	3	1	Clear*	Unkn	Unkn	Round	Single	Piles	373	28.0	0.0	2.25	1.06	2.6	0.69	1.3	1.9	1.3	1.0	12.0	30.0
374	54	VA	8/24/90	1430	3	1	Clear*	Unkn	Unkn	Round	Single	Piles	374	28.0	0.0	2.25	0.62	2.0	0.69	1.3	1.9	1.4	1.0	5.0	14.0
375	54	VA	3/29/91	1730	3	1	Clear*	Unkn	Unkn	Round	Single	Piles	375	28.0	0.0	2.25	1.63	3.5	0.69	1.3	1.9	1.5	1.0	6.0	18.0
376	55	VA	3/29/91	1430	2	1	Clear*	Non-coh	Unkn	Round	Single	Poured	376	30.0	0.0	2.0	3.7	2.5	55.0	84.0	1.5	1.5	1.0	5.5	16.0
377	55	VA	6/5/92	1030	2	1	Clear*	Non-coh	Unkn	Round	Single	Poured	377	30.0	0.0	2.0	5.51	10.5	55.0	84.0	1.5	2.1	1.0	8.5	36.0
378	55	VA	3/24/93	0930	2	1	Clear*	Non-coh	Unkn	Round	Single	Poured	378	30.0	0.0	2.0	6.45	10.5	55.0	84.0	1.5	1.8	1.0	12.0	45.0
379	56	VA	5/29/90	1100	1	1	Clear*	Non-coh	Unkn	Round	Single	Poured	379	29.5	0.0	2.0	4.08	7.1	37.0	75.0	2.0	0.2	1.0	47.0	19.0
380	56	VA	5/29/90	1100	2	1	Clear*	Unkn	Unkn	Round	Single	Poured	380	29.5	0.0	2.0	4.6	7.9	37.0	75.0	2.0	0.4	1.0	19.0	15.0
381	56	VA	3/30/91	1000	2	1	Clear*	Unkn	Unkn	Round	Single	Poured	381	29.5	0.0	2.0	4.47	8.5	37.0	75.0	2.0	0.8	1.0	10.0	17.0
382	56	VA	2/26/92	1000	2	1	Clear*	Unkn	Unkn	Round	Single	Poured	382	29.5	0.0	2.0	4.6	9.7	37.0	75.0	2.0	1.0	1.0	10.0	20.0
383	56	VA	3/4/93	1330	2	1	Clear*	Unkn	Unkn	Round	Single	Poured	383	29.5	0.0	2.0	4.79	9.9	37.0	75.0	2.0	0.8	1.0	12.0	20.0
384	56	VA	3/4/93	1730	2	1	Clear*	Unkn	Unkn	Round	Single	Poured	384	29.5	0.0	2.0	5.1	10.7	37.0	75.0	2.0	1.2	1.0	8.0	19.0

[UP/DN, upstream/downstream (1=upstream, 2=downstream, 0=unknown); D₅₀, median grain size; D₈₄, grain size for which 84 percent of sample is finer by weight; σ, geometric standard deviation of the grain size distribution; clear, clear-water scour; non-coh, non-cohesive; substantial, substantial; live, live-bed scour; L, left; R, right; P, pier; sediment transport condition based on comparison of measured velocity and computed incipient-motion velocity; 1 ft = 0.305 m]

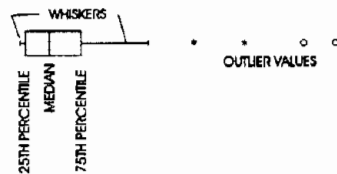
Table 6. Characteristics of principal variables of local scour at bridge piers.

Variable	Units	No.	Minimum	Maximum	Mean	Standard deviation	Median
Drainage area	sq. mi.	46	92.8	60,700	9,286	16,957	2,369
Channel slope	ft/ft,V/H	45	0.0	0.007	0.001	0.002	0.001
Pier length	ft	379	8.0	90.0	34.3	12.1	34.5
Pier skew	degree	384	0.0	43.0	4.0	8.0	0.0
Pier width	ft	384	0.95	15.0	4.2	3.0	3.4
Flow velocity	ft/s	384	0.50	14.7	4.59	2.78	3.90
Flow depth	ft	384	0.4	44.2	14.4	10.0	12.1
D ₅₀	mm	380	0.119	108.0	12.7	23.5	0.940
D ₈₄	mm	373	0.250	233.0	28.2	48.1	4.2
Sigma	--	373	1.30	12.1	3.35	2.18	2.40
Scour depth	ft	384	0.0	25.1	3.1	3.4	2.0
Error	ft	384	0.2	2.0	0.69	0.34	0.50
Side slope	ft/ft, H/V	325	1.5	51.0	7.9	5.8	6.4
Top width	ft	326	3.0	281.0	44.0	47.0	28.0

[H, horizontal; V, vertical; D₅₀, median grain size; D₈₄, grain size for which 84 percent of the sample is finer by weight; 1 ft = 0.305 m; 1 mi² = 2.59 km²]



EXPLANATION OF BOX PLOTS



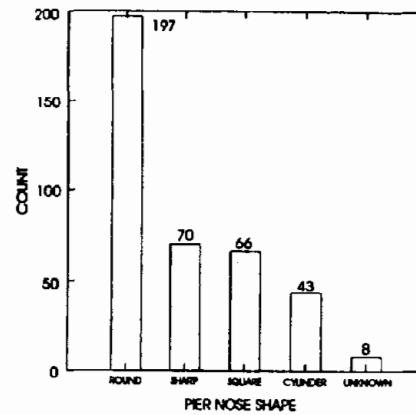
$$1 \text{ mi}^2 = 2.59 \text{ km}^2$$

Figure 22. Characteristics of: (A) drainage area, (B) log-transformed drainage area, (C) channel slope, and (D) log-transformed channel slope for scour measurement sites in data base.

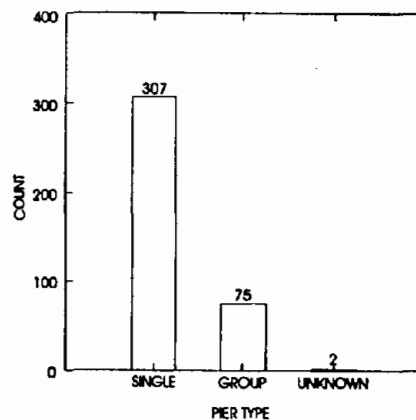
The geographic distribution of the 56 sites where scour was measured is shown in figure 3. The characteristics of the basin drainage area for the sites in the data base are shown in figure 22A. Basin area was not determined for 10 of the 56 sites. Basin area is often log-transformed (base 10 logarithms) for hydrologic analysis, as shown in figure 22B. Basin area indirectly affects the scour characteristics of the stream as the principal determinant of flow magnitude and duration, and as it relates to stream slope and sediment characteristics. The channel slope is shown in figure 22C for the 45 sites where it was determined from a survey of the channel profile or water-surface slope, or from a topographic map.

About one-half of the pier scour measurements were made at round-nosed (semicircular or elliptical-shaped nose) piers (figure 23A). Sharp (including lenticular) and square-nosed piers were measured 70 and 66 times, respectively, and cylindrical piers were measured 43 times. The pier was a single column above the foundation footing for 307 of the measurements, and it had more than one column for 75 measurements (figure 23B). The measured piers had poured footings for 117 of the measurements and pile foundations for 248 measurements (figure 23C).

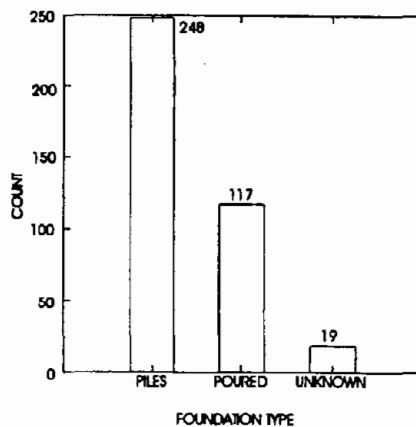
Scour measurements were made at piers with widths from 0.29 to 4.6 m (0.95 to 15 ft) (figure 24A). The median pier width is 1.04 m (3.4 ft) and 50 percent of the measurements have pier widths between 0.7 and 1.5 m (2.4 and 5.0 ft) (measurements within the box in figure 24A). A depth-weighted pier width was used for tapered or stepped-width piers. Although pier width is not a "natural" variable, it is shown log-transformed in figure 24B because this transformation improves the linearity of the



(A) PIER NOSE SHAPE



(B) PIER TYPE



(C) FOUNDATION TYPE

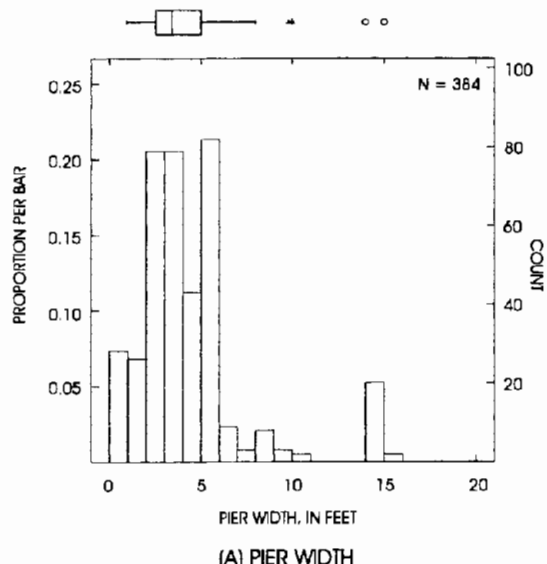
Figure 23. Characteristics of: (A) pier nose shape, (B) pier type, and (C) foundation type for scour measurements.

scour depth to pier width relation. Scour was measured at piers with lengths from 2.4 to 27.4 m (8 to 90 ft), and the most frequently measured pier lengths are between 10.7 and 11.6 m (35 and 38 ft) (figure 24C). Pier length was not recorded for five measurements. Pier length is significant to the local pier scour depth where the pier is skewed to the flow. About 70 percent of the measurements were made where the pier was aligned with the flow (zero skew, figure 24D). The limited-detail studies generally targeted these zero skew sites so that the effects of other factors on pier scour could be evaluated independent of the effects of skew.

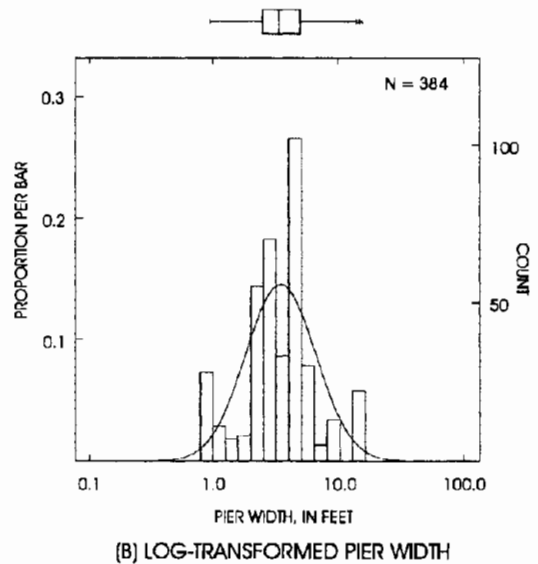
The pier scour velocity represents the local velocity just upstream of the pier, but outside the zone of locally accelerated flow, and is averaged over the measurement vertical. Measured velocities range from 0.15 to 4.5 m/s (0.5 to 14.7 ft/s), and the median velocity is 1.19 m/s (3.90 ft/s). The distribution of the measured velocities is illustrated in figure 25A and, when square-root transformed, they fit the normal distribution well (figure 25B). The distribution of flow depth measured upstream of the pier (not including the depth of scour) is shown in figure 25C. The median flow depth is 3.7 m (12.1 ft). A square-root transformation was also used for the measured flow depth to improve the symmetry of the distribution (figure 25D).

Bed material is one of the most variant and poorly documented factors affecting bridge scour. Bed material size distribution data for most of the scour measurement sites are contained in the national scour data base. The size distributions for non-cohesive bed material are summarized by the D_{50} , D_{84} , and the geometric standard deviation (tables 5 and 6; figures 26 and 27). D_{50} is the median bed material diameter for a sample, that is, the size for which one-half the sample is larger and one-half is smaller by weight. D_{84} is the particle size for which 84 percent of the sample is smaller by weight. D_{50} is typically used to characterize the size of streambed material. D_{84} may more effectively describe the effects of bed material size on scour because larger particles in the bed tend to exert more influence on channel erosion. The geometric standard deviation (σ_g) is a measure of the spread of grain sizes in a sample and is computed as the square root of the ratio of D_{84} to D_{16} . D_{84} and D_{16} particle sizes were not available for scour measurements made in Alaska, so D_{90}/D_{50} was used in the computation of σ_g and D_{90} for the listing of D_{84} . The topic of scour in cohesive streams requires further investigation and is not addressed in this investigation.

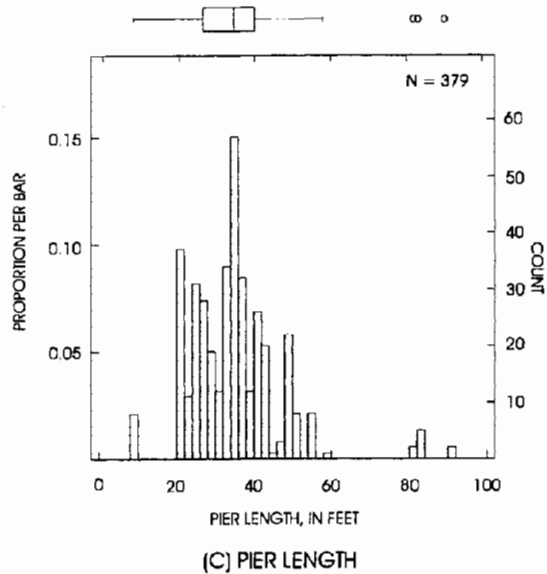
The percentage of the 384 scour measurements made in various sized bed materials (as classified by D_{50}) was as follows: about 1 percent less than sand-sized (less than 0.062 mm); about 61 percent sand-sized (from 0.062 to 2 mm); about 30 percent gravel-sized (2 to 64 mm); and about 8 percent larger than gravel-sized (larger than 64 mm) (figure 26A). D_{50} is not listed for four of the measurements made in cohesive bed materials. No transformation was found to make the distribution of D_{50} or D_{84} symmetric, but the log-transformation makes the data much more linear in relation to other variables (figure 26). Similarities between the distributions of σ_g and of the D_{50} and D_{84} grain sizes indicate that gradation is typically larger for larger bed material streams (figure 27). The log-transformed σ_g data are shown in figure 27B. Only nine of the scour measurements were made in bed materials known to be cohesive (figure 28) and most of those classified as "unknown" were very likely noncohesive, as indicated by the sampled bed material.



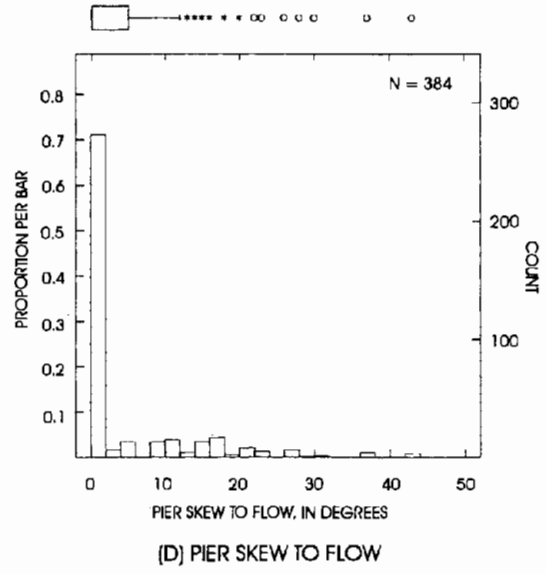
(A) PIER WIDTH



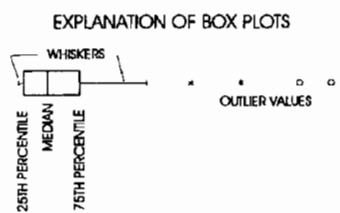
(B) LOG-TRANSFORMED PIER WIDTH



(C) PIER LENGTH

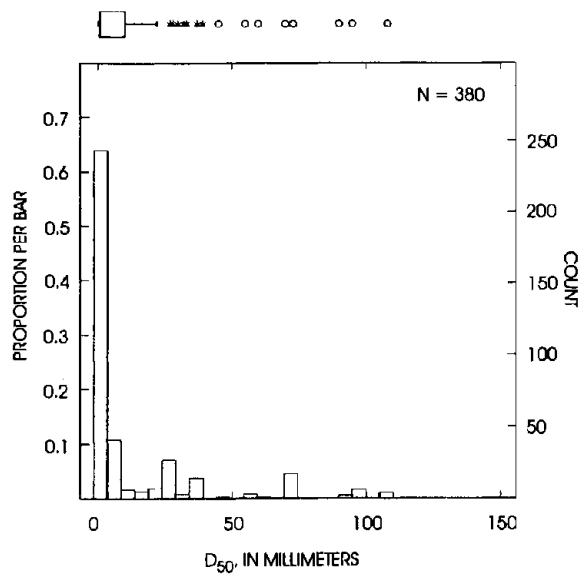


(D) PIER SKEW TO FLOW

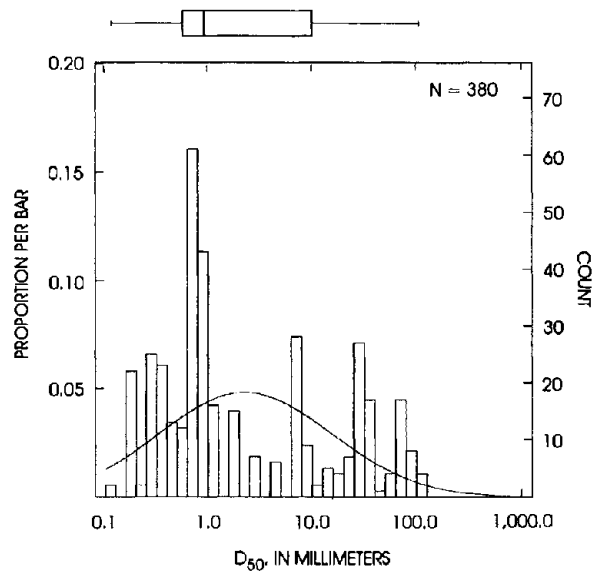


1 ft = 0.305 m

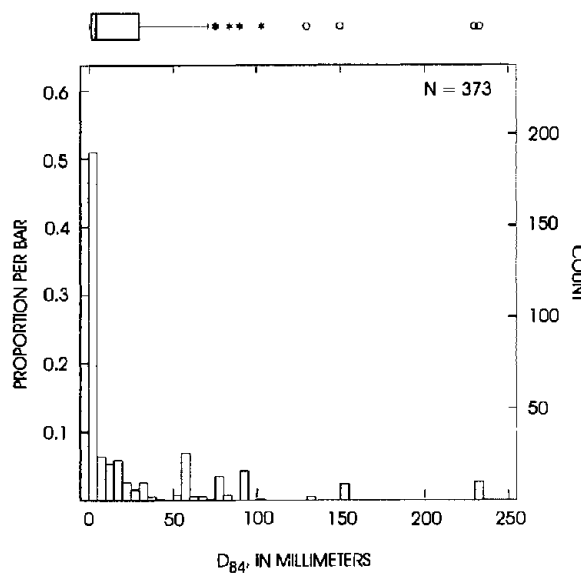
Figure 24. Characteristics of: (A) pier width, (B) log-transformed pier width, (C) pier length, and (D) pier skew to flow for scour measurements.



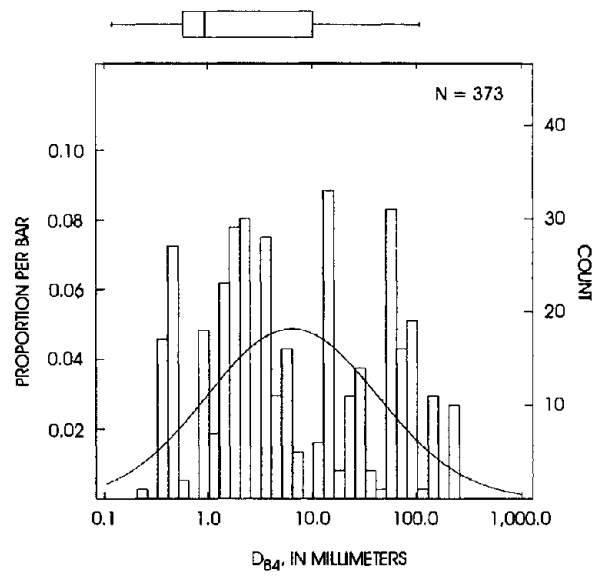
(A) D_{50} GRAIN SIZE



(B) LOG-TRANSFORMED D_{50} GRAIN SIZE



(C) D_{84} GRAIN SIZE



(D) LOG-TRANSFORMED D_{84} GRAIN SIZE

EXPLANATION OF BOX PLOTS

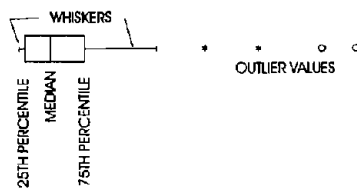
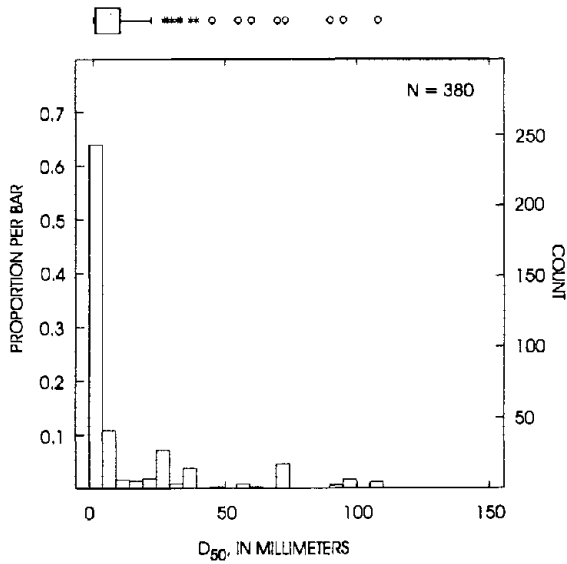
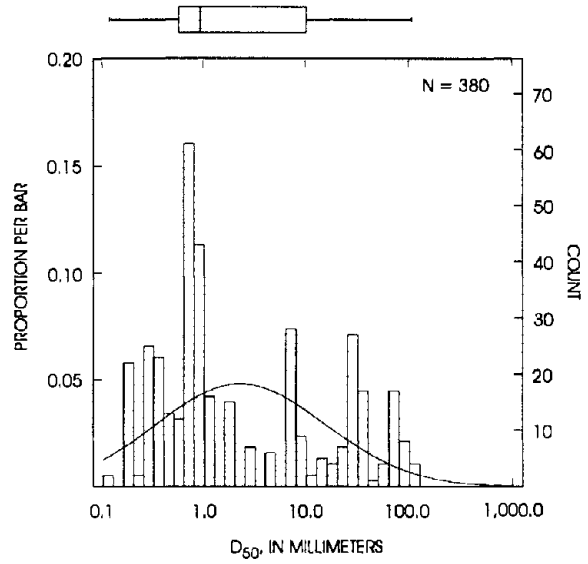


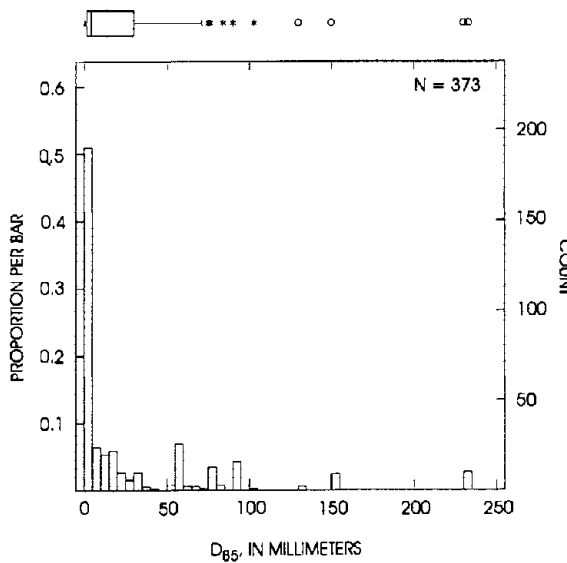
Figure 26. Characteristics of: (A) D_{50} grain size, (B) log-transformed D_{50} grain size, (C) D_{84} grain size, and (D) log-transformed D_{84} grain size.



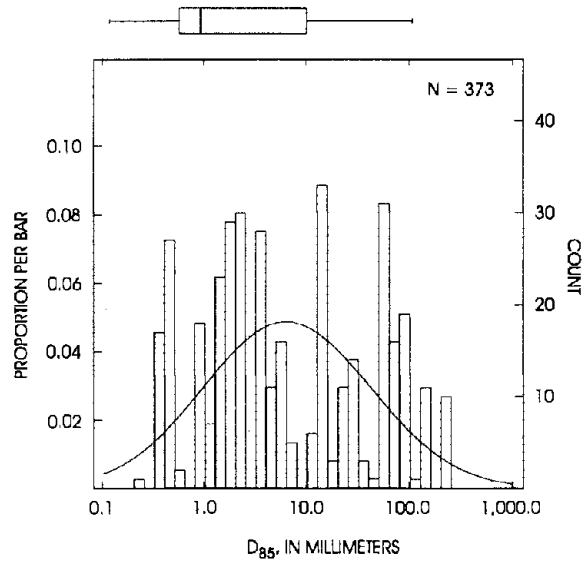
(A) D_{50} GRAIN SIZE



(B) LOG-TRANSFORMED D_{50} GRAIN SIZE



(C) D_{85} GRAIN SIZE



(D) LOG-TRANSFORMED D_{85} GRAIN SIZE

EXPLANATION OF BOX PLOTS

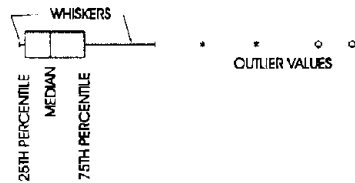


Figure 26. Characteristics of: (A) D_{50} grain size, (B) log-transformed D_{50} grain size, (C) D_{84} grain size, and (D) log-transformed D_{84} grain size.

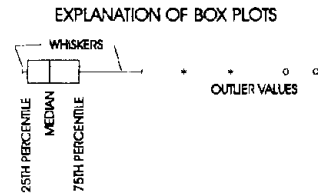
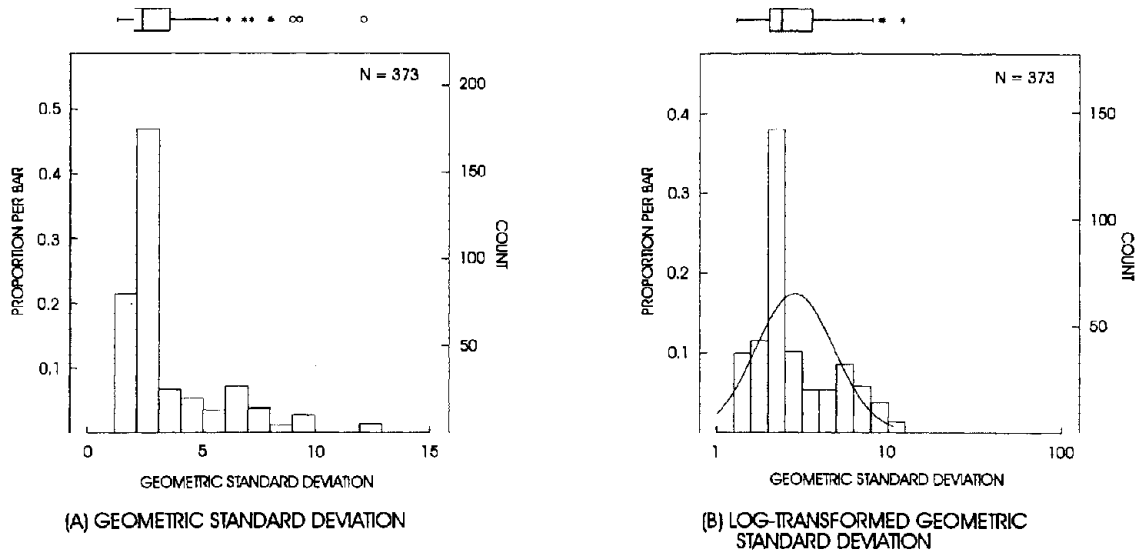


Figure 27. Characteristics of: (A) untransformed and (B) log-transformed geometric standard deviation (σ_g) of the bed material for scour measurements.

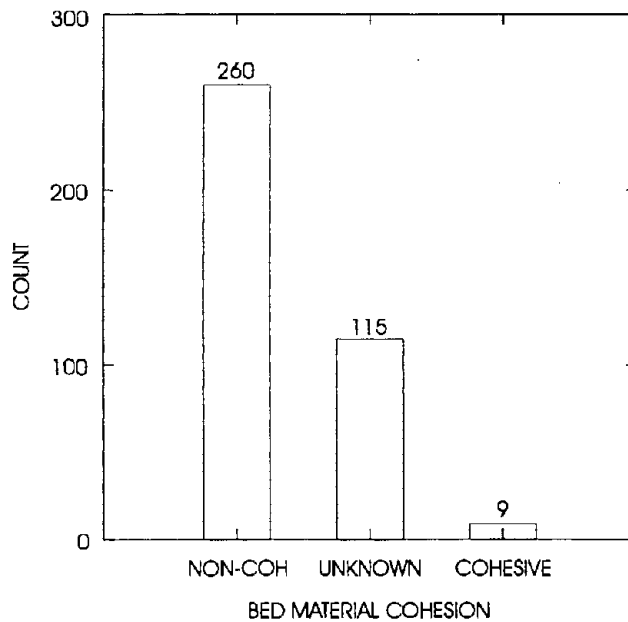
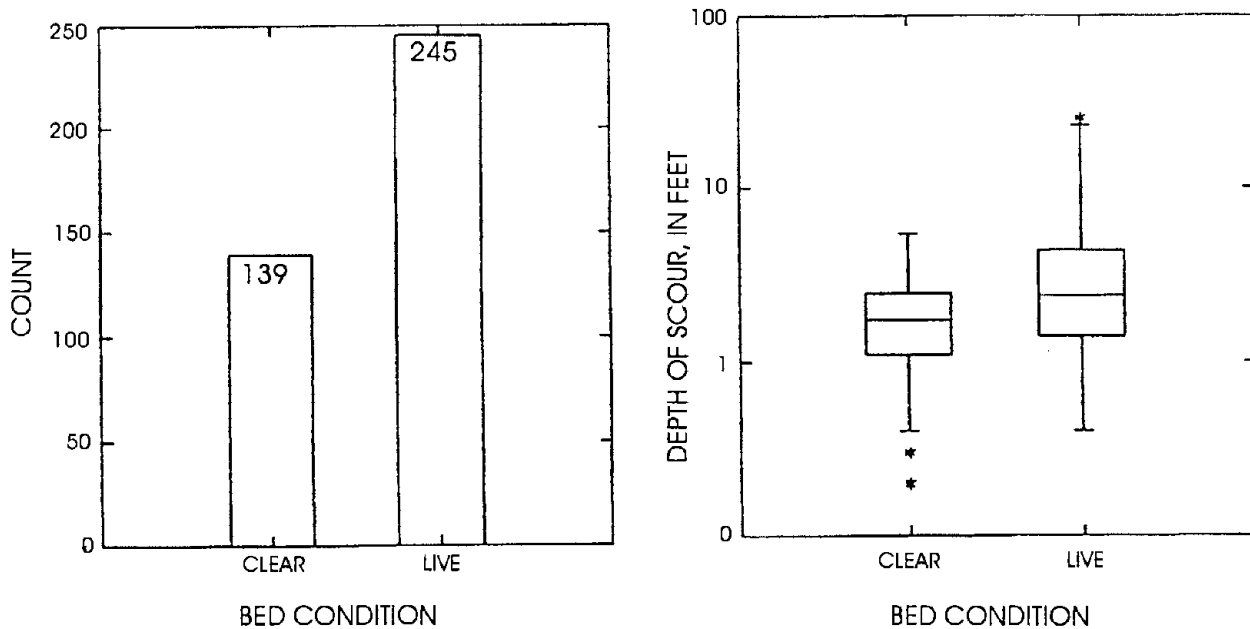


Figure 28. Classification of bed material cohesion for scour measurements.

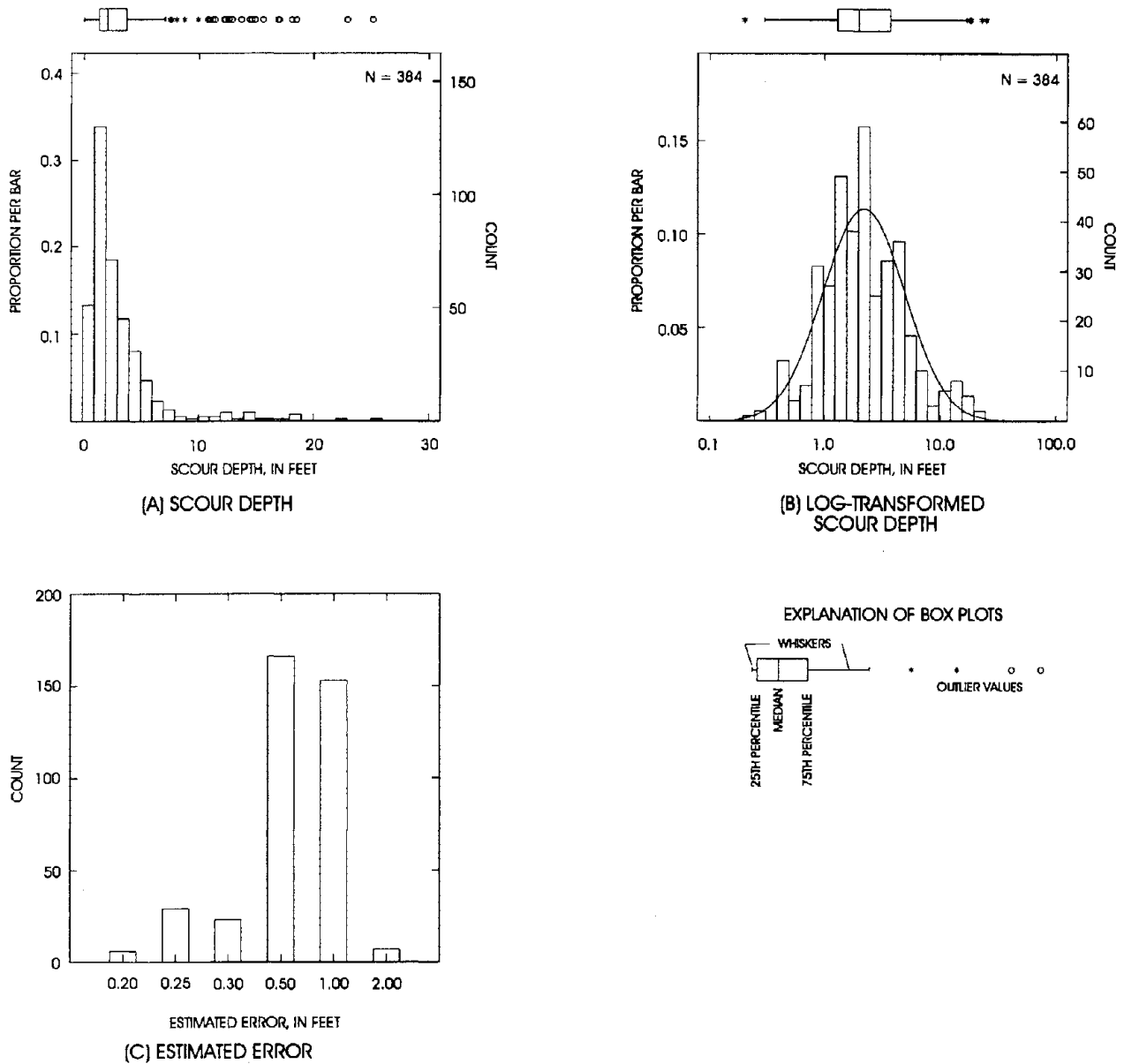
Scour measurements were classified as live bed or clear water based on the observations of the measurement crew or on the basis of whether the local measured velocity exceeded Neill's computed incipient motion velocity for the D_{50} grain size. The sediment transport conditions may be misclassified by either observation or computation; however, such errors are probably infrequent. Live-bed scour conditions were prevalent for 64 percent of the measurements in the national scour data base (figure 29).



1 ft = 0.305 m

Figure 29. Distribution and characteristics of scour depth measured under clear-water and live-bed conditions.

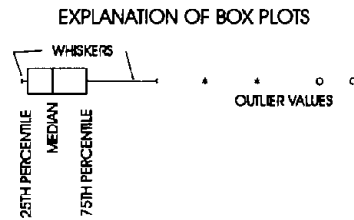
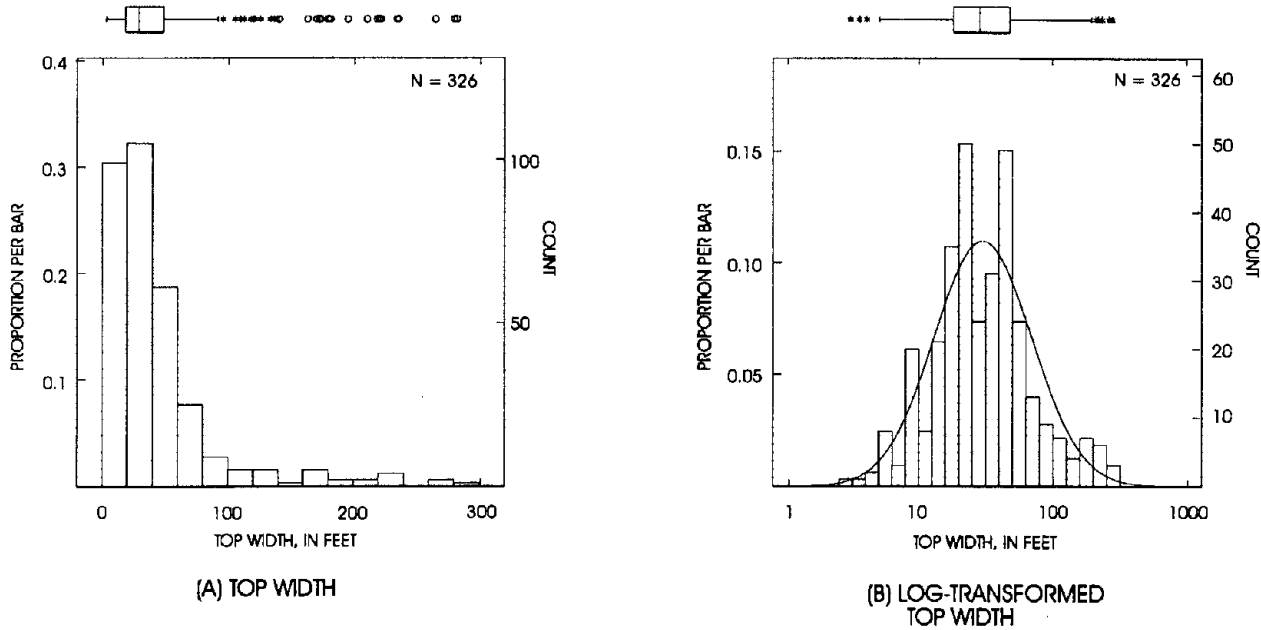
The characteristics of the local pier scour depth are illustrated in figure 30. The range of measured scour is 0 to 7.7 m (0 to 25.1 ft). The median measured scour depth is 0.6 m (2.0 ft), and about 13 percent of the scour depths were greater than 1.5 m (5 ft). The standard deviation about the mean for the measured scour is 1.0 m (3.4 ft) (table 6). The largest scour depths were usually recorded using boat measurement methods that generally provide good accuracy. Zero scour measurements are reported where significant scour was expected for the given bed material and velocity conditions. In these cases, zero scour measurements help define a threshold scour condition. The distribution of the \log_{10} -transformed scour depth data is more symmetrical and it fits fairly well by the normal distribution (figure 30B). The error of the scour depth is a function of the accuracy of the streambed elevation measurement and of the reference surface determination. The estimated accuracy of each scour depth was based on a qualitative analysis of these factors. Errors of measurement less than 0.15 m (0.5 ft) are usually measurements made on clear-water scour streams, where flood scour measurements were supplemented by inspection surveys of the scour hole before and after the flood. Errors between 0.15 and 0.3 m (0.5 and 1.0 ft) are reported for 83 percent of the measurements (figure 30C).



1 ft = 0.305 m

Figure 30. Characteristics of measured scour depth (y_s) for: (A) standard, (B) log-transformed units, and (C) estimated error of scour measurements.

The distributions of the untransformed and log-transformed scour hole top width are shown in figure 31. The horizontal top width of the scour hole for the measurements were determined along the line of the measured cross section. The median top width is 8.5 m (28 ft) and top widths range from 0.9 to 85.6 m (3 to 281 ft). The very large top widths were verified in the quality assurance and in the analysis of this variable; they are also seen to be typical (not extreme) outliers in the distribution of the \log_{10} -transformed data. Scour hole top width was not determined for 58 of the measurements.



1 ft = 0.305 m

Figure 31. Characteristics of top width of measured local scour holes in: (A) standard and (B) log-transformed units.

The distributions of the measured scour hole side slope are shown in figure 32. Slope was measured as the run over the rise (horizontal over vertical) using a horizontal reference frame at the pier. The horizontal reference frame was often inappropriate where the scour reference surface was sloping, so these results should be used with caution. The side slope was indeterminant for 59 of the measurements. As for all of the natural quantitative scour variables summarized here, the distribution of the untransformed data is right skewed and the \log_{10} -transformed data is more symmetrical and more normally distributed.

The summary information provided in the characterization of each of these primary scour variables is valuable in assessing the statistical characteristics of the variables and in evaluating whether the data have similar distributions whose relations may be analyzed using methods that assume linearity.

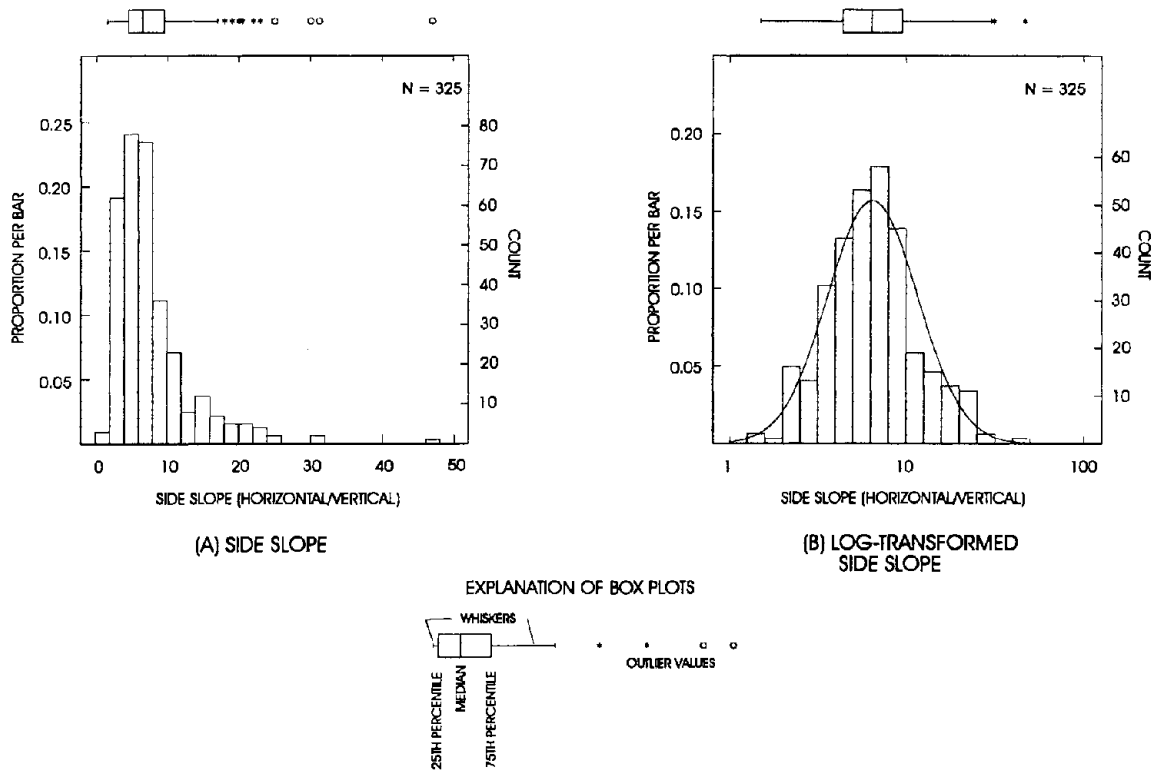


Figure 32. Characteristics of side slope of measured local scour holes in: (A) untransformed and (B) log-transformed units.

ANALYSIS OF LOCAL SCOUR PROCESSES AT BRIDGE PIERS

Local scour occurs at bridge piers because of interrelated processes controlled by several variables. These processes and variables were discussed in a previous section of this report. The processes are analyzed here by exploring the relation of measured scour depth to the pier width, pier shape, pier alignment, flow depth, flow intensity, sediment size, and sediment gradation. In exploring these relations using field data, it is important to remember that the measured scour depth is rarely in equilibrium with the concurrently measured deterministic variables and that the relative equilibrium of most measurement conditions is difficult to assess. Scour processes at bridges are particularly complex due to the dynamic sediment transport, flow depth, and flow intensity, which are rarely in a steady-state condition during floods. In addition to these factors, effective pier width may vary because of shifts in flow alignment or the combination of tapered piers and changing flow depths. Changing conditions cannot be assumed to occur uniformly across these variables, so their influence on scour depth, relative to each other, is also dynamic.

In a simplistic analogy to illustrate these dynamic conditions, we may think of scour depth or volume as a ship attached by ropes to its several "tug-boat" deterministic variables, as shown in figure 33. At the time of a measurement, some variables are exerting a significant influence (tight lines), while some are not (slack lines). The relative tension in the ropes of different variables is dynamic over a flood event. Additional ropes may be drawn between selected variables, such as flow depth and flow intensity. This concept is important in determining how to analyze and interpret field measurements of scour; for example, ordinary least-squares regression would usually not be adequate because the influence of the explanatory variable on the dependant variable is not constant in the data set. A weighted least squares would be preferable, but a weighting algorithm that measures the relative equilibrium of each measurement has not been determined. This concept highlights the value of laboratory studies, where the influence of all but the selected variables is turned off or controlled; it also highlights the limitations of laboratory studies in representing the dynamic conditions of a flooding stream.

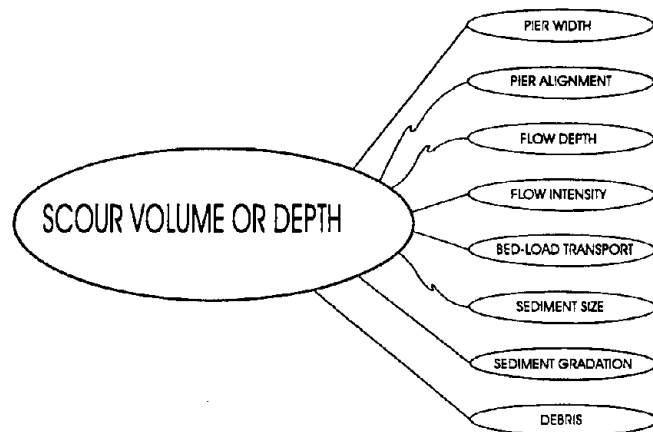


Figure 33. Illustrations of dynamic influence of variables on scour depth or volume.

Relations between selected variables are illustrated and analyzed using scatter plots. The plots are made in \log_{10} space for most of the relations, based on the distribution characteristics of the variables. The plotted points typically have a broad spread so that a smooth curve is useful to identify the trend of the relation. Locally weighted, scatter plot smoothing (LOWESS) curves are used in this exploratory analysis because they do not require any prior assumption as to the

mathematical function of the relations investigated. The LOWESS curve is also statistically robust (that is, relatively insensitive to outliers that affect the sample mean and variance). They are shown to highlight the trend of the relations illustrated on scatter plots of data and they do not have a mathematical definition. For each pair of data (x,y), the LOWESS method computes a plotting point from a weighted least-squares regression whose weights are a function of both the distance from x and the magnitude of the residual for that point from the previous regression (iterative procedure). As explained by Helsel and Hirsh (1992), "A point will receive a small weight, and therefore have little influence on the smoothed predicted y, if it is either far from the center of the window in the x direction or has a large residual in the y direction." The width of the regression "window" used was 70 percent of the data set for all of the LOWESS curves shown in this analysis.

Pier Width Effects

The effective pier width is probably the most influential deterministic parameter for local pier scour, and estimated scour varies directly with pier width in many design equations. Piers skewed to the flow alignment were generally avoided when selecting sites for scour measurements during the reconnaissance phase of this investigation. This was done so that the effect of other variables could be analyzed more directly. Piers were skewed to the flow in about 30 percent of the scour measurements reported here. The flow width, effectively blocked by a skewed non-cylindrical pier, is computed as:

$$b_e = (L \times \sin(\alpha) + b \times \cos(\alpha)) \quad (4)$$

where b_e is the effective pier width;
 L is the pier length;
 b is the pier width; and
 α is the skew of pier to flow.

Figure 34 illustrates the relation between effective pier width and local scour depth for the 374 non-zero scour measurements of this investigation. These variables have a more linear relation when \log_{10} is transformed. The Pearson linear correlation coefficient for scour depth and effective pier width is 0.51 for the \log_{10} -transformed variables.

The slope of the relation shown in figure 34 indicates that the influence of pier width on scour depth is linear in logarithmic space and thus is decreasing at a slow, linear rate in untransformed space. This slope agrees well with the results of Shen et al. (1969) from laboratory and field data compiled from five investigations. The LOWESS curve in figure 34 follows a \log_{10} slope of about 0.77. The local pier scour equation in *HEC-18: Evaluating Scour at Bridges* (Richardson et al., 1993) includes pier width to the 0.65 power. Larras' local scour equation is a function of pier width to the 0.75 power (Shen et al., 1969), and the Chinese scour equation includes pier width to the 0.6 power (Don Guang et al., 1992).

The relation shown in figure 34 indicates that a scour prediction equation of pier width times a constant, such as Breusser's, would tend to underpredict scour for smaller pier widths and to overpredict scour for larger pier widths if the curve were fit to the center of the data (minimized error). Similarly, the influence of pier width would tend to be underrated for smaller pier widths and overrated for larger ones when pier width is used with an exponent of 1 in the computation of local scour, as in many design equations. However, pier width (with an exponent of 1) remains the most obvious choice to non-dimensionalize the scour depth for non-dimensional data analysis.

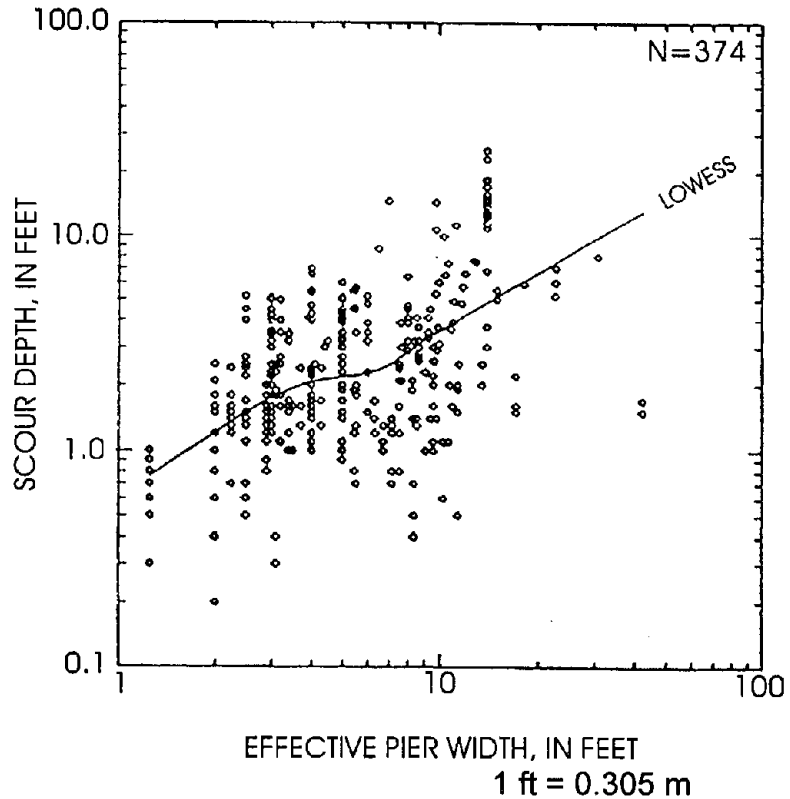


Figure 34. Relation of effect of pier width (b_e) and scour depth (y_{sp}).

Maximum y_{sp}/b (scour depth/pier width) values of 2.4 and 3.0 are suggested for Froude numbers in the range of less than and greater than 0.8, respectively, in *HEC-18: Evaluating Scour at Bridges* (Richardson et al., 1993). The pier scour design method presented by Melville and Sutherland (1988) is based upon a maximum scour depth of 2.4 pier diameters for a cylindrical pier, which is then modified by coefficients that account for other scour variables. The maximum y_{sp}/b for the 212 live-bed scour measurements presented by Dong Guang et al. (1992) is 3.1. The maximum y_{sp}/b for this data set is 2.6. However, when the pier width is corrected for skew using equation 5, the maximum y_{sp}/b_e value for this data set is 2.1.

Pier Alignment Effects

Most design methods account for skew of pier alignment to flood flow using a correction coefficient or by using the effective width of the pier as defined by equation 5. The coefficients from Laursen (1960) are often used, and *HEC-18: Evaluating Scour at Bridges* (Richardson et al., 1993) uses coefficients similar to those presented by Laursen. Froehlich (1988) uses the ratio of effective pier width to pier width (b_e/b) as an explanatory variable in his ordinary least-squares regression analysis of 66 field measurements of live-bed local scour (which include some measurements reported in this data base from Alaska (Norman, 1975) and Colorado (Jarrett and Boyle, 1986)). Froehlich's regression of y_{sp}/b on four dimensionless explanatory variables in logarithmic units yielded an exponent of 0.62 for b_e/b . The relation of dimensionless scour depth to dimensionless effective pier width is shown in figure 35 for the 111 measurements with piers

skewed to the flow. The 0.62 slope curve from Froehlich's equation is also shown. At large effective pier width ratios, the rate at which pier alignment influences local scour appears to decrease. This may be because the maximum scour under these conditions has moved to a location along the side of the pier and underneath the bridge, where limited-detail methods usually cannot obtain a measurement; yet the measurement made at the nose of the pier may have been recorded as the maximum scour.

For most of the analyses in this study, scour depth was normalized for pier width and made non-dimensional by dividing it by the effective pier width (b_e), in preference to unadjusted pier width (b), so that the effects of pier alignment would not obscure the exploration of other scour processes.

Pier Nose Shape Effects

Differences in the shape of the nose of a pier can cause scour depth to vary by ± 10 percent, according to *HEC-18: Evaluating Scour at Bridges* (Richardson et al., 1993) and based on laboratory flume investigations. The pressure field, vortices, and downward flow velocity will be more intense for a blunt-nosed pier than for a streamlined pier, resulting in larger scour depths. The field data do not support this finding, as illustrated in figure 36, where the square pier nose shape is seen to have smaller characteristic scour depths than the sharp, cylindrical, and round pier nose shapes. However, these results are probably less reliable than those from laboratory studies where pier shape effects have been analyzed independent of other factors. The field data represent

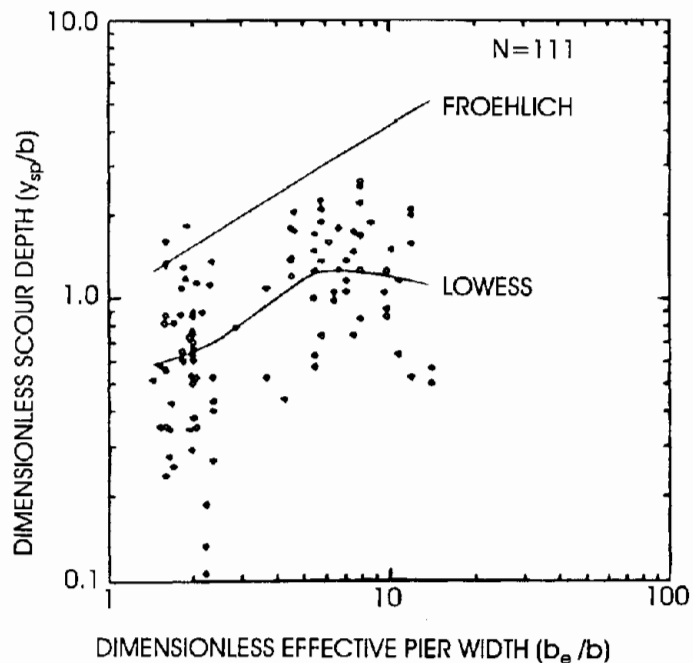


Figure 35. Relation of effective pier width to dimensionless scour depth for piers skewed to the flow.

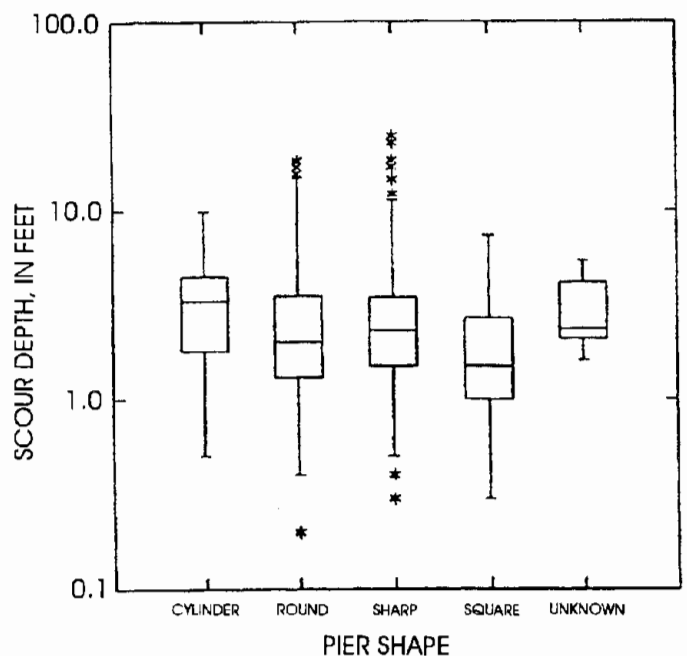


Figure 36. Distribution of scour depth data according to pier shape.

the combined results of several processes and only the most influential ones are likely to be apparent in this analysis. For example, Melville and Sutherland (1988) state that there is no effect from pier streamlining for skews greater than 10 to 15 degrees, and *HEC-18: Evaluating Scour at Bridges* (Richardson et al., 1993) states that the effect of pier shape is negligible for skew angles exceeding 5 degrees. The influence of even minor debris accumulations would also overwhelm pier shape effects.

Flow Depth Effects

The effect of approach flow depth on local scour depth has been somewhat disputed in previous literature. Laursen and Toch (1956) stated that the principal hydraulic parameter affecting scour is flow depth, not velocity. Shen et al. (1969) found the effect of flow depth on equilibrium scour depth to be very slight. In *HEC-18: Evaluating Scour at Bridges* (Richardson et al., 1993), the equation for dimensionless local scour depth includes a factor of flow depth over pier width (y_o/b) to the 0.35 power. More recent laboratory studies for clear-water scour have found the influence of scour depth to be significant only for depth to pier width ratios (y_o/b) less than about 3 (Ettema, 1980; Raudkivi and Ettema, 1983). At these smaller y_o/b ratios, scour reportedly increases with increasing flow depth because of decreasing interference of the surface bow wave with the horseshoe vortex at the base of the pier. Raudkivi and Ettema (1983) found that as sediment size increases, flow depth influences clear-water scour over a larger range in flow depth. They state that for fine sediments, the scour depth may be independent of flow depth at y_o/b greater than about 1; while for coarse sediments, flow depth may have an influence up to a y_o/b of about 6. These relations were found to also be applicable for live-bed scour (Chiew, 1984; Chiew and Melville, 1987) in analyses of laboratory-measured clear-water and live-bed scour data. In the design method presented by Melville and Sutherland (1988), local scour is computed using a flow depth correction factor when y_o/b is less than 2.6 and is computed independent of flow depth where y_o/b is larger than 2.6.

An analysis of the effect of flow depth on scour is difficult with field data because the flow depth is closely related to measured velocity and to pier width (because larger piers are typically found in deeper rivers). The relation between y_o/b_e and y_{sp}/b_e is shown in figure 37A in untransformed units. In an effort to evaluate the effect of flow depth apart from flow velocity, the y_{sp}/b_e values were normalized for flow intensity, which was evaluated as the ratio of measured velocity to critical incipient motion velocity (V_o/V_c). The relation between dimensionless flow depth and scour depth normalized for flow intensity is shown in figure 37B in untransformed units. This relation appears very poorly defined and is not improved by normalizing dimensionless scour depth for flow intensity. The Kendall's Tau monotonic correlation coefficients for the relations in figures 37A and 37B are 0.36 and 0.33, respectively. The LOWESS curves in figure 37 (A and B) indicate that flow depth has only a small influence on scour depth at y_o/b_e values greater than about 6, which would be in partial agreement with the laboratory-based results of Raudkivi and Ettema (1983), and Chiew and Melville (1987).

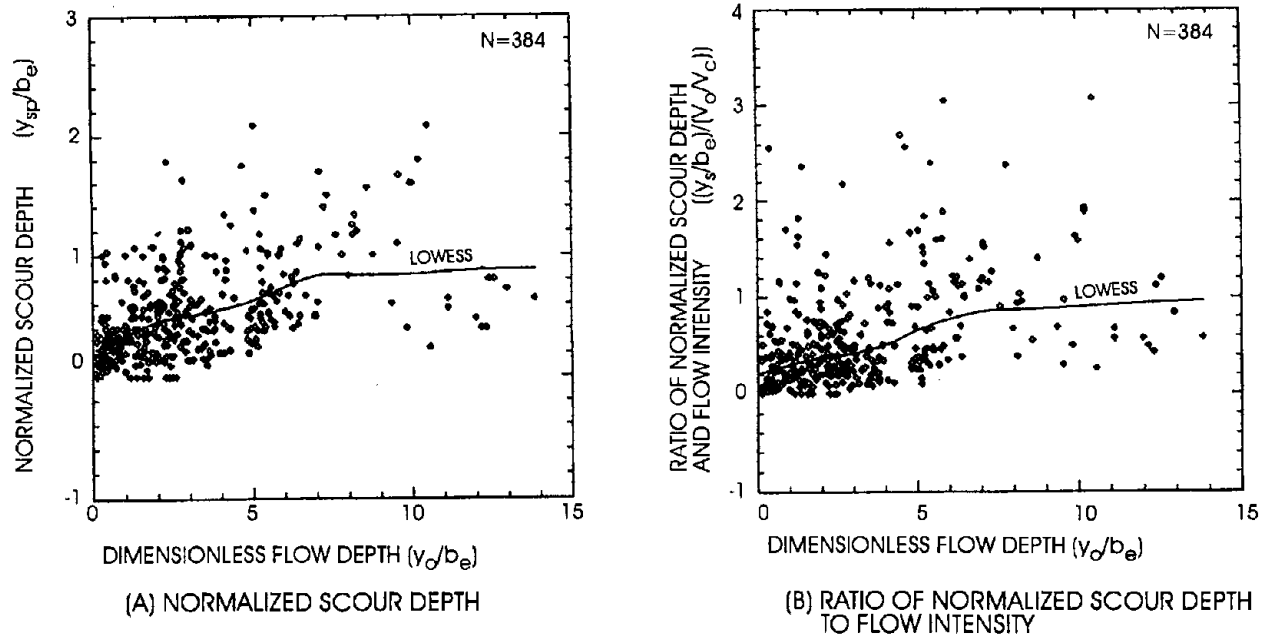
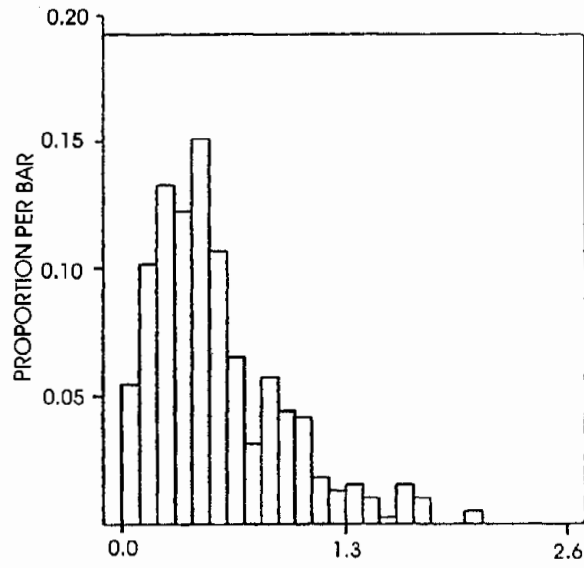


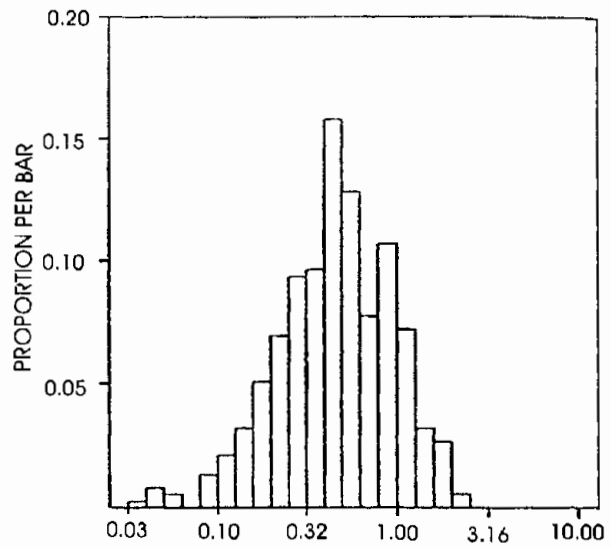
Figure 37. Relation of ratio of flow depth to effective pier width to: (A) scour depth normalized for pier width, and (B) scour depth normalized for pier width and flow intensity.

However, monotonic correlation coefficients do not improve for the subset of measurements at y_o/b_e values less than 6. Analyses did not identify a trend in this relation with sediment size, evaluated as the ratio of effective pier width to median grain size (b_e/D_{50}). However, about 89 percent of the data set had b_e/D_{50} values greater than 30, where grain size would not significantly affect the influence of flow depth according to previous research (Raudkivi and Ettema, 1983).

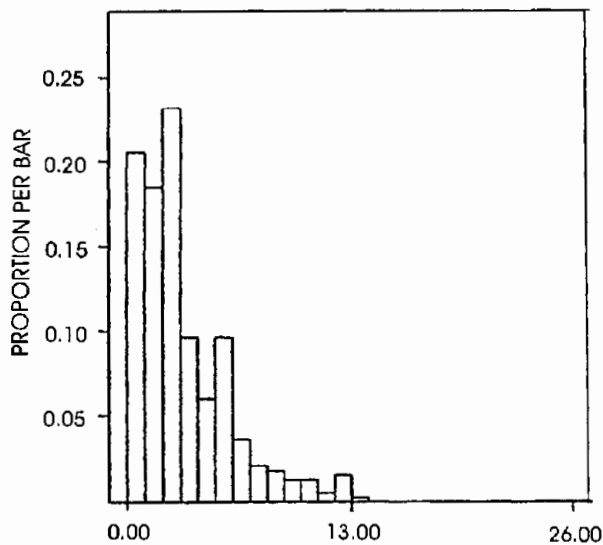
The analyses described above were made in untransformed units to facilitate comparisons with previous investigations also made in untransformed units. As discussed in the data summary, problems can arise when parameters having nonlinear data distributions are analyzed in a linear relation. Figure 38 shows that the untransformed y_{sp}/b_e and y_o/b_e are right skewed, while the \log_{10} -transformed data are comparatively symmetric. The relations of y_{sp}/b_e and $(y_{sp}/b_e)/(V_o/V_c)$ to y_o/b_e in \log_{10} space are illustrated for the 374 non-zero scour depths in figure 39 (A and B), where the relation appears much stronger and near linear. The Pearson linear correlation coefficients for figures 39 A and B are 0.54 and 0.50 (monotonic correlation is not altered by transformations). The \log_{10} slope of the curves in figure 39 (A and B) is between 0.4 and 0.5, so that in linear space, the influence of flow depth decreases at a uniform rate, but does not become insignificant over the range of measured data.



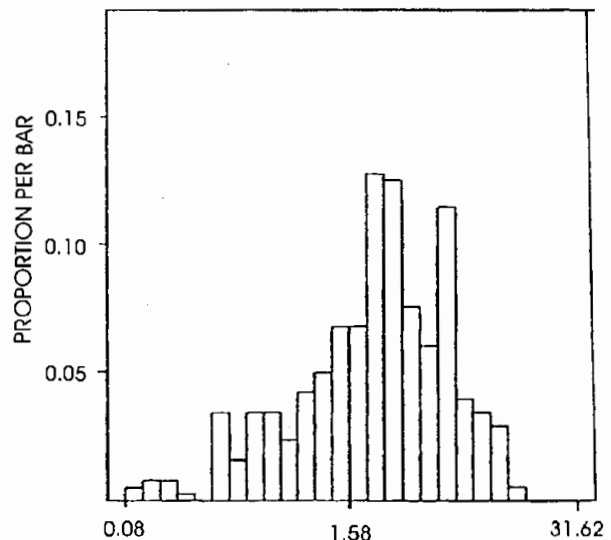
(A) NORMALIZED DEPTH OF SCOUR



(B) LOG-TRANSFORMED NORMALIZED DEPTH OF SCOUR



(C) DIMENSIONLESS DEPTH OF FLOW



(D) LOG-TRANSFORMED DIMENSIONLESS DEPTH OF FLOW

Figure 38. Characteristics of: (A) untransformed and (B) log-transformed scour depth to effective pier width ratio, and (C) untransformed and (D) log-transformed flow depth to effective pier width ratio.

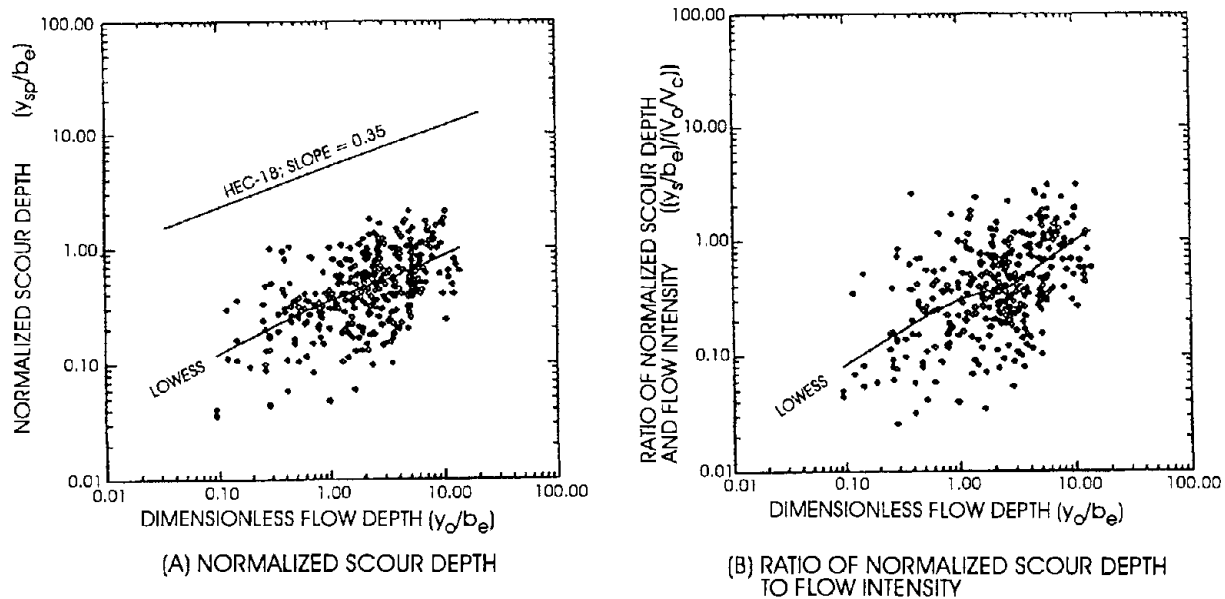


Figure 39. Relation of ratio of flow depth to effective pier width to: (A) scour depth normalized for pier width, and (B) scour depth normalized for pier width and flow intensity.

The relation for flow depth and scour depth defined in the local pier scour equation (referred to as the HEC-18 equation) presented in *HEC-18: Evaluating Scour at Bridges* (Hydraulic Engineering Circular 18, Richardson et al., 1993) is in general agreement with the measured data as shown in figure 39A. However, these results do not confirm the findings of previous investigations that scour becomes independent of flow depth above some upper limit of y_o/b_e . The LOWESS curves in figure 39 (A and B) do indicate a slight change in the relation at a y_o/b_e value of about 1, so that the relation could be driven by interfering horizontal vortices at shallower depths and by other processes at larger depths. The continued influence of flow depth at large y_o/b_e values could be due to the influence of other factors, such as velocity or bed-load transport, embedded in the flow depth factor. In figures 37B and 39B, scour depth was normalized for the influence of flow intensity, which is discussed in the next section.

Flow Intensity Effects

Flow intensity influences the local scour because it affects the initiation and rate of bed-load transport and the pressure field, downward flow velocity, and vortices generated around the pier. Several researchers (Neill, 1964; Bruessers et al., 1977; and others) have found that scour depth increases with increasing flow velocity to a maximum value at threshold sediment transport conditions, then decreases slightly and tends toward an equilibrium scour depth that is independent of further increases in flow velocity. Clear-water scour depth increases with increasing velocity because the local scouring energy increases while the sediment transport into the scour hole remains insignificant. Live-bed scour depth is related to the relative rate of sediment transport into and out of the local scour hole. In an analysis based on data from several investigations, Melville (1984) found that the relation of maximum scour depth to flow velocity has the form shown in figure 40, with a second peak beyond the one occurring near the threshold

between clear-water and live-bed sediment transport. Melville reported that the second peak occurs under plane bed form conditions, which exist at the transition between dune and anti-dune bed forms. Under those conditions, the shear stress due to bed form drag is at a minimum. As indicated in figure 40, Melville found that for fine sediments (defined as $D_{50} \leq 0.7$ mm), this second peak is greater than the one occurring near threshold velocity. Each of the bed materials used in Melville's (1984) investigation had a uniform gradation.

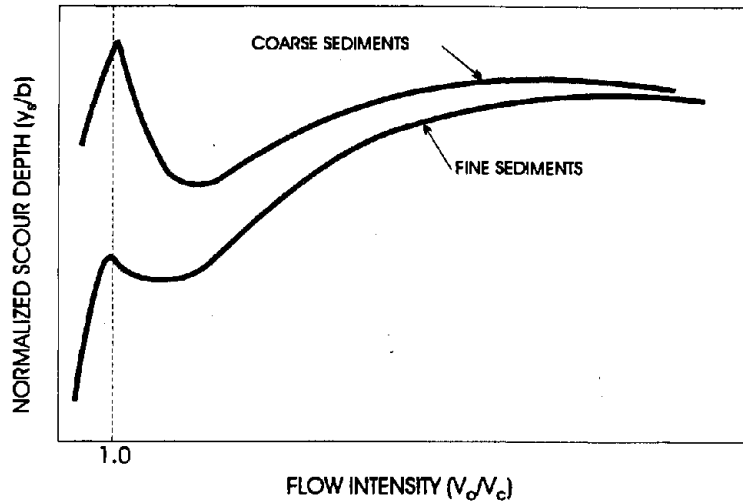


Figure 40. Relation of normalized maximum scour depth to flow intensity (v_o/v_c) (Melville, 1984).

In this investigation, three dimensionless variables were tested to quantify the effect of flow intensity on local scour. The first flow intensity variable is the ratio of measured velocity to critical incipient motion velocity (V_o/V_c) for the D_{50} -sized particle, where V_c is computed using equation 3. This variable provides a measure of flow intensity normalized for the critical sediment transport velocity for the bed material. Figure 41 shows the relation between this normalized velocity and y_{sp}/b_c . The second variable is similar to the first, but

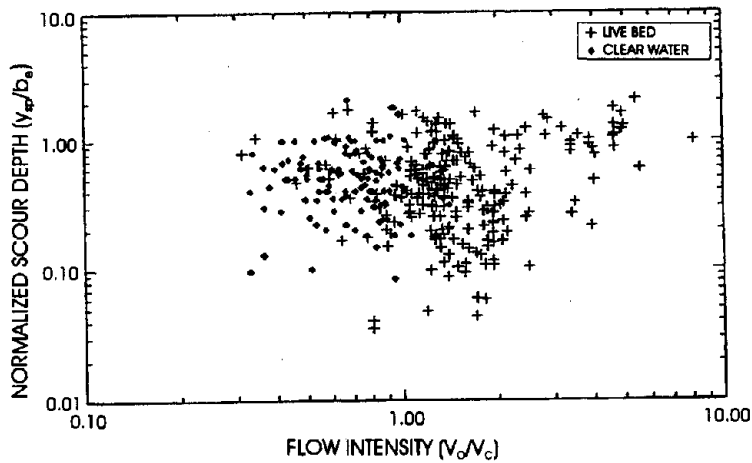


Figure 41. Relation of flow intensity variable v_o/v_c to normalized scour depth.

it includes a measure of sediment gradation, which influences both the formation of an armor layer in the channel and the availability of larger particles that may concentrate in the scour hole. This variable is computed as $[V_o - (V_{c(D84)} - V_c)]/V_c$, where $V_{c(D84)}$ is the critical incipient motion velocity for the D_{84} -sized particle computed using equation 3. This factor has the same form as one used by Melville and Sutherland (1988), except Melville and Sutherland used the critical incipient motion velocity for the median particle size of the armor layer (D_{50a}) rather than $V_{c(D84)}$. (Melville and Sutherland (1988) describe a method for estimating D_{50a} and use a formula to estimate average incipient motion velocity that is different from that used by Neill (1968).) Figure 42 shows the relation between this flow intensity variable and scour depth.

Observations on the relation of flow intensity to scour depth from figures 41 and 42 are similar; however, the second variable (figure 42) may be a more representative measure of flow intensity effects. In general, these figures indicate a very weak relation between scour depth and flow intensity. Scour depth appears to increase with increasing flow intensity for clear-water conditions; however, both linear and monotonic correlation coefficients for the clear-water measurements in these plots are less than 0.1. The variance of the data is significantly

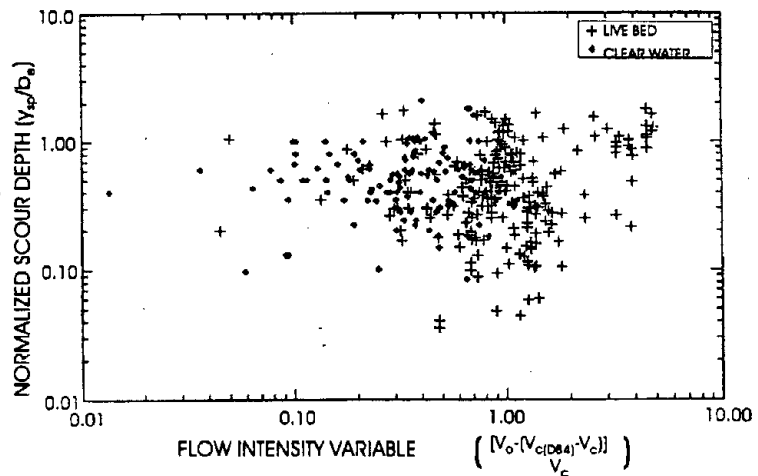


Figure 42. Relation of flow intensity variable $[v_o - (v_{c(D84)} - v_c)]/v_c$ and normalized scour depth.

greater in the vicinity of threshold conditions ($V_o/V_c = 1.0$), which may reflect relatively unsteady conditions associated with threshold sediment transport. The data may indicate a decrease in scour depth between V_o/V_c values of 1 and 2, as laboratory studies have found for equilibrium scour conditions. Scour depth appears to be insensitive to flow intensity where these flow intensity variables are greater than 2. The relations do not indicate that scour depth increases to a second peak at large values of V_o/V_c . The results from figures 41 and 42 are not conclusive and additional analysis of this relation is being performed.

Laboratory studies have found that the relation of scour depth and flow intensity is represented by a series of curves differentiated by both sediment size and flow depth; thus, a smoothing algorithm may not be appropriate and LOWESS curves were not drawn on these scatter plots. This may account for the large scatter in these plots and the very poor general correlation of scour depth and flow intensity. However, comparisons of these relations for data subsets, defined by sediment size and flow depth classes, did not demonstrate such secondary relations or curve series. The sediment transport classifications (live bed or clear water) made by the measurement personnel do not always agree with the ratio of measured to critical velocity, as seen in figure 41.

The third variable used to quantify flow intensity is the Froude number, a commonly used measure of energy in open channel flow. The Froude number is computed as $\frac{V_o}{\sqrt{gy_o}}$. The local

scour design equations from *HEC-18: Evaluating Scour at Bridges* (Richardson et al., 1993) and Froehlich (1988) include the Froude number to the 0.43 power and the 0.20 power, respectively. The relation of the Froude number to scour depth for the data of this report is shown in figure 43.

The data of this figure indicate that scour depth decreases slightly with increasing Froude number, which does not support the relation in the equation from HEC-18 (Richardson et al., 1993). Figure 43 shows the Froude number to be a poor indicator of flow intensity effects. This may be due to the influence of the square root of flow depth in the denominator of the Froude number and because the Froude number is not normalized for the sediment transport conditions of the measurement.

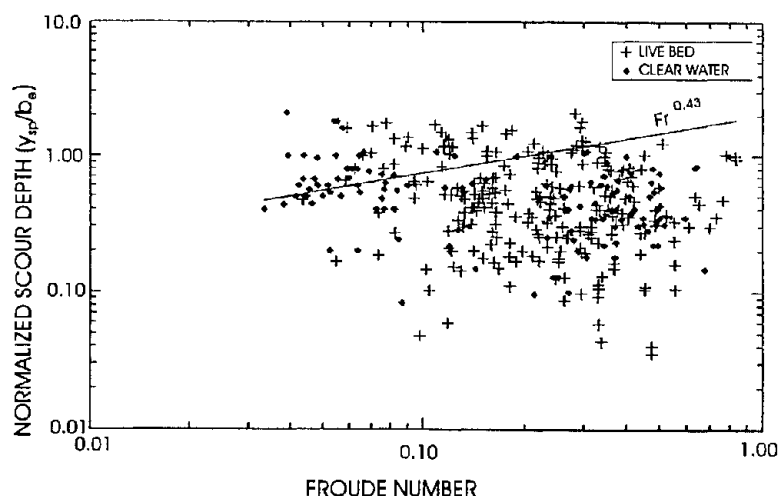


Figure 43. Relation of Froude number to normalized scour depth.

Sediment Size Effects

The principal effect of sediment size on local scour is its influence on the initiation and rate of bed material transport into the scour hole. That effect is evaluated in computations of critical velocity for incipient motion. In laboratory investigations reported by several researchers (Ettema, 1980; Chiew, 1984; Raudkivi and Ettema, 1983; Raudkivi, 1986; Chiew and Melville, 1987), equilibrium scour depth has been shown to decrease with increasing bed material size at pier width to median sediment size ratios (b/D_{50}) less than about 50 for both clear-water and live-bed conditions. According to these researchers, larger particles reduce the local scour because they more effectively dissipate the energy of the downward flow velocity where it intersects the bed, and because they are physically large with respect to the groove eroded by the downward velocity where it intersects the bed at the base of the pier. Chiew and Melville (1987) showed that y_{sp}/b increases with logarithmic b/D_{50} in a nearly linear relation up to a b/D_{50} value of about 50.

The direct effect of sediment size on local scour depth is not accounted for in most scour prediction formulas; for example, the local pier scour equation of HEC-18 (Richardson et al., 1993) does not include a sediment size factor. Froehlich (1988) used the ratio of pier width to median sediment size in his local scour regression analysis and computed an exponent of 0.08 for this ratio. Dong Guang et al. (1992) reported a sediment size correction coefficient based on a regression analysis of 40 field measurements of local scour under clear-water conditions. This coefficient is used in the Chinese local scour equations and is computed as a function of D_{50} (or average D) to the -0.07 power. The results of Froehlich and Dong Guang are similar; however, they are derived using the method of ordinary least-squares regression on field data, which is problematic as discussed previously. Melville and Sutherland's (1988) design method uses a sediment size factor developed from Ettema's (1980) clear-water and Chiew's (1984) live-bed scour data and is computed as a function of $\log(2.24(b/D_{50}))$.

Figure 44 illustrates the scatter plot of the sediment size versus scour depth parameters for the measurements where the b_e/D_{50} is less than 100. The 88 measurements shown in figure 44 came from 17 sites and have a D_{50} ranging from 10.2 to 108 mm. Several methods were used to analyze this relation, including an analysis using D_{84} ; however, no discernable effect of sediment size on local scour was apparent, as indicated in figure 44. The non-concurrence of these results with previous investigations may be due to non-equilibrium conditions, scale factors (in the case of model data), or to differences between characteristics of the sampled sediment and of sediment in the local scour hole.

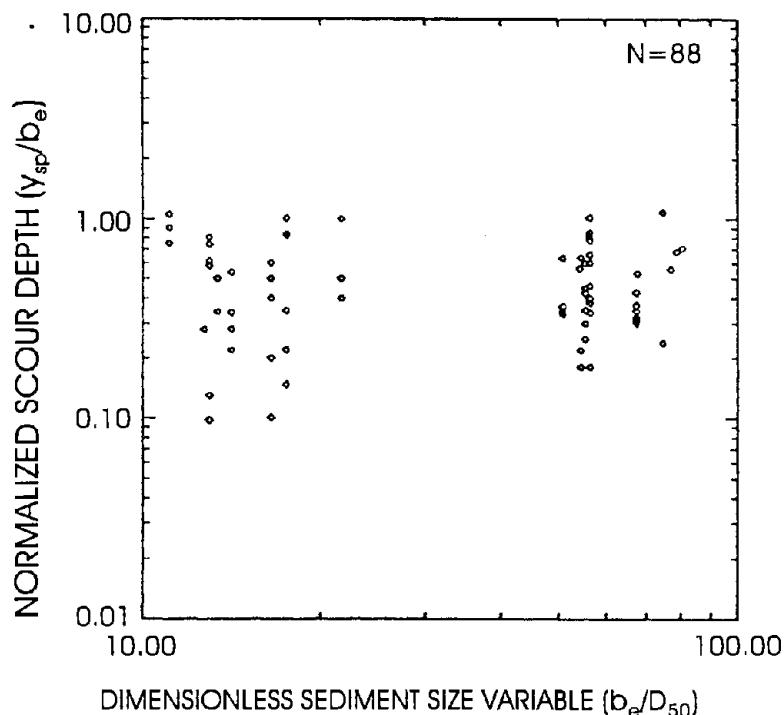


Figure 44. Relation of dimensionless sediment size variable to normalized scour depth.

Bed material sampling methods are typically designed to obtain samples that represent the general stream channel as it affects sediment transport. Bed material samples that represent the channel may not represent the scour hole sediments, although the two are typically similar. Observations and limited sampling of sediments, both in local scour holes and in the channel, indicate that differences may exist, with larger particles being found in the scour hole. Larger particles may accumulate in a scour hole because it requires more energy to roll these particles up the slope and out of the scour hole rather than along the bed (effectively increasing the critical shear stress at this location).

The lack of correlation between sediment size and scour depth for this data set is inconclusive. These data may not indicate a relation for reasons described above; however, additional analysis of these data and of the process is warranted. Specifically, investigations of the comparative size distributions of sediment in the channel and in local scour holes and of the potential scale distortion of model results for bed material analyses would contribute to understanding this process.

Sediment Gradation Effects

Natural streams do not have uniform-sized channel bed material. Bed material transport begins with relatively small particles at velocities less than the incipient motion velocity of D_{50} -sized particles and initiates a gradual process of selective bed material transport. As finer particles are removed, larger particle sizes (where they occur in adequate number) may be

concentrated and form an armor layer at the surface that limits erosion until flow intensities are adequate to move the armor layer particles. Sediment gradation is one measure of the capacity of a channel to have an armor layer. The process of selective transport of graded sediments affects the equilibrium scour depth in general, not only for the case where an armored surface is formed. The median sediment size becomes less descriptive of bed material characteristics as the sediment gradation increases. Sediment gradation was found to have a strong influence on the time rate of scour and on equilibrium scour depth for clear-water conditions in investigations by Raudkivi and Ettema (1977) based on laboratory data. Raudkivi and Ettema (1977) found that for clear-water conditions, the equilibrium scour depth in graded sediment with a geometric standard deviation (σ_g) of about 3.5 could be about 80 percent less than that in a uniform-sized sediment. Raudkivi and Ettema (1983) present these results as a gradation factor that is the ratio of equilibrium scour depth in a graded sediment to that in a uniform sediment. Raudkivi and Ettema (1977, 1983) show data used to develop their relation that have a range of D_{50} from 0.55 to 6.00 mm and a range of σ_g from 1 to about 4.6. Mellville and Sutherland (1988) discuss the influence of σ_g for clear-water and live-bed conditions based on results obtained by Baker (1986) using sediments with a D_{50} of 0.6 mm and with σ_g ranging from 1.3 to 5.2. These results indicate that the influence of sediment gradation is less significant under live-bed conditions and tends to decrease as velocities increase.

Sediment gradation is usually not accounted for in scour design methods. The flow intensity variable used in the design method of Melville and Sutherland (1988) accounts for sediment gradation indirectly. The computation of their flow intensity variable includes the critical velocity for the median particle size of the general bed material D_{50} and of the armor layer D_{50a} . The D_{50a} particle size is computed as a function of σ_g and D_{50} , and its critical velocity represents a limiting armor condition.

The relation between dimensionless scour depth (y_{sp}/b_e) and σ_g for the field measurements of this investigation is shown in figures 45 and 46 for clear-water and live-bed conditions, respectively. The relation is difficult to evaluate with field data because the influence of gradation may not be in equilibrium with the scour depth at the time of the measurement. The LOWESS smoothing of the data makes the general trend of the data more apparent. The relations defined in figures 45 and 46 are similar in form. The scour tends to decrease as σ_g increases from a near uniform condition to a value of about 2.8. The trend of the smoothing and the lower boundary of the data appears to reverse at a σ_g of about 2.8; however, an upper envelope curve of the data would indicate that scour decreases with σ_g for the range of measured data. These results may indicate that the data come from separate populations. The median value of both D_{50} and D_{84} is notably lower for the measurements where σ_g is less than 2.8, compared to measurements where σ_g is greater than 2.8.

The relation between σ_g and y_{sp}/b_e appears reasonable for σ_g less than 2.8. The slope of the relation for the live-bed condition agrees well with the result in Raudkivi and Ettema (1977), which is shown in figures 45 and 46 for a y_{sp}/b_e of 2.4. For the clear-water case, the relation is at least in the expected direction for a σ_g of less than 2.8. It is not reasonable that y_{sp}/b_e would increase as σ_g increases from 2.8 and for a group of measurements with larger characteristic sediment sizes. The apparent relation for a σ_g greater than about 2.8 may represent effects of other parameters embedded in sediment gradation.

A dimensionless sediment size factor was derived from the product of σ_g and D_{50} divided by b_e . The relation of this sediment factor to y_{sp}/b_e is shown in figure 47. This relation indicates a very moderate decrease in scour depth with increasing σ_g and D_{50} , up to a $(\sigma_g D_{50})/b_e$ value of about 0.001. In general, this figure illustrates the minor influence of sediment characteristics on scour depth for the measured data of this investigation.

Analysis of the relation of local scour depth to sediment size and gradation based on these data is continuing. Laboratory studies using sediments with a large σ_g would be valuable. In the data of this study, the direct influence of sediment size on local scour is not apparent and local scour appears to decrease as sediment gradation increases from a uniform gradation to a σ_g of about 2.8. Scour depth appears to be larger for smaller, more uniform sediments (figure 47).

Analyses of these data provide information on local scour processes at bridge piers and on the relation of scour depth to selected explanatory variables that may be used in scour design equations. Predicted scour depths are compared with observed scour for several equations in the following section.

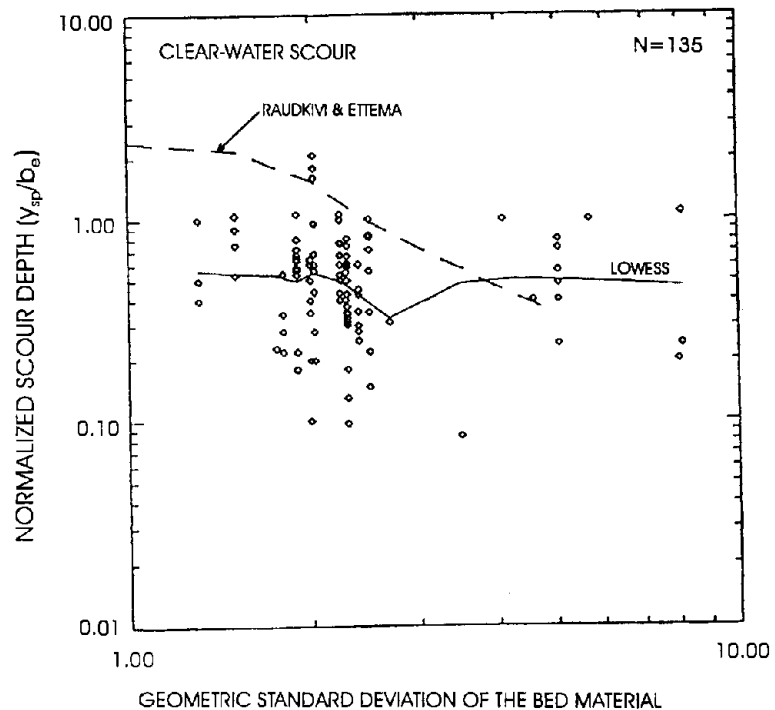


Figure 45. Relation of the geometric standard deviation of the bed material (σ_g) to normalized scour depth (y_{sp}/b_e) for clear-water scour measurements compared with relation in Raudkivi and Ettema (1977).

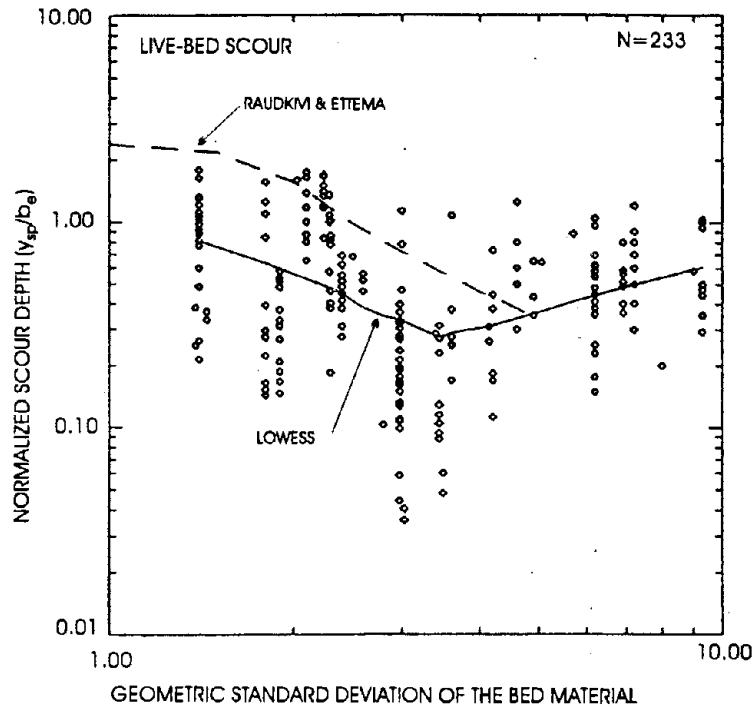


Figure 46. Relation of geometric standard deviation of the bed material (σ_g) to normalized scour depth (y_{sp}/b_e) for live-bed scour measurements compared with relation in Raudkivi and Ettema (1977).

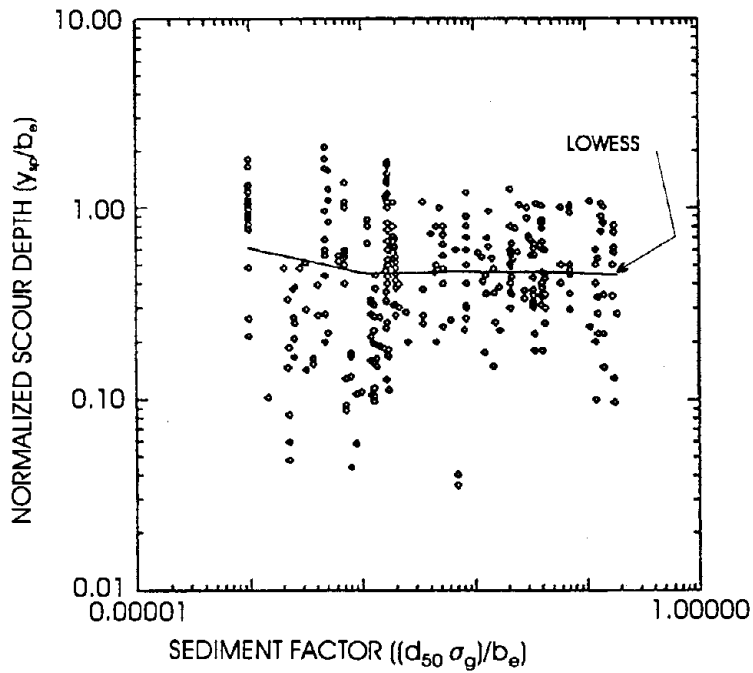


Figure 47. Relation of sediment factor to normalized scour depth.

Page Intentionally Left Blank

EVALUATION OF SELECTED PIER SCOUR EQUATIONS

A literature review of bridge scour equations by McIntosh (1989) found that more than 35 equations have been proposed for estimating the local scour at bridge piers. Numerous equations also have been developed for prediction of scour at abutments and scour that is a result of channel-width contractions. Most local-scour equations are based on research with scale models in laboratory flumes with cohesionless, uniform bed material and limited field verification (McIntosh, 1989). The contraction- and local-scour equations produce a wide range of scour-depth estimates for the same set of conditions (Anderson, 1974; Hopkins et al., 1980; Richards, 1991). This range of estimates is probably due largely to the unique conditions that were modeled in each investigation, differences in how the equations were developed, and differences in how model data were interpreted. Differences between scour predictions and scour measurements at bridge sites are also common. These differences may be due largely to the broad range of deterministic scour variables in the field that are difficult to reproduce and are often not modeled in the laboratory, and due to dynamic dissimilarity between field conditions and laboratory investigations. In evaluating and applying scour prediction equations, it is valuable to know their limitations, the conditions for which they were developed, how the underlying data were interpreted, and the methods used to develop the equations. However, some of this information is not available in the literature for many of the equations.

Data used to develop scour equations have been collected and analyzed using several methods. Studies have used different scour depth reference surfaces, as discussed previously. Several scour studies have been conducted in flumes under clear-water conditions. In studies conducted under live-bed conditions, scour depth is typically measured under equilibrium sediment transport conditions and the recorded depth is averaged over the periodic changes in bed elevation caused by the passage of dunes. Therefore, equations that are based on live-bed laboratory data often compute equilibrium scour. Some researchers assume that the scour measured in the field represents equilibrium conditions, whereas others have assumed that it represents the maximum scour associated with the passage of the dune trough. The extent to which the equilibrium or maximum condition is represented in a field measurement usually cannot be determined without repeated measurements, and this factor brings uncertainty into the measured scour in comparisons with the depth of scour computed from published equations.

Different methods have been used to develop pier scour equations from laboratory and field data. Most equations were developed by fitting a curve or curves to envelop all or most of the scour data. These equations will compute values that exceed the observed values from which they were developed. Some equations were developed by the method of ordinary least-squares regression and will compute scour depths equal to or less than the measured depths for one-half of the data set from which they are developed. For design purposes, it may be desirable to use an equation that computes the maximum depth of scour that could be expected, effectively including a factor of safety. Alternatively, an accurate predictive equation would allow a designer to assign a risk-based factor of safety to a given scour estimate. This report describes the method used to develop the evaluated equations where that information was available.

Review and evaluation of all published equations were beyond the scope of this study; therefore, a limited number of equations were selected. A consistent notation for variables is used for presentation and discussion of the equations in this report; consequently, the notation used here may not be identical to the notation in the references cited. The variables are defined in the text the first time they are introduced. A complete listing of the variables is provided in the "Symbols" section at the front of this report. Many of the equations are dimensionless; therefore, any system of units can be used as long as they are used consistently. If an equation is not dimensionless, the units are defined with the equation in which they are required.

Description of Equations

AHMAD EQUATION

Ahmad (1953) concluded from previous investigations of scour around spur dikes that local scour is not influenced by grain sizes within the range typical of the alluvial plains of West Pakistan (0.1 to 0.7 mm). He stated that this conclusion may not be valid for the entire range of bed material grain sizes. Ahmad (1962) reanalyzed the work of Laursen (1962) with a special emphasis on scour in sand-bed streams in West Pakistan and developed the following equation:

$$y_p = K q^{2/3} \quad (5)$$

where

$$y_p = y_o + y_{sp} \quad (6)$$

- y_p is scoured depth of flow at the bridge pier, including local pier scour;
- y_o is depth of flow just upstream of the bridge pier or abutment, excluding local scour;
- y_{sp} is depth of pier scour below the ambient bed;
- q is discharge per unit width just upstream from the pier; and
- K is a coefficient that is a function of boundary geometry, pier width, pier shape, and the angle of the approach flow. On the basis of numerous model studies, Ahmad (1962) suggested that the coefficient should be in the range of 1.7 to 2.0 for piers and abutments. For this investigation, it was assumed to be 1.8.

Equation 5 is dimensional, with y_p in feet and q in cubic feet per second per foot. Solving equations 5 and 6 for y_{sp} yields the Ahmad equation:

$$y_{sp} = K q^{2/3} - y_o \quad (7)$$

Equation 7 is dimensional, with y_{sp} and y_o in feet and q in cubic feet per second per foot.

BLENCH-INGLIS EQUATIONS

Inglis (1949) performed numerous experiments on model bridge piers and developed an empirical formula by fitting a curve to the plotted data. Blench (1962) reduced Inglis' (1949) original formula to the form:

$$\frac{y_p}{y_r} = 1.8 \left(\frac{b}{y_r} \right)^{0.25} \quad (8)$$

where

$$y_r = \left(\frac{q^2}{f_b} \right)^{2/3} \quad (9)$$

and b is the width of the bridge pier;
 y_r is the regime depth of flow; and
 f_b is the bed factor.

Equation 9 is dimensional with y_r in feet, q in cubic feet per second per foot, and f_b treated as a constant. Blench (1951) stated that the bed factor was related to the sediment load characteristics and defined it as:

$$f_b = \frac{V^2}{y} \quad (10)$$

where V is the average velocity of the section; and
 y is the average depth of the section.

Equation 10 is dimensional, with y in feet and V in feet per second. Lacey (1936) proposed a rough estimate for the bed factor based on grain size; this relation was modified by other researchers, including Blench (1951, 1969), and is as follows:

$$f_b = 1.9 \sqrt{D_{50}} \quad (11)$$

where D_{50} is the median grain size of the bed material.

Equation 11 is dimensional with D_{50} in millimeters. The value of the coefficient in equation 11 varies in the literature; but a value of 1.9 is common. In applying regime theory to bridge scour, if the average velocity and depth in equation 10 can be approximated by the conditions just upstream of the pier, then equations 6, 8, 9, and 10 can be solved to obtain equation 12 for y_{sp} , which will be referred to as the "Blench-Inglis I equation":

$$y_{sp} = 1.8 b^{0.25} q^{0.5} \left(\frac{y_o}{V_o^2} \right)^{0.25} - y_o \quad (12)$$

where V_o is the velocity of the approach flow just upstream from the bridge pier or abutment.

Equation 12 is dimensional, with y_{sp} , b , and y_o in feet; q in cubic feet per second per foot; and V_o in feet per second. If the bed factor is estimated based on grain size, equations 6, 8, 9, and 11 can be solved to obtain equation 13 for y_{sp} , which will be referred to as the "Blench-Inglis II equation":

$$y_{sp} = 1.8 b^{0.25} \left(\frac{q^2}{1.9 \sqrt{D_{50}}} \right)^{0.25} - y_o \quad (13)$$

Equation 13 is dimensional, with y_{sp} , b , and y_o in feet; q in cubic feet per second per foot; and D_{50} in millimeters.

SIMPLIFIED CHINESE EQUATIONS

Gao et al. (1992) presented scour equations that have been used in China for more than 20 years by highway and railway engineers. These equations were developed from laboratory and field data for both live-bed and clear-water scour at bridge piers. Gao et al. (1992) define critical velocity of the bed material by the equation from Zang et al. (1981):

$$V_c = \left(\frac{y_o}{D_m} \right)^{0.14} \left(17.6 \left[\frac{\rho_s - \rho}{\rho} \right] D_m + 6.05E(-7) \left[\frac{10 + y_o}{D_m^{0.72}} \right] \right)^{0.5} \quad (14)$$

where V_c is the critical (incipient motion) velocity for the D_m -sized particle;
 D_m is the mean grain size of the bed material;
 ρ_s is the density of the sediment particles; and
 ρ is the density of water.

Equation 14 is dimensional, with V_c in meters per second, and y_o and D_m in meters.

Many hydraulic model experiments were conducted to relate the velocity in the approach section to the critical velocity in the accelerated flow region around the pier for the mean bed material size (D_m). Data from these experiments were analyzed using multiple-regression analysis to develop the following relation:

$$V_c' = 0.645 \left(\frac{D_m}{b} \right)^{0.053} V_c \quad (15)$$

where V_c' is the approach velocity corresponding to critical velocity and incipient scour in the accelerated flow region at the pier.

Equation 15 indicates that the accelerated flow velocity will be about 1.5 to 3 times the approach flow velocity for pier widths and median grain sizes found in many streams in the United States. Gao and Xu (1989) used V_c' in defining the following dimensionless variable to account for the influence of flow intensity on scour depth:

$$y_{sp} \approx \left(\frac{V_o - V_c'}{V_c - V_c'} \right) \quad (16)$$

Gao and Xu (1989) found scour depth to vary with this flow intensity variable in a linear relation for clear-water conditions, and in an exponential relation for live-bed conditions. In analyses of model experiment data in China, scour depth was found to relate weakly to flow depth and bed material size to exponents of 0.15 and -0.07, respectively. The relation of scour depth and pier width was defined using pier width with an exponent of 0.6. These relations, as well as a coefficient for pier shape and flow alignment were used to derive the following equation:

$$y_{sp} = 0.46 K_\xi b^{0.6} y_o^{0.15} D_m^{-0.07} \left(\frac{V_o - V_c'}{V_c - V_c'} \right)^c \quad (17)$$

where K_ξ is a coefficient for pier shape and flow alignment; and c is an exponent related to the bed material transport condition, defined as $c=1$ if $V_o \leq V_c$ and $c < 1$ if $V_o > V_c$.

Equation 17 is dimensional, with y_{sp} , y_o , b , and D_m in meters. Pier shape coefficients for equation 17 were formulated for 10 types of piers as a function of pier flow alignment by the Academy of Railway Sciences of China (1975) and were described in a detailed table. Gao et al. (1992) defined a simplified pier shape coefficient and developed two simplified equations for clear-water and live-bed conditions. The "Simplified Chinese scour equation" for clear-water conditions is defined as:

$$y_{sp} = 0.78 K_s b^{0.6} y_o^{0.15} D_m^{-0.07} \left(\frac{V_o - V_c'}{V_c - V_c'} \right) \quad (18)$$

where K_s is the simplified pier shape coefficient defined as 1.00 for cylinders, 0.8 for round-nosed piers, and 0.66 for sharp-nosed piers.

Equation 18 is dimensional, with y_{sp} , y_o , b , and D_m in meters. The "Simplified Chinese scour equation" for live-bed conditions, in which flow intensity is related exponentially to scour depth, is defined as:

$$y_{sp} = 0.65 K_s b^{0.6} y_o^{0.15} D_m^{-0.07} \left(\frac{V_o - V_c'}{V_c - V_c'} \right)^c \quad (19)$$

Equation 19 is dimensional, with y_{sp} , y_o , b , and D_m in meters. The exponent c in equation 19 for live-bed conditions is computed using the following equation, which was derived from a regression analysis of 212 groups of field data for live-bed scour conditions:

$$c = \left(\frac{V_c}{V_o} \right)^{9.35 + 2.23 \log D_m} \quad (20)$$

Equation 20 is dimensional, with D_m in meters. The exponent c will always be less than 1, so that the scour depth computed by the Simplified Chinese equation for live-bed conditions is always less than that computed by the Simplified Chinese equation for clear-water conditions. The median grain size, D_{50} , was substituted for the mean grain size, D_m , in equations 19 and 20 for comparison of predicted and observed scour depths in this report.

CHITALE EQUATION

Chitale (1962) conducted a series of experiments on a 1:65 scale model of the Hardings Bridge in India to determine the influence of the approach flow depth and sediment size on scour around piers. In four experiments, the bed of the flume contained 0.32-mm sand, except for the area in the immediate vicinity of the piers where sands having mean diameters of 0.16 mm, 0.24 mm, 0.68 mm, or 1.51 mm were placed. Each experiment was run until the scour depth reached equilibrium. Chitale (1962) made the following observations:

1. For flow aligned with the pier, the location of maximum scour depth was always at the nose of the pier, and scour at the sides of the pier was 5 to 15 percent less than at the nose.
2. There is a linear relation between the approach flow velocity and the ratio of scour depth to approach flow depth.
3. The approach flow depth has an influence on the scour depth.

Although some scatter of the data was evident, Chitale (1962) chose the Froude number to characterize the relative depth of the scour hole, and developed the following equation:

$$\frac{y_{sp}}{y_o} = -5.49 F_o^2 + 6.65 F_o - 0.51 \quad (21)$$

where F_o is the Froude number of the approach flow, defined as $F_o = \frac{V_o}{\sqrt{g y_o}}$; and g is the acceleration of gravity.

Solving equation 21 for y_{sp} results in the "Chitale equation":

$$y_{sp} = y_o (-5.49 F_o^2 + 6.65 F_o - 0.51) \quad (22)$$

The Chitale equation does not account for sediment size effects; however, a visual analysis of the Chitale data indicates that bed material size can affect the relative depth of scour by as much as a factor of 2 for Froude numbers less than 0.2, and to a lesser extent for Froude numbers greater than 0.2 (Chitale, 1962).

FROEHLICH EQUATIONS

Froehlich (1988) compiled field measurements of local scour at bridge piers from the reports of several investigations. All of the data sets were assumed to represent scour depth at equilibrium sediment transport conditions. Froehlich (1988) analyzed only measurements that appeared to have been made in live-bed conditions based on the critical mean-velocity relation presented by Neill (1968). Froehlich (1988) selected dimensionless variables and used linear regression analysis of these live-bed data to develop the following equation:

$$\frac{y_{sp}}{b} = 0.32 \phi F_o^{0.2} \left(\frac{b_e}{b} \right)^{0.62} \left(\frac{y_o}{b} \right)^{0.46} \left(\frac{b}{D_{50}} \right)^{0.08} \quad (23)$$

where b_e is the width of the bridge pier projected normal to the approach flow, as defined by equation 4; and

ϕ is a coefficient based on the shape of the pier nose (1.3 for square-nosed piers, 1.0 for round-nosed piers, 0.7 for sharp-nosed piers).

Solving equation 23 for y_{sp} results in:

$$y_{sp} = 0.32 b \phi F_o^{0.2} \left(\frac{b_e}{b} \right)^{0.62} \left(\frac{y_o}{b} \right)^{0.46} \left(\frac{b}{D_{50}} \right)^{0.08} \quad (24)$$

which will be referred to as the “Froehlich equation.” The predicted scour using equation 24 is less than or equal to the measured scour for one-half of the data set from which it was developed because it was developed using least-squares regression. A design scour depth, for which the predicted scour is greater than the measured scour for all cases in the data set, can be computed as the sum of the pier width (b) and y_{sp} from equation 24. Froehlich (1988) recommended, for design purposes, that the depth of scour computed by equation 24 be increased by the width of the pier. This will be referred to as the “Froehlich Design equation.”

HYDRAULIC ENGINEERING CIRCULAR 18 (HEC-18) EQUATION

The Federal Highway Administration report *HEC-18: Evaluating Scour at Bridges* (Richardson et al., 1993) presents the following equation that was developed using a compilation of laboratory data for scour at circular piers.

$$\frac{y_{sp}}{y_o} = 2.0 K_1 K_2 K_3 \left(\frac{b}{y_o} \right)^{0.65} F_o^{0.43} \quad (25)$$

where K_1 is a coefficient based on the shape of the pier nose (1.1 for square-nosed piers, 1.0 for circular- or round-nosed piers, 0.9 for sharp-nosed piers, and 1.0 for a group of cylinders);

K_2 is a coefficient based on the ratio of the pier length to pier width (L/b) and the alignment of the approach flow to the bridge pier, defined as:

Angle	L/b = 4	L/b = 8	L/b = 12
0°	1	1	1
15°	1.5	2	2.5
30°	2	2.75	3.5
45°	2.3	3.3	4.3
90°	2.5	3.9	5.0

K_3 is a coefficient based on the channel bed conditions defined as:

Bed Condition	Dune Height	K_3
Clear-water scour	N/A	1.1
Plane bed or anti-dunes	N/A	1.1
Small dunes	0.6 to 3.0 m	1.1
Medium dunes	3.0 to 9.1 m	1.1 - 1.2
Large dunes	> 9.1 m	1.3

Solving equation 25 for y_{sp} results in the "HEC-18 equation," defined as:

$$y_{sp} = 2.0 y_o K_1 K_2 K_3 \left(\frac{b}{y_o} \right)^{0.65} F_o^{0.43} \quad (26)$$

Richardson et al. (1993) stated that no correction for pier shape should be made if the alignment of the approach flow is greater than 5 degrees, because the influence of pier shape is not significant at these greater angles.

INGLIS-POONA EQUATIONS

Experiments were conducted at the Central Water and Power Research Station in Poona, India, in 1938 and 1939 to study scour around a single pier. These studies were done in a flume with sand having a mean diameter of 0.29 mm. On the basis of these studies, Inglis (1949) presented the formula (Joglekar, 1962):

$$\frac{y_p}{b} = 1.7 \left(\frac{q^{2/3}}{b} \right)^{0.78} \quad (27)$$

which may be solved for y_{sp} to obtain the "Inglis-Poona I" equation, defined as:

$$y_{sp} = 1.7 b \left(\frac{q^{2/3}}{b} \right)^{0.78} - y_o \quad (28)$$

Equations 27 and 28 are dimensional, with y_{sp} , y_o , and b in feet and q in cubic feet per second per foot. This relation is not dimensionally homogeneous; therefore, it may not be universally applicable to other bridge scour data. From the same set of experimental data, Inglis (1949) developed a dimensionally homogeneous equation that when solved for y_{sp} , is defined as:

$$y_{sp} = 1.73 b \left(\frac{y_o}{b} \right)^{0.78} - y_o \quad (29)$$

which has units as defined for equation 28 and will be referred to as the "Inglis-Poona II" equation.

LARRAS EQUATION

Larras (1963) compiled scour data from field investigations of several French rivers and scale-model investigations, and developed the "Larras" equation:

$$y_{sp} = 1.42 K_{S2} b^{0.75} \quad (30)$$

where K_{S2} is a coefficient based on the shape of the pier nose (1.0 for cylindrical piers and 1.4 for rectangular piers).

Equation 30 is dimensional, with y_{sp} and b in feet.

The Larras equation is a function of pier width and shape only. Because Larras' field measurements were only point measurements of scour depth made after a flood had passed, those data may not represent the depth of equilibrium scour (Shen et al., 1969).

LAURSEN EQUATION

Laursen used the results of his investigation of scour in a long contraction to develop equations for scour at bridge piers and abutments. Laursen stated: "The flow at the crossing cannot be considered uniform, but the solutions for the long contraction can be modified to describe the scour at bridge piers and abutments with the use of experimentally determined coefficients" (Laursen, 1962, p. 170). Numerous flume experiments were conducted to evaluate the importance of the alignment of the piers to the flow, the length to width ratio of the piers, the approach flow velocity and depth, and the sediment size. The dimensionless Laursen equation for pier scour is:

$$\frac{b}{y_o} = 5.5 \left(\frac{y_{sp}}{y_o} \right) \left(\left[\left(\frac{1}{11.5} \right) \left(\frac{y_{sp}}{y_o} \right) + 1 \right]^{1.70} - 1 \right) \quad (31)$$

Equation 31 requires an iterative solution procedure to determine y_{sp} . The depth of scour (y_{sp}) from equation 31 must be corrected for the misalignment of the pier to the flow and (if the pier is aligned to the flow) for the pier nose shape, so that:

$$y_{sp} = K_{S1} K_{\alpha L} y_{sp} \quad (32)$$

where K_{S1} is a coefficient based on the shape of the pier nose, which is set to 1.0 if the pier is skewed to the flow and is otherwise defined in table 7; and $K_{\alpha L}$ is a coefficient based on the pier length and alignment to the approach, and is defined in figure 48.

Table 7. Pier shape coefficients (Laursen, 1962).

Nose Form	Length-Width Ratio	K_{S1}
Rectangular	--	1.0
Semicircular	--	0.9
Elliptic	2:1	0.8
	3:1	0.75
Lenticular	2:1	0.80
	3:1	0.70

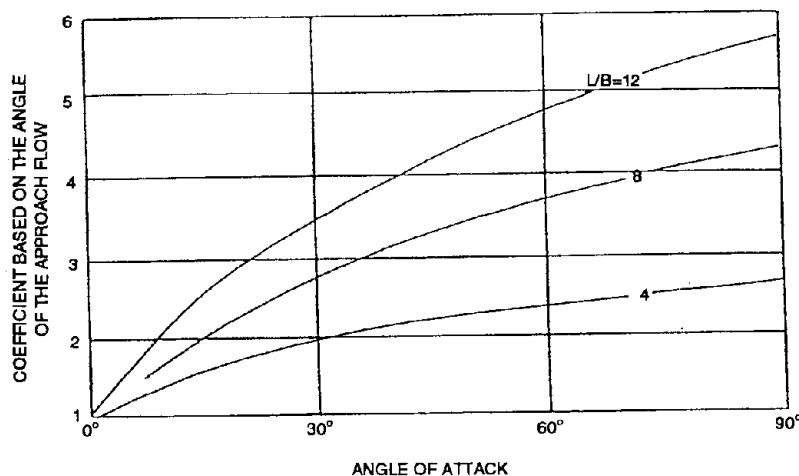


Figure 48. Effect of angle of attack (Laursen, 1962, p. 177).

Laursen found that the depth of scour was not strongly influenced by the flow velocity or sediment size for live-bed conditions. Laursen (1962) concluded that the maximum depth of live-bed scour is uniquely determined by the pier geometry and that the width of the scour holes may be estimated as $2.75y_{sp}$.

SHEN EQUATIONS

Shen et al. (1969) conducted a series of experiments and determined that the basic mechanism of local scour is the vortex systems caused by the pressure field induced by the pier. Further analysis of the vortex systems indicated that the strength of the horseshoe vortex is a function of the dimensionless pier Reynolds number, defined as:

$$R_p = \frac{V_o b}{\nu} \quad (33)$$

where ν is the kinematic viscosity of water.

According to Shen et al. (1969),

“Since the horseshoe vortex system is the mechanism of local scour and the strength of the horseshoe vortex system is a function of the pier Reynolds number, the equilibrium depth of scour should be functionally related to the pier Reynolds number.”

Data from several investigations were used to evaluate the influence of the pier Reynolds number on the depth of scour around bridge piers. The analysis indicated that scour depth increases rapidly to a maximum with increasing pier Reynolds number, then begins to decrease as the pier Reynolds number continues to increase. A least-squares regression of the data with pier Reynolds numbers less than 50,000 resulted in the following equation:

$$y_{sp} = 0.00073 R_p^{0.619} \quad (34)$$

Equation 34 is dimensional, with y_{sp} in feet.

This equation generally envelops the data from which it was developed and will be referred to as the “Shen” equation. Shen et al. (1969) found that this equation does not adequately account for the pier shape and the size of the bed material. They concluded that this equation could be used to provide a conservative estimate of clear-water scour, but that it was too conservative to be used for live-bed conditions. They suggested use of the equations by Larras (1963) and Breusers (1964 to 1965) for live-bed conditions.

Shen et al. (1969) also analyzed the pier Froude number, described in Maza and Sanchez (1964), as an explanatory variable for scour depth. They found that for pier Froude

numbers less than 0.2 and fine sands ($D_{50} < 0.52$ mm), the depth of scour increased rapidly as the pier Froude number increased. However, for pier Froude numbers greater than 0.2 and coarser sands, the depth of scour increased only moderately for increases in the pier Froude number. From that analysis, Shen et al. (1969) developed two equations, referred to as the “Shen-Maza” equations and defined as:

$$y_{sp} = 11.0 b F_p^2 \quad \text{for} \quad F_p < 0.2 \quad (35)$$

$$y_{sp} = 3.4 b F_p^{0.67} \quad \text{for} \quad F_p > 0.2 \quad (36)$$

where F_p is the pier Froude number, defined as $\frac{V_o}{\sqrt{gb}}$.

Equation 35 is fundamentally the same equation developed by Maza and Sanchez (1964) and is applicable when the pier Froude numbers are less than 0.2. Note that the pier width cancels out in equation 35; therefore, it is based only on velocity and is unlikely to represent general observed scour conditions.

Application of Equations to Measured Data

Laboratory conditions are often designed to isolate specific scour processes so that the resulting equations may not account for the complex and dynamic conditions found in the field. Field conditions are often assumed to be steady state and uniform when equations based on laboratory investigations are used to estimate or predict scour at bridges. Equations used in this report were used to estimate scour for both live-bed and clear-water conditions, except for the Simplified Chinese equation, which has coefficients specific to clear-water and live-bed conditions.

Methods and coefficients that correct for pier flow alignment are not consistent among the equations and often are not addressed in the original documentation of the equation. The Laursen and HEC-18 equations provide coefficients to correct estimated scour for skew, and the Froehlich equation uses effective pier width computed by equation 4 to account for skew. The Simplified Chinese equation does not include the skew correction of the original Chinese equation, which is a function of skew and pier shape, so the Simplified Chinese equation was applied only to measured data where the pier is aligned to the approach flow. The other selected equations do not provide a correction for skew, so they were applied using the effective pier width computed by equation 4.

Many equations do not account for the effect of pier shape or only provide corrections for a limited number of pier shapes. Laursen's equation does not specify a shape correction for pile groups, so pile groups were classified as round-nosed or circular piers (as described in

Richardson et al., 1993). Pile groups were treated as cylinders for the Simplified Chinese equation. Blench-Inglis I and II, Inglis-Poona I and II, Chitale, Ahmad, and Shen equations contain no procedure to correct the estimated scour for pier shape, and no corrections were used in this evaluation. The Larras equation specifies only square-nosed and circular pier shapes. For this evaluation of the Larras equation, sharp-nosed piers and pile groups were classified as circular piers.

Comparison of Observed and Computed Scour

The criteria for evaluating equations using comparisons of computed and observed (measured) scour depths should not be based on minimized errors of estimate for most pier scour equations. Some of the selected equations were not developed to predict observed scour, but to estimate the maximum probable scour for a given set of conditions for design applications. Design curves and equations are generally developed to not underestimate the data, so there is a bias for negative residual errors (observed minus computed scour). Best fit and regression equations are intended to predict the mean of the data. The criteria for evaluating equations will depend on the intended use of the equations. Equations that accurately estimate the maximum depth of scour and rarely underestimate the scour will be preferred for most design applications. Methods that could predict observed scour for the broad range of measurement conditions would probably be more complex than those reviewed here and would include methods to account for the time-dependent scour processes such as soil erodibility.

Differences between observed and computed scour depths for the selected equations are illustrated in box plots of the residuals (observed scour and computed scour) in figure 49. The equations produced a wide range of residuals, with most equations having maximum absolute errors of 6.1 m (20 ft) or greater. Ratios of computed scour to observed scour are illustrated in the box plots in figure 50. All of the equations frequently computed scour that was at least twice the observed depth of scour and occasionally computed scour that was at least 10 times the observed values. The negative values in figure 50 reflect situations where the equation computed a negative depth of scour. The equations were not developed for infilling (negative scour) conditions, and these negative values are shown only to illustrate the widely varied results that can be obtained. None of the equations consistently computed a depth of scour that closely matched the observed depth of scour for the measured conditions, as illustrated in figures 49 and 50. Figures 49 and 50 indicate that the Simplified Chinese, HEC-18 (CSU), Froehlich, Froehlich Design, Larras, Shen, Inglis-Poona II, and Blench-Inglis I equations predicted the observed scour more closely than did the other selected equations. Predicted scour depths from these equations were compared with observed scour depths in scatter plots.

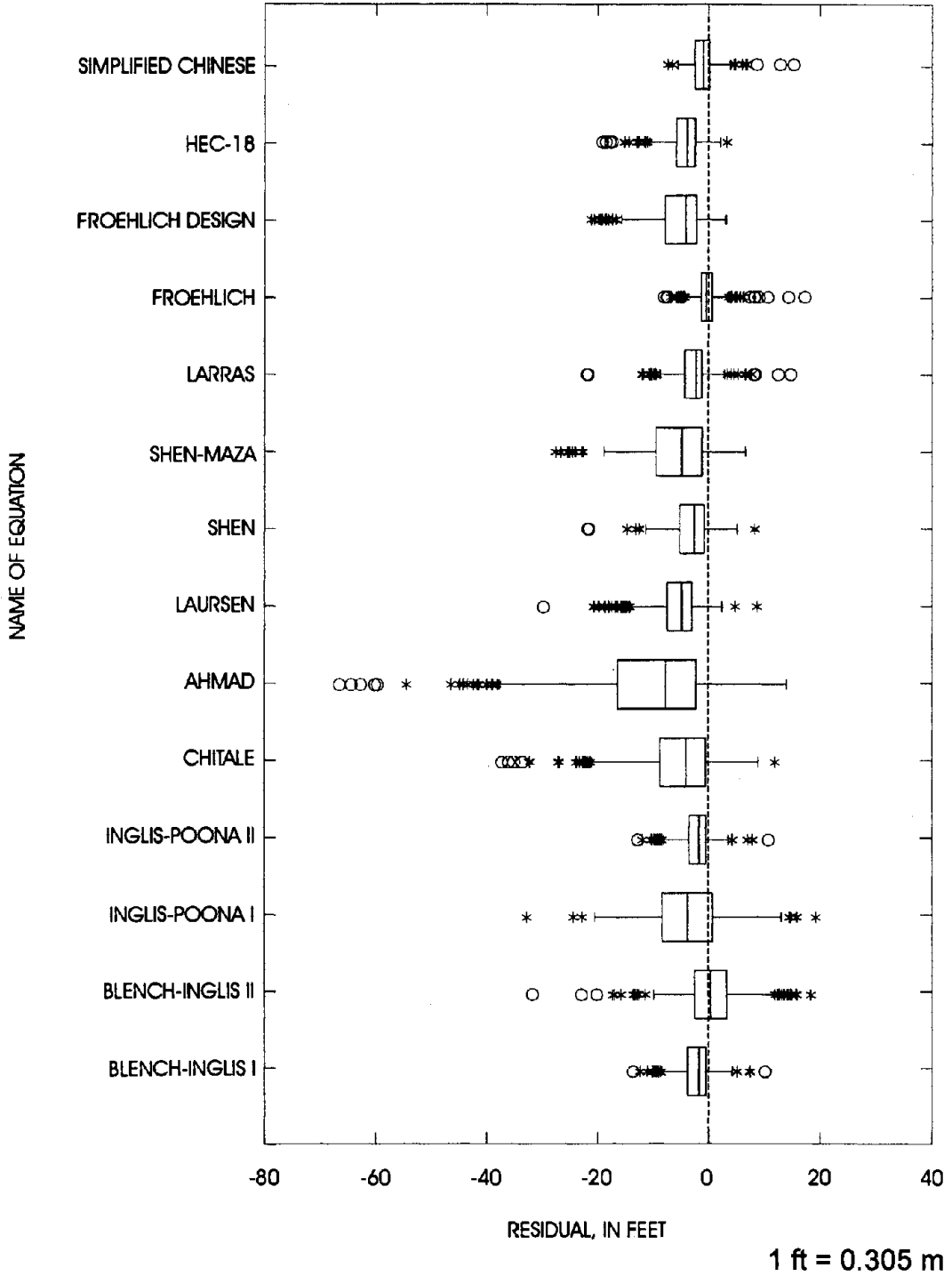
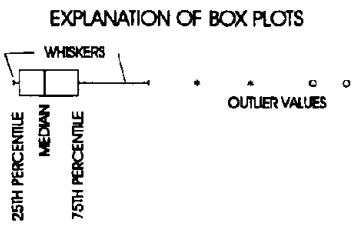


Figure 49. Box plot of residuals for all data.

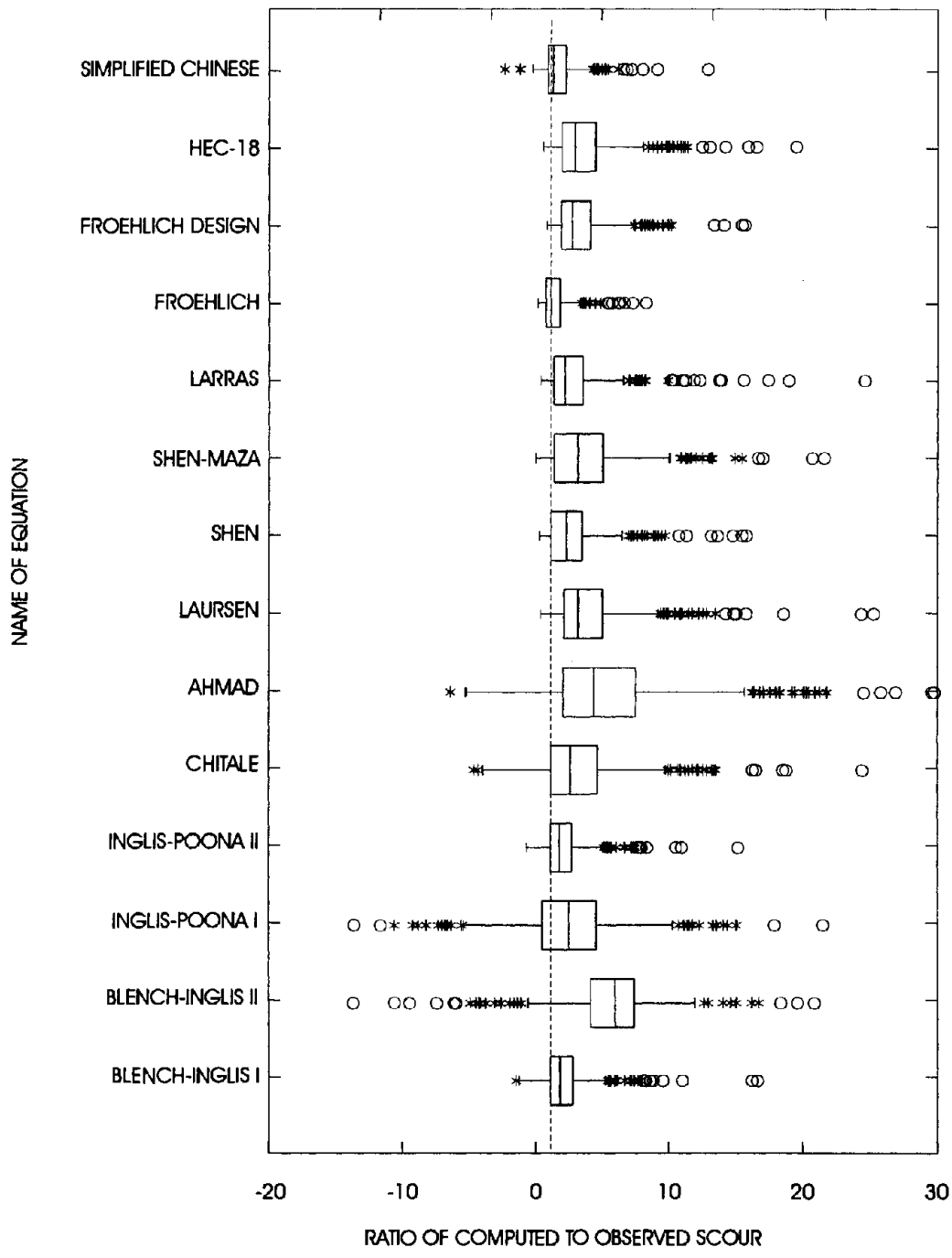
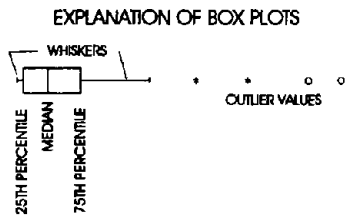


Figure 50. Box plot of ratio of computed to observed scour for all data.

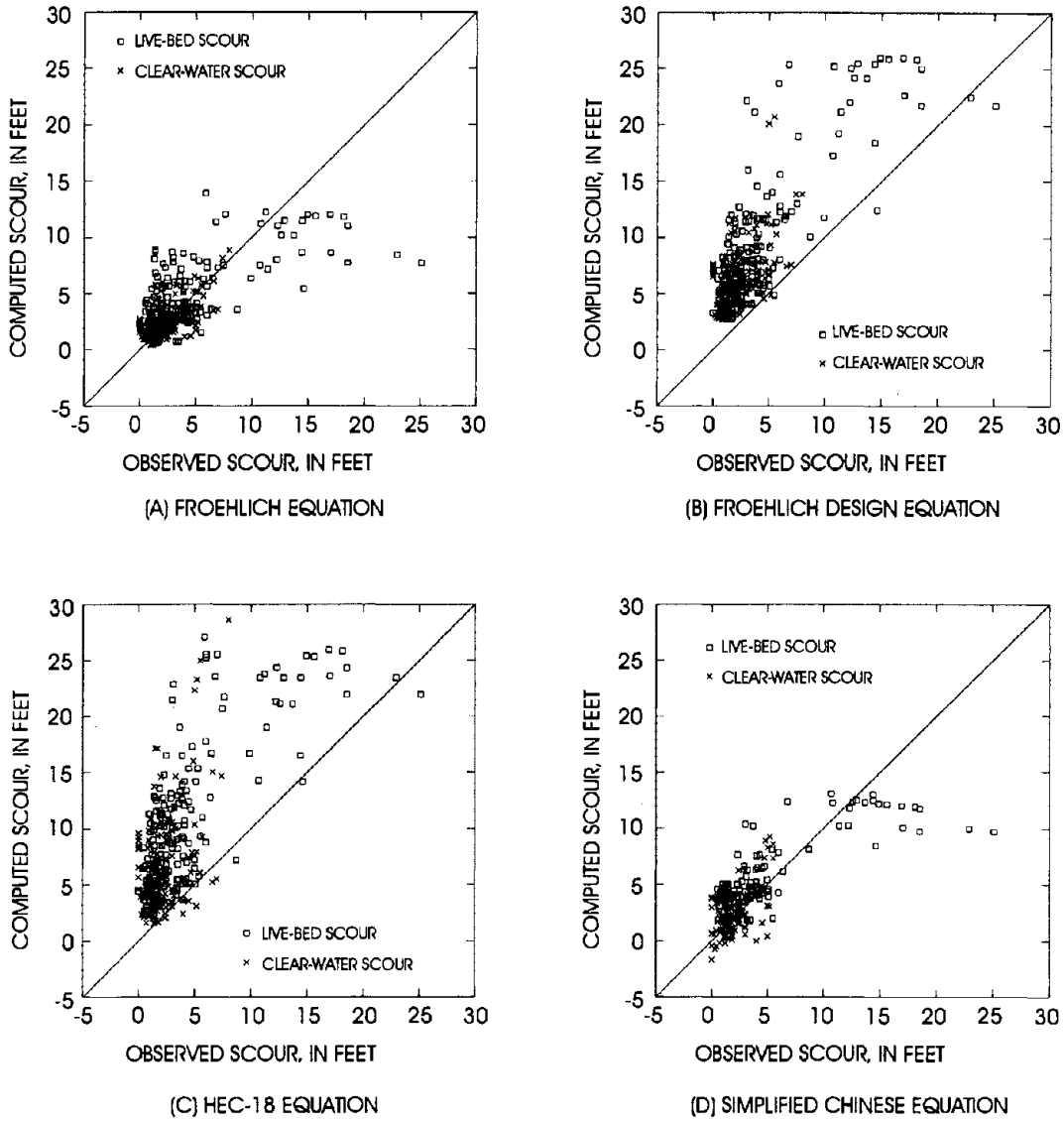
The scatter plots of predicted and observed scour depths shown in figures 51 through 54 reveal additional information about the performance of the eight equations. Figures 51 and 52 compare depth of scour computed by the selected equations to the observed scour with live-bed and clear-water conditions identified. The Froehlich equation (figure 51A) and the Simplified Chinese equation (figure 51D) fit the center of the data fairly well; however, they underestimate the scour for the larger observed values. The factor of safety included in the Froehlich Design equation (figure 51B) is successful at moving nearly all of the data above the line-of-equality. Figure 51C shows that the HEC-18 equation also provided conservative results with very few cases where the depth of scour was underestimated. Although the HEC-18 and Froehlich Design equations seldom underestimated the observed scour, the spread above the line-of-equality is quite large, indicating large overestimation for many measurements. The Shen, Blench-Inglis I, Larras, and Inglis-Poona II equations shown in figure 52 have less spread above the line-of-equality, but have underestimated the scour for several of the observed values.

Figures 51 and 52 indicate that live-bed scour is estimated with greater accuracy than clear-water scour. The trend of the live-bed data is more parallel to the line-of-equality than is the trend of the clear-water data. For six of the eight equations, the trend of the clear-water data is steeper than the live-bed data and the line-of-equality. The Froehlich and Simplified Chinese equations have the least scatter for clear-water conditions. The Froehlich equation includes an explanatory variable for sediment size. The Simplified Chinese equation is defined uniquely for live-bed and clear-water conditions, and also includes a term to account for the flow intensity. Thus, it is not surprising that these two equations performed better for clear-water conditions than did the other six equations, which have no method to account for the difference between live-bed and clear-water conditions.

The scatter plots of predicted and observed scour depths shown in figures 53 and 54 were plotted with measurements having piers aligned to the flow identified separately from those skewed to the flow. The Simplified Chinese equation was not applied to piers skewed to the flow and, therefore, only contains data for piers aligned with the flow. All of the equations tended to overestimate the depth of scour at piers skewed to the flow. This overestimation could be the result of several factors. The effective pier width was used for equations that did not directly account for skew. The effective pier width and/or coefficients used by the various equations may overcompensate for the effect of skewed piers. The measured data may not represent the maximum depth of scour that typically occurs downstream from the nose along the sides of the pier for piers skewed to the flow. The HEC-18 and Froehlich equations include factors that account for skew, but do not appear to perform better than those that do not account for skew.

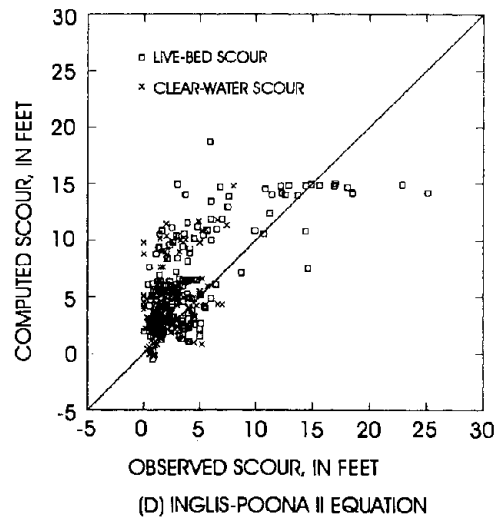
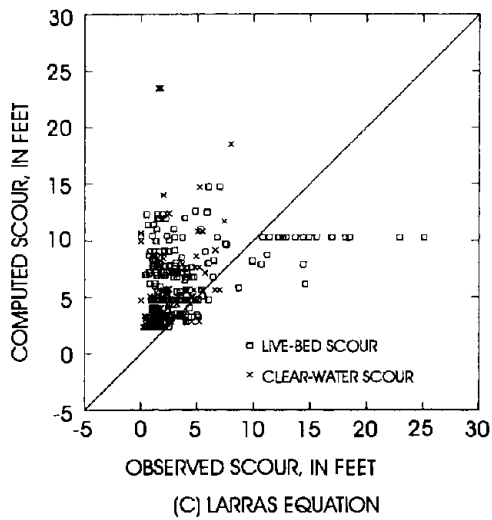
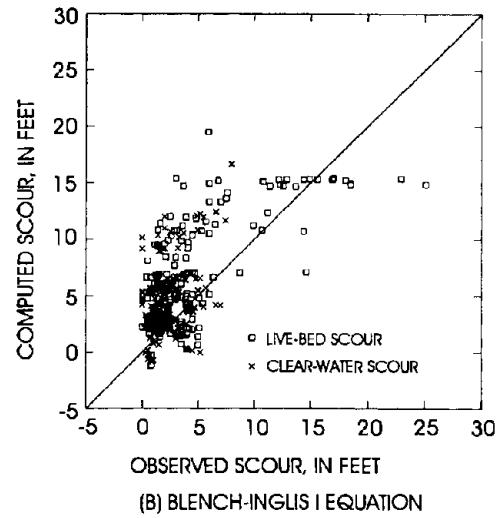
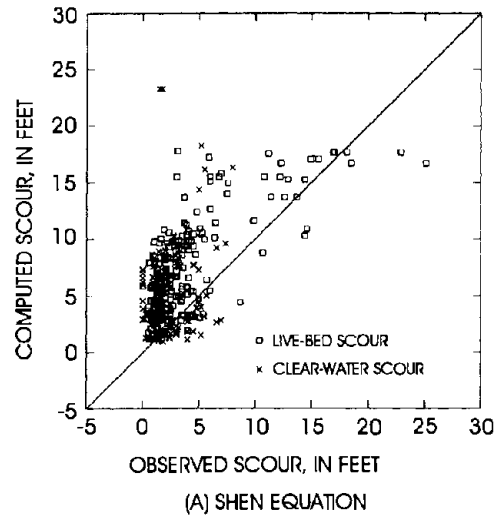
None of the equations accurately computed the depth of scour for the full range of measured conditions. The Froehlich and Simplified Chinese equations provided a reasonable "best fit" for observed scour depths less than 3 m (10 ft), but typically underestimated observed scour depths greater than 3 m (10 ft). The Shen equation had less scatter than the Froehlich Design or HEC-18 equation, but underestimated the scour for many measurements. Although the Froehlich Design and HEC-18 equations overestimate the scour for many measurements, they seldom underpredict the measured scour and may be preferable for bridge design. The

overestimated depths of scour from the Froehlich Design and CSU equations may result in oversized bridge foundations. Therefore, more accurate, but conservative, equations are needed to provide the design engineer with the information required to develop a safe and economical design.



1 ft = 0.305 m

Figure 51. Comparison of computed and observed scour for: (A) Froehlich, (B) Froehlich Design, (C) HEC-18, and (D) Simplified Chinese equations with live-bed and clear-water scour identified.



1 ft = 0.305 m

Figure 52. Comparison of computed and observed scour for: (A) Shen, (B) Blench-Inglis I, (C) Larras, and (D) Inglis-Poona II equations with live-bed and clear-water scour identified.

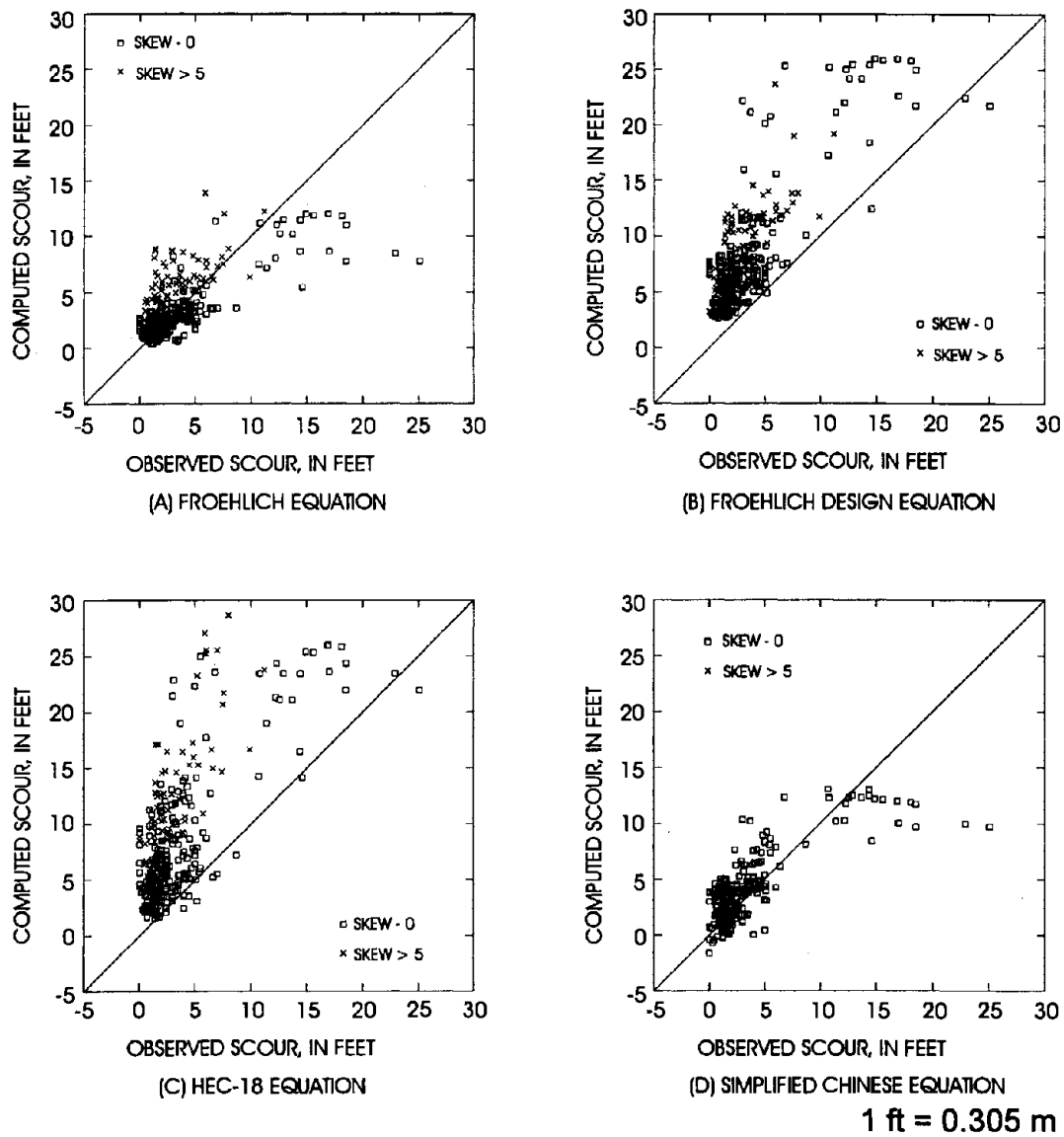
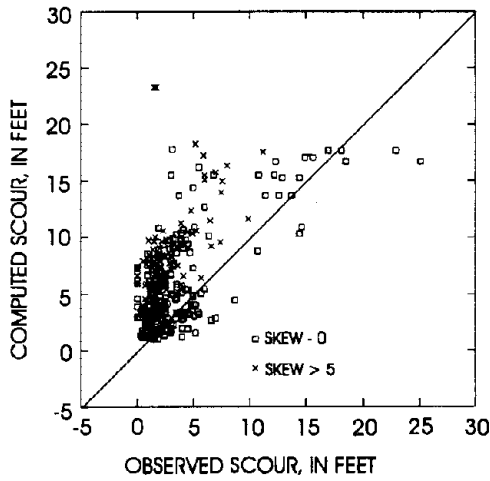
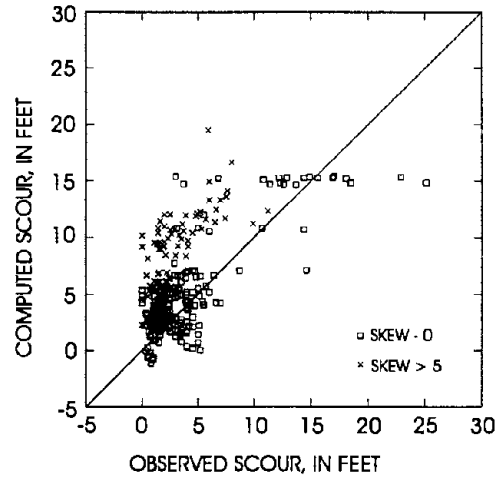


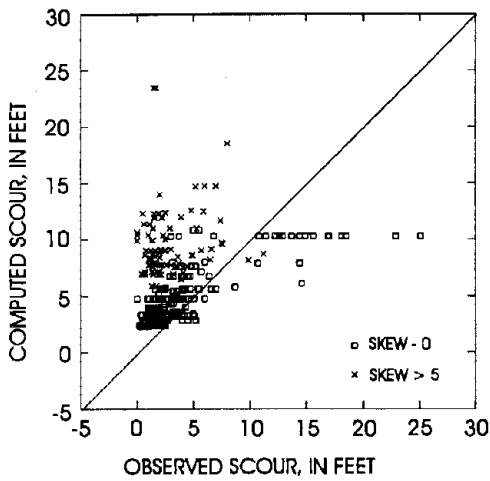
Figure 53. Comparison of computed and observed scour for: (A) Froehlich, (B) Froehlich Design, (C) HEC-18, and (D) Simplified Chinese equations with skew of pier to flow categorized.



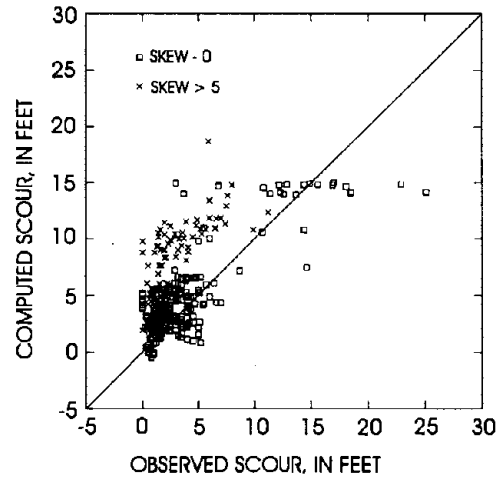
(A) SHEN EQUATION



(B) BLENCH-INGLIS I EQUATION



(C) LARRAS EQUATION



(D) INGLIS-POONA II EQUATION

1 ft = 0.305 m

Figure 54. Comparison of computed and observed scour for: (A) Shen, (B) Blench-Inglis I, (C) Larras, and (D) Inglis-Poona II equations with skew of pier to flow categorized.

Page Intentionally Left Blank
116

SUMMARY AND CONCLUSIONS

The processes of river channel scour at bridge foundations are complex and interrelated. Methods to predict scour at bridges are often of unknown accuracy because of inadequate knowledge about the scour processes. Field measurements of bridge scour are essential to extend our understanding of scour processes and to evaluate scour prediction methods.

Investigations to collect scour data during flood events require considerable preparation, including site reconnaissance, site selection, site establishment, and development of a scour measurement plan. The scope of a bridge scour measurement may be limited (for the purpose of exploring relations between scour and explanatory variables and evaluating published equations) or detailed (for the purpose of describing and understanding complex scour processes). Instrumentation and techniques specific to limited-detail and detailed bridge scour measurements have been developed in this and other investigations. Collection of bridge scour data sets requires methods and instrumentation to measure streambed elevation, water velocity, bed material, and sediment transport at bridges during floods. Methods are also required for deploying the instruments, measuring the horizontal position of instruments, and storing the collected data. A major reason for the increased success in obtaining scour data sets in the last few years is the development of improved instrumentation and techniques for measuring bridge scour. Further developments will continue to improve the potential quantity and accuracy of bridge scour measurements, especially for detailed data sets.

The channel geometry data of a scour measurement must be interpreted in order to quantify the depth of scour. The scour depth for a data set is defined by the vertical distance between the scoured channel and a reference surface that represents the channel geometry for a baseline condition. Inconsistent methods of determining scour reference surfaces can produce scour depths that vary by as much as 100 percent. Consistent and representative methods of determining scour reference surfaces are required in regional analysis of scour depths and in compilations of data from different investigators. Reference surfaces should be selected so that the local, contraction, general, and long-term process components of total scour may be quantified separately. The reference surface for local scour is one that represents the ambient channel geometry at the measurement location in the absence of the flow obstruction. The contraction scour reference surface should represent the mean bed elevation of an uncontracted section at the measurement location. Determination of scour references requires judgment; however, consistent methodology will facilitate transferability of scour data and scour analyses.

A computer data base management system for bridge scour data provides a repository for the data of past and ongoing investigations and facilitates preparation, compilation, and analysis of these data. The Bridge Scour Data Management System (BSDMS) prompts users for over 200 data set attributes and provides descriptions of those attributes so that the data sets are recorded as completely as possible using consistent definitions. Each bridge site is stored as a data set that includes all of the scour measurement and related data for that site. The program is interactive and is portable to workstations and DOS computers.

The data base of this report contains 384 local pier scour data sets measured at 56 sites in 14 States. This investigation tried unsuccessfully to make measurements of contraction scour and local scour at bridge abutments; however, these measurements are very difficult to obtain and, when measured, to interpret conclusively. Investigations are needed that have specific objectives and methods to obtain measurements of these types of scour, for which field data are particularly lacking. This is especially important because methods to estimate contraction scour and local scour at bridge abutments are regarded as less reliable than those for estimating local scour at bridge piers.

The distributions of the data for most of the quantitative variables are right (positive) skewed, as is typical for water resources and watershed data. A base 10 logarithmic transformation improved the symmetry of the distribution for most of the variables and the linearity of the relations between variables. About one-half of the pier scour measurements were made at round-nosed piers. The measurements were classified according to live-bed or clear-water sediment transport conditions, and about 64 percent were made under live-bed conditions. The range of measured scour depth is zero to 7.7 m (25.1 ft). About 47 percent of the measured scour depths were less than 0.6 m (2 ft), while about 13 percent were greater than 1.5 m (5 ft). The estimated error of the measured scour depth was between 0.15 and 0.3 m (0.5 and 1 ft) for 83 percent of the measurements.

Scour processes are typically dependent on multiple, interrelated variables, so that the relation between scour depth and a single variable may have several curves that represent data subgroups defined by the values of a third variable. In the analysis of field scour measurements, it is important to realize that measured scour depths are unlikely to represent equilibrium conditions for the concurrent deterministic variables, and the relative equilibrium of most measurement conditions is difficult to assess. These observations indicate that some analytical procedures that do not assume constant variance and independent observations in the data set would be preferable to those that do make these assumptions. For example, an ordinary least-squares regression may not be adequate to define a functional scour-depth relation, because the influence of the explanatory variable on the scour depth is not constant in the data set. This observation also underscores the benefits of laboratory studies to investigate specific relations under controlled steady-state conditions, and the limitations of laboratory results when applied to the much more complex conditions actually occurring in the field.

Measured pier widths range from 0.29 to 4.6 m (0.95 to 15 ft) and most of the pier widths were between 0.6 and 1.8 m (2 and 6 ft). The influence of pier width on measured scour was found to decrease with increasing pier width so that when local scour depth is computed as a linear function of pier width, the influence of pier width tends to be underrated for smaller pier widths and overrated for large ones. Scour depth and pier width have an approximately linear relation in logarithmic space, with a slope between about 0.65 and 0.8. The maximum ratio of scour depth to effective pier width for the data of this study is 2.1. About 70 percent of the measurements were made where the piers were aligned with the flow. The alignment of piers to the flow was found to have a significant influence on scour depth, while the effect of pier nose shape was not apparent in these field data.

The influence of flow depth on scour appears to decrease at a uniform rate over the range of measured data, but does not become insignificant at large ratios of flow depth to pier width. The relation of scour depth and flow depth, where both variables are normalized for effective pier width, is approximately linear in logarithmic space. Measured scour depths increase with flow intensity under clear-bed conditions and appear nearly independent of flow intensity for live-bed conditions. The field data do not indicate any direct influence of sediment size on scour depth; however, this may be due to differences between the sampled bed material and bed material in the scour hole. The relation of sediment gradation and measured scour depth was not conclusive. The data indicate that scour depth decreases with gradation from a uniform condition to a geometric standard deviation of about 2.8; but a relation is not evident at larger values of geometric standard deviation.

Comparison of computed and observed depths of scour showed that none of the selected equations accurately estimate the depth of scour for all of the conditions measured. The Froehlich and Simplified Chinese equations fit the data reasonably well for observed scour depths less than 3 m (10 ft), but generally underestimate the depth of scour for observed depths of scour greater than 3 m (10 ft). The Froehlich Design and HEC-18 equations were the only equations that did not underestimate the scour depth for several measurements; however, they often overestimated the scour by large amounts, which would result in overdesigned bridge foundations.

Additional field research, data collection, and data analysis are needed to understand and model the complex interrelated processes responsible for scour at bridges. Instrumentation and techniques for making field measurements of scour currently allow most of the necessary data to be collected, and future instrumentation development should allow the complex processes to be more fully measured in the field. Analysis and modeling of these processes will provide improved understanding of scour processes and contribute to the reliability and economy of bridge foundation designs that benefit the traveling public.

Page Intentionally Left Blank

120

REFERENCES

- Abdel-Rahmann, N.M., 1964, The effect of flowing water on cohesive beds: Contribution no. 56, Versuchsanstalt für Wasserbau und Erdbau an der Eidgenössischen Technischen Hochschule, Zurich, Switzerland, pp. 1-114.
- Academy of Railway Sciences of China, 1964, Selection of local scour data of piers, Symposium on Scour of Bridge Crossings in China (in Chinese).
- Ahmad, Mushtaq, 1962, Discussion of "Scour at bridge crossings," by E.M. Laursen: Transactions of the American Society of Civil Engineers, vol. 127, part I, no. 3294, pp. 198-206.
- Ahmad, Mushtaq, 1953, Experiments on design and behavior of spur dikes, *in* Minnesota International Hydraulics Convention, Minneapolis, MN, 1953, Proceedings: Minneapolis, MN, St. Anthony Falls Hydraulic Laboratory, pp. 145-159.
- Anderson, A.G., 1974, Scour at bridge waterways—A review: Federal Highway Administration Report no. FHWA-RD-75-089, 29 pp.
- Andrews, E.D., and Smith, J.D., 1992, A theoretical model for calculating marginal bedload transport rates of gravel, *in* Dynamics of Gravel-Bed Rivers, eds. Billi, P., Hey, R.D., Thorne, C.R., and Tacconi, P.: John Wiley and Sons, Ltd, pp. 41-52.
- Ashmore, P.E., Yuzyk, T.R., and Herrington, R., 1988, Bed-material sampling in sand-bed streams: Environment Canada, Report no. IWD-HQ-WRB-SS-88-4, Ottawa, Canada, 87 pp.
- Baker, C.J., 1986, Local scour at bridge piers in non-uniform sediment: Auckland, New Zealand, University of Auckland, Master of Engineering thesis, School of Engineering Report no. 402.
- Blench, Thomas, 1969, Mobile-bed fluviology: Edmonton, Alberta, Canada, The University of Alberta Press, 221 pp.
- Blench, Thomas, 1962, Discussion of "Scour at bridge crossings," by E.M. Laursen: Transactions of the American Society of Civil Engineers, vol. 127, part I, no. 3294, pp. 180-183.
- Blench, Thomas, 1951, Regime theory for self-formed sediment-bearing channels: Proceedings of the American Society of Civil Engineers, vol. 77, separate no. 70.
- Blodgett, J.C., 1989, Monitoring scour at the State Route 32 bridge across the Sacramento River at Hamilton City, California: Proceedings of the Bridge Scour Symposium, October 1989, U.S. Federal Highway Administration Report no. FHWA-RD-90-035, pp. 211-226.

- Blodgett, J.C., 1986, Rock riprap design for protection of stream channels near highway structures, vol. 1: Hydraulic Characteristics of Open Channels: U.S. Geological Survey Water-Resources Investigations Report 86-4127, 60 pp.
- Breusers, H.N.C., 1964-1965, Scour around drilling platforms: Bulletin, Hydraulic Research 1964 and 1965, International Association of Hydraulic Research, vol. 19, p. 276.
- Breusers, H.N.C., Nicollet, G., and Shen, H.W., 1977, Local scour around cylindrical piers: Journal of Hydraulic Research, vol. 15(3), pp. 211-252.
- Butch, G.K., 1992, written communication.
- Carlson, G.H., 1991, U.S. Geological Survey, written communication.
- Chang, F.M., 1980, Scour at bridge piers—Field data from Louisiana files: U.S. Federal Highway Administration Report no. FHWA-RD-79-105, 34 pp.
- Chiew, Y.M., 1984, Local scour at bridge piers: Auckland, New Zealand, University of Auckland, Ph.D. dissertation, School of Engineering Report no. 355.
- Chiew, Y.M., and Melville, B.W., 1987, Local scour around bridge piers: Journal of Hydraulic Research, vol. 25(1), pp. 15-26.
- Chitale, S.V., 1962, Discussion of "Scour at bridge crossings," by E.M. Laursen: Transactions of the American Society of Civil Engineers, vol. 127, part I, no. 3294, pp. 191-196.
- Colby, B.R., and Hembree, C.H., 1955, Computations of total sediment discharge, Niobrara River near Cody, Nebraska: U.S. Geological Survey Water-Supply Paper 1593, 17 pp.
- Edwards, T.K., and Glysson, G.D., 1988, Field methods for measurement of fluvial sediment: U.S. Geological Survey Open-File Report 86-531, 118 pp.
- Ettema, Robert, 1980, Scour at bridge piers: Auckland, New Zealand, University of Auckland, School of Engineering Report no. 216.
- Federal Interagency Sedimentation Project, 1952, The design of improved type of suspended-sediment samplers, Interagency Report 6: Minneapolis, MN, St. Anthony Falls Hydraulics Laboratory, 103 pp.
- Flaxman, E.M., 1963, Channel stability in undisturbed cohesive soils: Journal of the Hydraulics Division, American Society of Civil Engineers, vol. 89, no. HY2, Proceedings Paper 3462, March, pp. 87-96.

- Froehlich, D.C., 1989, Local scour at bridge abutments, *in* Ports, M.A., ed., Hydraulic Engineering—Proceedings of the 1989 National Conference on Hydraulic Engineering: New York, American Society of Civil Engineers, pp. 13-18.
- Froehlich, D.C., 1988, Analysis of on-site measurements of scour at piers, *in* Abt, S.R., and Gessler, Johannes, eds., Hydraulic Engineering—Proceedings of the 1988 National Conference on Hydraulic Engineering: New York, American Society of Civil Engineers, pp. 534-539.
- Gao Dong Guang, Posada G., Lilian, and Nordin, C.F., 1992, Pier scour equations used in the People's Republic of China: Fort Collins, CO, Colorado State University, Department of Civil Engineering, Draft.
- Gao Dong Guang, and Xu Guoping, 1989, Research on local scour mechanism of piers and revision of equations; Research report revision of Code of Investigation and Design of Highway Bridge Crossings in China, Xian Highway Transport University (in Chinese).
- Harrington, R.A., and McLean, D.G., 1984, Field observations of river bed scour on the Peace River near Fort Vermilion, Alberta: Canadian Journal of Civil Engineering, vol. 11, pp. 782-797.
- Helsel, D.R., and Hirsch, R.M., 1992, Statistical methods in water resources: Elsevier Science Publishers, 522 pp.
- Hopkins, G.R., Vance, R.W., and Kasraie, Behzad, 1980, Scour around bridge piers: U.S. Federal Highway Administration Report no. FHWA-RD-79-103, 124 pp.
- Hubbell, D.W., 1964, Apparatus and techniques for measuring bedload: U.S. Geological Survey Water-Supply Paper 1748, 74 pp.
- Inglis, S.C., 1949, The behavior and control of rivers and canals: Poona, India, Poona Research Station, Publication 13, part II, Central Water Power Irrigation and Navigation Report, 478 pp.
- International Organization for Standardization (ISO), 1992, Liquid flow measurement in open channels, Sampling and analysis of gravel-bed material: ISO Reference no. ISO 9195:1992(E), 9 pp.
- Jarrett, R.D., and Boyle, J.M., 1986, Pilot study for collection of bridge-scour data: U.S. Geological Survey Water-Resources Investigation 86-4030, 30 pp.
- Jobson, H.E., and Froehlich, D.C., 1988, Basic hydraulic principles of open-channel flow: U.S. Geological Survey Open File Report 88-707, Reston, VA, 150 pp.

Joglekar, D.V., 1962, Discussion of "Scour at bridge crossings," by E.M. Laursen: Transactions of the American Society of Civil Engineers, vol. 127, part I, no. 3294, pp. 183-186.

Jones, J.S., 1993, personal communication.

Kittle, J.L., Jr., Hummel, P.R., and Imhoff, J.C., 1989, ANNIE-IDE, A system for developing user interfaces for environmental models (programmers guide): U.S. Environmental Protection Agency Report no. EPA/600/3-89/034, Environmental Research Laboratory, Athens, Georgia.

Klingeman, P.C., 1973, Hydrologic evaluation in bridge pier scour design: Journal of the Hydraulics Division, American Society of Civil Engineers, vol. 99, no. HY12, pp. 2175-2184.

Lacey, Gerald, 1936, Discussion of "Stable channels in erodible material," by E.W. Lane: Proceedings of the American Society of Civil Engineers, vol. 237, no. 5, pp. 775-779.

Lacey, Gerald, 1930, Stable channels in alluvium: London, United Kingdom, Minutes and Proceedings of the Institution of Civil Engineers, vol. 229, Paper 4736, pp. 259-284.

Lagasse, P.F., Schall, J.D., Johnson, F.L., Richardson, E.V., Richardson, J.R., and Chang, F.M., 1991, Stream stability at highway structures: U.S. Federal Highway Administration Hydraulic Engineering Circular 20, Publication FHWA-IP-90-014, 195 pp.

Land, Garland, 1992, Arkansas Department of Transportation, oral communication.

Landers, M.N., Jones, J.S., and Trent, R.E., 1994, Brief summary of national bridge scour data base, *in* Cotroneo, G.V., and Rumer, R.R., eds., Hydraulic Engineering '94: American Society of Civil Engineers, New York, pp. 41-45.

Landers, M.N., and Mueller, D.S., 1993, Reference surfaces for bridge scour depths, *in* Shen, H.W., Su, S.T., and Wen, Feng, eds., Hydraulic Engineering '93: American Society of Civil Engineers, New York, pp. 2075-2080.

Landers, M.N., Mueller, D.S., and Martin, G.R., 1996, Bridge Scour Data Management System Users Manual, U.S. Geological Survey Open File Report 95-754.

Landers, M.N., Mueller, D.S., and Trent, R.E., 1993, Instrumentation for detailed bridge-scour measurements, *in* Shen, H.W., Su, S.T., and Wen, Feng, eds., Hydraulic Engineering '93: American Society of Civil Engineers, New York, pp. 2063-2068.

Larras, Jean, 1963, Profondeurs maximales d'érosion des fonds mobiles autour des piles en rivière [Maximum depth of erosion in shifting bed around river piles]: Paris, France, Annales des Ponts et Chaussées, vol. 133, no. 4, pp. 411-424.

- Laursen, E.M. 1980, Predicting scour at bridge piers and abutments—A study to advance the methodology of assessing the vulnerability of bridges to floods for the Arizona Department of Transportation: Tucson, AZ, University of Arizona.
- Laursen, E.M., 1963, An analysis of relief bridge scour: Journal of the Hydraulics Division, American Society of Civil Engineers, vol. 89, no. HY3, pp. 93-118.
- Laursen, E.M., 1962, Scour at bridge crossings: Transactions of the American Society of Civil Engineers, vol. 127, part I, no. 3294, pp. 166-209.
- Laursen, E.M., 1960, Scour at bridge crossings: Journal of the Hydraulics Division, American Society of Civil Engineers, vol. 86, no. HY2, pp. 39-54.
- Laursen, E.M., 1958, The total sediment load of streams: Proceedings of the American Society of Civil Engineers, vol. 84, no. HY1, Paper 1530.
- Laursen, E.M., and Toch, A., 1956, Scour around bridge piers and abutments: Iowa Highway Research Board, Bulletin no. 4, 60 pp.
- Leopold, L.B., Wolman, M.G., and Miller, J.P., 1964, Fluvial processes in geomorphology: W.H. Freeman, San Francisco.
- Liu, H.K., Chang, F.M., and Skinner, M.M., 1961, Effect of bridge constriction on scour and backwater: Fort Collins, CO, Colorado State University, Department of Civil Engineering, Report CER60HKL22, 118 pp.
- Maza Alvarez, J.A., and Sanchez Bribiesca, J.L., 1964, Contribucion al estudio de la socavacion local en pilas de puente: Porta Alegre, Brazil Universidade Federal do Rio Grande do Sul, August.
- McIntosh, J.L., 1989, Use of scour prediction formulae, in Proceedings of the Bridge Scour Symposium: U.S. Federal Highway Administration Report no. FHWA-RD-90-035, pp. 78-100.
- Melville, B.W., 1984, Live-bed scour at bridge piers: Journal of Hydraulic Engineering, American Society of Civil Engineers, vol. 110, no. 9, pp. 1234-1247.
- Melville, B.W., and Sutherland, A.J., 1988, Design method for local scour at bridge piers: Journal of the Hydraulics Division, American Society of Civil Engineers, vol. 114, no. 10, pp. 1210-1225.
- Mueller, D.S., and Landers, M.N., 1994, Real-time data collection of scour at bridges, *in* Pugh, C.A., ed., Proceedings of Symposium on Fundamentals and Advancements in Hydraulic Measurements and Experimentation: American Society of Civil Engineers, New York, August, pp. 104-113.

- Mueller, D.S., and Landers, M.N., 1993, Development of bridge-scour instrumentation for inspection and maintenance personnel, *in* Shen, H.W., Su, S.T., and Wen, Feng, eds., Hydraulic Engineering '93: American Society of Civil Engineers, New York, pp. 2045-2050.
- Murillo, J.A., 1987, The scourge of scour: Civil Engineering, American Society of Civil Engineers, vol. 57, no. 7, pp. 66-69.
- Neill, C.R., 1968, Note on initial movement of coarse uniform bed material: Journal of Hydraulic Research, International Association of Hydraulic Research, vol. 27, pp. 247-249.
- Neill, C.R., 1965, Measurements of bridge scour and bed changes in a flooding sand-bed river: Proc. Institute of Civil Engineering, London, vol. 30, pp. 415-435, Discussion in vol. 36 (1967), pp. 397-421.
- Neill, C.R., 1964, River-bed scour: Research Council of Alberta Contribution no. 281, Canadian Good Roads Association, 37 pp.
- Neill, C.R., ed., 1973, Guide to bridge hydraulics: Project Committee on Bridge Hydraulics, Roads and Transportation Association of Canada, University of Toronto Press, ISBN 0-8020-1961-7, 191 pp.
- Norman, V.W., 1975, Scour at selected bridge sites in Alaska: U.S. Geological Survey Water-Resources Investigation 32-75, 171 pp.
- Porterfield, George, 1972, Computation of fluvial sediment discharge: U.S. Geological Survey Techniques of Water-Resources Investigations, Book 3, Chapter C3, 66 pp.
- Posey, C.J., 1974, Tests of scour protection for bridge piers: Journal of Hydraulic Engineering, American Society of Civil Engineers, vol. 100, no. 12, pp. 1773-1783.
- Rantz, S.E., et al., 1982, Measurement and computation of streamflow: U.S. Geological Survey Water-Supply Paper 2175, 631 pp.
- Rudkivi, A.J., 1986, Functional trends of scour at bridge piers: Journal of Hydraulic Engineering, American Society of Civil Engineers, vol. 112, no. 6, pp. 1-13.
- Raudkivi, A.J., and Ettema, Robert, 1983, Clear-water scour at cylindrical piers: Journal of the Hydraulics Division, American Society of Civil Engineers, vol. 109, no. 3, pp. 338-350.
- Raudkivi, A.J., and Ettema, Robert, 1977, Effect of sediment gradation on clear-water scour: Journal of the Hydraulics Division, American Society of Civil Engineers, vol. 103, no. 10, pp. 1209-1212.
- RD Instruments, 1993, Direct-reading broadband acoustic Doppler current profiler technical manual: San Diego, CA, 224 pp.

- Richards, N.A., 1991, Review of channel stability assessment techniques, pier scour equations, and countermeasures: Fort Collins, CO, Colorado State University, Department of Civil Engineering, Paper submitted for fulfillment of CE695BV, 80 pp.
- Richardson, E.V., Harrison, L.J., and Davis, S.R., 1991, HEC-18: Evaluating scour at bridges: U.S. Federal Highway Administration Hydraulic Engineering Circular 18, Publication FHWA-IP-90-017, 191 pp.
- Richardson, E.V., Harrison, L.J., Richardson, J.R., and Davis, S.R., 1993, HEC-18: Evaluating scour at bridges: U.S. Federal Highway Administration Hydraulic Engineering Circular 18, Publication FHWA-IP-90-017, revised April 1993, 238 pp.
- Richardson, E.V., and Richardson, J.R., 1989, Bridge scour, *in* Proceedings of the Bridge Scour Symposium: U.S. Federal Highway Administration Report no. FHWA-RD-90-035.
- Richardson, E.V., Simons, D.B., and Julien, P.Y., 1990, Highways in the river environment: U.S. Federal Highway Administration Publication FHWA-HI-90-016, 719 pp.
- Richardson, E.V., Simons, D.B., Karaki, Susumu, Mahmood, Khalid, and Stevens, M.A., 1975, Highways in the river environment: Hydraulic and environmental design considerations: U.S. Federal Highway Administration, 476 pp.
- Santoro, B.C., 1991, Velocity profiles and scour depth measurements around bridge piers: Transportation Research Record 1319, Transportation Research Board, Washington, D.C., pp. 137-142.
- Shen, H.W., Schneider, V.R., and Karaki, Susumu, 1969, Local scour around bridge piers: Journal of the Hydraulics Division, American Society of Civil Engineers, vol. 95, no. HY6, pp. 1919-1940.
- Shields, A., 1936, Anwendung der aehnlichkeitsmechanik und der turbulenz-forschung auf die geschiebebewegung: Berlin, Mitteilungen der Preuss, Versuchsanst fur Wasserbau und Schiffbau, Heft 26.
- Shirole, A.M., and Holt, R.C., 1991, Planning for a comprehensive bridge safety assurance program: Transportation Research Record 1290, pp. 137-142.
- Skinner, J.V., 1986, Measurement of scour depth near bridge piers: U.S. Geological Survey, Water-Resources Investigations Report 85-4106, 33 pp.
- Smerdon, E.T., and Beasley, R.P., 1961, Critical tractive forces in cohesive soils: Agricultural Engineering, St. Joseph, MI, January, pp. 26-29.
- Sundborg, A., 1956, The river Klaralven, a study of fluvial processes: Geografiska Annaler, pp. 127-316.

- Tison, L.J., 1961, Local scour in rivers: *Journal of Geophysical Research*, vol. 66(12), pp. 4227-4232.
- Trent, R.E., and Landers, M.N., 1991, Chasing floods and measuring scour: *Transportation Research Record* 1290, vol. 2, pp. 236-244.
- U.S. Federal Highway Administration, 1988, Scour at bridges: *Federal Highway Administration Technical Advisory* 5140.20, 132 pp.
- Vanoni, V.A., ed., 1975, *Sedimentation engineering*: American Society of Civil Engineers, New York, 745 pp.
- Ward, J.R., and Harr, C.A., eds., 1990, *Methods for collection and processing of surface-water and bed-material samples for physical and chemical analyses*: U.S. Geological Survey Open-File Report 90-140, 71 pp.
- White, C. M., 1940, Equilibrium of grains on bed of stream: *Proceedings of the Royal Society of London, Series A*, vol. 174, pp. 332-334.
- Yuzyk, T.R., 1986, *Bed material sampling in gravel-bed streams*: Environment Canada, Report no. IWQ-HQ-WRB-SS-86-8, Ottawa, Canada, 74 pp.
- Zang, RuiJin et al., 1981, *River sediment engineering*, vols. 1 and 2; Teaching and Research Section of River Mechanics and Engineering, Wuhan Institute of Hydraulic and Electric Engineering, Water Resources Press, China (in Chinese).
- Zhuravl'ov, M.M. 1978, New method of estimation of local scour due to bridge piers and its substantiation: *Trans. 109*. Ministry of Transport Construction, State All-Union Scientific Research Institute on Roads, 20 pp.